HYDROXYL FUNCTIONALITIES OF MID
RANK BRITISH COALS

VOLUME I

Harminder Singh Manak

A thesis submitted for the Degree of Doctor of Phil

The University of Aston in Birmingham

January 1996

The University of Aston in Birmingham

Hydroxyl functionalities of middle rank British Coals

Harminder Singh Manak

Doctor of Philosophy

1996

Most of the new processes involving the utilisation of coal are based on hydroliquefaction, and in order to assess the suitability of the various coals for this purpose and to characterise coals in general, it is desirable to have a detailed and accurate knowledge of their chemical constitution and reactivity. Also, in the consumption of coals as chemical feed stocks, as in hydroliquefaction, it is advantageous to classify the coals in terms of chemical parameters as opposed to, or in addition to, carbonisation parameters. In view of this it is important to realise the functional groups on the coal hydrocarbon skeleton. In this research it was attempted to characterise coals of various rank (and subsequently their macerals) *via* methods involving both microwave-driven and bench top derivatisation of the hydroxyl functionalities present in coal. These hydroxyl groups are predominantly in the form of hindered phenolic groups, with other alcoholic groupings being less important, in the coals studied here. Four different techniques were employed, three of which - stannylation, silylation and methylation - were based on *in situ* analysis. The fourth technique - acetylation - involved derivatisation followed by analysis of a leaving group. The four different techniques were critically compared and it is concluded that silylation is the most promising technique for the evaluation of the hydroxyl content of middle rank coals and coal macerals. Derivatisation *via* stannylation using TBTO was impeded due to the large steric demand of the reagent and acetylation did not successfully derivatise the more hindered phenolic groups. Three novel methylation techniques were investigated and two of these show great potential. The information obtained from the techniques was correlated together to give a comprehensive insight into the coals and coal macerals studied.

Keywords : Coal, Microwaves, Hydroxyl, Macerals.

To My Family

Acknowledgements

I would like to express my sincere gratitude and thanks to Professor W. R. McWhinnie for his encouragement, unfailing interest and supervision during the course of this research. I would like to thank the E.P.S.R.C and The Coal Research Establishment for funding this research, in particular Dr Paul Burchill for his interest and help during the past three years. I am grateful to Dr Mike Perry for providing the N.M.R data and coming in on the weekends in order to finish my analyses and to Dr Saied for providing the XPS data. Many thanks are due to the technical staff within the chemistry department for their time and patience, with a special thanks to Steve Ludlow whose assistance over the past three years has been very much appreciated. I would like to thank Rita and the members of the research group both past and present for making my time at Aston an interesting, entertaining and enjoyable one. Thanks are also due to Dr Parisa Monsef-Mirzai for her constructive criticisms and helpful suggestions throughout this work. I would like to acknowledge Dr Colin Snape of the University of Strathclyde for his help in supplying the phenolic resins and carrying out the carbon-13 analyses. I am also indebted to Riz and Johnny for keeping me amused with their eccentric humour, wit and observations during the course of this research, and finally I would like to express my thanks to my family for their support and encouragement during the course of this work.

LIST OF CONTENTS

Page

TITLE PAGE 1

SUMMARY 2

DEDICATION 3

ACKNOWLEDGEMENTS 4

LIST OF CONTENTS 5

LIST OF TABLES 10

LIST OF FIGURES 14

1. INTRODUCTION

1.1 GENERAL INTRODUCTION 26

1.2 SHORT HISTORY OF COAL 28

1.2.1 General History 28
1.2.2 Coal Reserves 28

1.3 GENESIS OF COAL 29

1.3.1 Background 29
1.3.2 The biochemical stage of coalification 29
1.3.3 The geochemical stage of coalification 30

1.4 CLASSIFICATION OF COAL 31

1.4.1 Coalification / Rank 31
1.4.2 Proximate analysis 33
1.4.3 Ultimate analysis 34
1.4.4 Heating / Calorific value 35

1.5 STRUCTURE OF COAL 36

1.5.1 General Introduction 36
1.5.2 Literature review 37
1.5.3 Mineral matter in coal 43

1.6 HETEROATOMS IN COAL 44

1.6.1 Nitrogen in coal 44
1.6.2 Sulphur in coal 44

1.7 OXYGEN IN COAL 46

1.7.1 General Introduction 46
1.7.2 Literature review 46
1.7.3 Why look at the O functionality ? 50

1.8 MICROWAVES IN CHEMICAL SYNTHESIS 53

1.8.1 General Introduction 53
1.8.2 What are microwaves ? 53
1.8.3 Microwave heating mechanisms 54
1.8.4 Literature review 57

2. EXPERIMENTAL

2.1 PHYSICAL METHODS 65

2.1.1 FT-IR Spectroscopy 65
2.1.2 NMR Spectroscopy 65
2.1.3 Gas Chromatography 65
2.1.4 X-ray photoelectron Spectroscopy (XPS) 65

2.2 MICROWAVE EQUIPMENT 67

2.2.1 Sharp Carousel II R-84801 67
2.2.2 Digestion vessels 67
2.2.3 MES-1000 microwave system 70
2.2.4 Microwave procedure 76

2.3 MODEL COMPOUNDS 78

2.4 DRYING OF COALS 80

2.5 SEPARATION OF COAL MACERALS 82

2.6 STANNYLATION PROCEDURE 84

2.6.1 Stannylation with tributyltin chloride 84
2.6.2 Stannylation with bis-tributyltin oxide (TBTO) 84

2.7 ACETYLATION PROCEDURE 87

2.7.1 Acetylation of coal - classical method 87
2.7.2 Acetylation of coal - microwave method 87

2.8 SILYLATION PROCEDURE 89

2.9 METHYLATION PROCEDURE 90

2.9.1 Method 1 - methyl iodide 90
2.9.2 Method 2 - methyl formate 90
2.9.3 Method 3 - phase-transfer 90

3. STANNYLATION

3.1 INTRODUCTION 91

3.2 EXPERIMENTAL 96

3.2.1 Testing of microwave-receptor solvents 96
3.2.2 Model compounds 97
3.2.3 Coals and coal macerals 97

3.3 RESULTS AND DISCUSSION 99

3.3.1 Selection of microwave-receptor solvents 99
3.3.2 Investigation into the distribution of microwave radiation in the microwave cavity 106
3.3.3 Stannylation of model compounds 108
3.3.4 Stannylation of coals 153
3.3.5 Stannylation of Creswell macerals 181
3.3.6 Stannylation of Cortonwood macerals 207

4. ACETYLATION

4.1 INTRODUCTION 237

4.1.1 General Introduction 237
4.1.2 Literature review 237
4.1.3 Coal macerals 240

4.2 EXPERIMENTAL 245

4.2.1 Separation of coal macerals 245
4.2.2 Scanning electron microscope (SEM) 245
4.2.3 Reflectance measurements 245
4.2.4 Acetylation of coals and coal macerals 249

4.3 RESULTS AND DISCUSSION 250

4.3.1 Separation of coal macerals 250
4.3.2 Acetylation of Creswell and Creswell macerals 274
4.3.3 Acetylation of Cortonwood and Cortonwood macerals 298
4.3.4 General conclusions 321

5. SILYLATION

5.1 INTRODUCTION 324

5.1.1 General Introduction 324
5.1.2 Literature review 324

5.2 EXPERIMENTAL 328

5.3 RESULTS AND DISCUSSION 330

5.3.1 Silylation of resins 330
5.3.2 Silylation of Creswell and Creswell macerals 356
5.3.3 Silylation of Cortonwood and Cortonwood macerals 384
5.3.4 General conclusions 409

6. METHYLATION

6.1 INTRODUCTION 416

6.1.1 General Introduction 416
6.1.2 Literature review 416

6.2 EXPERIMENTAL 422

6.2.1 Method 1 - methyl iodide 422
6.2.2 Method 2 - methyl formate 422
6.2.3 Method 3 - phase-transfer 422

6.3 RESULTS AND DISCUSSION 423

6.3.1 Methylation using methyl iodide 423
6.3.2 Methylation using methyl formate 435
6.3.3 Methylation via phase-transfer 447
6.3.4 General conclusions 453

7. CONCLUSIONS

7.1 CONCLUSIONS 455

7.2 FUTURE WORK 459

LIST OF REFERENCES..... 460

APPENDICES..... 470

Appendix I - FT-IR of model compounds..... 470
Appendix II - FT-IR of reagents..... 474
Appendix III - Calculations for % O in coals and coal macerals..... 480

LIST OF TABLES

		Page
Table 1.01	Classification of the different variety of coals by rank	31
Table 1.02	Analyses of Oxygen functionality in coals (wt% maf basis)	48
Table 1.03	Work done on Oxygen functionalities in coal 1963 - 1981	49
Table 1.04	Dielectric loss tangents (tand) for some common solvents	56
Table 1.05	A comparison of reaction times and yields in representative reactions using classical and microwave procedures	58
Table 1.06	The temperature of 50 cm^3 of several solvents after heating for 1 minute at 560 watts in an open vessel in a microwave oven	60
Table 1.07	Microwave heating of common solvents	61
Table 1.08	Microwave heating of solids	62
Table 1.09	The wt% of precursor intercalated using mechanical shaking and microwave methods	63
Table 3.01	^{119}Sn chemical shifts for TBTO derivatives for several phenols and selected thiols and alcohols	93
Table 3.02	Data on microwave-receptor solvents	99
Table 3.03	Selection of microwave solvents	100
Table 3.04	Temperature of water relative to its position on the microwave turntable	106
Table 3.05	Data for model compounds	112
Table 3.06	Stannylation of model compounds using reflux methods	129
Table 3.07	Stannylation of model compounds using microwave methods	129
Table 3.08	GC analyses of stannylated model compounds	137
Table 3.09	Chemical shifts for stannylated model compounds	151
Table 3.10	Analytical data for coals	154
Table 3.11	Absorption bands in the IR spectra of coal	157
Table 3.12	IR absorptions of organotin compounds	158
Table 3.13	Stannylation of the different particle sizes of Creswell coal	163
Table 3.14	Stannylation of Cortonwood, Gedling and Ollerton coals in the microwave oven	180
Table 3.15	IR analysis of the stannylated Creswell macerals	190

Table 3.16	XPS Results for the stannylated Creswell macerals	206
Table 3.17	IR analysis of the stannylated Cortonwood macerals	212
Table 4.01	The source materials of macerals	242
Table 4.02	General trends of the three maceral groups found in coals	244
Table 4.03	Yields from the density fractions of Creswell coal ≤32 μm	250
Table 4.04	Reflectance measurements for the Creswell coal and Creswell macerals	256
Table 4.05	Ultimate analysis for the Creswell coal macerals	256
Table 4.06	Proximate analysis for the Creswell coal macerals	257
Table 4.07	Calculation of Oxygen in the Creswell macerals on a dmmf basis	258
Table 4.08	Yields from the density fractions of Cortonwood coal ≤32 μm	259
Table 4.09	Reflectance measurements for the Cortonwood coal and Cortonwood macerals	265
Table 4.10	Ultimate analysis for the Cortonwood coal macerals	267
Table 4.11	Proximate analysis for the Cortonwood coal macerals	268
Table 4.12	Calculation of Oxygen in the Cortonwood macerals on a dmmf basis	269
Table 4.13	Yields from the density fractions of Kellingley coal ≤32 μm	270
Table 4.14	Yields from the density fractions of Gedling coal ≤32 μm	272
Table 4.15	Analytical data for the raw Creswell coal ≤32 μm	277
Table 4.16	Titration results for the Creswell coal macerals using the mw hydrolysis technique	278
Table 4.17	Titration results for the Creswell coal macerals using the reflux hydrolysis technique	280
Table 4.18	Comparison of total titration values obtained using the mw hydrolysis and reflux hydrolysis techniques for the Creswell macerals	283
Table 4.19	Titration values for the acetylation of the raw Creswell coal	284
Table 4.20	Calculation of the percentage O_{OH} / O_{total} for the Creswell coal and Creswell macerals	297
Table 4.21	Analytical data for the raw Cortonwood coal ≤32 μm	298
Table 4.22	Titration results for the Cortonwood coal macerals	302

Table 4.23 Calculation of the percentage O_{OH} / O_{total} for the Cortonwood.... 314
coal macerals

Table 4.24 MES-1000 reaction parameters for the acetylation of the..... 315
phenol-formaldehyde resin

Table 5.01 Results from the SPE / CP ^{13}C MASNMR analysis of the..... 349
silylated pure phenol-formaldehyde resin and the silylated
1 : 1 co-resite

Table 5.02 Calculation of the degree of silylation for the..... 354
phenol-formaldehyde resin and the (formerly) 1 : 1 co-resite

Table 5.03 MES-1000 reaction parameters for the silylation of the Creswell... 357
coal and Creswell macerals

Table 5.04 Summary of the IR results for the silylation of the Creswell coal... 369
and Creswell macerals

Table 5.05 Resonance peaks from the ^{29}Si MASNMR analysis of the..... 374
silylated Creswell coal and silylated Creswell macerals

Table 5.06 Integration values from ^{29}Si MASNMR for the silylated..... 374
Creswell coal and silylated Creswell macerals

Table 5.07 Results from the weighings of the silylated coal and laponite..... 376
standard peaks for the Creswell coal and Creswell macerals

Table 5.08 Integration values from the deconvoluted ^{29}Si MASNMR spectra. 380
for the silylated Creswell coal and Creswell macerals and the
laponite standards

Table 5.09 Results from the weighings (deconvolution method) of the..... 380
silylated coal and laponite standard peaks for the Creswell coal
and Creswell macerals

Table 5.10 Results for the % O (as phenolic -OH) from the silylation of the.... 382
Creswell coal and Creswell macerals

Table 5.11 The results for the % O_{OH} / O_{total} from the silylation of the..... 383
Creswell coal and Creswell macerals

Table 5.12 MES-1000 reaction parameters for the silylation of the..... 384
Cortonwood coal and Cortonwood macerals

Table 5.13 Summary of the IR results for the silylation of the Cortonwood..... 394
coal and Cortonwood macerals

Table 5.14 Resonance peaks from the ^{29}Si MASNMR analysis of the..... 399
silylated Cortonwood coal and silylated Cortonwood macerals

Table 5.15 Integration values from ^{29}Si MASNMR for the silylated..... 399
Cortonwood coal and silylated Cortonwood macerals

Table 5.16 Results from the weighings of the silylated coal and laponite..... 400
standard peaks for the Cortonwood coal and Cortonwood macerals

Table 5.17 Integration values from the deconvoluted ^{29}Si MASNMR spectra. 401
for the silylated Cortonwood coal and Cortonwood macerals and
the laponite standards

Table 5.18 Results from the weighings (deconvolution method) of the..... 406
silylated coal and laponite standard peaks for the Cortonwood
coal and Cortonwood macerals

Table 5.19 Results for the % O (as phenolic -OH) from the silylation of the.... 407
Cortonwood coal and Cortonwood macerals

Table 5.20 The results for the % O_{OH} / O_{total} from the silylation of the..... 408
Cortonwood coal and Cortonwood macerals

Table 5.21 Width-at-half-height from the ^{29}Si MASNMR spectra for the..... 413
silylated resins / coal products

Table 6.01 Methylation of model compounds using methyl formate..... 444

LIST OF FIGURES

		Page
Fig 1.01	Diagrammatic interpretation of the structure of coal.....	37
Fig 1.02	Hayatsu's 'rings'.....	39
Fig 1.03	Proposed structural elements of coal.....	39
Fig 1.04	Model structure for 80% vitrain.....	40
Fig 1.05	Model structure for 80% vitrain II.....	41
Fig 1.06	Shinn's retrograde synthesis used to derive his hypothetical coal.... model	42
Fig 1.07	Order of reactivity of the oxygen functionalities in coal.....	51
Fig 1.08	The position of microwaves in the electromagnetic spectrum.....	54
Fig 1.09	The effect of dielectric constant on the heating rate of various..... organic liquids	59
Fig 2.01	FTS-40A FT-IR Spectrometer.....	66
Fig 2.02	Digestion vessel assembly.....	69
Fig 2.03	MES-1000 microwave extraction system.....	70
Fig 2.04	Microwave reaction vessel for temperature and pressure control...	72
Fig 2.05	Schematic representation of the pressure control system.....	74
Fig 2.06	Schematic representation of the temperature control system.....	75
Fig 2.07	MES-1000 Reaction vessel linked up with temperature and..... pressure monitoring devices	77
Fig 2.08	Synthesis of phenol-formaldehyde resin.....	78
Fig 2.09	Di- and tri-substituted model compounds.....	79
Fig 2.10	Drying of coal and coal macerals.....	81
Fig 2.11	Rotary evaporation of derivatised coal.....	86
Fig 2.12	Filtration of derivatised coal.....	86
Fig 3.01	Reflux apparatus for the stannylation of coals and model..... compounds	98
Fig 3.02	IR spectra of the stannylated Creswell coal <500>212 μm using.... nitromethane, acetonitrile and nitromethane + toluene solvents	101
Fig 3.03	IR spectra of the stannylated Creswell coal <500>212 μm using.... acetonitrile, acetonitrile + nitromethane and acetonitrile + toluene	102

Fig 3.04 ^{119}Sn MASNMR spectrum of the stannylated Creswell coal..... 103
<500>212 μm using acetonitrile + nitromethane solvent

Fig 3.05 Variation in the temperature of 100 cm^3 water relative to its..... 107
starting position on the microwave turntable

Fig 3.06 IR spectra of 2,6-dimethylphenol after 15 mins stannylation with.. 109
Bu_3SnCl in the mw oven and the unreacted 2,6-dimethylphenol

Fig 3.07 IR spectra of 2,6-dimethylphenol after 15, 30, 45 and 60 mins..... 110
stannylation with Bu_3SnCl in the mw oven (4000 - 2000 cm^{-1})

Fig 3.08 IR spectra of 2,6-dimethylphenol after 15, 30, 45 and 60 mins..... 111
stannylation with Bu_3SnCl in the mw oven (2000 - 400 cm^{-1})

Fig 3.09 IR spectrum of 2,6-dimethylphenol after 4 days stannylation..... 114
via reflux with Bu_3SnCl and acetonitrile

Fig 3.10 IR spectra of 2,6-dimethylphenol after 4 days stannylation via..... 115
reflux with Bu_3SnCl and toluene and unreacted 2,6-dimethylphenol

Fig 3.11 IR spectrum of 2,6-dimethylphenol after 2 hrs stannylation..... 118
via reflux with TBTO and toluene

Fig 3.12 IR spectra of 2,6-diisopropylphenol after 2 hrs stannylation via..... 119
reflux with TBTO and toluene and unreacted 2,6-diisopropylphenol

Fig 3.13 IR spectrum of 2,6-diphenylphenol after 2 hrs stannylation via..... 120
reflux with TBTO and toluene

Fig 3.14 IR spectrum of 2-phenylphenol after 2 hrs stannylation via reflux.. 121
with TBTO and toluene

Fig 3.15 IR spectrum of 2,6-di-tert-butylphenol after 24 hrs stannylation..... 122
via reflux with TBTO and toluene

Fig 3.16 IR spectra of 2,6-di-tert-butylphenol after 72 hrs stannylation via.. 123
reflux with TBTO and toluene and unreacted 2,6-di-tert-butylphenol

Fig 3.17 IR spectra of 2,6-di-tert-butylphenol after 24 hrs stannylation via.. 124
ultrasound bath using TBTO and toluene and unreacted
2,6-di-tert-butylphenol

Fig 3.18 IR spectrum of the stannylated 2,6-dimethylphenol after 1 min..... 125
mw heating

Fig 3.19 IR spectrum of the stannylated 2,6-diisopropylphenol after..... 126
1 min mw heating

Fig 3.20 IR spectrum of the stannylated 2-phenylphenol after 1 min..... 127
mw heating

Fig 3.21 IR spectrum of the stannylated 2,6-diphenylphenol after 1 min..... 128
mw heating

Fig 3.22 GC plot of the stannylated 2,6-dimethylphenol compound (reflux method) 131

Fig 3.23 GC plot of the stannylated 2,6-dimethylphenol compound (microwave method) 132

Fig 3.24 GC plot of the stannylated 2,6-diisopropylphenol compound (reflux method) 133

Fig 3.25 GC plot of the stannylated 2,6-diisopropylphenol compound (microwave method) 134

Fig 3.26 GC plot of the stannylated 2,6-diphenylphenol compound (reflux method) 135

Fig 3.27 GC plot of the stannylated 2,6-diphenylphenol compound (microwave method) 136

Fig 3.28 ^{117}Sn nmr of TBTO 139

Fig 3.29 ^{119}Sn nmr of TBTO 140

Fig 3.30 ^{117}Sn nmr of the stannylated 2,6-dimethylphenol compound (reflux method) 141

Fig 3.31 ^{119}Sn nmr of the stannylated 2,6-dimethylphenol compound (reflux method) 142

Fig 3.32 ^{119}Sn nmr of the stannylated 2,6-dimethylphenol compound (microwave method) 143

Fig 3.33 ^{119}Sn nmr of the stannylated 2,6-diisopropylphenol compound (reflux method) 144

Fig 3.34 ^{119}Sn nmr of the stannylated 2,6-diisopropylphenol compound (microwave method) 145

Fig 3.35 ^{119}Sn nmr of the stannylated 2,6-diphenylphenol compound (reflux method) 146

Fig 3.36 ^{119}Sn nmr of the stannylated 2,6-diphenylphenol compound (microwave method) 147

Fig 3.37 ^{117}Sn nmr of the stannylated 2-phenylphenol compound (reflux method) 148

Fig 3.38 ^{119}Sn nmr of the stannylated 2-phenylphenol compound (reflux method) 149

Fig 3.39 ^{119}Sn nmr of the stannylated 2-phenylphenol compound (microwave method) 150

Fig 3.40 IR spectrum of the raw Creswell coal <500>212 µm 156

Fig 3.41 IR spectra of the stannylated Creswell coal <500>212 μm..... 159
after 5, 10 and 30 mins of mw heating

Fig 3.42 IR spectra of the stannylated Creswell coal <500>212 μm..... 160
after 24 hrs reflux

Fig 3.43 IR of the stannylated Creswell coal <212>90 μm after 5 mins..... 161
mw heating

Fig 3.44 IR of the stannylated Creswell coal <212>90 μm after 24 hrs..... 162
reflux in toluene

Fig 3.45 IR of the stannylated Creswell coal ≤90 μm after 5 mins..... 164
mw heating

Fig 3.46 IR of the stannylated Creswell coal ≤90 μm after 5, 45 and..... 165
75 and 120 mins mw heating

Fig 3.47 IR of the stannylated Creswell coal ≤90 μm after 24 hrs reflux..... 166
in toluene

Fig 3.48 ^{119}Sn MASNMR of the stannylated Creswell coal..... 168
<500>212 μm after 30 mins mw heating

Fig 3.49 ^{119}Sn MASNMR of the stannylated Creswell coal..... 169
<212>90 μm after 5 mins mw heating

Fig 3.50 ^{119}Sn MASNMR of the stannylated Creswell coal..... 170
<212>90 μm after 24 hrs reflux in toluene

Fig 3.51 ^{119}Sn MASNMR of the stannylated Creswell coal..... 171
≤90 μm after 120 mins mw heating

Fig 3.52 IR of the raw Cortonwood coal ≤212 μm..... 173

Fig 3.53 IR of the stannylated Cortonwood coal ≤212 μm after..... 174
5 mins and 60 mins mw heating

Fig 3.54 IR of the raw Gedling coal ≤212 μm..... 175

Fig 3.55 IR of the stannylated Gedling coal ≤212 μm after 5, 30 and..... 176
60 mins of mw heating

Fig 3.56 IR of the stannylated Gedling coal ≤212 μm after 60 mins..... 177
mw heating

Fig 3.57 IR of the stannylated Ollerton coal ≤212 μm after 60 mins..... 178
mw heating

Fig 3.58 IR of the stannylated Ollerton coal ≤212 μm after 5 mins..... 179
and 120 mins mw heating

Fig 3.59a IR of the Creswell ≤32 μm exinite maceral..... 182

Fig 3.59b IR of the Creswell ≤32 μm vitrinite maceral..... 183

Fig 3.59c IR of the Creswell ≤32 μm inertinite maceral..... 184

Fig 3.60 IR comparison of the Creswell ≤32 μm macerals..... 185

Fig 3.61 IR of the stannylated Creswell ≤32 μm exinite after 60 mins..... 186
mw heating

Fig 3.62 IR of the stannylated Creswell ≤32 μm vitrinite after 60 mins..... 187
mw heating

Fig 3.63 IR of the stannylated Creswell ≤32 μm inertinite after 60 mins..... 188
mw heating

Fig 3.64 IR comparison of the stannylated Creswell ≤32 μm macerals..... 189

Fig 3.65 IR comparison of 24 hr soxhlet-extracted stannylated Creswell..... 191
≤32 μm vitrinite and the normal stannylated Creswell ≤32 μm
vitrinite maceral

Fig 3.66 IR comparison of solution obtained from stannylated..... 192
Creswell ≤32 μm soxhlet-extraction and toluene

Fig 3.67a ^{13}C CP MASNMR of the Creswell ≤32 μm exinite maceral..... 194

Fig 3.67b ^{13}C CP MASNMR of the Creswell ≤32 μm vitrinite maceral..... 195

Fig 3.67c ^{13}C CP MASNMR of the Creswell ≤32 μm inertinite maceral..... 196

Fig 3.68 ^{119}Sn MASNMR of the TBTO reagent..... 197

Fig 3.69a ^{119}Sn CP MASNMR of the stannylated Creswell ≤32 μm..... 198
exinite maceral

Fig 3.69b ^{119}Sn CP MASNMR of the stannylated Creswell ≤32 μm..... 199
vitrinite maceral

Fig 3.69c ^{119}Sn CP MASNMR of the stannylated Creswell ≤32 μm..... 200
inertinite maceral

Fig 3.70a XPS of the stannylated Creswell ≤32 μm exinite maceral..... 202

Fig 3.70b XPS of the stannylated Creswell ≤32 μm exinite maceral II..... 203

Fig 3.71 XPS of the stannylated Creswell ≤32 μm vitrinite maceral..... 204

Fig 3.72 XPS of the stannylated Creswell ≤32 μm inertinite maceral..... 205

Fig 3.73a IR of the Cortonwood ≤32 μm exinite maceral..... 208

Fig 3.73b IR of the Cortonwood ≤32 μm vitrinite maceral..... 209

Fig 3.73c IR of the Cortonwood ≤32 μm inertinite maceral..... 210

Fig 3.74 IR comparison of the Cortonwood ≤32 μm macerals..... 211

Fig 3.75	IR of the stannylated Cortonwood ≤32 μm exinite after 60 mins mw heating	213
Fig 3.76	IR of the stannylated Cortonwood ≤32 μm vitrinite after 60 mins mw heating	214
Fig 3.77	IR of the stannylated Cortonwood ≤32 μm inertinite after 60 mins mw heating	215
Fig 3.78a	^{13}C CP MASNMR of the Cortonwood ≤32 μm exinite maceral	217
Fig 3.78b	^{13}C CP MASNMR of the Cortonwood ≤32 μm vitrinite maceral	218
Fig 3.78c	^{13}C CP MASNMR of the Cortonwood ≤32 μm inertinite maceral	219
Fig 3.79a	^{119}Sn CP MASNMR of the stannylated Cortonwood ≤32 μm exinite	220
Fig 3.79b	^{119}Sn CP MASNMR of the stannylated Cortonwood ≤32 μm vitrinite	221
Fig 3.79c	^{119}Sn CP MASNMR of the stannylated Cortonwood ≤32 μm inertinite	222
Fig 4.01	Schematic representation of the apparatus used for coal reflectance measurements	246
Fig 4.02	Optical parts of a typical reflectance measuring microscope	248
Fig 4.03	Reflectance histogram of the raw Creswell coal	252
Fig 4.04	Reflectance histogram of the Creswell exinite maceral	253
Fig 4.05	Reflectance histogram of the Creswell vitrinite maceral	254
Fig 4.06	Reflectance histogram of the Creswell inertinite maceral	255
Fig 4.07	Reflectance histogram of the raw Cortonwood coal	261
Fig 4.08	Reflectance histogram of the Cortonwood exinite maceral	262
Fig 4.09	Reflectance histogram of the Cortonwood vitrinite maceral	263
Fig 4.10	Reflectance histogram of the Cortonwood inertinite maceral	264
Fig 4.11	Photograph of raw Cortonwood coal (x437 magnification)	265
Fig 4.12	Photograph of the Cortonwood vitrinite maceral fraction (x437 magnification)	266
Fig 4.13	Photograph of the Cortonwood inertinite maceral fraction (x437 magnification)	267
Fig 4.14	SEM micrograph of raw Kellingley coal	271
Fig 4.15	SEM micrograph of a single particle of Kellingley coal	271

Fig 4.16 Photograph showing the bimacerites and trimacerites in..... 273
Gedling raw coal

Fig 4.17 Photograph showing the bimacerites and trimacerites in the..... 273
Gedling vitrinite fraction

Fig 4.18 Plot of the titration of liberated acetic acid with 0.1015N NaOH.... 281
for the Creswell exinite maceral

Fig 4.19 Plot of the titration of liberated acetic acid with 0.1015N NaOH.... 281
for the Creswell vitrinite maceral

Fig 4.20 Plot of the titration of liberated acetic acid with 0.1015N NaOH.... 282
for the Creswell inertinite maceral

Fig 4.21 Plot of the titration of liberated acetic acid with 0.1015N NaOH.... 285
for the raw Creswell coal

Fig 4.22 IR of the raw Creswell coal..... 286

Fig 4.23 IR of the acetylated raw Creswell coal..... 287

Fig 4.24 IR comparison of the unreacted and stannylated raw..... 288
Creswell coal

Fig 4.25 IR of the acetylated Creswell exinite maceral..... 290

Fig 4.26 IR comparison of Creswell exinite and the Creswell..... 291
exinite after acetylation and hydrolysis

Fig 4.27 IR of the acetylated Creswell vitrinite maceral..... 292

Fig 4.28 IR of the acetylated Creswell inertinite maceral..... 293

Fig 4.29 IR comparison of the Creswell inertinite and the..... 294
Creswell inertinite after acetylation and hydrolysis

Fig 4.30 IR of the acetylated Creswell macerals and the acetylated raw..... 295
Creswell coal

Fig 4.31 IR of the Creswell macerals after acetylation and hydrolysis and... 296
the raw Creswell coal

Fig 4.32 Plot of the titration of liberated acetic acid with 0.1015N NaOH.... 299
for the Cortonwood exinite maceral

Fig 4.33 Plot of the titration of liberated acetic acid with 0.1015N NaOH.... 300
for the Cortonwood vitrinite maceral

Fig 4.34 Plot of the titration of liberated acetic acid with 0.1015N NaOH.... 301
for the Cortonwood inertinite maceral

Fig 4.35 IR of the raw Cortonwood coal..... 304

Fig 4.36 IR of the acetylated raw Cortonwood coal..... 305

Fig 4.37 IR comparison of the raw Cortonwood coal and the acetylated..... 306
Cortonwood coal

Fig 4.38 IR of the acetylated raw Cortonwood coal after 2 hrs and 3 hrs..... 307
mw heating

Fig 4.39 IR of the acetylated raw Cortonwood coal using the MES-1000..... 308
mw oven

Fig 4.40 IR of the acetylated Cortonwood exinite maceral..... 310

Fig 4.41 IR of the acetylated Cortonwood vitrinite maceral..... 311

Fig 4.42 IR of the acetylated Cortonwood inertinite maceral..... 312

Fig 4.43 IR comparison of the acetylated Cortonwood macerals and the..... 313
acetylated raw Cortonwood coal

Fig 4.44 Temperature and pressure profile (for the first 30 mins) for the..... 316
acetylation of the phenol-formaldehyde resin

Fig 4.45 IR of the phenol-formaldehyde resin..... 317

Fig 4.46 IR of the acetylated phenol-formaldehyde resin after 4 hrs..... 318
mw heating

Fig 4.47 IR comparison of the phenol-formaldehyde resin and the..... 319
acetylated phenol-formaldehyde resin

Fig 4.48 IR of the phenol-formaldehyde resin after acetylation and..... 320
hydrolysis

Fig 5.01 Zirconium dioxide rotor used for quantitative ^{29}Si MASNMR..... 329
measurements

Fig 5.02 IR of phenol-formaldehyde resin..... 331

Fig 5.03 IR of silylated phenol-formaldehyde resin after 1 hr and 2 hrs..... 332
mw heating

Fig 5.04 IR of silylated phenol-formaldehyde resin after 2 hrs mw heating.. 333

Fig 5.05 IR comparison of the silylated phenol-formaldehyde resin and..... 334
the unreacted phenol-formaldehyde resin

Fig 5.06 IR of the 1:1 co-resite..... 335

Fig 5.07 IR of the silylated 1:1 co-resite after 1 hr and 2 hrs mw heating..... 336

Fig 5.08 IR of the silylated 1:1 co-resite after 2 hrs mw heating..... 338

Fig 5.09 IR of the 3:1 co-resite..... 339

Fig 5.10 Multispectral IR display of the phenol-formaldehyde resin and..... 340
the 1:1 and 3:1 co-resites

Fig 5.11 IR of the silylated 3:1 co-resite after 1 hr and 2 hrs mw heating..... 341

Fig 5.12 IR of the silylated 3:1 co-resite after 2 hrs mw heating..... 342

Fig 5.13 IR comparison of the silylated 3:1 co-resite and the..... 343
unreacted 3:1 co-resite

Fig 5.14 Qualitative ^{29}Si CP MASNMR of the silylated..... 344
phenol-formaldehyde resin (2 hrs mw heating)

Fig 5.15 Qualitative ^{29}Si CP MASNMR of the silylated 1:1 co-resite..... 345
(2 hrs mw heating)

Fig 5.16 Quantitative ^{29}Si CP MASNMR of the silylated 3:1 co-resite..... 346
(2 hrs mw heating)

Fig 5.17a ^{13}C SPE MASNMR of the silylated phenol-formaldehyde resin.... 350
(1 hr mw heating)

Fig 5.17b ^{13}C CP MASNMR of the silylated phenol-formaldehyde resin..... 351
(1 hr mw heating)

Fig 5.18a ^{13}C SPE MASNMR of the silylated 1:1 co-resite..... 352
(1 hr mw heating)

Fig 5.18b ^{13}C CP MASNMR of the silylated 1:1 co-resite..... 353
(1 hr mw heating)

Fig 5.19 Temperature / pressure profile for the silylated raw..... 358
Creswell coal

Fig 5.20 Temperature / pressure profile for the silylated Creswell..... 358
exinite maceral

Fig 5.21 Temperature / pressure profile for the silylated Creswell..... 359
vitrinite maceral

Fig 5.22 Temperature / pressure profile for the silylated Creswell..... 360
inertinite maceral

Fig 5.23 IR of the silylated raw Creswell coal (4 hrs mw heating)..... 362

Fig 5.24 IR comparison of the silylated raw Creswell coal and the..... 363
unreacted raw Creswell coal

Fig 5.25 IR of the silylated Creswell exinite maceral..... 364

Fig 5.26 IR of the silylated Creswell vitrinite maceral..... 365

Fig 5.27 IR of the silylated Creswell inertinite maceral..... 366

Fig 5.28 IR comparison of the silylated Creswell inertinite and the..... 367
unreacted Creswell inertinite

Fig 5.29 IR comparison of the silylated Creswell macerals..... 368

Fig 5.30 Quantitative ^{29}Si MASNMR of the silylated raw Creswell coal.... 370

Fig 5.31 Quantitative ^{29}Si MASNMR of the silylated Creswell..... 371
exinite maceral

Fig 5.32 Quantitative ^{29}Si MASNMR of the silylated Creswell..... 372
vitrinite maceral

Fig 5.33 Quantitative ^{29}Si MASNMR of the silylated Creswell..... 373
inertinite maceral

Fig 5.34 Deconvoluted ^{29}Si MASNMR spectrum for the silylated..... 377
raw Creswell coal

Fig 5.35 Deconvoluted ^{29}Si MASNMR spectrum for the silylated..... 378
Creswell exinite maceral

Fig 5.36 Deconvoluted ^{29}Si MASNMR spectrum for the silylated..... 379
Creswell vitrinite maceral

Fig 5.37 Temperature / pressure profile for the silylated raw..... 385
Cortonwood coal

Fig 5.38 Temperature / pressure profile for the silylated..... 385
Cortonwood exinite maceral

Fig 5.39 Temperature / pressure profile for the silylated..... 386
Cortonwood vitrinite maceral

Fig 5.40 Temperature / pressure profile for the silylated..... 386
Cortonwood inertinite maceral

Fig 5.41 IR of the silylated raw Cortonwood coal (4 hrs mw heating)..... 388

Fig 5.42 IR comparison of the silylated raw Cortonwood coal and..... 389
the unreacted raw Cortonwood coal

Fig 5.43 IR of the silylated Cortonwood exinite maceral..... 390

Fig 5.44 IR of the silylated Cortonwood vitrinite maceral..... 391

Fig 5.45 IR of the silylated Cortonwood inertinite maceral..... 392

Fig 5.46 IR comparison of the silylated Cortonwood macerals..... 393

Fig 5.47 Quantitative ^{29}Si MASNMR of the silylated raw Cortonwood..... 395
coal

Fig 5.48 Quantitative ^{29}Si MASNMR of the silylated Cortonwood..... 396
exinite maceral

Fig 5.49 Quantitative ^{29}Si MASNMR of the silylated Cortonwood..... 397
vitrinite maceral

Fig 5.50 Quantitative ^{29}Si MASNMR of the silylated Cortonwood..... 398
inertinite maceral

Fig 5.51 Deconvoluted ^{29}Si MASNMR spectrum for the silylated raw..... 402
Cortonwood coal

Fig 5.52 Deconvoluted ^{29}Si MASNMR spectrum for the silylated..... 403
Cortonwood exinite maceral

Fig 5.53 Deconvoluted ^{29}Si MASNMR spectrum for the silylated..... 404
Cortonwood vitrinite maceral

Fig 5.54 Deconvoluted ^{29}Si MASNMR spectrum for the silylated..... 405
Cortonwood inertinite maceral

Fig 6.01 IR of the methylated 2,6-dimethylphenol product..... 424
(methyl iodide method)

Fig 6.02 IR of the methylated 2,6-dimethylphenol product and the..... 426
unreacted 2,6-dimethylphenol (methyl iodide method)

Fig 6.03 IR of Iodomethane..... 427

Fig 6.04 IR of Iodomethane and the methylated 2,6-dimethylphenol..... 428
product (methyl iodide method)

Fig 6.05 IR of the methylated 2,6-dimethylphenol product using..... 429
dried CH_3I (methyl iodide method)

Fig 6.06 IR of the methylated 2,6-dimethylphenol product using..... 430
dried CH_3I and normal CH_3I (methyl iodide method)

Fig 6.07 IR of the new batch of Iodomethane..... 431

Fig 6.08 IR comparison between the impure and new batch of..... 432
Iodomethane

Fig 6.09 IR of methylated 2,6-dimethylphenol product using the..... 433
new batch of CH_3I (methyl iodide method)

Fig 6.10 IR of the ppt obtained from the methylation of..... 434
2,6-dimethylphenol using the new batch of CH_3I
(methyl iodide method)

Fig 6.11 IR of the methylated 2,6-dimethylphenol product..... 437
(methyl formate method)

Fig 6.12 IR of the methylated 2,6-diisopropylphenol product..... 438
(methyl formate method)

Fig 6.13 IR of the methylated 2,6-di-tert-butylphenol product..... 439
(methyl formate method)

Fig 6.14 IR of the methylated 2,6-diphenylphenol product..... 440
(methyl formate method)

Fig 6.15 IR of the methylated 2-phenylphenol product..... 441
(methyl formate method)

Fig 6.16 IR of the methylated 2,4,6-tri-tert-butylphenol product..... 442
(methyl formate method)

Fig 6.17 IR of the methylated 2,4,6-tri-tert-butylphenol product and..... 443
CTAB (methyl formate method)

Fig 6.18 IR of the methylated 2,6-dimethylphenol product after..... 445
30 mins and 120 mins mw heating (methyl formate method)

Fig 6.19 IR of the methylated 2,6-dimethylphenol product after..... 446
6 hrs mw heating (methyl formate method)

Fig 6.20 IR of the methylated 2,6-dimethylphenol product after..... 448
24 hrs reflux (methyl formate method)

Fig 6.21 IR of the methylated 2,6-dimethylphenol product after..... 449
48 hrs reflux (methyl formate method)

Fig 6.22 Methylation via phase-transfer..... 447

Fig 6.23 IR of methylated 2,6-dimethylphenol (phase-transfer method)..... 451

Fig 6.24 IR comparison of methylated 2,6-dimethylphenol and..... 452
unreacted 2,6-dimethylphenol (phase-transfer method)

INTRODUCTION

1.1 GENERAL INTRODUCTION

Our way of life and very existence depends on the convenient and efficient utilisation of accessible energy. In today's prevailing climate the world's primary source of energy is fossil fuel - petroleum, natural gas and coal. This source of energy is converted into electricity, fuel and heat, which is employed in a range of diverse applications and processes. Perhaps the greatest disadvantage of fossil fuel is that it is an exhaustible commodity. Because of this drawback, one of two actions should be implemented in the near future; the first of these is to find a viable alternative means of mass power generation - solar power, hydropower, nuclear power and power from renewable biomass are some options. But in most cases a major scaling-up of the process is required if the increasing energy demands of the future are to be met. The second course of action involves the implementation of existing methods, especially those involving the more abundant fossil fuels - most prominently coal, on a more efficient, economical and environmentally-acceptable level (although coal is already considered to be a relatively clean fuel).

In the early 1970s, the Organisation of Petroleum Exporting Countries OPEC imposed an oil embargo - this caused the price of crude oil to spiral upwards, resulting in the cost of crude oil quadrupling almost overnight. This shock to the world economy outlined the dangers of relying on a predominantly imported energy source. All of a sudden there was a renewed interest in coal and coal research, which had been fairly inactive since the early 1960s. Research into coal now took on a new impetus. The sharp drop in crude oil prices in the mid-1980s, however, helped to check this momentum and succeeded in turning the focus back to oil. But the alternative use of coal, instead of oil, is expected in the future for several reasons, some of which are outlined below :

1) The large reserves of coal world-wide will ensure that coal remains a crucially important energy source.

2) The disadvantage of relying on fossil fuel imported from politically volatile territories of the world (as exhibited by the Gulf War 1990-1991).

3) The 'lost faith' in alternative sources of energy, such as nuclear power (as exhibited by the Chernobyl nuclear reactor meltdown 1986) and the dependence of other forms of energy on weather conditions (solar power and wind-generated power) and local geography (hydropower).

4) The expansion of new markets, particularly in the Third World.

5) Improved technology becoming available for more efficient coal combustion and transformation of coal to synthetic fuel or desired chemicals.

More than 1 billion tons of coal are burned every year and it supplies about 30% of the world's energy requirements (down from 60% in 1950). The value of coal may be illustrated by its diverse applications to contemporary industry - electricity, transportation fuels, manufacture of chemicals (plastics, medicines, fertilisers, etc), providing chemicals for extracting metals from their ore and providing process heat i.e heat used for boiling, melting, annealing, etc in the metal and chemical industry.

Research into coal is an important requisite to avoid shortcomings in the future and must continue, so that the required technology is available when it is needed, to re-establish the energy gulf which will be left when oil and gas reserves are depleted. For these reasons it is vital to gain a comprehensive insight into the composition and physical nature of coal.

1.2 SHORT HISTORY OF COAL

1.2.1 General history

Essentially carbon is little more than a trace element in the earth's crust and yet it is our greatest source of energy. The majority of this attainable carbon is in the form of fossil fuels.

Historically, coal was used as a source of heat as early as AD300. By AD1000 it was being used on a large scale by the Chinese and it was the Venetian traveller Marco Polo who brought knowledge of coal to the western world in 1295. Sea coals and other surface coals burned with a very smoky flame due to their inorganic matter and consequently coal developed a reputation as being a dirty fuel. Large scale coal mining began in Britain in the mid-16th century. By the 17th century there was a severe shortage of wood, and coal soon became a primary fuel. Also, as charcoal became scarcer a substitute was required for iron-ore smelting - this came in the form of coke from coal. It was the large scale production of this inexpensive iron that gave impetus to the Industrial Revolution. The world production in coal increased by 500% in the 50 years following 1865. In the 20th century the consumption of coal was the same in 1970 as it was in 1912[1]. There was increased production during the war years followed by a slump in favour of oil and natural gas in the 1950s. In the 1970s coal production increased because of the oil price shocks. The revival, however, faded in the mid-1980s with the advent of price cuts in the oil industry.

Though the future is constantly changing and unpredictable, one thing is almost certain - coal will continue to play an active and participating role in energy conversion for the foreseeable future.

1.2.2 Coal Reserves

From known coal deposits, estimates of coal reserves are calculated to be in the region of 1.5 x 10^{12} tonnes world-wide. However, if the coal which is inferred to exist from geological observations is also taken into account this figure is propelled upwards to 12 x 10^{12} tonnes world-wide[2]. The vast majority of this coal is located in the Soviet Union (approximately 7 x 10^{12} tonnes - 90% of which can be found in Siberia), followed by the United States (approximately 3 x 10^{12} tonnes) and China - these are the 3 main areas of coal deposits. Canada, West Germany, Australia and Great Britain have lesser amounts.

1.3 GENESIS OF COAL

1.3.1 Background

Coal is a fossil formed by the action of temperature, time and pressure on plant debris. It consists mainly of the elements C and H with lesser amounts of O, S and N, and has associated with it various amounts of moisture and mineral deposits.

The origins of coal can be traced back to approximately 300 - 400 million years ago, when warm and humid climates favoured the growth of huge tropical ferns and giant trees in vast swamps. The dead plants fell into the boggy waters and through land subsidence and other changes in the local water regime, the debris was inundated and gradually covered by silts. These silts were then buried under increasingly thick inorganic sediments and were progressively compacted and chemically altered by heat to produce coal. There are 2 stages of coal formation:

1.3.2 The biochemical stage of coalification

When a plant dies in an arid environment, decomposition sets in almost immediately converting the plant to carbon dioxide and water (with lesser amounts of ammonia and sulfur) until nothing remains but the inorganic constituents of the plant. With this process atmospheric oxygen acts as the main agent initiating decay. If, however, the plant dies in water, the main agent initiating decay is anaerobic bacteria. This decaying process when the plant is in the water, involves decomposition of the plant tissue by removing oxygen and hydrogen via carbon dioxide and methane (marsh gas) respectively, and as water. In this instance much more O and H are lost in comparison with the amount of C lost - consequently a carbon-rich residue is built up. Decomposition is terminated when the intermediate decomposition product's (organic acids and phenols) concentrations have built up to such levels that they are lethal to the bacteria. A cycle of swamp formation and destruction by flooding or eventual drying out follows, resulting in the deposition of a series of coal seams separated by other inorganic sediment. As more plant debris amasses, the material at the bottom becomes increasingly compressed and this compressed plant material and residual organic debris (along with sulfur and inorganic entities) is called "peat". This process is called "peatification" and its formation signals the end of the biochemical stage of coalification. Peat may contain 30 - 35% O, about 60% C (on a dry, ash-free basis - daf basis) and up to 90% moisture.

In summary, the biochemical stage of coalification consists of the decomposition of the plant material by bacteria and fungi in a waterlogged environment, to eventually give rise to the formation of peat. This process usually takes a few thousand years.

An important point to note at this stage, is that not all the plant material decomposes at the same rate - this gives rise to the discrete remains of different types of plant material, which may be distinguished microscopically. These remains are called "macerals" and the study of these macerals is known as "petrology" (the analysis of these macerals is known as petrographic analysis). Macerals are covered in greater depth in chapter 4.

1.3.3 The geochemical stage of coalification

This stage took millions of years, during which the peat was slowly transformed, via changes in temperature and pressure, into coal. The geochemical stage starts with the deposition of layers of new sediment building up on the peat. As the layers accumulate, the pressure compacts the peat and buries it deeper into the earth. Consequently the peat is exposed to elevated temperatures and the combined effect of temperature and pressure transforms the peat into brown coal and lignite - these materials contain recognisable plant fragments and partially coalified material. Moisture contents for brown coals are in the region of 60 - 70%, whereas for lignites they are 30 - 40%. Lignites also contain approximately 70% C (daf basis) and approximately 20 - 25% O. The next materials to form under the continual changes in temperature and pressure over thousands of years are bituminous coals - these have significantly more carbon (up to 88%) and less oxygen compared to lignite (their precursor). Anthracite is the highest rank of coal and geologically the oldest. Formation involved tremendous pressures during which rocks themselves folded and buckled. Anthracite is approximately 94% C and no traces of the original plant material is discernible in this form of coal.

The main factors affecting the degree of coalification appear to be temperature, and to a lesser extent, pressure and time. Generally the youngest coals appear near the surface and the oldest are deepest from the surface. Because the temperature of rock strata increases as you get nearer to the earth's core, the oldest coals have usually been subjected to the highest temperatures and therefore the greatest chemical change.

1.4 CLASSIFICATION OF COAL

1.4.1 Coalification / Rank

Coalification or rank indicates the extent of geological maturity of the coal. It is the name given to the development of the series of substances peat, brown coal and lignite (brown coal is less mature), sub-bituminous, bituminous (this is sub-divided on the basis of volatile matter into low-, middle- and high volatile bituminous coal)* and anthracite, with graphite (pure carbon) being the final maturation product of coal. It should be noted that peat and lignite are comparatively rare in the UK.

The combination of pressure and time during the geochemical coalification stage progressively eliminated the H and O through water, methane and carbon dioxide. Consequently the C content increased and the H and O content decreased as coalification proceeded. The O content dropped sharply in going from lignite to bituminous coal, but the H content was preserved. A significant reduction in H does occur, however, on formation of anthracite. Increased temperature or prolonged exposure to heat during the geochemical stage resulted in increased coalification or rank.

Table 1.01 Classification of the different variety of coals by rank

Type of Coal	Approx. composition. wt%		
	C	H	O
WOOD	49	7	44
PEAT	60	6	34
LIGNITE	70	5	25
SUBBITUMINOUS	75	5	20
BITUMINOUS	85	5	10
ANTHRACITE	94	3	03

In going from wood to anthracite, pressure, temperature and time are increasing and there is increasing aromaticity.

*The volatile matter content is the % loss in weight when a sample of crushed coal is heated to 900°C, under standard conditions, with allowances being made for moisture and mineral matter content. It decreases with increasing coal rank from about 40% in lower rank coals to about 5% in higher rank coals.

Brown coal and lignite have very high moisture and volatile matter contents. They ignite easily, have a low calorific value and burn with a smoky flame. Plant remains, such as spores and pollen, may be observed in lignite deposits. Sub-bituminous coals (sometimes called black lignite) are also easily ignited, but these burn with a cleaner flame compared to lignites. The main attraction of sub-bituminous coals is that they have a very low sulfur content. Bituminous coals are used the most extensively - they tend to have low moisture and volatile matter contents and their heating value is generally higher than sub-bituminous coal. Finally, anthracite has very low moisture, sulfur and volatile matter content and burns with a clean, hot, smokeless flame. It is jet black, has a high lustre and is more expensive than other forms of coal.

Generally as rank increases the reactivity, moisture and volatile matter content decrease. The coals also become blacker and harder, more stable and burn more efficiently with a cleaner flame (containing less smoke and soot). Low rank coal is typically 79% C, middle rank 88% C and high rank 94% C.

1.4.2 Proximate Analysis

The proximate analysis determines the amount of moisture, volatile matter and ash in a sample of coal, and from these determinations a value for the amount of fixed carbon is calculated.

The procedure for determination is as follows; firstly a sample of the coal is heated gently to 105°C to remove the water - the % loss in weight gives the % moisture in the coal. After removal of the moisture, the temperature is increased and the sample is heated in an inert atmosphere (to prevent the coal burning) at 900 ± 5°C for 7 minutes, which results in a further weight loss due to a mixture of gases (including CO_2 and CH_4) escaping and the condensation of an oily liquid and a tar. Collectively these three components are known as the volatile matter. The solid material left behind after the volatile matter has been driven off is a black char with a semblance to charcoal. When air is allowed into the apparatus this char burns to leave behind an inorganic solid called ash (ash is composed mainly of Al, Ca, Fe, Mg, P, K, Si, Na, S and Ti - all combined with oxygen). The amount of coal material in the char is called the fixed carbon (it is called 'fixed' carbon because it does not volatilise) and the value for fixed carbon is calculated by :

100 - (moisture + volatile matter + ash)%

The only fuel components of the coal are the volatile matter and the fixed carbon. Moisture and ash are unreactive components which hinder heat generation. Ash is also an unwanted by-product which must be removed from the combustor and disposed off. The ratio of volatile matter : fixed carbon can help to predict how the coal will combust - the volatile matter will vaporise and burn with a long smoky flame, whereas fixed carbon will burn with a short, smokeless, hot flame.

The volatile matter, ash and fixed carbon are reported on a moisture-free basis, because moisture can be influenced by falling rain, humidity in the air and coal standing in an arid environment. Volatile matter and fixed carbon may also be reported on a dry, ash-free (daf) basis by multiplying by 100 / 100 - (moisture + ash).

1.4.3 Ultimate Analysis

The ultimate analysis gives an indication of the elemental composition of the coal with respect to C, H, N and S. From these values the %O is calculated by difference.

The C and H are determined by burning the coal and collecting the CO_2 and H_2O given off in absorbents, which have been weighed beforehand. The mass of CO_2 and H_2O is determined and from this the mass, and hence %C and %H in the original sample is calculated.

A common method for S determination is to convert the S into sodium sulphate and then to convert this further into barium sulphate, which is highly insoluble in water. The barium sulphate can subsequently be collected, dried and its mass determined to find out how much S was originally present. This method does not distinguish between the different types of S.

Nitrogen is usually determined by conversion to ammonia, followed by addition to a known amount of acid. The amount of acid remaining after neutralisation of the ammonia is calculated and from this the amount of ammonia, and hence original N in the coal, is calculated.

The %O content is determined by difference :

$$\%O = 100 - (C + H + N + S)\%$$

Coal has been shown to contain nearly all the elements, except noble gases and radioactive elements, in trace amounts.

1.4.4 Heating / Calorific value

This is the amount of energy obtained from heating a sample of coal. A known quantity is burned inside a reaction vessel, which is then immersed in a known quantity of water - this results in the temperature of the surrounding water being raised. Because the amount of heat required to raise the temperature of a given mass of water by 1°F is known (the specific heat capacity of water), the heating value for the coal may be calculated. The unit of measurement is usually the British thermal unit - this is the heat required to raise the temperature of 1 lb of water by 1°F. Values for coal vary from between 6000 to over 14000 Btu/lb. Oil has a value of approximately 20 000 Btu/lb and natural gas about 22 000 Btu/lb.

1.5 STRUCTURE OF COAL

1.5.1 General Introduction

Physically and chemically coal is a heterogeneous material consisting of two classes of material :

(a) Organic carbonaceous macerals, which can be sub-divided into 3 maceral groups - exinite / liptinite, vitrinite and inertinite.
(b) Inorganic crystalline minerals.

Coal has a complex, statistical, non-uniform structure made up of small condensed aromatic units, or layers, with functional groups located mainly at the peripheral edges, and some degree of cross-linking and hydrogen-bonding. It consists predominantly of C and H with lesser amounts of O, N and S and other trace elements. Because the units are pseudo-planar (not strictly planar due the presence of heteroatoms) they show some tendency to pack in a parallel orientation to each other. The lower rank coals tend to have small layers randomly orientated and connected by cross-links making the structure highly porous, whereas the middle rank coals show a greater degree of orientation and a greater tendency towards parallel stacking. In this case there are less cross-links and fewer pores. Finally, higher rank coals tend to show a growth in individual layers and there is a significant increase in the degree of orientation - the pores in higher rank coal are usually elongated parallel to the stacks of layers.

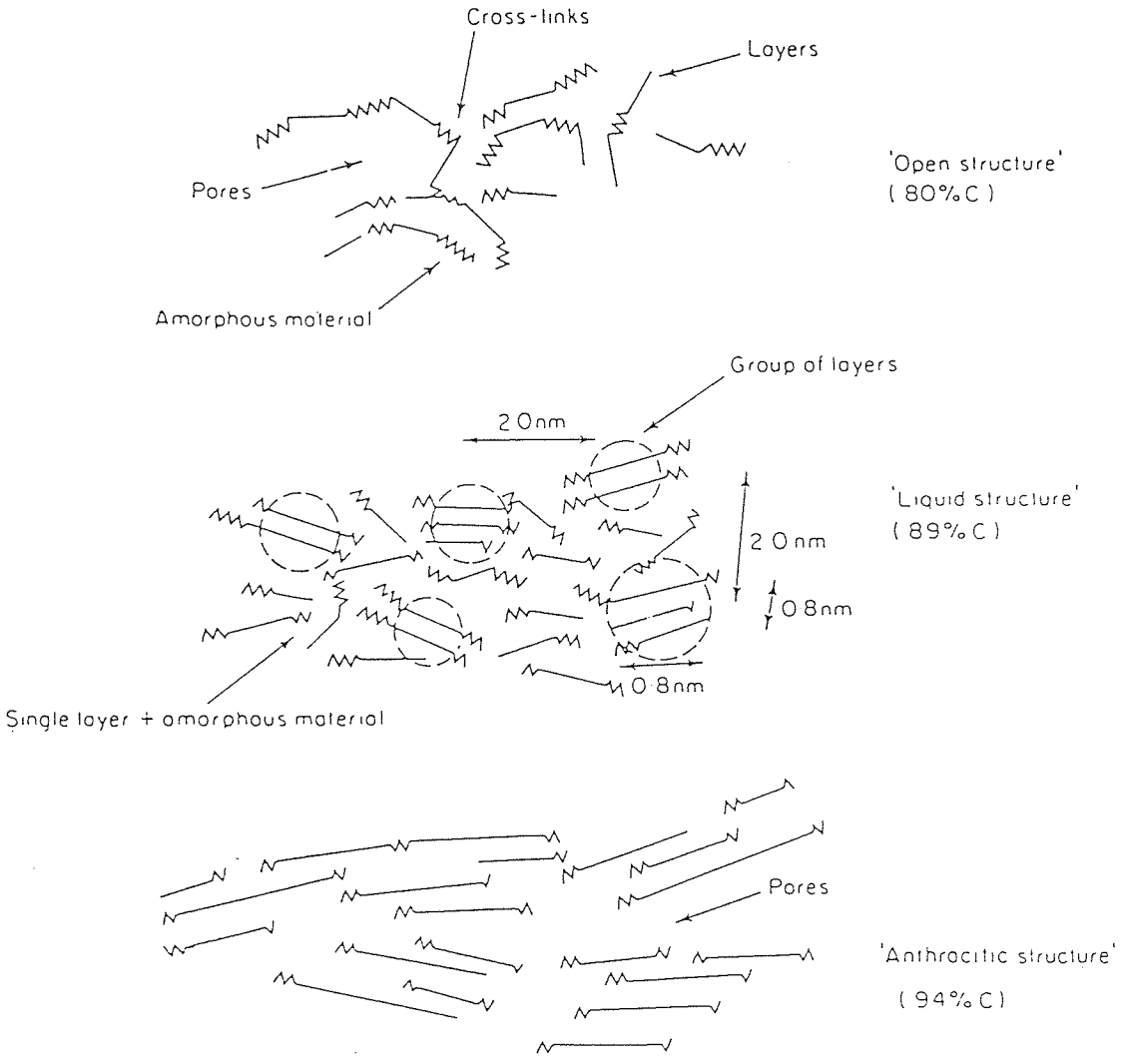

Fig1.01

Diagrammatic interpretation of the structure of coal (Hirsch 1954)[3]

1.5.2 Literature review

It is generally agreed that the origins of coal lie in the decomposition of plant material[4-6]. Much of the early work on determining coal structure was carried out in the 1950s and is summarised in a recent book by Van Krevelen[4]. The early conclusions that Van Krevelen came to about coal were : that it was a high m.wt polymeric material with a non-uniform structure, was strongly aromatic - with aromaticity increasing with rank, and the average structural unit consisted of about 20 carbon atoms and 4 - 5 rings (although larger structures were expected for anthracite). A comprehensive review by Tingey and Morrey (1973)[7], however, refuted this claim. They assumed that if coal was completely made up of condensed benzene rings, the average number of rings for lower rank coals is 2, increasing to 3-5 rings for higher rank coals. These results were based on total carbon rather than fixed carbon and represent a lower value than that arrived at by Van Krevelen.

Attempts to determine the m.wt of coals have been made by Larsen et al[8] and Heredy[9] by depolymerisation of the coal via cleavage of the methylene bridges, using phenol as a solvent and BF_3 as catalyst. Number average molecular weights of about 1000 were obtained for Bruceton coal by Larsen. Larsen also obtained good results using a reductive alkylation technique, whereby the coal was treated with an alkali metal in THF in the presence of a small amount of naphthalene. In this reaction the coal 'polyanion' was produced and this was alkylated by an alkyl halide - ether bridges and C-C bonds were also cleaved. Makabe et al[10] also managed to obtain promising results by extracting coal in pyridine by reacting it with NaOH in ethanol. More recent work has been carried out by Philip et al[11] on the application of matrix assisted laser desorption ionisation (MALDI) to coals and coal-derived materials using sinapinic acid as the matrix. By this method molecular masses of up to 270 000 units have been obtained for Point of Ayr coal and it has been shown that fragments in the mass range of 1000 - 5000 units appear to predominate in coals and coal-derived liquids.

Retcofsky and Friedel[12] have shown that conventional broad-line ^{13}C nmr techniques indicate that for all coals 83% C and higher, the position of maximum intensity is near the chemical shift value for liquid benzene - this appears to indicate relatively high aromaticity. In the ^{13}C nmr spectra of coal it is possible to resolve 4 types of C : simple aromatic, quaternary aromatic, oxygen-bonded aromatic and simple aliphatic. Since Retcofsky's experiments, results have been enhanced by using cross-polarisation ^{13}C nmr, but resonances remain fairly broad due to anisotropic chemical shift effects. Better results for aromaticity were obtained by Bartuska et al[13] who employed magic-angle spinning to reduce the line-broadening due to ^{13}C / ^{1}H interactions.

In 1975 Hayatsu et al[14] had positively identified 35 aromatic acids from coal, including several heterocyclic compounds containing O and S. He achieved this by reacting the coal with 0.4M sodium dichromate at 250°C to effect oxidation.

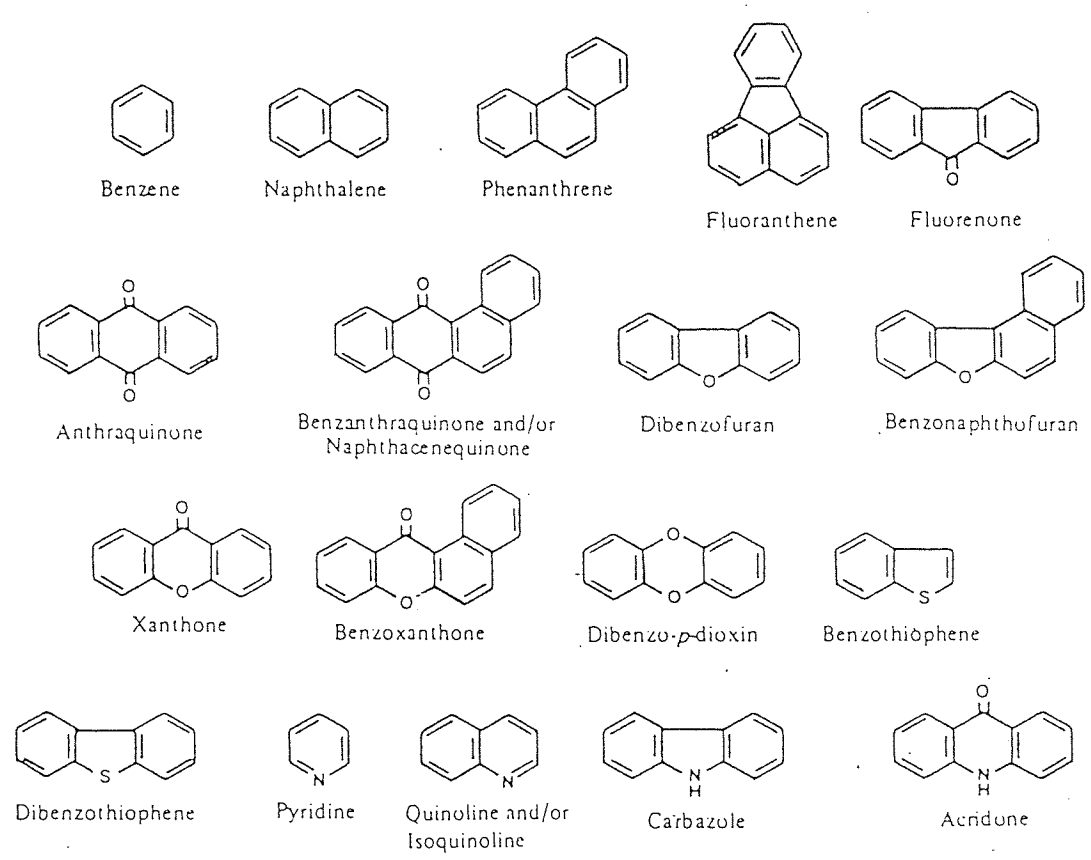

Fig1.02 Hayatsu's 'rings'

In the late 1950s P.H.Given[15] proposed a three-dimensional model structure for coal based on the average composition :

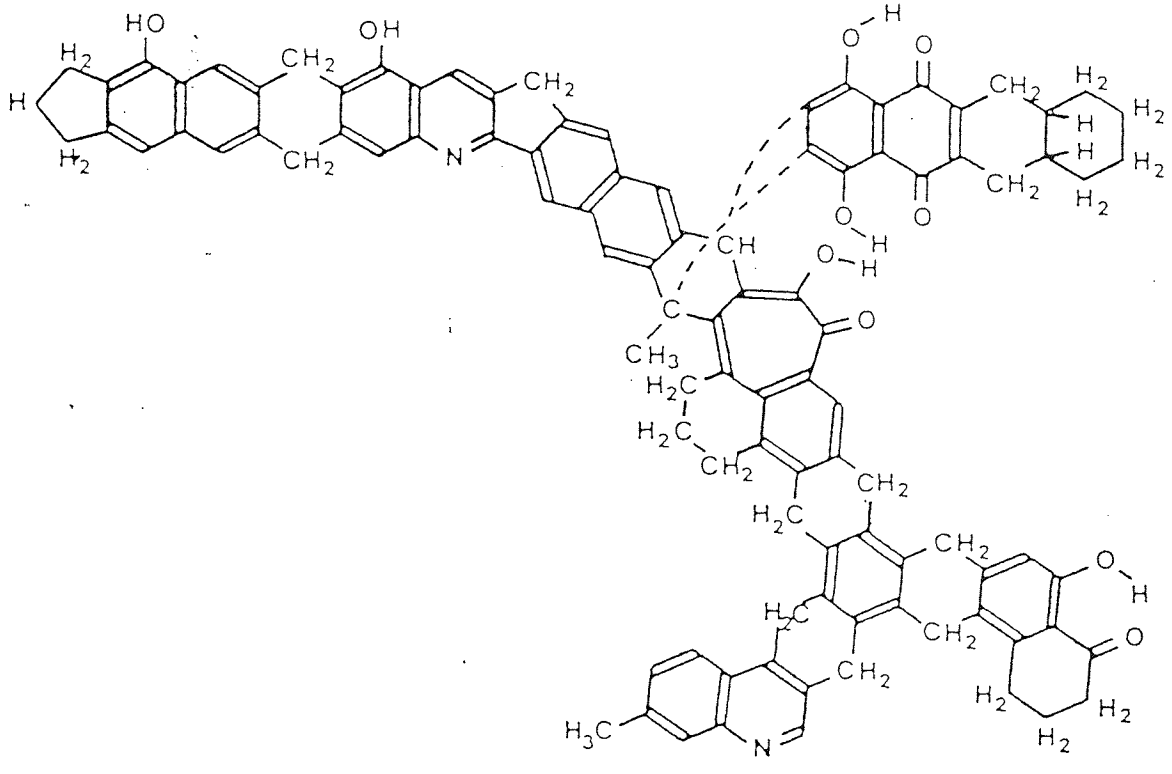

Fig1.03 Proposed structural elements of coal (Given 1960)

Later W.H.Wiser[16] presented a finer model which showed the locations of a number of relatively weak bonds, which possibly account for the rapid breakdown of coal into smaller, more soluble fragments during coal liquefaction.

Then in 1979 Pitt[17] presented a model on which he labelled possible dimerisation locations.

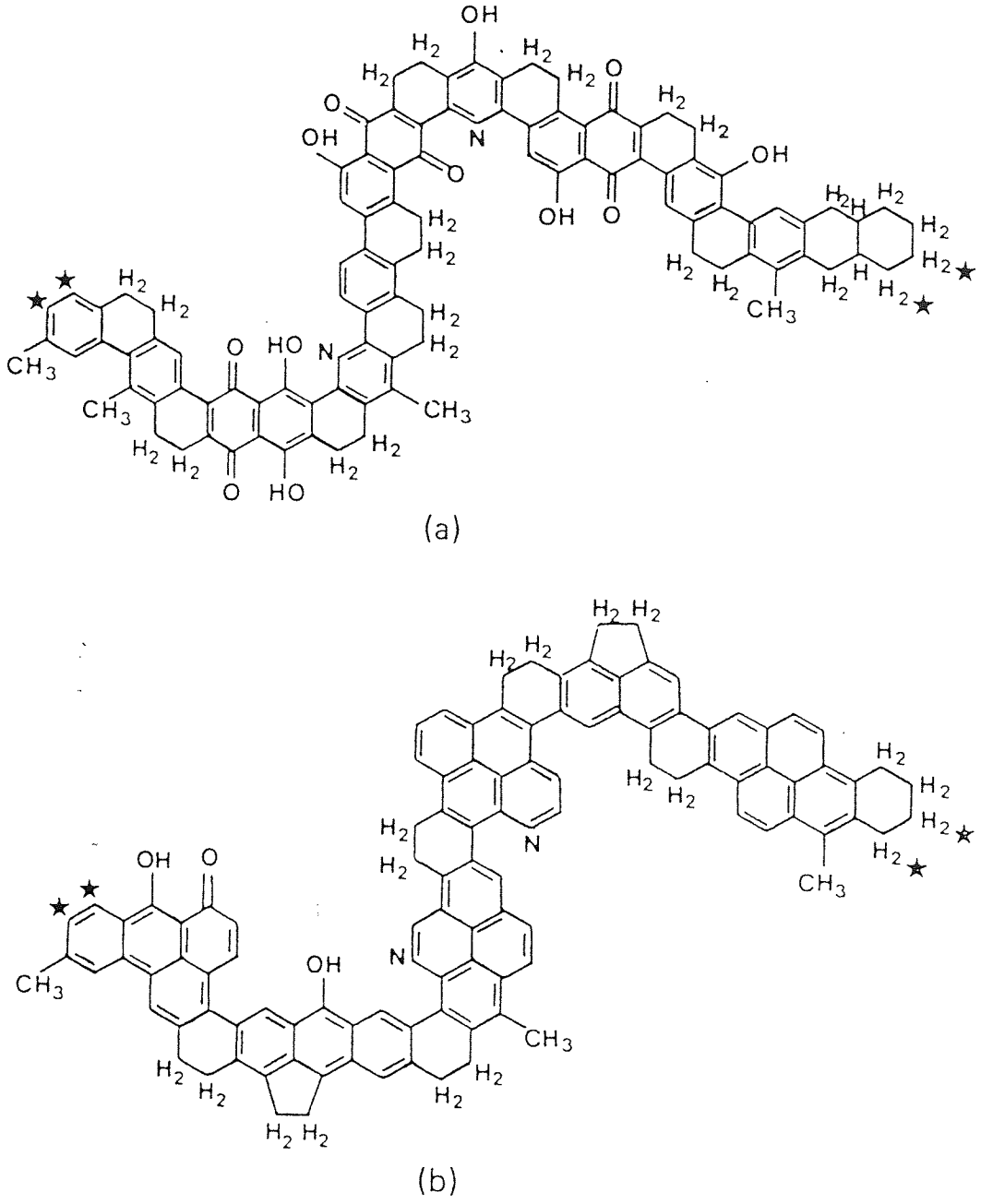

Fig1.04

Model structure for 80% vitrain. Asterisks indicate where dimerisation could occur (Pitt 1979)

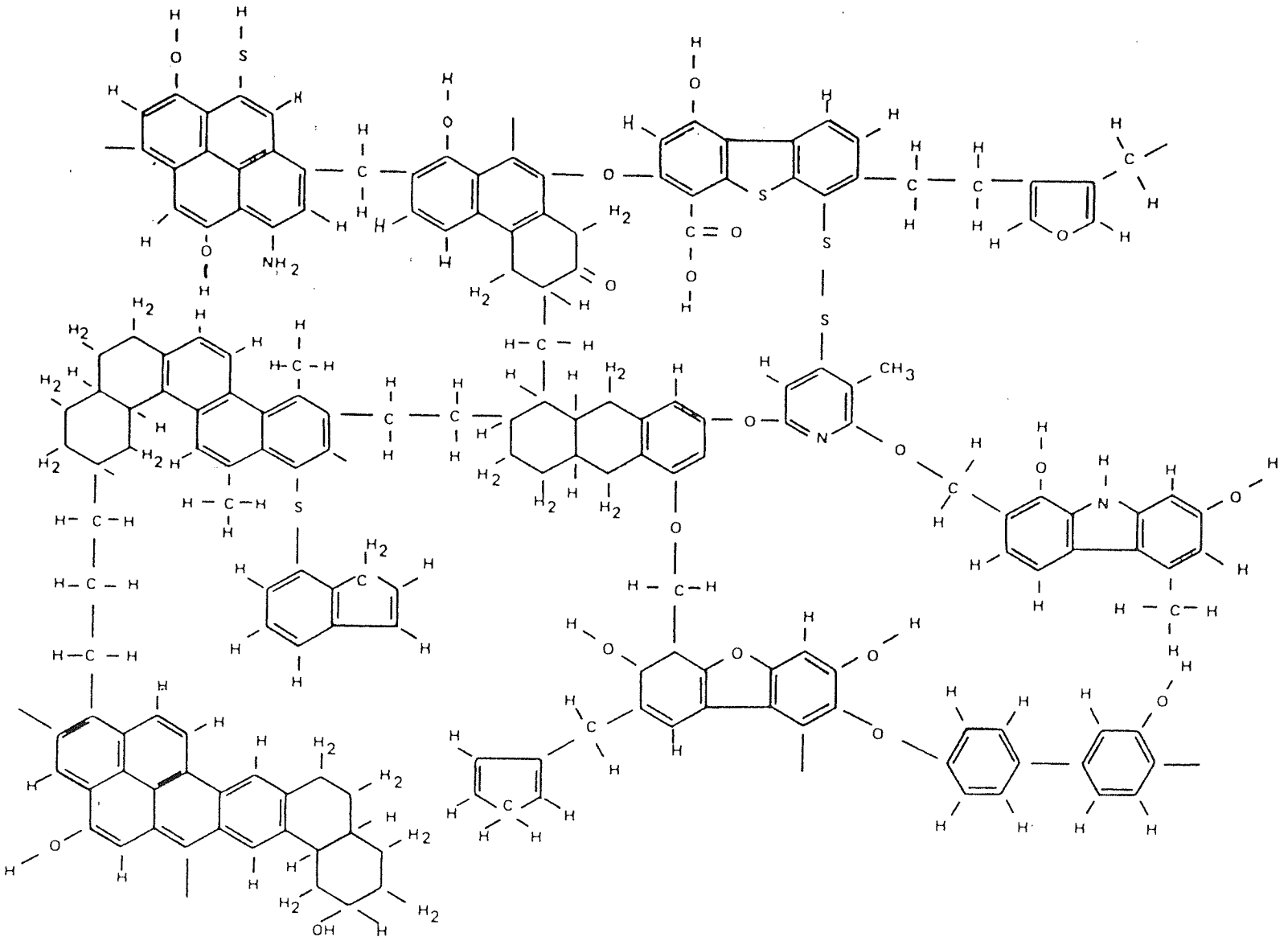

Fig 1.05

Model structure for 80% vitrain. Asterisks indicate where dimerisation could occur (Pitt 1979)

More recent work in structural determination has been carried out by J.H.Shinn[18] who has managed to construct a coal model using the technique of "retrograde synthesis". This technique involves gathering all the analytical data on the parent coal and consolidating this by information obtained from the liquefaction products i.e elemental distribution, aromaticity and functional group chemistry.

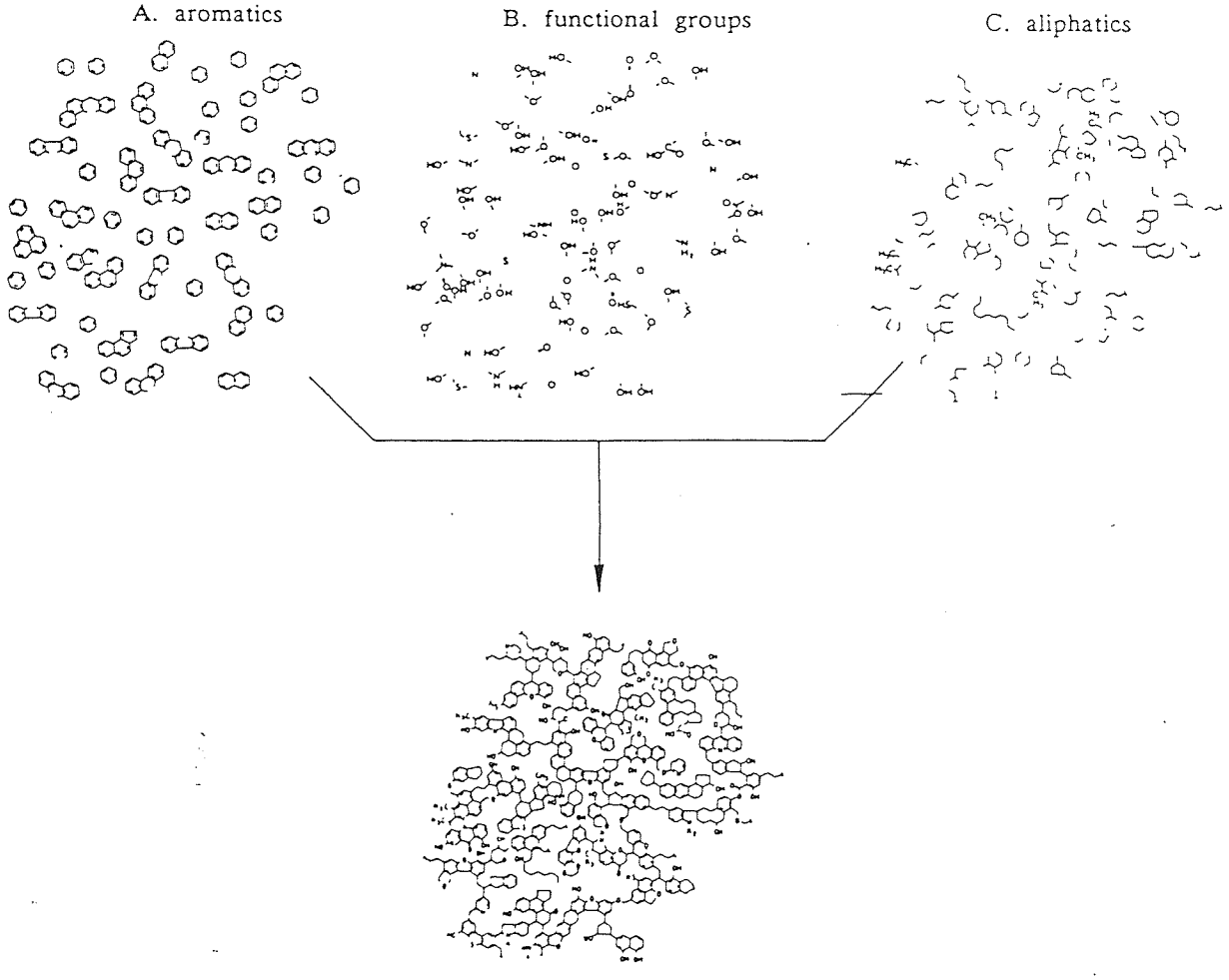

Fig1.06

Shinn's retrograde synthesis used to derive his hypothetical coal model.

1.5.3 Mineral matter in coal

The mineral matter in coal may be acquired in several ways. The first of these is from the plants themselves - during their lifetime they can accumulate inorganic matter, for example silica deposits in the cell walls. Once dead in the boggy water, this new medium provides a good transport for inorganic ions and mineral grains (these are mineral particles eroded from rocks, which blend with the coal as discrete grains of minerals e.g clay and quartz - these are referred to as "detrital" minerals and are usually macroscopic in size), which become incorporated into the peat and lignite via ion-exchange processes during the biochemical phase of coalification. Even after the coal has been compacted, water may still percolate through the cracks and seams to deposit minerals - this is the mechanism for pyrite (FeS_2) deposition. Pyrite is an example of a "disseminated" mineral crystallite - this is inherent mineral matter that is finely divided (usually < 0.1mm) and distributed throughout the coal. Calcite, kaolinite and pyrite are commonly disseminated in fusain (a coal maceral).

Procedures for the removal of mineral matter in coal rely on the difference in specific gravity between the mineral matter and the bulk coal. Methods include baum jig washing, dense medium washing and froth flotation.

Ash is the residue of mineral matter after complete combustion of the coal and consequently the mineral matter is usually calculated from the ash content using the "Parr" formula:

$$MM = 1.08A - 0.55S$$

MM = mineral matter : A = ash content : S = sulfur content.

1.6 HETEROATOMS IN COAL

1.6.1 Nitrogen in coal

In coal N is a minor constituent and tends to compose about 1% of all coals regardless of rank. Work looking into the nature of N in coals appears to indicate that it is present mainly in heterocyclic form - pyridine, quinoline and carbazole have all been identified in coal-based liquids[19].

Nitrogen emissions from coal are not as significant as sulfur emissions. Nitrogen oxides (NO_x) are produced when coal, and other fossil fuel, is burnt in air. The main components are nitric oxide NO - this constitutes approximately 95% vol. emissions, nitrogen dioxide NO_2 and trace amounts of nitrous oxide N_2O. These oxides arise mainly from 2 sources : organic N in the coal and atmospheric N (which only contributes to NO_x formation at higher temperatures). At higher concentrations NO_2 contributes to respiratory disorders and NO can inhibit the transport of oxygen by haemoglobin. NO_x can also affect some plant life and are a contributory factor to air pollution and smog formation.

It is important to note, however, that coal combustion is responsible for only about 5% of the NO_x released into the atmosphere. The bulk of the emissions derive from N-based fertilisers and car exhausts.

1.6.2 Sulfur in coal

Sulfur may be present at up to 8 - 9% in some coals. It occurs in 3 different forms in coal:

1. Organic sulfur	this is organically bound to the coal and makes up about half of the total S in low rank coal. It is mainly the remains of plant tissue, which has not yet significantly coalified.
2. Pyritic sulfur	this is mainly in the form FeS_2 and makes up the bulk of the S in bituminous coals*
3. Sulphate sulfur	this is mainly in the form of metal sulphates and contributes only a very small percentage to the total sulfur.

*Much of this pyrite has its origins in the bacterial activity during coalification - a by-product of the bacterial activity on S compounds is the gas H_2S. This reacts with iron-containing compounds in the water to produce iron sulphides, which are gradually transformed to pyrite.

Heterocyclic compounds such as benzothiophene and dibenzothiophene have been identified in coal[20] and Attar and Dupuis[21] have shown that thiol (-SH) groups are significantly higher in lignite and high-volatile bituminous coals compared to low-volatile bituminous coals. Aliphatic sulphides (R-S-R) are present at 18 - 25% and thiophenic sulfur is the major organic component in higher rank coals. It has been proposed that condensation reactions, during the coalification process, are responsible for the changes in going from -SH through R-S-R to thiophenic S.

During combustion the organic S and the pyrite is converted mainly into SO_2 with trace amounts of SO_3 - these are known collectively as SO_x. These gases can affect the respiratory system, corrode buildings and inhibit the growth of crops. Approximately 15% of the S is retained in the ash and a large proportion of the SO_x is converted to 'acid rain'.

There are 3 methods of reducing SO_x emissions :

1. Coal cleaning - large particles of pyrite may be removed by washing and smaller particles by fine grinding
2. Removal during combustion - one method is by the addition of limestone during low temperature processes
3. Flue gas desulfurisation (FGD) - the SO_x is removed in a large 'scrubber' using limestone and gypsum.

The other major heteroatom component in coal is oxygen and this will be discussed in the next section.

1.7 OXYGEN IN COAL

1.7.1 General Introduction

In coal the primary oxygen functional groups consist of phenols (R-OH), ethers (R-O-R), carbonyl groups - in particular ketones (R-CO-R) and carboxylic acids (R-COOH). The oxygen content generally decreases as the rank of the coal increases and the nature of oxygen groups present depend upon the rank of the coal. Methoxyl functional groups only occur in low rank coals, whereas carboxylic acid groups are found mainly in low-middle rank coals - coals with < 80% C. Phenolic and carbonyl groups make up the main oxygen functionalities in coals up to about 90% C. Carboxylic, phenolic and methoxyl structures are predominantly found attached to ring-structures and as a consequence - because the degree of aromaticity increases with rank - diminish or become less prevalent as the rank increases.

1.7.2 Literature review

The first important point to note is that, when considering the oxygen content of coal, the amount of moisture in the sample and the oxygen present as mineral matter - pertaining to silicates, sulphates, carbonates, oxides, etc - should be taken into account. Coal may absorb moisture (particularly on its surface) on prolonged exposure to the atmosphere and hence can vary greatly in moisture content. For these underlying reasons it is imperative that the sample for analysis has the moisture removed and the oxygen present as mineral matter is subtracted from the total oxygen content, when determining the organic oxygen present.

Much of the early work on the characterisation of coal was carried out in the 1950s by research headed by Dirk Van Krevelen[22-23]. In fact when Van Krevelen[24] was asked what he thought the single most important aspect of coal was with respect to its applications, he had no hesitation in saying "research on the composition of coal".

As early as 1932 Heathcoat and Wheeler[25] determined the %OH in coal as a function of rank. They found that the %OH in low rank coals was as little as 13%. Later work by Blom et al[26] (1957) used an acetylating procedure to show that the OH content fell from about 8% to 0.5% in going from lignite to 90% carbon coals. These results showed good agreement with future work carried out by Hammack et al[27] and Friedman et al[28] using trimethylsilylation techniques. From his results Friedman concluded that the hydroxyl groups were predominantly phenolic / acidic in character with little evidence for alcoholic or weakly acidic hydroxyl groups. Higher results for -OH content were obtained by Horton[29] (1947) using ketene as an acetylating reagent.

Carboxyl groups in coal have been determined by H.Schafer[30] (1970) via ion-exchange using barium acetate followed by subsequent titration of the liberated acetic acid. The exchange reaction was conducted at pH 8.2 to prevent formation of phenolic acids. It was shown that carboxyl groups only exist in appreciable amounts in brown coals and lignites. At 83% carbon, carboxyl groups were found to be no longer present. A similar trend was observed for methoxyl groups, but in this instance, most of the methoxyl functionality has disappeared at 75% carbon and only about 0.2% remained at 80% carbon. The carbonyl structure, however, persists at higher percentages of carbon. Ihnatowicz[31] and Blom et al[32] found that carbonyl oxygen contents were in the region of 0.2 - 0.8% for 83% carbon and higher.

Work on the aliphatic oxygen constituents of coal has been carried out by Deno et al[33], who managed to degrade coal into fragments of m.wt below 400 by using a mixture of aqueous hydrogen peroxide and trifluoroacetic acid to oxidise the coal. This technique destroyed the aromatic rings while leaving the aliphatic structure effectively intact. Functional group analysis showed that the main oxygen-containing groups were carboxyl, carbonyl, methoxyl and hydroxyl functionalities.

A contemporary method available for the determination of total oxygen in coal is neutron activation analysis - this involves a nuclear reaction, whereby the sample is irradiated with thermal neutrons from a nuclear reactor and the resulting number and energies of the γ-rays and x-rays emitted by the radioactive isotope are measured. The drawback of using this technique is that it is very costly, requires a nuclear reactor and has all the hazards associated with radiation.

Ruberto and Cronauer[34] have studied the oxygen content of sub-bituminous coal and managed to break down the individual components. The conclusion they came to was that there appears to be a significant amount of oxygen in the form of ether α- or β- to the aromatic groups and in the form of furan. Ruberto and Cronauer's findings are outlined in Table 1.02.

Table 1.02

Analyses of Oxygen functionality in coals (wt% maf basis)

Coal	Burning Star (bituminous)	Belle Ayr (subbituminous)
Oxygen content as :		
Hydroxylic (-OH)	2.4	5.6
Carboxylic (-COOH)	0.7	4.4
Carbonylic (=C=O)	0.4	1.0
Etheric (-O-)	2.8	0.9
Total :	6.3	11.9
Oxygen by difference :		
Ash basis	5.9	16.2
Mineral matter basis	—	16.0

From Ruberto and Cronauer[34] (1978 p.61) maf = moisture, ash-free.

In 1979 R.Liotta at al[35-37] developed a novel O-alkylation technique for the selective alkylation of acidic hydroxyl groups in coal. This was a two-step process utilising iodomethane under very mild reaction conditions. The products were analysed by FT-IR and ^{13}C nmr to identify and quantify the hydroxyl / carboxylic acid groupings present.

Table 1.03 gives a concise summary of the work done on oxygen functionalites between 1963 - 1981.

Table 1.03 Work done on Oxygen functionalities in coal 1963 - 1981[38]

Coal Rank[a]	Hydroxy / Carbonyl	Amount present[b]	Reference(s)
High-volatile bituminous	Phenolic OH	0.8 - 6.3%	Heredy et al (1965)
	Phenolic OH	2.3 - 5.8%, 35 - 39% of all O	Brown and Wyss (1955)
Japanese (60 - 84% C)	Phenols in extracts, amount depending on solvent	0.5 - < 5% OH	Yokoyama et al (1967)
Coal (83% C)	Phenolic OH	2.3 meq/g	Brooks and Maher (1954)
Australian Greta (82.4% C)	Phenolic OH	1.6 meq/g	Maher and O' Shea (1967)
Illinois No.6	Phenolic OH	5 OH groups / 100 C atoms	Gethner (1982); Liotta et al (1983)
Vitrinite (84% C)	Phenolic OH	2.5 meq/g	Halleux et al (1959, 1961)
Bituminous (80 - 94% C)	Total acids	0.64 - 6.2% OH, 37 - 62% of all O	Vaughan and Swithenbank (1970)
Low rank	Total acids	4 - 9 meq/g	Schafer (1970); Maher and Schafer (1976)
HVA. HVB, HVC subbituminous, etc	Total acids	1.0 - 6.5% OH, 34 - 62% of all O[c]	Abdel-Baset et al (1978)
	Total acids	3.5 - 6.5% OH, 34 - 75% of all O[c]	Yarzab et al (1979)
Bituminous and subituminous	Total acids	2.4 - 5.6% OH 0.7 - 4.4 % COOH	Ruberto et al (1977)
Australian brown (63% C)	Total acids	5% OH, 5% COOH	Evans and Hooper (1981)
Bituminous and subbituminous	Total carbonyl	0.4 - 1.0%	Ruberto et al (1977)
Australian brown (63% C)	Total carbonyl	3%	Evans and Hooper (1981)

[a]Amounts in this column are weight percentages relative to coal.
[b]Amounts in this column are weight percentages relative to coal unless indicated otherwise.
[c]Percentages of oxygen of this functionality relative to overall oxygen

Recent work on the structural elucidation of -OH groups in coal includes work done by Cannon at al[39], who have identified -OH functional groups in coal tars using FT-IR - apparently there is a strong similarity between the IR of the parent coal and the respective tars, with the tars giving better resolved spectra compared to the coal matrix. Dadey at al[40] have also looked at -OH groups in coal via derivatisation with diphenylphosphinyl chloride i.e by introducing a ^{31}P (which is a 100% abundant magnetic nucleus) label into the coal. The signals corresponding to phosphinate ethers were then integrated to produce a quantitative measure of the -OH content of the sample.

Contemporary acetylation work has been carried out by Bailey et al[41] who have acetylated a rank series of coals using a variety of reagents. They concluded that the percentage of oxygen present in the coals as -OH was much higher when determined with ketene (a toxic gas generated from the pyrolysis of acetone) compared with derivatisation by other 'conventional' reagents. The greater reaction is probably due to the fact that a smaller, more reactive reagent is being employed. Acetylation will be looked at in greater depth in chapter 4.

A very recent paper by Monsef-Mirzai et al[42] has looked at the measurement of hydroxyl groups in coal using microwave methodology and derivatisation with silylating reagents. Good results were obtained for 11 different coals of varying rank using a new mixture of derivatising reagents followed by quantitative ^{29}Si nmr analysis. Silylation will be discussed further in chapter 5.

Hydroxyl groups in coal may be detected with a reasonable degree of certainty by employing spectroscopic methods and the hydroxyl content may be measured by conversion into derivatives e.g acetylation, silylation, alkylation, etc ; but because of the heterogeneous nature of these systems, there is always the ambiguity as to whether the reactions have progressed to completion / equilibrium - and indeed a method-dependant scatter of results is observed in the literature.

1.7.3 Why look at the O functionality ?

Direct coal liquefaction processes involve the thermal solubilisation of the coal in solvents, which are usually procured from the coal. The preliminary step, for a process at about 400°C, is primarily a thermal one where bonds with energy < 55 kcal / mol are broken. Consequently aliphatic ether bridges are the first to rupture during coal liquefaction. An order of reactivity of the oxygen functionalities in coal (with respect to bond energies) has been drawn up by Mitchell[43] (see fig.1.07).

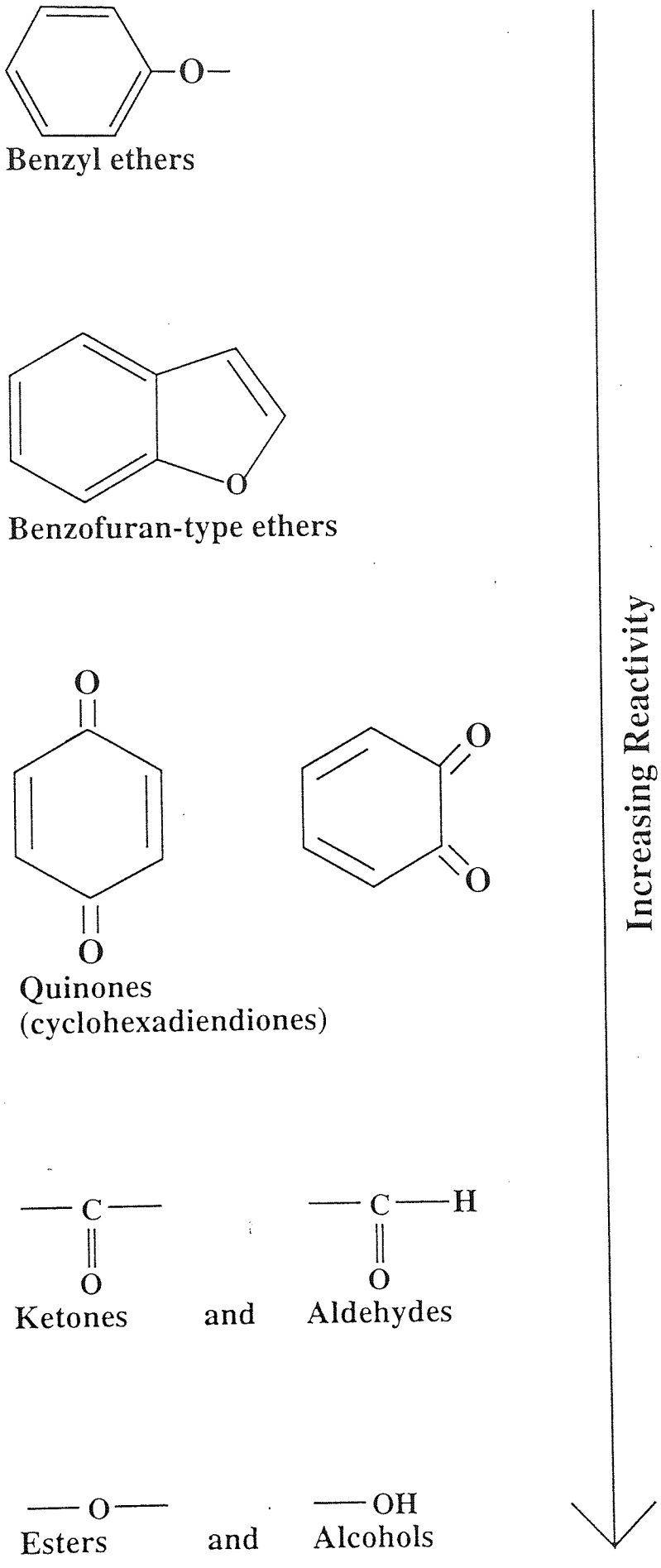

Fig1.07 Order of reactivity of the oxygen functionalities in coal

Cronauer et al[44] have stressed the detrimental effects caused by the presence of phenolic -OH groups during liquefaction - additional reaction time and an increased hydrogen input, allied with powerful catalysts, are required in order to overcome this costly obstruction and ensure complete reaction of the phenol and furan groups. Consequently the hydroxyl groups and in particular the phenolic groups, are a very important class of compound in coal liquefaction. The characterisation of these phenolic groupings are therefore vital for the further development and understanding of these liquefaction processes.

Another reason for the investigation of phenolic (and carboxylic acid) groups in coal is that they are very polar and capable of entering into hydrogen-bonding within the coal. This can lead to the creation of a secondary structure in coal, which again hinders liquefaction. Work in this thesis is aimed at altering these acidic hydroxyl groups chemically via derivatisation, in order to obtain quantitative information without altering the generic nature of the coal matrix. Data obtained will allow us to study the environment of the phenolic groups and give a measure of the amount of hydroxyl functionality present in the coal.

1.8 MICROWAVE TECHNOLOGY IN CHEMICAL SYNTHESIS

1.8.1 General Introduction

The application of microwave energy to chemical synthesis has undergone intensive investigation over the last decade or so. The technique is especially well suited to the production of small scale specialist materials of high purity e.g enantiomeric and diastereomeric products and other asymmetric syntheses. The main driving force for the development of microwave technology is the need for an efficient, environmentally clean technology which can help to reduce waste products and other pollutants. Another reason for the rapid growth in microwave research is the increasing availability and development of hardware for use both in laboratories and, perhaps more importantly, on an industrial scale - this is largely due to advances in the field of microelectronics in the 1970s. A wide range of organic and inorganic reactions have been accelerated using microwave techniques and the rapid synthesis of these compounds can be attributed primarily to superheating effects, which occur as the result of the effective coupling of microwaves to the polar solvent in the containment vessel. Another advantage of microwaves is that large temperature gradients in the reaction are avoided. The position, size and shape of the sample also affects the heating, as the microwaves tend to 'cut' into the sample. For coupling of microwave radiation with molecules in solution, a dipole moment is required - on irradiation with microwaves, di-electric losses occur (due to dipolar polarisation in the microwave field) which cause friction and result in the build up of heat.

1.8.2 What are microwaves ?

Microwaves are electromagnetic radiation situated between the infrared and radio frequency regions of the electromagnetic spectrum. They cover the frequency range 300 MHz to 30 GHz corresponding to wavelengths between 1.0 m and 10.0 cm. The high frequency range 1.2 - 30 GHz is used for radar, and the other frequencies are used in telecommunications. Industrial and domestic microwaves usually operate at a frequency of 2.45 GHz. Microwaves do not produce changes in molecular structure, but cause molecular motion via exposing the molecules to non-ionising radiation. This radiation causes the migration of ions and the rotation of dipoles.

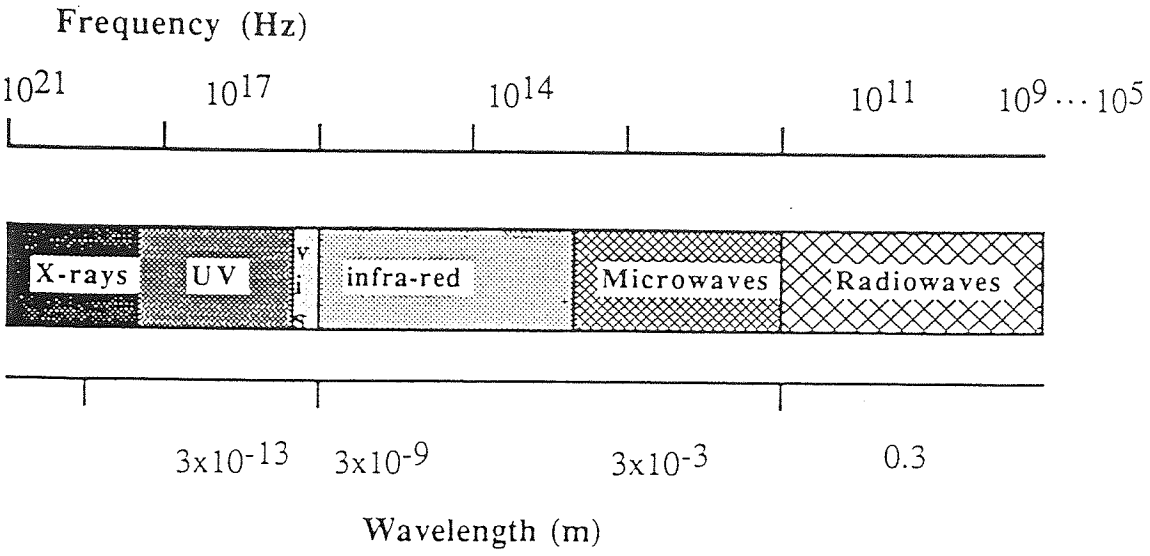

Fig1.08 The position of microwaves in the electromagnetic spectrum

1.8.3 Microwave heating mechanisms

Microwave heating of solids and liquids has been shown to occur via two mechanisms[45-46], which both arise from the induction of a force on charged particles by the electromagnetic wave. Consequently more polar materials will absorb greater microwave radiation to emit more heat. The 2 mechanisms are :

(i) Dielectric polarisation / dipolar rotation

Dielectric heating transpires when an oscillating electromagnetic field induces dipoles in a material and the associated relaxation times are too long to allow the polarisation to follow the reversal of the field. The subsequent time lag between fluctuations in the field and those of the induced dipoles is evident as energy absorption and heating. Dielectric polarisation is affected by both frequency and temperature. The total polarisation of material is composed of 2 main components :

(a) Dipolar polarisation

This is due to the permanent dipoles within the absorbing material due to the different electronegativities of the atoms. This phenomenon is characterised by dielectric parameters :

$$\tan\delta = \frac{\varepsilon''}{\varepsilon'}$$

$\tan\delta$ = loss tangent - this defines the ability of a material to convert electromagnetic energy into heat energy. δ is the angle between the charging current and the vector sum of the charging current and the loss current[45]. Loss tangents decrease with increasing temperature ($\tan\delta$ values for selected solvents are presented in Table 1.04).

ε'' = loss factor - this gives an indication of the efficiency with which the electromagnetic energy can be converted into heat. The loss factor for non-polar liquids / solutions is very low and the values for polar liquids, such as alcohols, are usually quite high.

ε' = dielectric constant - this represents the capacity of the molecule to be polarised by the electromagnetic field.

Table1.04

Dielectric loss tangents (tanδ) for some common solvents[45-46]

Solvent	Temperature °C	Frequency (GHz)	Loss tangent,tanδ
Water	25	0.3	0.015
	25	3.0	0.15
	25	10.0	0.54
	05	3.0	0.28
	21	2.58	0.16
	50	2.58	0.10
	65	2.58	0.094
	98	2.58	0.090
Methanol	25	0.3	0.081
	25	3.0	0.64
	25	10.0	0.81
	21	2.58	0.81
	46	2.58	0.70
	65	2.58	0.65
Ethanol	25	0.3	0.27
	25	3.0	0.25
	25	10	0.065
n-Propanol	25	0.3	0.42
	25	3.0	0.68
	25	10.0	0.087
n-Butanol	25	0.3	0.55
	25	3.0	0.46
Ethylene glycol	25	0.3	0.16
	25	3.0	1.0
	25	10.0	0.79
Tetrahydrofuran	21	2.58	0.065
	40	2.58	0.060
	60	2.58	0.057
	65	2.58	0.055
n-Heptane	25	3.0	1.0×10^{-4}
	25	10.0	1.0×10^{-3}
Tetrachloromethane	25	3.0	4.1×10^{-4}
	25	10.0	1.4×10^{-3}

(b) Interfacial polarisation

This arises from the build up of charges at interfaces between materials of different dielectric constants.

(ii) Ionic conductance

This phenomena occurs when the charged particles are mobile, thereby inducing a current due to the incident electromagnetic field. It is dependent on frequency and to a lesser extent on temperature.

The absorption of microwave energy determines the penetration depth into the irradiated medium i.e the higher the absorption, the less the penetration.

Microwave heating also has distinct advantages over conventional heating via conductive methods. During conductive heating the containment vessel must first be heated up before the energy is transferred to the solution. In order to heat the solution a thermal gradient must be established via convection currents and only a small proportion of the solution will be at the same temperature as the external vessel wall. With microwave heating the whole of the solution is heated up instantaneously resulting in a rapid attainment of its boiling-point and, if the sample is an enclosed environment, superheating of the sample will occur.

1.8.4 Literature review

Microwaves have been used in chemical synthesis as far back as 1975, when microwave heating was used to increase the rate of acid dissolution of samples in an open beaker[47]. Later this technology evolved into the heating of reagents in sealed containers to effect superheating of the reactants. Microwave-driven reactions have been shown to be superior to conventional methods in their ability to dramatically reduce reaction times and in some cases give cleaner reactions - there is very little evidence to suggest that microwaves significantly alter the pathway of a reaction, as can happen with ultrasound. Microwave energy may be applied to solid, liquid or gaseous phases and even heterogeneous systems.

Much of the early pioneering work was carried out in the mid-1980s by Richard N. Gedye et al[48-49] at the Laurentian University in Canada. His work concluded that organic compounds could be synthesised up to 1240 times faster in sealed teflon vessels in a microwave oven compared to synthesis by conventional reflux methods (see Table 1.05).

Table 1.05

A comparison of reaction times and yields in representative reactions using classical and microwave procedures.

Compound synthesised	Procedure followed	Reaction time	Average[b] yield	$\frac{k_{microwave}}{k_{classical}}$
Hydrolysis of benzamide to benzoic acid in water				
C_6H_5COOH	Classical	1 hour	90	
C_6H_5COOH	Microwave	10 min	99	6
Oxidation of toluene to benzoic acid in water				
C_6H_5COOH	Classical	25 min	40	
C_6H_5COOH	Microwave	5 min	40	5
Esterification of benzoic acid with methanol				
$C_6H_5COOCH_3$	Classical	8 hours	74	
$C_6H_5COOCH_3$	Microwave[a]	5 min	76	96
S_N2 reaction of 4-cyanophenoxide ion with benzyl chloride in methanol				
$NCC_6H_4OCH_2C_6H_5$	Classical	16 hours	89	
$NCC_6H_4OCH_2C_6H_5$	Microwave	4 min[c]	93	240
$NCC_6H_4OCH_2C_6H_5$	Classical	12 hours	65	
$NCC_6H_4OCH_2C_6H_5$	Microwave	35 sec[c,d]	65	1240

[a]Very high pressures developed and the study of this reaction was halted.

[b]The average yields are based on isolated yields and represent the average of at least two experiments. The S_N2 reaction was followed by titrating the chloride ion.

[c]Value for one run only.

[d]The reaction was done in a 50 cm^3 teflon bomb.

Gedye also proposed that the rate enhancement was predominately due to the superheating of the solvent and further that the rate of microwave energy absorption was dependent on the dielectric constant of the solvent :

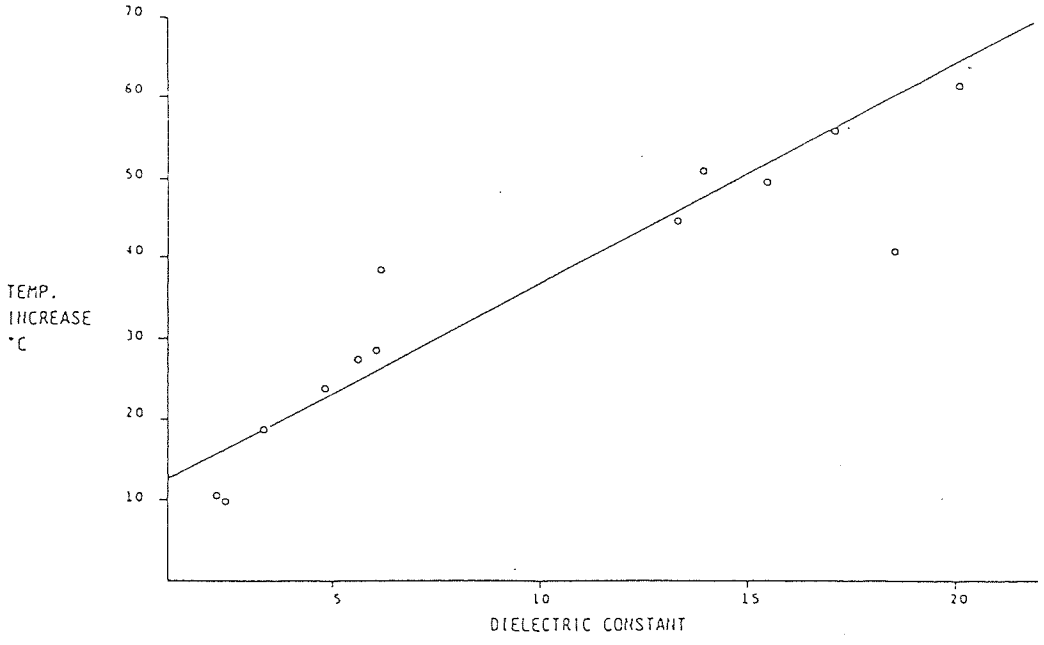

Fig1.09 The effect of dielectric constant on the heating rate of various organic liquids.

Table 1.06

The temperature of 50 cm^3 of several solvents after heating for 1 minute at 560 watts in an open vessel in a microwave oven.

Solvent	Temperature °C after 1min.	Boiling point °C
Water	81	100
Methanol	65	65
Ethanol	78	78
1-Propanol	98	97
1-Butanol	109	117
1-Pentanol	106	137
1-Hexanol	92	158
1-Chlorobutane	76	78
1-Bromobutane	95	101
Acetic acid	110	119
Ethyl acetate	73	77
Methylene chloride	41	41
Chloroform	49	61
Acetone	56	56
N,N-Dimethylformamide	131	153
Diethyl ether	32	35
1,4-Dioxane	53	101
1-Butylamine	70	77
Tripropylamine	56	157
Hexane	25	68
Heptane	26	98
Carbon tetrachloride	28	77

It can be seen from Table 1.06 that the more polar solvents absorb microwaves more readily. When carrying out microwave reactions rapid heating creates very high pressures in the reaction vessel - these increased pressures can lead to deformation of the vessel and subsequently a possible explosion. To try to avert such a disaster Gedye recommended that the volume of the reaction mixture should be kept down to between 10 - 15% of the volume of the container. Further work by Gedye et al[50] on elimination-substitution reactions of bromooctanes showed that microwaves did not significantly alter the product composition of a reaction i.e the reaction pathway is not critically altered.

Mingos and Baghurst[45] have also shown that the direct interaction of microwaves with liquids results in very rapid and direct heating (see Table 1.07).

Table 1.07 Microwave heating of common solvents

Solvent	Normal boiling point (°C)[a]	Temperature attained in 1min. (°C)[b]	Superheated temperature (°C)	Extent of superheat (°C)
Water	100	81	105	5
Methanol	65	65	84	19
Ethanol	78	78		
1-Propanol	97	97		
2-Propanol	82		108	26
1-Butanol	117	109	138	21
2-Butanol	98		127	29
t-Butanol	83		112	29
1-Pentanol	136	106	157	21
2-Pentanol	119		135	16
t-Pentanol	102		115	13
1-Hexanol	158	92		
1-Heptanol	176		208	32
Diethyl ether	35	32	60	25
THF(tetrahydrofuran)	67		103	36
n-Hexane	68	25		
n-Heptane	98	26		
Acetone	56	56	89	33
2-Butanone(MEK)	80		110	30
Cyclohexanone	155		186	31
Acetic acid	119	110		
Ethyl acetate	77	73	102	25
Acetonitrile	82		120	38
DMF(Dimethylformamide)	153	131		
Trichloromethane	61	49	89	28
Tetrachloromethane	77	28		
1-Chlorobutane	78	76		
1-Bromobutane	101	95		

[a]Pressure 1013 mbar

[b]50 cm^3 heated at 560 W, 2.45 GHz for 1min : Initially at 'room' temperature.

The largest temperature rises occur in liquids for which the dielectric loss factors are high, such as alcohols. As can be seen from Table 1.07 the liquids show significant superheating effects. It is also possible that superheating may occur locally in the body of a liquid - this could happen if the microwave energy is rapidly absorbed into the liquid, followed by relatively slow mixing and transport processes for its dissipation - this could explain unusual reaction rate enhancements. Abramovitch[51] proposed that the most rapid temperature rises occur where high dipole moments are coupled with low heat capacities.

Work has also been carried out on the heating of solids in microwaves[45] (see Table 1.08). The heating is thought to take place via dielectric and conduction mechanisms.

Table 1.08 Microwave heating of solids

Material	Heating time (min)	Temperature attained°C
Al	6	577
C	1	1283
Co_2O_3	3	1290
CuCl	13	619
$FeCl_3$	4	41
$MnCl_2$	1.75	53
NaCl	7	83
Ni	1	384
NiO	6.25	1305
$SbCl_3$	1.75	224
$SnCl_2$	2	476
$SnCl_4$	8	49
$ZnCl_2$	7	609
CaO	30	83
CeO_2	30	99
CuO	0.5	701
Fe_2O_3	30	88
Fe_3O_4	2	510
La_2O_3	30	107
MnO_2	30	321
PbO_2	7	182
Pb_3O_4	30	122
SnO	30	102
TiO_2	30	122
V_2O_5	9	701
WO_3	0.5	532

The values in the top part of the table refer to 25g samples at 1 kW, 2.45 GHz.
The values in the lower part of the table refer to 5-6g samples at 500 W, 2.45 GHz.

Good reviews of the applications of microwaves to organic synthesis are given by Abramovitch[51] and Mingos[45]. Investigations have also been carried out on the utilisation of microwave technology in the field of inorganic chemistry and heterogeneous systems.

Meek et al[52] have reported a microwave heating process for the preparation of Ni-Al_2O_3 powder from solutions of aluminium and nickel nitrates, whilst Bauer at al[53] have developed a continuous process for the manufacture of dielectric mixed oxide ceramics from mixed nitrate solutions. Kozuka and McKenzie[54] have managed to prepare metal carbides by heating the oxides with graphite in a domestic microwave oven at 700W. Baghurst et al[45,55] have also carried out a great deal of work on the synthesis of organometallic transition metal co-ordination complexes. Another field where microwaves have been successfully employed is the intercalation of organic and organometallic compounds into layered structures - the main problem normally encountered in this type of reaction is that the intercalation processes are kinetically very slow and reactions may not proceed to completion, even after several days of refluxing. Chatakondu et al[56] have succeeded in intercalating pyridines into α-$VOPO_4$ - a layered mixed oxide - with a microwave exposure time of only 5 minutes at 80bar and 200°C. Similarly, Ashcroft et al[57] have intercalated organotin compounds into laponite (a synthetic smectite clay). The aryltin precursors were incorporated as tin(IV) oxide pillars with benzene produced as a by-product. The microwave preparations were irradiated for 5 minutes, whereas conventional mechanical shaking was carried out over a 1 week period (see Table 1.09).

Table 1.09

The wt% of precursor intercalated using mechanical shaking and microwave methods.

Intercalated compound	wt% intercalated Mechanical shaking	wt% intercalated Microwave method
$(Ph_3Sn)_2O$	10	33
Ph_3SnCl	45	75
Ph_2SnCl_2	38	44

The possible use of microwaves in the sphere of coal research was outlined by Bailey et al[58] (1990), who stated that microwaves are able to effect internal heating of a suitable polar medium, in which the coal is suspended, during derivatisation. This is due to the fact that coal is effectively transparent to microwave irradiation. Preliminary work was carried out by Bailey et al[41] (1992) on the acetylation of a rank series of coals and the results showed that microwave-driven acetylation produced higher values in shorter experimental time compared with conventional reflux methods. Work has also been done by McWhinnie et al[59] on the pyrolysis of coal in a microwave oven using various metal oxide receptors and graphite - it was found that the method was very effective for transferring the non-carbon elements - H, O, S and N into the liquid tar phase. More recent work has involved the use of microwaves in the silylation of hydroxyl functional groups in coal[42] - this will be discussed further in chapter 5.

CHAPTER 2

2.1 PHYSICAL METHODS

2.1.1 FT-IR Spectroscopy

Fourier transform infrared spectroscopy was carried out using a Bio-rad FTS-40A spectrometer incorporating a 600 microwatt 632.8 nm CW class II laser. KBr discs (4000 - 400 cm^{-1}) were used for solid samples and NaCl discs (4000 - 625 cm^{-1}) for liquid samples, with a KBr beamsplitter. For analysis in the far infrared region, a mylar beamsplitter was used with CsI discs (4000 - 145 cm^{-1}).

2.1.2 NMR Spectroscopy

The nmr spectra were obtained on a Brucker AC300 spectrometer, for which the static field of the superconducting magnet was 7.04 T. The analyses were carried out by the Aston University Department of Chemical Engineering and Applied Chemistry. Solid samples were spun at the magic angle with a rotor speed of approximately 4000 Hz and analysed using multinuclear or solid state probes.

2.1.3 Gas Chromatography

Gas chromatography analyses were carried out on an ATI unicam 610 series gas chromatograph instrument using an initial temperature setting of 200°C, a final setting of 300°C, a flame ionisation detector (FID) temperature of 330°C and a temperature rate of 1°C min^{-1}. The column was 2 metres in length and contained silicon grease on a diatomite support. The carrier gas was nitrogen with a flow rate of 30 cm^3min^{-1}.

2.1.4 X-ray photoelectron Spectroscopy (XPS)

XPS measurements were carried out on a Fisons VG Escalab 200D spectrometer. The source consisted of Mg K_α radiation and analyses were carried out using a 20 or 50 eV analyser, a dwell time of 50 or 100 ms and 2 - 8 scans.

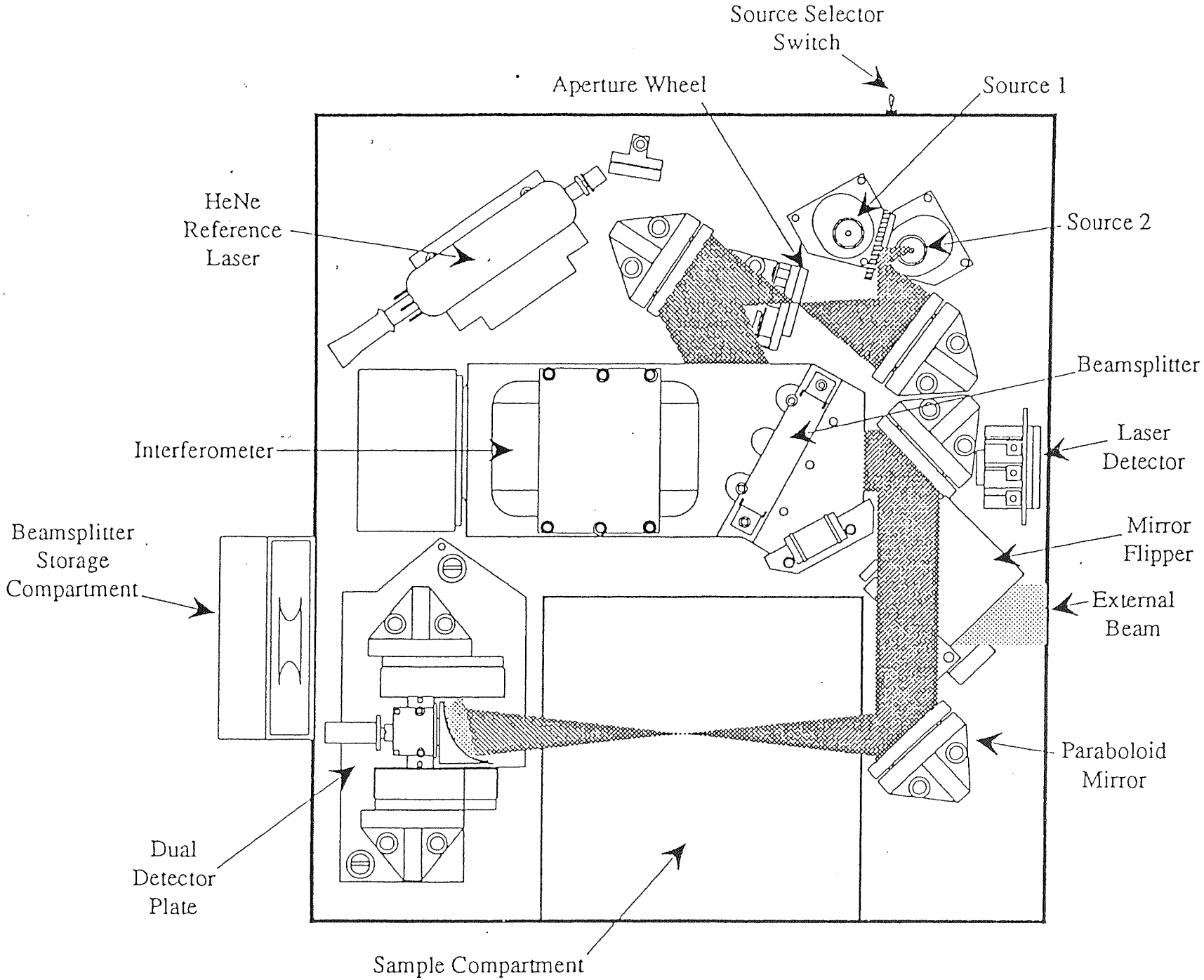

Fig2.01 FTS-40A FT-IR Spectrometer

2.2 MICROWAVE EQUIPMENT

2.2.1 Sharp Carousel II R-84801

This is a domestic microwave with a power rating of 650 watts and an operational frequency of 2.45 GHz. Much of the early work in this thesis was conducted on this instrument. The Carousel II R-84801 was not modified or adapted in any way for use in the laboratory, but for safety reasons it was used under a fume hood.

2.2.2 Digestion vessels

The containment vessels used in conjunction with the Carousel II R-84801 microwave consisted of teflon PFA digestion vessels - supplied by CEM* - incorporating relief valves and venting nuts. These digestion vessels had a volume of 100 cm^3 and were transparent to microwave energy.

The digestion vessels were sealed shut using CEM capping stations and the safety relief valve remained sealed up to an internal pressure of 830 ± 70 kPa (tested by CEM at 50% microwave power (270 watts) using 30 cm^3 water). Above this pressure the vessel cap flexed and the pressure was relieved. When the pressure fell below 830 ± 70 kPa the cap resealed itself to maintain the pressure inside the vessel.

The digestion vessels are made from teflon (a fluoropolymer), have a melting-point of approximately 300°C and are very resistant to chemical attack - teflon PFA has no known solvent at temperatures up to 150°C. Teflon PFA is a soft plastic which is easily scratched and can become discoloured when exposed to strong acids.

With prolonged use of the vessels, they may undergo physical defects :

(a) Absorption

Compounds may become absorbed in the fluoropolymer matrix. There is very low absorption of ionic inorganic materials, but hydrocarbon solvents may be absorbed at their boiling-point, giving rise to about a 1% weight increase of the teflon PFA vessel. Higher absorptions can occur when halogenated solvents are used. Absorption is affected by physical parameters such as temperature.

(b) Environmental Stress Cracking (ESC)

This results in failure of the vessel due to exposure to a chemical environment under conditions of mechanical and/or thermal stress.

(c) Creep

This is permanent deformation due to an applied force. Increased pressures result in greater creep and higher temperatures lead to a greater increase in the rate of creep. On release of the pressure the vessel will partially return to its original shape. If the vessels are cooled quickly, for example immersed in cold water, deformation will be less than if they are allowed to cool slowly.

The CEM digestion vessels have a lifetime of between 50-100 digestions.

*CEM is a registered trademark.

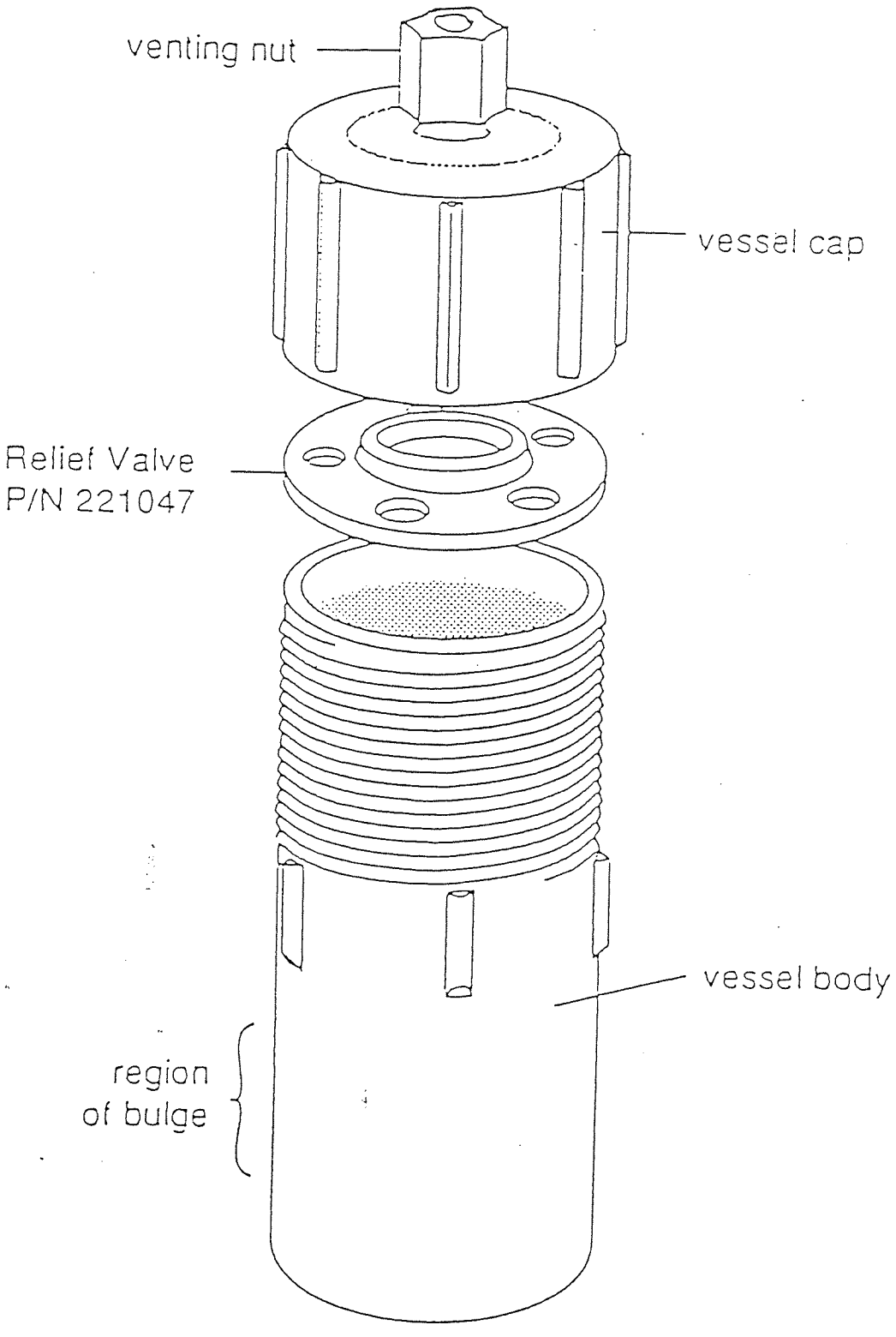

Fig2.02 Digestion vessel assembly

2.2.3 MES-1000 microwave system

For the latter part of the investigation an MES (microwave extraction system) -1000 was acquired. The main features of this system are; a fluoropolymer-coated cavity fitted with a cavity exhaust fan (exhaust air flow = 157 ft^3min^{-1} or $4.5m^3min^{-1}$), a direct drive alternating turntable, a tin-oxide semiconductor gas sensor designed for detecting organic solvents, exhaust-tubing to vent fumes, a digital programmable computer (30 multistep programs consisting of up to 5 stages each) and 3 inlet/outlet ports to accommodate control lines. The MES-1000 delivers approximately 950 ± 50 watts of microwave energy at a frequency of 2450MHz at full power. The % power may be programmed in at 1% increments to control the rate of heating and a microcomputer controls and monitors operations.

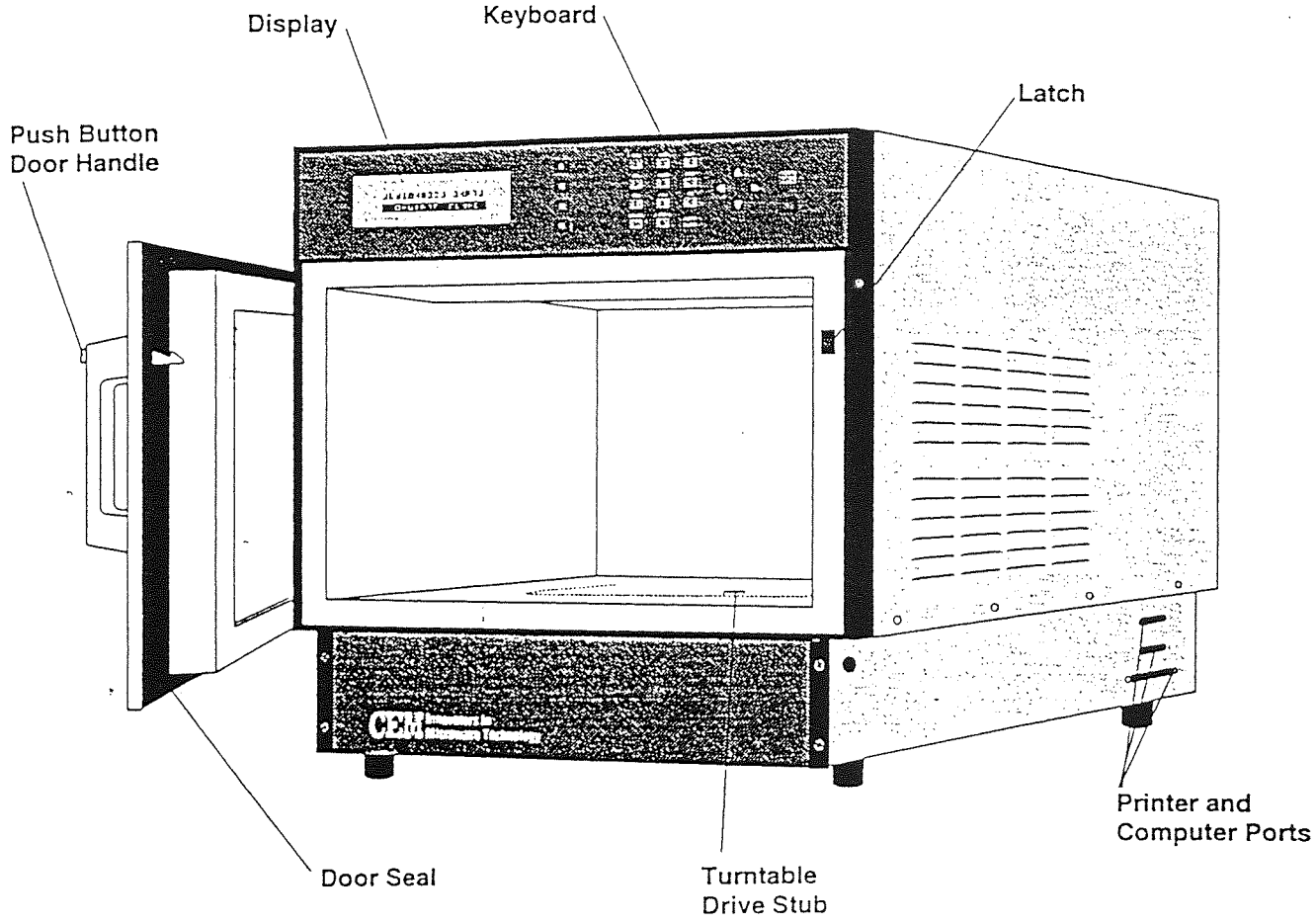

Fig2.03 MES-1000 microwave extraction system

The MES-1000 is also equipped with a pressure monitoring device and a fibreoptic temperature probe. Heating stops when a set temperature or pressure is attained - effectively the pressure monitor acts as a baristat and the temperature monitor as a thermostat.

The reaction vessel used in conjunction with the MES-1000 is manufactured from teflon and encased in an Ultem* polyetherimide outer body and cap. The cap has three outlets - the first of these is located at the top of the cap and is for the thermowell which holds the fibreoptic probe. The other two outlets for the pressure sensing line and the rupture membrane are both located at the side of the cap. At temperatures below 250°C the vessel is resistant to attack from most chemicals. The vessel, encased in the polyetherimide sleeve - which is also transparent to microwaves - can be used at temperatures up to 200°C and pressures up to 200 psig or 1279 kPa (although a lower pressure limit is recommended, because the pressure can fluctuate very rapidly by ± 5 - 10 psig resulting in rupture of the pressure membrane, which is not designed to handle pressures over 200 psig).

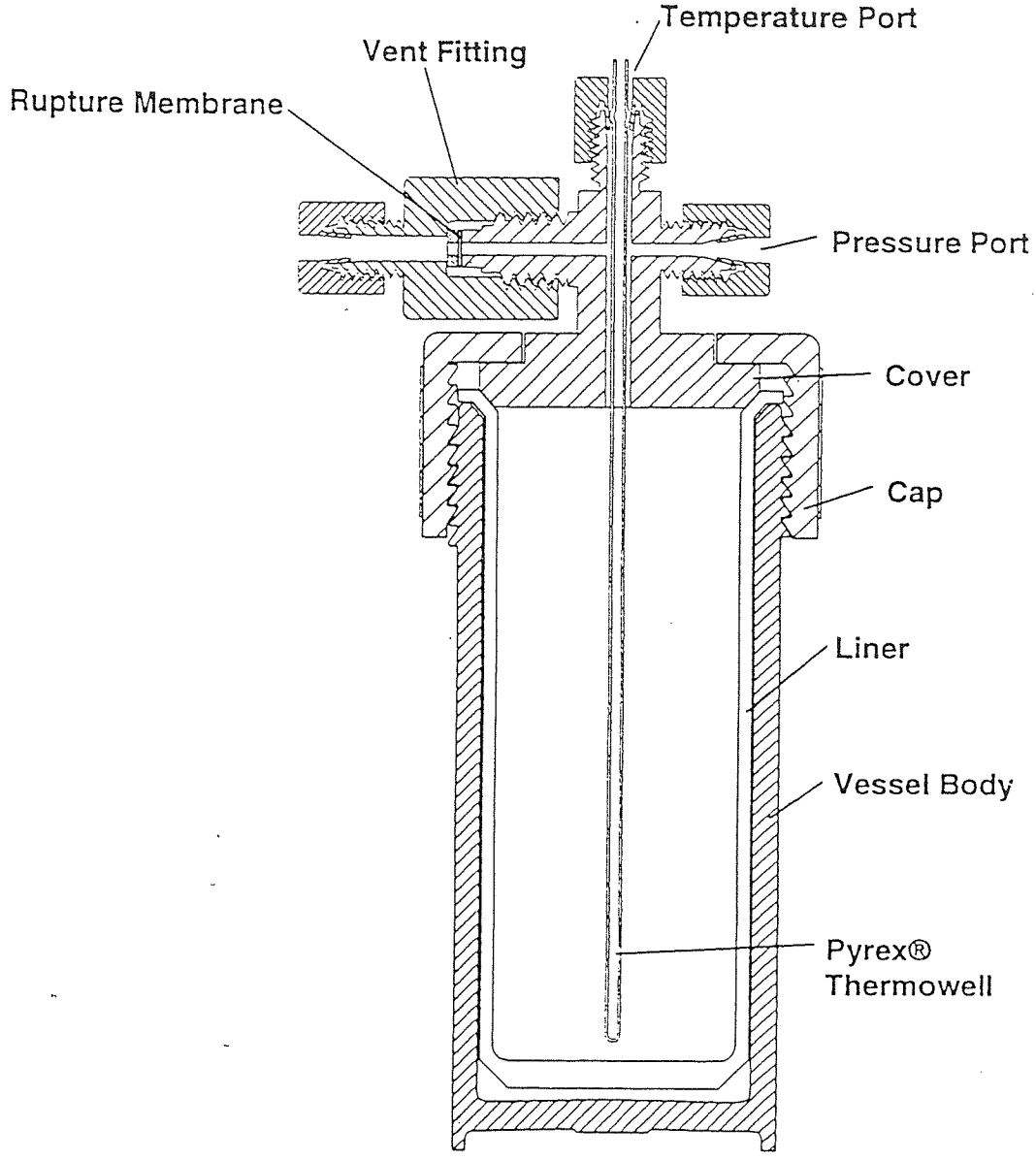

Fig2.04 Microwave reaction vessel for temperature and pressure control

The pressure is controlled by an onboard pressure control system. Tubing is attached to the sample vessel and routed outside the microwave cavity through one of the inlet / outlet ports. The pressure is sensed by a transducer and displayed graphically and digitally on the LCD display screen. A feedback signal to the system's magnetron regulates microwave power output to maintain the selected pressure.

The temperature control system consists of a fibreoptic probe (which is microwave immune) inserted into a Pyrex thermowell located in the control vessel. This is fed to a temperature control board mounted on the system CPU board outside the microwave cavity. Again, a feedback signal to the system's magnetron regulates microwave power output to maintain the selected temperature. The temperature sensor is a phosphor located at the tip of the probe.

The notable advantage of using this microwave control system over a domestic microwave is that the user has precise control of operating conditions i.e temperature and pressure, thereby introducing a whole new set of reaction parameters. The safety considerations are also greatly enhanced by the presence of a solvent detection system, the pressure rupture membrane, a cavity exhaust fan, the polyetherimide sleeve, three door safety interlocks and an interlock monitoring system to prevent microwave emissions when the door is open, and the fine control over reaction conditions.

*Ultem is a registered trademark of the General Electric Company.

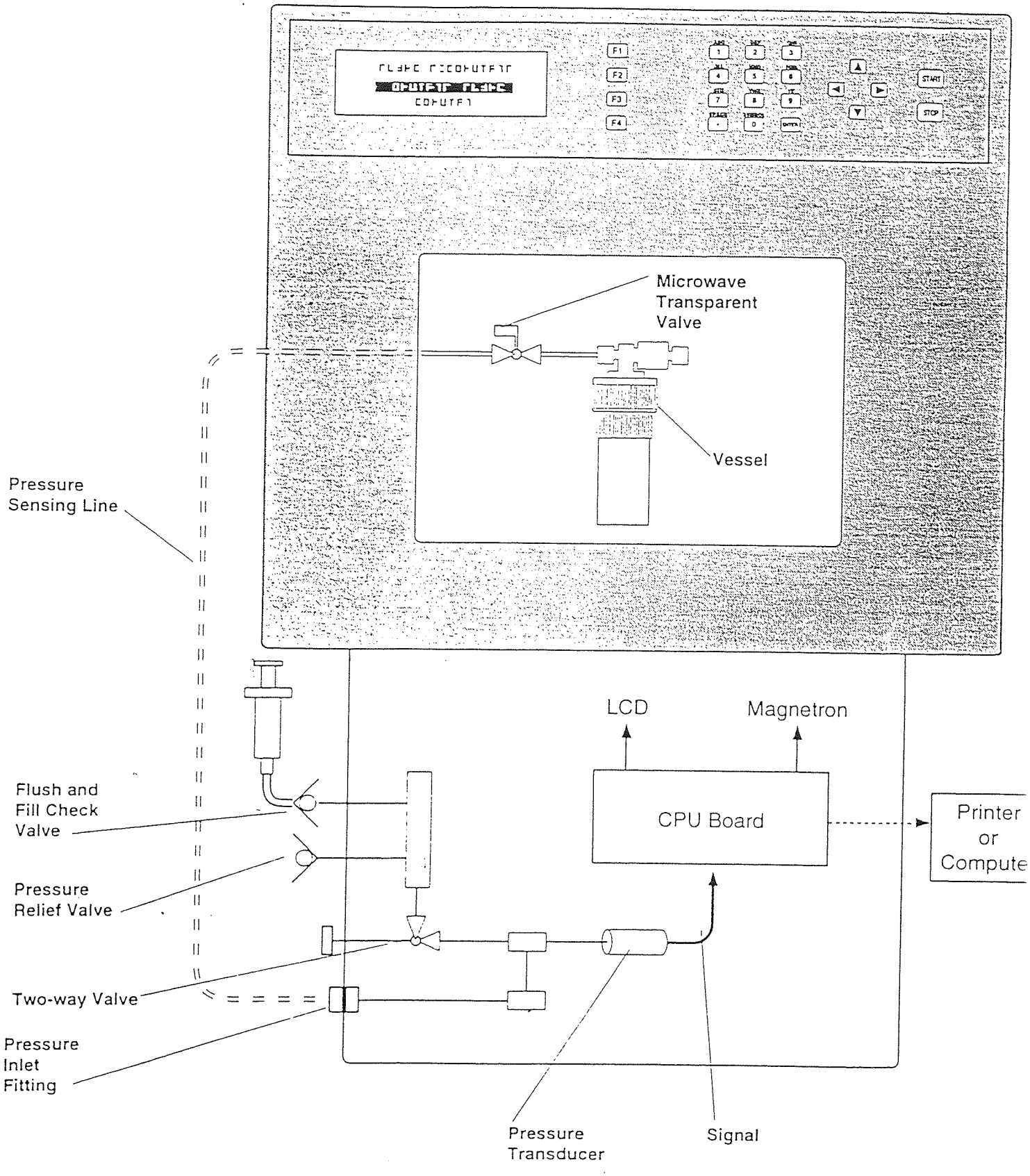

Fig2.05 Schematic representation of the pressure control system

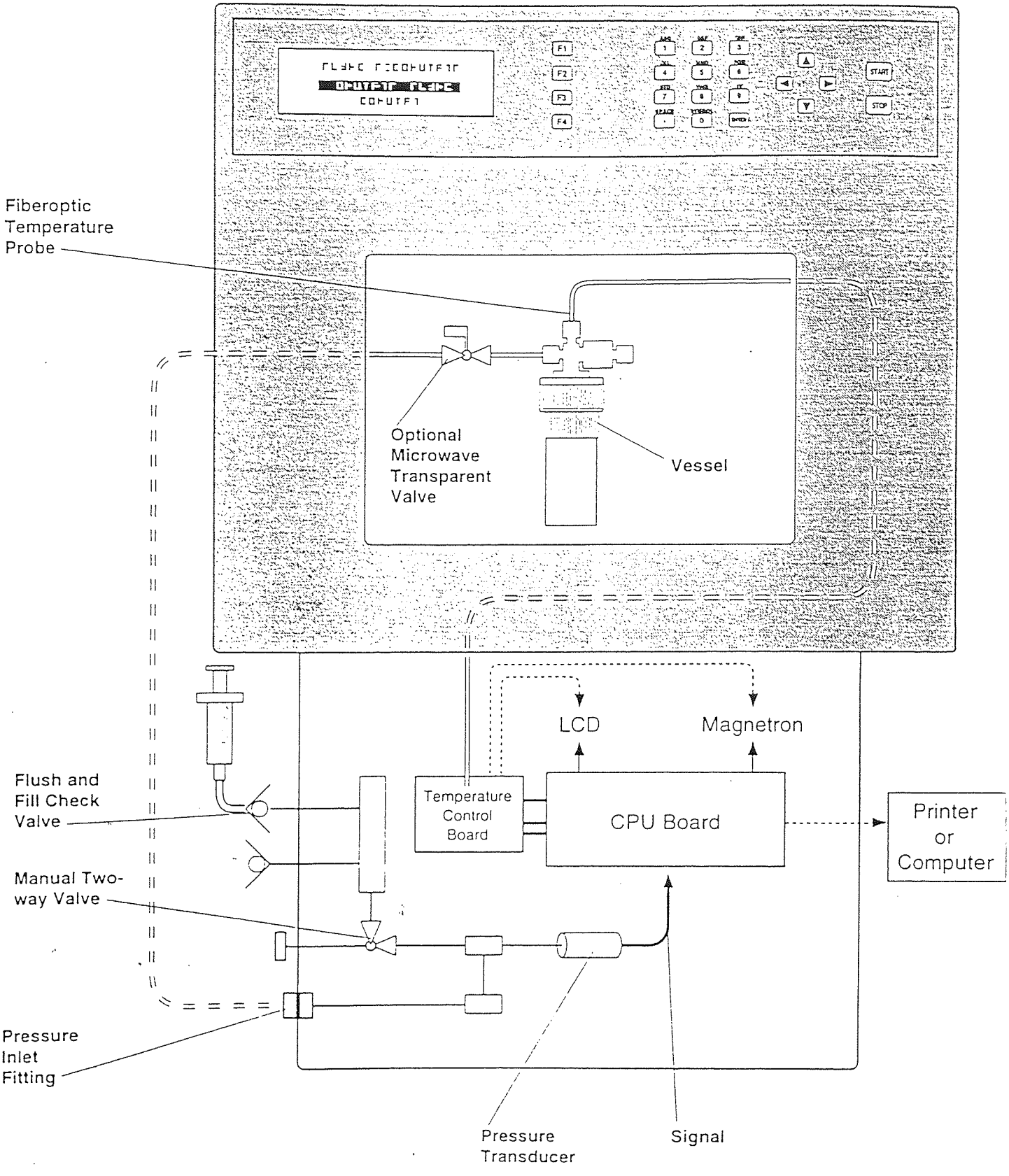

Fig2.06 Schematic representation of the temperature control system

2.2.4 Microwave procedure

(a) Sharp Carousel II R-84801

The reactants were weighed into the teflon digestion vessel and the lid was screwed on and tightened using the capping stations. The containment vessel was then placed in the microwave cavity. The power level was set at a medium-high level and the reactants were subjected to one minute bursts of microwave irradiation followed by subsequent cooling in a beaker of cold water - care should be taken to ensure that the level of the water in the beaker does not go near the 'lip' of the digestion vessel, as this can lead to water entering the digestion vessel and contaminating the reaction products. This procedure was repeated until the reaction had proceeded to completion. After completion of the reaction the digestion vessel was allowed to cool, before the cap was opened using the capping stations. The reason for this procedure is to ensure that the gas pressure inside the container has reduced to a safe level. If the cap were to be opened without cooling i.e straight after a reaction, there would be a large venting of high pressure heated gas, which could burn, blind or scald the operator!

It should be noted here that the microwave reaction times indicated in the results and derivatisation chapters refer to the time spent only in the microwave i.e not the total time of microwave heating plus the digestion vessel cooling time.

(b) CEM-1000 Microwave System

The reactants were weighed into the open teflon vessel and the vessel was placed in its polyetherimide sleeve. Next the cap was screwed on hand-tight and the apparatus was placed inside the microwave cavity. The pressure sensing line, pressure rupture line and fibreoptic probe were then attached to the containment vessel. A 'test' rotation of the turntable was initiated to ensure that the lines did not cross over or entangle themselves, before the parameters were programmed into the computer and the reaction started. With this procedure there was no need for cooling of the reagents after subsequent bursts of microwave irradiation, because of the in-built safety features of the CEM-1000.

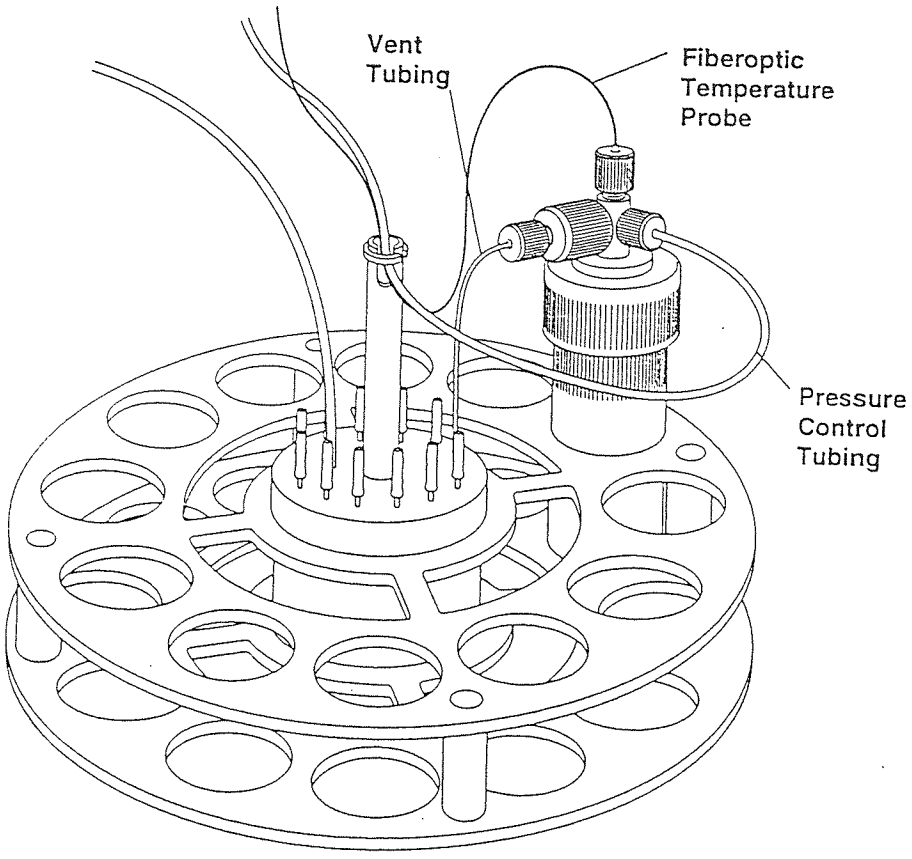

Fig2.07 MES-1000 Reaction vessel linked up with temperature and pressure monitoring devices

2.3 MODEL COMPOUNDS

The model compounds used in this study consisted of di- and tri-substituted phenols with varying degrees of steric hindrance. They were supplied by the Aldrich Chemical Company. The model compounds were :

1) 2,6-dimethylphenol (99+% purity)
2) 2,6-diisopropylphenol (97% purity)
3) 2,6-di-tert-butylphenol (99+% purity)
4) 2,6-diphenylphenol (97% purity)
5) 2-phenylphenol (99+% purity)
6) 2,4,6-tri-tert-butylphenol (96% purity)

Subsequently phenolic resins were also used as model compounds, because these were thought to give a closer approximation to the structure of the coal compared to the phenolic compounds above. The phenolic resins were synthesised under the supervision of Dr Colin Snape at the University of Strathclyde, Scotland. Three phenolic resins were supplied :

1) 1 : 1 Phenol-formaldehyde resin
2) 1 : 1 2,6-di-tert-butylphenol : phenol co-resite
3) 3 : 1 Phenol : 2,6-di-tert-butylphenol co-resite

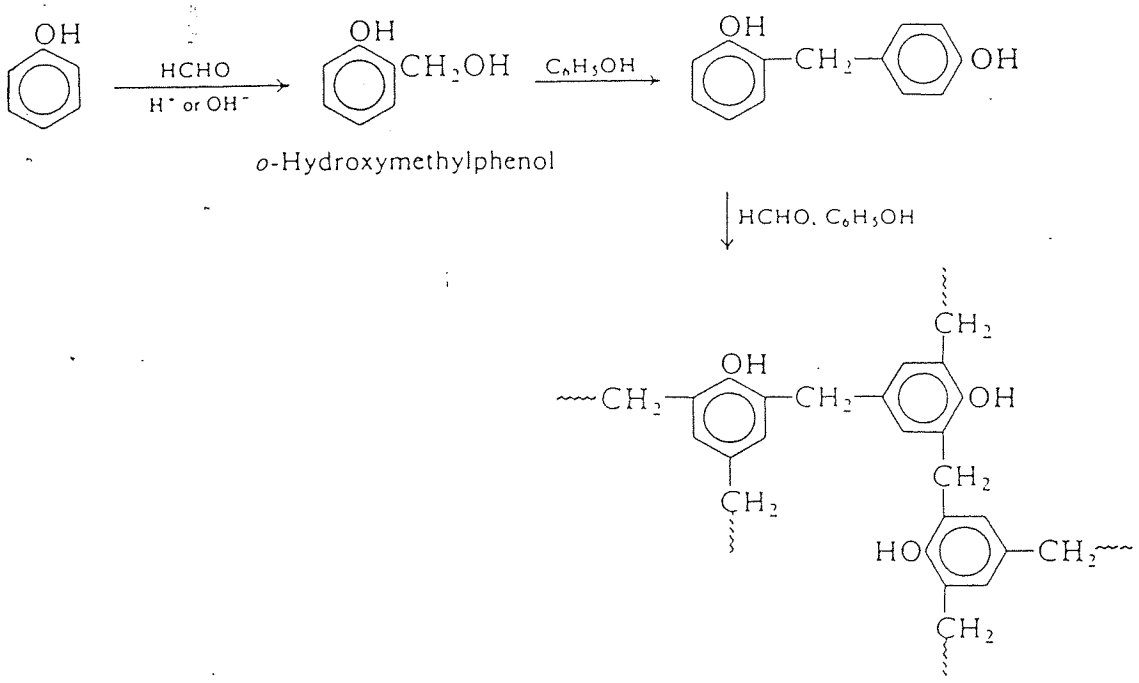

Fig2.08 Synthesis of phenol-formaldehyde resin

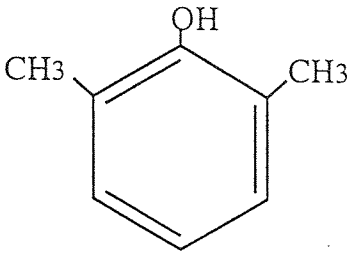

2,6-dimethylphenol

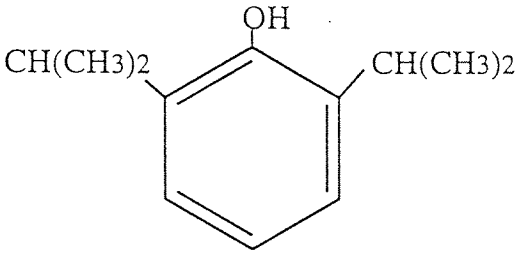

2,6-diisopropylphenol

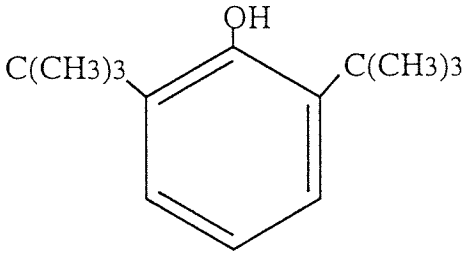

2,6-di-tert-butylphenol

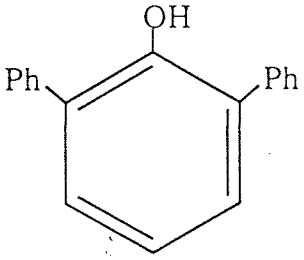

2,6-diphenylphenol

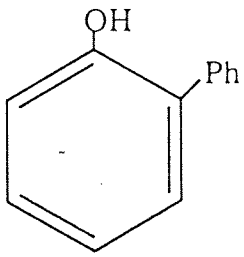

2-phenylphenol

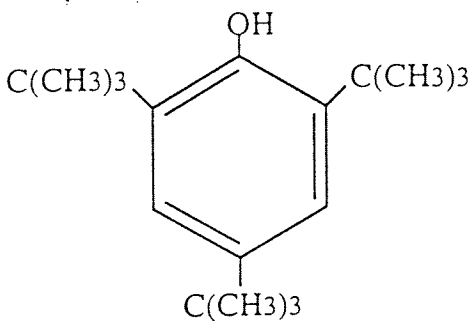

2,4,6-tri-tert-butylphenol

Fig2.09 Di- and tri-substituted model compounds

2.4 DRYING OF COALS

The coals and coal macerals were dried by heating at 110°C under a dry N_2 atmosphere, for at least 24 hrs, in a Gallenkamp dryer. After drying of the coals and coal macerals there was a significant reduction in the -OH stretching band at 3200 - 3600 cm^{-1} in the FT-IR spectrum indicating adsorbed moisture had been removed from the samples. One of the problems associated with the drying of coals and coal macerals is that it is very difficult to remove tenaciously held moisture, such as water-of-constitution associated with silicates, from within the coal matrix - consequently, there is a possibility that small amounts of residual moisture will still remain even after prolonged periods of drying.

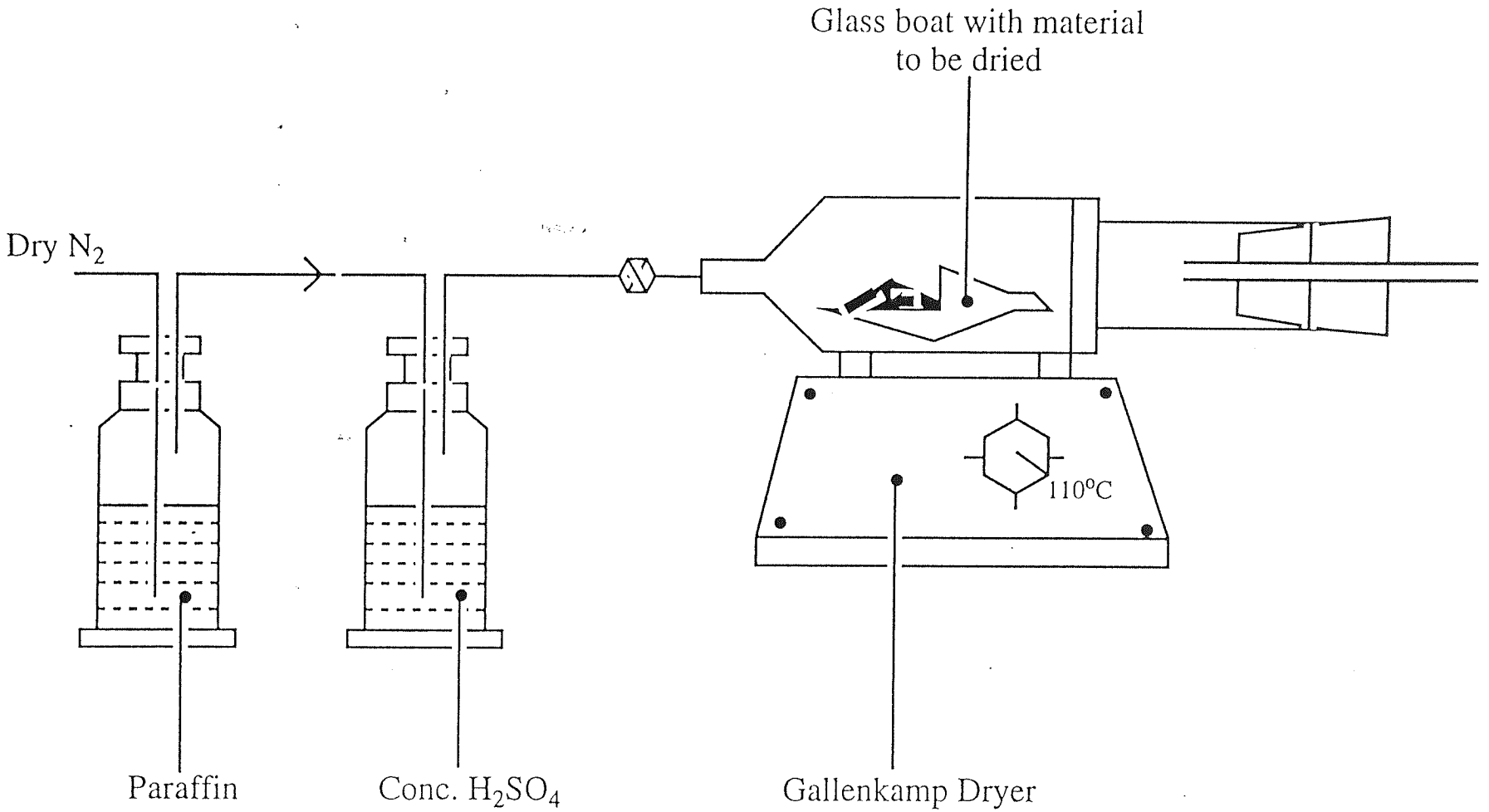

Fig2.10 Drying of coal and coal macerals

2.5 SEPARATION OF COAL MACERALS

It is possible to separate coal macerals because different bulk macerals have different relative densities i.e separation can be effected by using gravitational methods. The coals were ground down using a dry grinding technique at the Coal Research Establishment (CRE). This involved first breaking up the large chunks of coal in a "jaw-crusher" followed by fine grinding in a gyro-mill until the desired particle size was obtained, the coal was then passed through a 32 μm sieve. It was important to grind down the coal as finely as possible for two reasons :

(a) to liberate as much mineral matter as possible (as this would have an effect on the overall density of the macerals)

(b) to effectively disassociate the individual macerals and reduce the relative amounts of bi- and tri-macerals

The instrument used for the separations was the Jouan CR4-22 centrifuge equipped with an internal thermostat. Each cycle was operated at 4000 rpm for 1 hr at a temperature of 16°C. The rotor radius on the centrifuge was 185 mm.

40g of the ground coal was weighed into a beaker and 800 cm^3 of the appropriate density solution was added to give 20% w/v dispersion (the solution densities were made up using combinations of two of the following solvents : cyclohexane d=0.779 1,2-dichloroethane d=1.256 and carbon tetrachloride d= 1.594). The mixture was stirred and the beaker was then placed in an ultrasound bath for 5 mins to ensure that most of the coal particles were discrete.

The solution was then equally divided up and weighed (to 2 dp) into 4 stainless steel centrifuge tubes and placed in the centrifuge. After checking that there was no imbalance due to the tubes, the programmed cycle was switched on. On completion of the cycle the liquid layer was decanted from the centrifuge tubes and filtered using a Hartley funnel under vacuum (No.1 Whatman filter paper was used). The filtered coal was then placed in an oven at approximately 80°C at -1bar to dry overnight.

The next density solution was then prepared and used to wash out the precipitated coal from the centrifuge tubes into a beaker. The volume was made up to 800 cm^3 and the beaker was again placed in an ultrasound bath for 5 mins. The procedure was then repeated as outlined above and so on for subsequent density separations. This cycle was repeated 3 - 4 times for each coal to build up appreciable amounts of each maceral.

The density fractions were specific gravity : < 1.25 (exinite / liptinite), 1.25 - 1.35 (vitrinite), 1.35 - 1.45 (inertinite), 1.45 - 1.55 (fusinite and mineral matter) and > 1.55 (heavier mineral matter). The like-maceral fractions from each run were collected together and analysed using reflectance measurements (see Chapter 4).

2.6 STANNYLATION PROCEDURE

2.6.1 Stannylation with tributyltin chloride

(a) microwave method

2.26g 2,6-dimethylphenol was added to 5 cm^3 tributyltin chloride and 5 cm^3 acetonitrile (the microwave receptor) in a teflon digestion vessel. The digestion vessel was then heated using microwave radiation. The acetonitrile was rotary evaporated off and the sample analysed by FT-IR.

(b) reflux method

2.26g of 2,6-dimethylphenol was added to 5 cm^3 tributyltin chloride and 5 cm^3 acetonitrile in a 50 cm^3 round-bottomed flask. The solution was then refluxed for 4 days on a stirrer-hotplate, followed by rotary evaporation of the acetonitrile and analysis by FT-IR.

2.44g of 2,6-dimethylphenol was added to 3.3 cm^3 tributyltin chloride and 20 cm^3 toluene in a 50 cm^3 round-bottomed flask. The solution was refluxed for 4 days on a stirrer-hotplate, followed by rotary evaporation of the toluene and analysis by FT-IR.

2.6.2 Stannylation with bis-tributyltin oxide (TBTO)

(a) microwave method - model compounds

20 mmol of the sterically-hindered phenolic compound was put into a teflon digestion vessel, along with 12 mmol (an excess) of the stannylating reagent bis-tributyltin oxide (TBTO). The microwave receptor - either 10 cm^3 acetonitrile or 5 cm^3 acetonitrile + 5 cm^3 toluene - was then added and the digestion vessel was sealed shut using the capping stations. The sample was then subjected to bursts of microwave radiation with intermittent cooling. The acetonitrile (and toluene) and water (if produced) were then distilled off using a Heidolph VV2000 rotary evaporator and the product was cooled and analysed.

(b) microwave method - coal samples

1.0g of coal along with 5 cm^3 TBTO (stannylating reagent) and the microwave receptor - either 10 cm^3 acetonitrile or 5 cm^3 acetonitrile + 5 cm^3 toluene - were placed in the digestion vessel. The vessel was then sealed and subjected to bursts of microwave radiation with intermittent cooling to prevent the pressure building up to dangerously high levels. On completion of the reaction, the sample was cooled and the coal was filtered using a No.4 sintered-glass crucible under suction filtration and washed with toluene or acetonitrile. Finally the coal was dried (in a glass boat) by placing it in a Gallenkamp dryer at approximately 110°C over dry nitrogen and leaving it overnight.

(c) reflux method - model compounds

20 mmol of the sterically-hindered phenolic compound was weighed into a 50 cm^3 round-bottomed flask, along with 12 mmol (an excess) of TBTO (the stannylating reagent). Next 20 cm^3 of toluene solvent was added and the round-bottomed flask was fitted with a Dean-Stark trap and a condenser. The mixture was then refluxed using a stirrer-hotplate for the appropriate time (usually 2 hrs). The product was then cooled and analysed.

(d) reflux method - coal samples

1.0g of coal was weighed into a 50 cm^3 round-bottomed flask along with 5 cm^3 of TBTO and 20 cm^3 of toluene. The round-bottomed flask was fitted with a Dean-Stark trap and a condenser and the mixture was then refluxed using a stirrer-hotplate for the appropriate time (usually 24 hrs). The coal was then filtered using a sintered-glass crucible No.4 under suction filtration and washed with toluene. Finally the coal was dried (in a glass boat) by placing it in a Gallenkamp dryer at approximately 110°C over dry nitrogen and leaving it overnight.

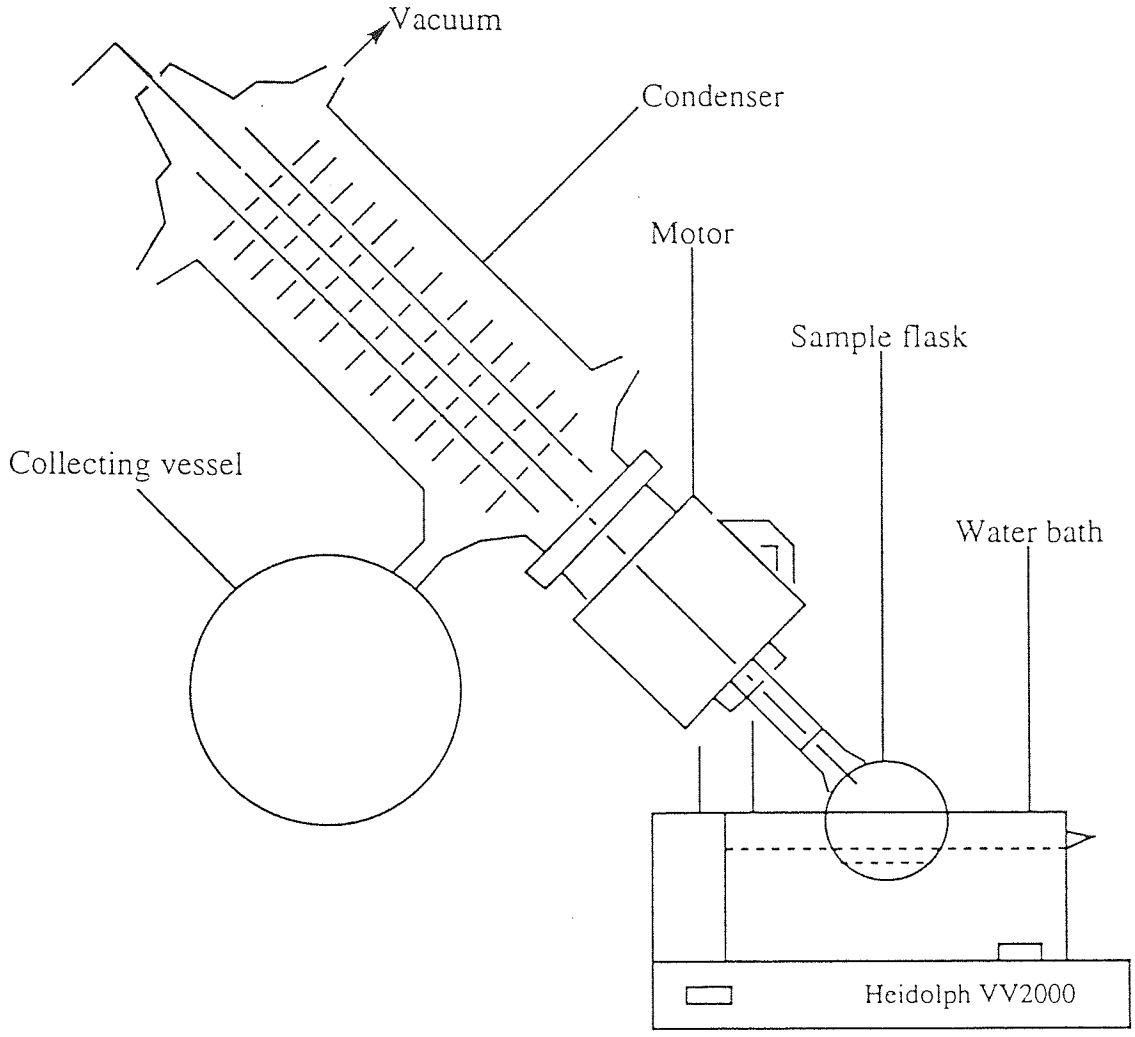

Fig2.11 Rotary evaporation of derivatised coal

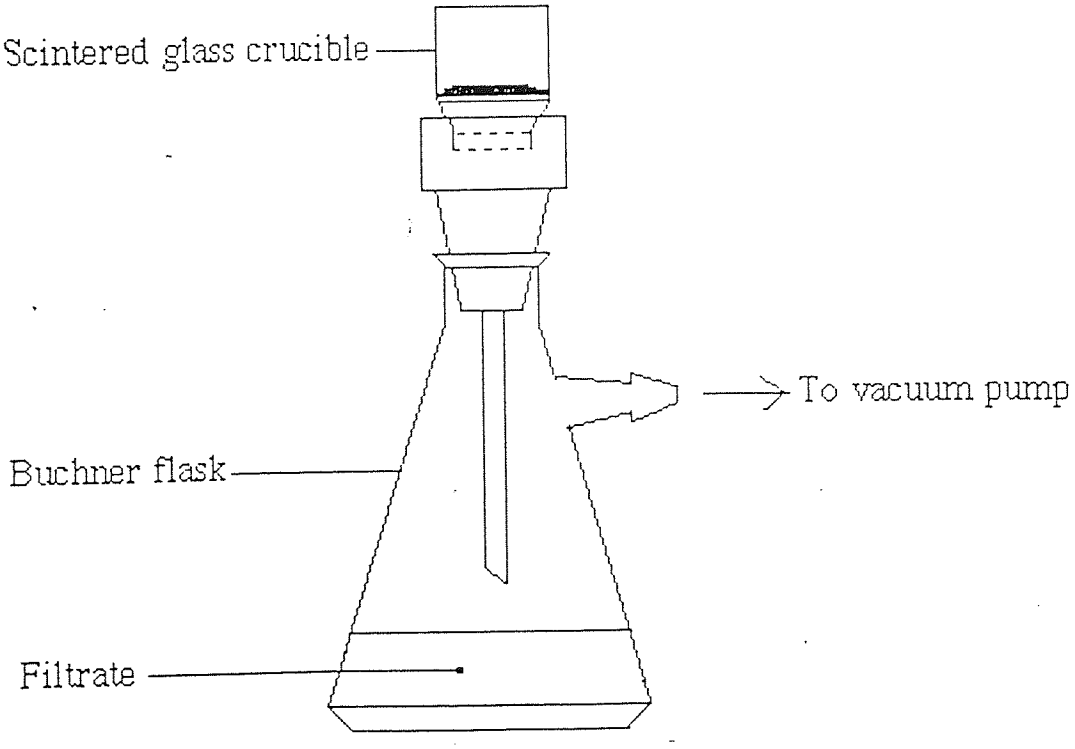

Fig2.12 Filtration of derivatised coal

2.7 ACETYLATION PROCEDURE

2.7.1 Acetylation of coal - classical method

0.5g of the coal was acetylated using a mixture of 3.3 cm^3 acetic anhydride $(CH_3CO)_2O$ and 6.7 cm^3 pyridine C_5H_5N. The reagents were put into a round-bottomed flask fitted with a condenser and refluxed using a stirrer-hotplate for the appropriate time. The contents were then poured onto distilled water, stirred and the acetylated coal filtered off. The precipitate was then washed thoroughly until the effluent was free of acid, as indicated by litmus paper, and dried at 100°C under a dry N_2 blanket overnight. The measurement of the acetyl groups in the acetylated coal, and hence the amount of hydroxyl groups in the original sample, was determined by alkaline hydrolysis followed by acidification, distillation and titration of the liberated acetic acid. The distillation was carried out stepwise until the titre reached a blank value.

The dried acetylated coal (0.10g) was hydrolysed by refluxing with 10 cm^3 of 0.3M barium hydroxide solution (barium hydroxide is quite insoluble in water and should be made up using lukewarm water just before required) for the appropriate time (usually 24 hrs). After cooling, the reaction mixture was filtered, acidified with a few drops of phosphoric acid (H_3PO_4) and distilled. After 20 cm^3 of distillate had been collected it was titrated against 0.1015N NaOH using phenolpthalein indicator - the solution went from colourless in the presence of acid to pink when the solution was neutral. The procedure was then repeated several times by adding 20 cm^3 aliquots of distilled water and continuing the distillation until a constant titre, equal to the blank titre, was obtained. The titrations were carried out using an Interflon 5.0 cm^3 micro burette. The respective titres were then added together to give the total titre, from which the acetyl content of the coal was calculated.

2.7.2 Acetylation of coal - microwave method

0.5g of the coal was acetylated using a mixture of 3.3 cm^3 acetic anhydride $(CH_3CO)_2O$ and 6.7 cm^3 pyridine C_5H_5N. The reagents were put into a teflon digestion vessel with the cap sealed, placed in the microwave cavity and subjected to microwave radiation for the appropriate reaction time. The contents were then poured onto distilled water, stirred and the acetylated coal filtered off. The precipitate was then washed thoroughly until the effluent was free of acid, as indicated by litmus paper, and dried at 100°C under a dry N_2 blanket overnight. The measurement of the acetyl groups in the acetylated coal, and hence the amount of hydroxyl groups in the original sample, was determined by alkaline hydrolysis followed by acidification, distillation and titration of the liberated acetic acid. The distillation was carried out stepwise until the titre reached a blank value.

The dried acetylated coal (0.10g) was hydrolysed either in the microwave oven by adding 10 cm^3 0.3M barium hydroxide to the coal in the containment vessel and subjecting the heterogeneous mixture to microwave radiation or by reflux (see 2.7.1). After cooling, the reaction mixture was filtered, acidified with a few drops of phosphoric acid (H_3PO_4) and distilled. After 20 cm^3 of distillate had been collected it was titrated against 0.1015N NaOH using phenolpthalein indicator - the solution went from colourless in the presence of acid to pink when the solution was neutral. The procedure was then repeated several times by adding 20 cm^3 aliquots of distilled water and continuing the distillation until a constant titre, equal to the blank titre, was obtained. The titrations were carried out using an Interflon 5.0 cm^3 micro burette. The respective titres were then added together to give the total titre, from which the acetyl content of the coal was calculated.

2.8 SILYLATION PROCEDURE

The sample to be silylated (1.0g resin / 0.5g coal) was first dried overnight in the Gallenkamp dryer at 110°C over dry N_2. The sample was then weighed into a teflon digestion vessel along with 2 cm^3 N-(trimethylsilyl) imidazole (TMSI) and 8 cm^3 acetonitrile (CH_3CN) and heated in the microwave. Microwave heating times varied depending on the sample. After reaction the sample was filtered using a No.4 sintered-glass crucible, washed thoroughly using dry acetonitrile and dried overnight at 110°C over dry N_2 in the Gallenkamp dryer.

2.9 METHYLATION PROCEDURE

2.9.1 Method 1 - methyl iodide

The sample (3.26 mmol phenolic compound) and 6.52 mmol of silver tetrafluoroborate ($AgBF_4$) were dissolved, with stirring, in 11.0 cm^3 of dichloroethane under an inert atmosphere of argon. The methyl iodide (6.52 mmol) was then introduced via a syringe and the mixture was left to stir overnight. On completion of the reaction the mixture was filtered and washed with an excess of acetonitrile. The filtrate was then rotary evaporated to remove the solvent and the residue (if a solid) was dried overnight at 110°C over dry N_2.

2.9.2 Method 2 - methyl formate

The dried sample (10 mmol phenolic compound) was added to 50 mmol methyl formate ($HCOOCH_3$), 0.30 mmol cetyltrimethylammonium bromide catalyst and 7 cm^3 acetonitrile solvent. For the microwave method the reagents were put into a sealed teflon digestion vessel, placed in a microwave and irradiated with microwaves (usually for 30 mins). The bench top method involved refluxing the reagents (usually for 24 hrs). On completion of reaction the sample was rotary evaporated or filtered and washed with acetonitrile, depending on whether a solution or solid in solution were obtained.

2.9.3 Method 3 - phase transfer

10 mmol of the phenolic compound, 20 mmol of 0.2M sodium hydroxide solution and 20 mmol of methyl iodide were placed in a separating funnel to give two immiscible layers. 1.0 cm^3 of 15-crown-5 ether was then added and the mixture was agitated and left to stand for two days. After two days the mixture was separated and silver nitrate ($AgNO_3$) was added to the aqueous solution to see how much silver iodide (AgI) precipitated. The layer containing the methylated phenol compound was rotary evaporated to isolate the product.

STANNYLATION

3.1 INTRODUCTION

The hydroxyl group, and in particular the phenolic group (which constitutes the bulk of the hydroxyl functionality in middle rank coals) is one of the more abundant oxygen-containing functional groups in coal. Consequently it has a significant influence on the behaviour and properties of coal during processes such as hydroliquefaction - the nature, degree of hydrogen bonding (polarity) and the amount of hydroxyl functionality present are all factors which have a bearing on the quality of products obtained, and a knowledge of these characteristics can give a useful indication as to which solvent(s) are suitable for the solubilisation processes.

Much work has been done in the past on attempting to gain a comprehensive insight into the distribution and nature of these hydroxyl groups in coals (section 1.7.2). Most of these methods involve multi-step derivatisation of the hydroxyl functionality with the appropriate reagents.

One group of reagents which have been utilised in the determination of hydroxyl functionalities in coal are those derived from Group 14 elements. Silylation work[28,42] has been carried out with some success, resulting in the quantitative derivatisation of some of the more hindered phenolic groups in coal. The derivatising reagent favoured in these cases is the trimethylsilyl- reagent.

Work has also been carried out using organotin reagents. John Larsen et al[60] (1982) developed a method for incorporating ^{119}Sn into coal for the purpose of structural elucidation. The procedure involves refluxing the sample with bis(tributyltin) oxide $(n\text{-}Bu_3Sn)_2O$ in toluene solvent followed by subsequent analysis via Mössbauer spectroscopy. The work concluded that, for Illinois No.6 and Rawhide (Wyodak) - both low rank coals with appreciable amounts of oxygen - nearly all the reacted tin had a trigonal bipyramidal structure. For this type of structure to exist it was proposed that a heteroatom was in close proximity to both the derivatised hydroxyl group and the tin, and that this heteroatom co-ordinated directly with the tin. From these conclusions it can be inferred that the hydroxyl groups (for the coals studied) were paired with heteroatoms and the nature of this pairing in the solid coal was in the form of hydrogen bonding.

Further work was carried out by Esfandir Raffi et al[61] on the characterisation of phenols from coal liquefaction products by using ^{119}Sn nuclear magnetic resonance spectroscopy. Raffi and his co-workers succeeded in stannylating 33 phenols (as well as some alcohols, thiols and thiophenols) by using the bis(tributyltin) oxide (TBTO) reagent in toluene solvent.

Table 3.01

^{119}Sn chemical shifts for TBTO derivatives for several phenols and selected thiols and alcohols[61]

Compound	$\delta(^{119}Sn)^a$ ppm
2-chlorophenol	124.7
α-naphthol	118.4
2-phenylphenol	115.5
β-naphthol	114.9
4-chlorophenol	114.3
4-phenylphenol	111.4
2,6-dimethylphenol	109.0
phenol	108.2
2-methylphenol	108.0
4-tert-butylphenol	108.0
4-methylphenol	107.0
2-ethylphenol	106.8
3-ethylphenol	106.8
2,5-dimethylphenol	106.5
4-methoxyphenol	106.2
4-ethylphenol	106.0
2,3-dimethylphenol	105.9
2,4,6-trimethylphenol	105.6
3-methylphenol	105.5
3,5-dimethylphenol	104.8
2-isopropylphenol	104.8
4-isopropylphenol	104.8
3,4-dimethylphenol	104.7
2,3,5-trimethylphenol	104.5
5-isopropyl-2-methylphenol	104.3
2,4-dimethylphenol	103.6
2-isopropyl-5-methylphenol	103.2
2,4-dimethyl-6-isopropylphenol	102.9
2-indanol	102.7
resorcinol	102.2
2-tert-butylphenol	101.0
hydroquinone	99.6
benzyl alcohol	99.0
2-tert-butyl-4-methylphenol	98.5
cyclohexanol	92.5
1-butanol	89.8
2-octanol	81.8
thiophenol	79.5
4-methylthiophenol	77.6
2-hydroxyquinoline	75.7
benzylthiol	73.0
1-butanethiol	72.1
8-hydroxyquinoline	70.1
1-methylcyclohexanol	63.2

[a]All chemical shifts of neat liquids are reported as relative to tetramethyltin

$\delta^{119}Sn(TBTO) = 83.0$ ppm

The work in this chapter involves further research into the derivatisation of hydroxyl groups in coals and coal macerals via stannylation. Experiments were first carried out on substituted phenols, which acted as model compounds for the hydroxyl groups in coal, and then progressed to the coals and coal macerals.

The first stage of this work involved the testing and selection of suitable microwave solvents with which to carry out the microwave reactions. Five different solvents / mixtures of solvents were tested on a reaction known to work using acetonitrile and from these, two suitable solvents were selected for the microwave work.

The distribution of the microwave radiation within the microwave cavity was also mapped, thus ensuring that the reaction vessel could be positioned, such that in successive experiments it was exposed to the same microwave flux.

The next step involved work with the model compounds (di- and tri-substituted phenols). These were reacted with two different tin reagents :

(a) Tributyltin chloride Bu_3SnCl

(b) Bis(tributyltin) oxide $(n\text{-}Bu_3Sn)_2O$ (TBTO)

Tributyltin chloride and bis(tributyltin) oxide were supplied by Aldrich and both reagents were of 96% purity.

The objective was to incorporate the tin into the model compounds and use this as a magnetic label to determine the chemical shifts of the respective model compounds (with respect to a tetramethyltin standard). The isotope ^{119}Sn has a natural abundance of 8.45% compared to a ^{29}Si abundance of only 4.71%. The phenol compounds were reacted under both conventional (reflux) and microwave conditions to compare the rate and efficiency under different operating conditions.

The final step was to stannylate the four coals - Gedling and Ollerton (low-middle rank coals) and Creswell and Cortonwood (silkstone) (middle rank coals) - and the Creswell and Cortonwood macerals. The aim was to form C-O-Sn linkages with the coal -OH groups, so that investigations into the environment of the metal, and hence the hydroxyl functionality, could be carried out using spectroscopic techniques. As with the model compounds, reactions were compared using both bench top (reflux) and microwave techniques.

The TBTO reagent has a much larger steric requirement than the trimethylsilyl-derivatising reagent because of the difference in size between Sn and Si (both Group 14 elements). It is this feature of tin which may enable us to map out the steric environment of the coals, as well as affording valuable data on the -OH content. This may be done by derivatising the various hydroxyl functionalities in the coal / coal maceral using a tin reagent and then comparing the amount of derivatisation achieved via stannylation with that effected by using an alternative derivatising technique, such as silylation. Because we would expect less derivatisation for a larger reagent, we would be able to determine the proportion of more sterically-hindered groups in the sample by collating the two methods.

3.2 EXPERIMENTAL

3.2.1 Testing of microwave-receptor solvents

The five solvents / mixtures of solvents tested were :

1. Acetonitrile
2. Acetonitrile : Toluene
3. Acetonitrile : Nitromethane
4. Nitromethane : Toluene
5. Nitromethane

All the reactions were carried out in the Sharp Carousel II R-84801 with the microwave oven on a medium-high setting. The reaction involved the stannylation of 1.0g Creswell coal (particle size <500>212 μm) with 5 cm^3 TBTO and 10 cm^3 of the solvent / solvent mixture (in the case when there was a mixture of solvents, 5 cm^3 of each solvent was used giving a consistent total solvent volume of 10 cm^3). The reagents were placed in a 100 cm^3 CEM teflon digestion vessel and the cap was tightened using capping stations. The digestion vessel was then placed in the centre of the microwave turntable and microwave heating was initiated. The total microwave heating time was 5 minutes (with the sample subjected to 1 minute bursts of microwave radiation followed by 1 minute cooling by immersing the digestion vessel in a 500 cm^3 open beaker containing 250 cm^3 H_2O. This cycle was repeated until the sample had been subjected to 5 minutes of microwave heating).

The coal was then filtered and dried and analysed subjectively using FT-IR. The coal products from the most promising solvent / mixture of solvents were also analysed using solid-state ^{119}Sn MASNMR.

The distribution of microwaves within the microwave cavity of the Sharp Carousel II R-84801 was tested by heating 100 cm^3 distilled H_2O in a 250 cm^3 open beaker, placed at different positions on the turntable, for 1 minute. The initial temperature of the water was room temperature (18 °C). After 1 minute in the microwave oven, the temperature of the water was quickly measured and then plotted relative to the beaker's position on the turntable.

3.2.2 Model compounds

For FT-IR plots of the model compounds (di- and tri-substituted phenols) please refer to Appendix I.

The procedure for the stannylation of model compounds using the tributyltin chloride reagent is outlined in section 2.6.1. The microwave reaction was carried out in the Sharp Carousel II R-84801 on a medium-high setting using the 100 cm^3 digestion vessels.

The procedure for the stannylation of model compounds using the bis(tributyltin) oxide reagent is outlined in sections 2.6.2(a) and 2.6.2(c). The microwave reaction was carried out in the Sharp Carousel II R-84801 on a medium-high setting using the 100 cm^3 digestion vessels.

The products were analysed using GC, FT-IR and ^{119}Sn MASNMR.

3.2.3 Coals and coal macerals

The coals used in this study were supplied by the CRE Sample Bank*.

The procedures for the stannylation of the coals using the TBTO stannylating reagent are outlined in sections 2.6.2(b) and 2.6.2(d). The microwave reaction was carried out in the Sharp Carousel II R-84801 on a medium-high setting using the 100 cm^3 digestion vessels.

The coal macerals were separated using facilities at CRE, Stoke Orchard, as described in section 2.5, and the stannylation of these macerals is outlined in section 2.6.2(b).

The coals and coal macerals were analysed using FT-IR, ^{119}Sn MASNMR and XPS.

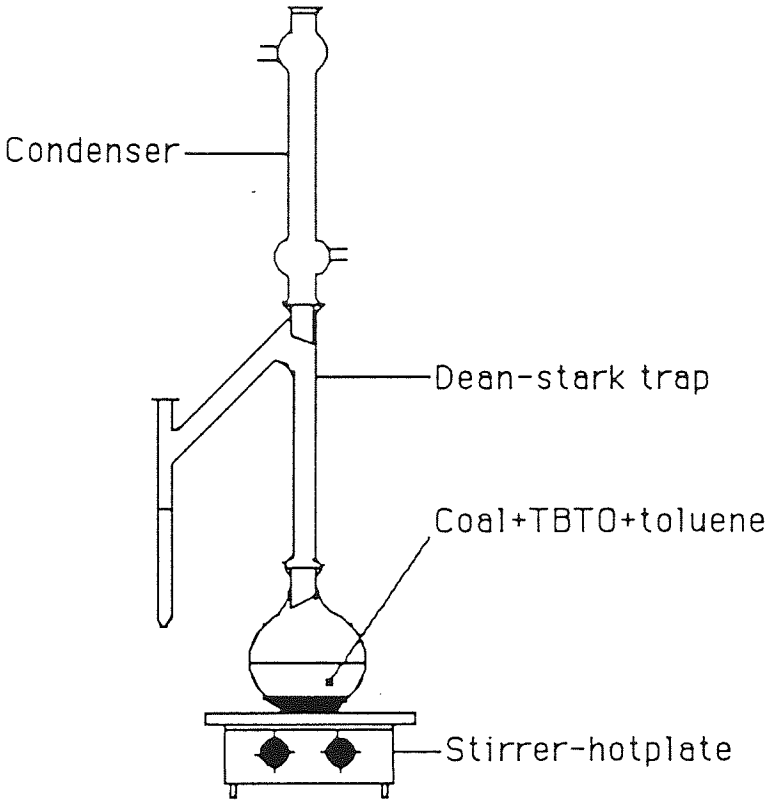

Fig 3.01

Reflux apparatus for the stannylation of coals and model compounds.

* The CRE Coal Bank was established in 1982 to supply universities and other research organisations with small quantities of representative and well characterised UK coals. By doing this it hopes to achieve comparability of results through the use of common samples and to co-ordinate research in the UK. The CRE Coal Bank currently comprises 22 coals ranging from high volatile bituminous coals to anthracite.

3.3 RESULTS AND DISCUSSION

3.3.1 Selection of microwave-receptor solvents

Before experimentation could proceed it was important to select suitable microwave solvents for both the coal and model compound reactions. Three different solvents were investigated - acetonitrile, toluene and nitromethane. Toluene was used in conjunction with both acetonitrile and nitromethane because of its low microwave receptivity. An acetonitrile / nitromethane mixture was also tested.

Table 3.02 Data on microwave-receptor solvents

microwave solvent	m.wt	b.pt °C	density (g cm^{-3})	formula	hazards
Acetonitrile	41.0	82	0.79	CH_3CN	flammable lachrymator
Toluene	92.14	111	0.87	$C_6H_5CH_3$	flammable toxic
Nitromethane	61.03	101	1.20	CH_3NO_2	toxic

The reactions were carried out as outlined in section 3.2.1 with each reaction mixture heated for 5 minutes in the microwave oven on a medium-high setting. The reaction used to test the solvents was the stannylation of 1.0g Creswell coal of particle size <500>212 μm with 5 cm^3 TBTO reagent and 10 cm^3 solvent. The reactions were carried out using the solvents / mixture of solvents shown in Table 3.03 :

Table 3.03 Selection of microwave solvents

REACTION No.	SOLVENT	VOLUME cm^3
1	acetonitrile	10.0
2	acetonitrile : toluene	5.0 : 5.0
3	acetonitrile : nitromethane	5.0 : 5.0
4	nitromethane : toluene	5.0 : 5.0
5	nitromethane	10.0

After reaction was complete the coal was filtered, dried and analysed by FT-IR. The IR spectra obtained are shown in fig 3.02 and fig 3.03. The main region of interest is where the hydrogen-bonded OH can be found - approximately 3600 - 3200 cm^{-1}. The reaction taking place is the stannylation of the hydroxyl groups in the coal by the TBTO reagent :

$$2\,R\text{-}OH + (Bu_3Sn)_2O \rightarrow 2\,R\text{-}O\text{-}SnBu_3 + H_2O$$

As can be seen from the IR spectra, reactions utilising nitromethane solvent and the nitromethane : toluene mixture of solvents did not appear to show any significant reaction, whereas the acetonitrile, acetonitrile : nitromethane and acetonitrile : toluene solvent reactions indicate that some reaction has taken place by the 'flattening' of the IR peak and / or reduction in -OH stretching frequencies in the 3600 - 3200 cm^{-1} region of the IR spectrum. The acetonitrile solvent appears to show the best extent of reaction, with a reduction in intensity of the 3600 - 3200 cm^{-1} band and the spectrum becoming more well-defined in the 'fingerprint' region (2000 - 500 cm^{-1}) - this is probably due to the reduction in hydrogen-bonding effected by stannylation. A peak at approximately 730 cm^{-1} also corresponds to a Sn-O asymmetric stretch, as found in the reagent. The acetonitrile : nitromethane reaction product was analysed by ^{119}Sn MASNMR with ^{1}H decoupling (fig 3.04), but no ^{119}Sn peaks were observed. This may be due to the fact that ^{119}Sn has long relaxation times in Creswell coal or another factor to consider is that, when this analysis was carried out, a broad band ^{119}Sn amplifier was not yet available for the Bruker AC 300, as it was for subsequent ^{119}Sn spectra - this may be the reason why the instrument had difficulty detecting the ^{119}Sn signal.

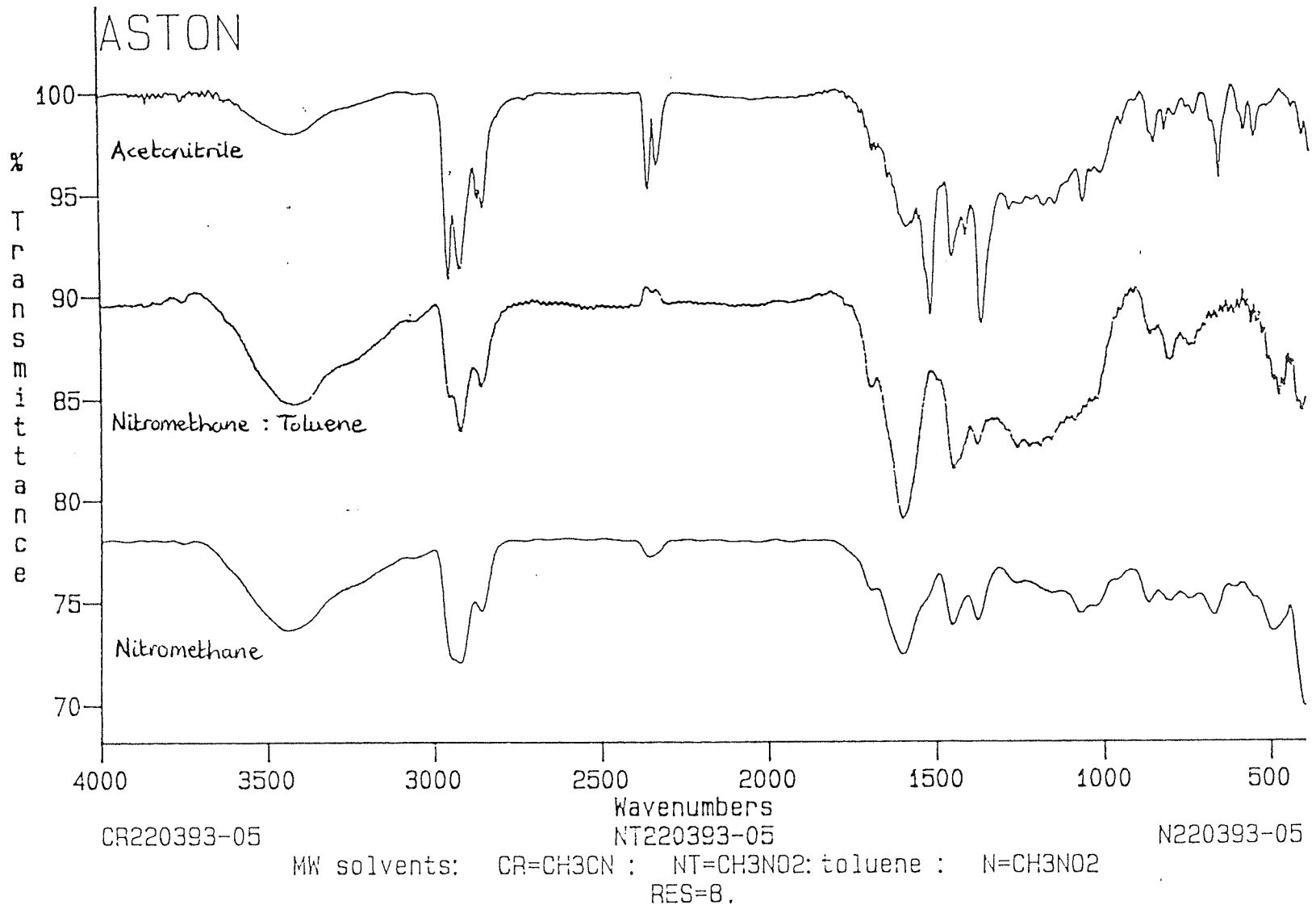

Fig3.02
IR spectra of the stannylated Creswell coal <500>212 μm using nitromethane, acetonitrile and nitromethane + toluene solvents

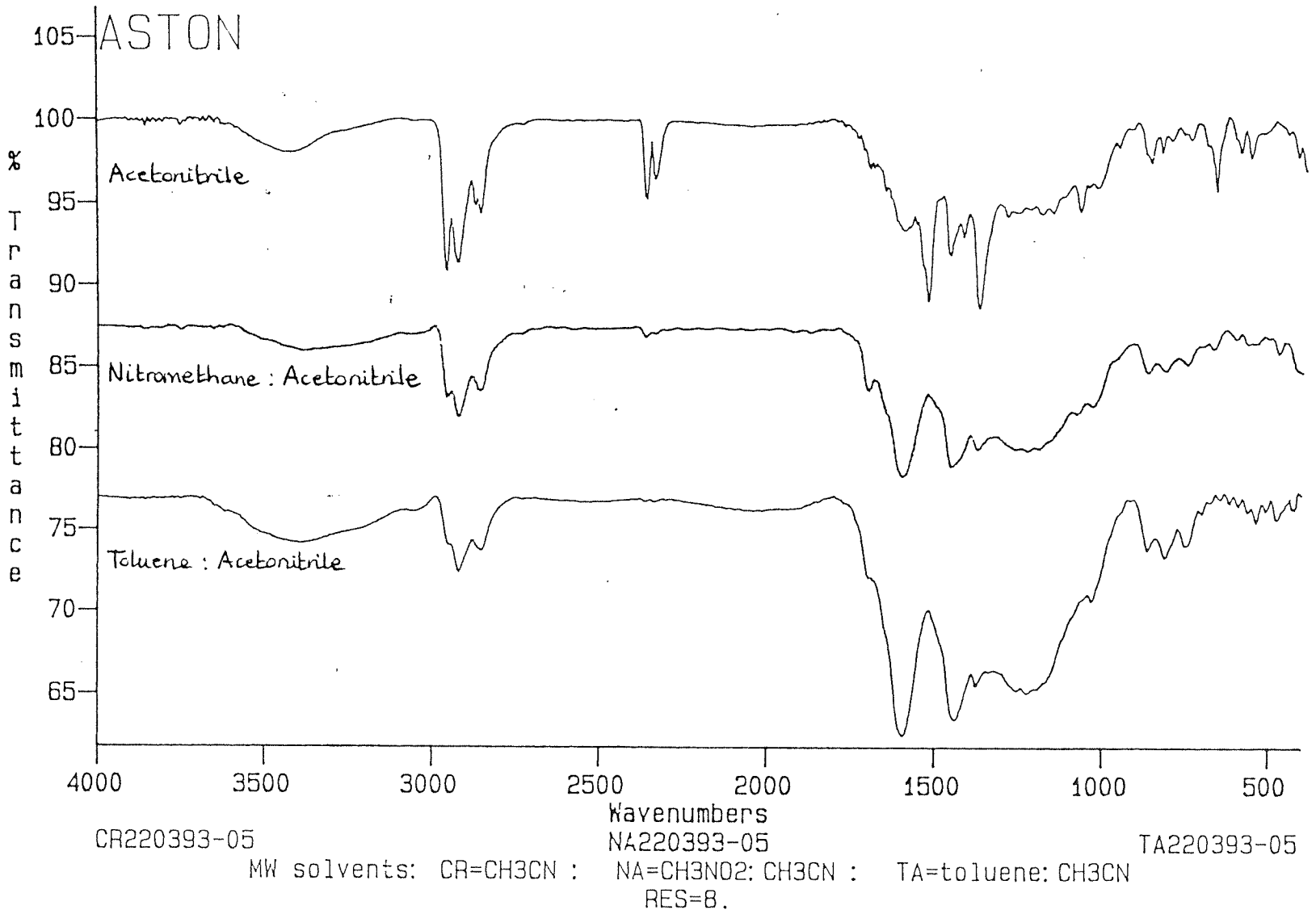

Fig3.03
IR spectra of the stannylated Creswell coal <500>212 μm
using acetonitrile, acetonitrile + nitromethane and acetonitrile + toluene

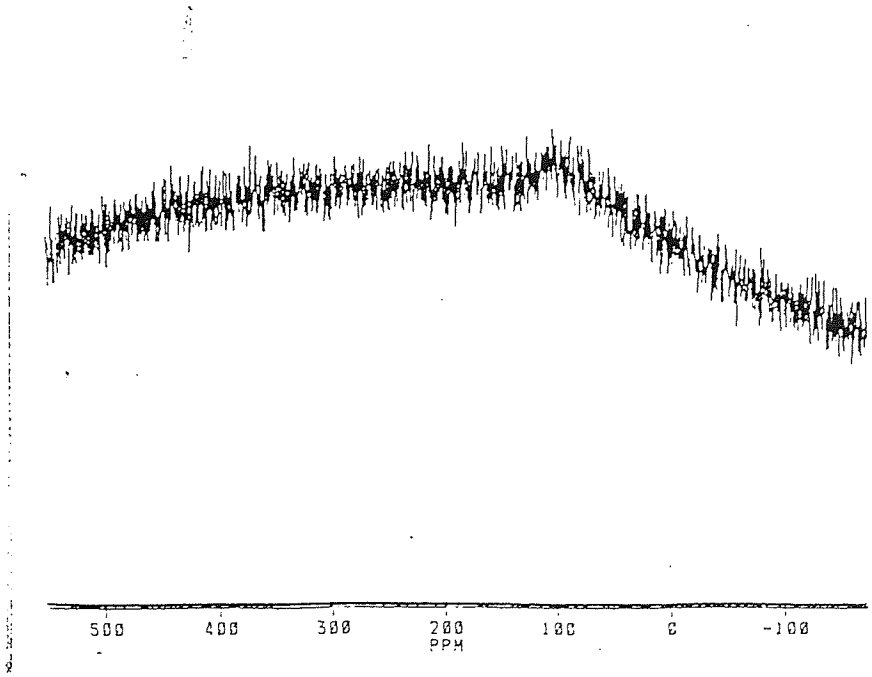

Fig3.04
^{119}Sn MASNMR spectrum of the stannylated Creswell coal <500>212 μm using acetonitrile + nitromethane solvent

A major drawback of using nitromethane (either by itself or as a mixture) is that the solvent tended to superheat very rapidly (within 10 - 20 seconds) compared to acetonitrile. This led to high temperatures and very high pressures building up in the digestion vessel. Subsequently the relief valve vented allowing the pressurised gas / solvent to escape, leaving behind less solvent for the ensuing reaction. One reason for this rapid superheating may lie with the structure of nitromethane. The nitromethane molecule is fairly acidic (pKa = 10.2) due to the fact that the conjugate base is resonance-stabilised :

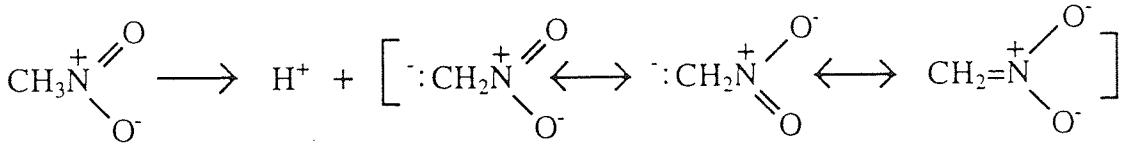

These resonance structures and the formation of the methylnitronate ion may result in the solvent being more receptive to microwave irradiation. Because of this rapid superheating of nitromethane it is necessary to cool the digestion vessel for prolonged time periods (2 - 3 minutes) after relatively short periods of microwave radiation (10 - 20 seconds) - this can be very time consuming, especially when long microwave heating times are required. Another negative factor relating to the use of nitromethane as a microwave solvent is that greater deformations occur in the digestion vessels due to the increased pressures.

After careful consideration it was decided that acetonitrile was the optimum solvent for our purposes. It has a dipole moment of 3.92 D and a dielectric constant of 36.2 (at 25°C)[62]. Rate acceleration is achieved via an Arrhenius effect due to the superheating of the solvent and the acetonitrile extracts the minimum amount of labile components from the coal under experimental conditions - previous work involving GC / MS analysis has also shown that, of the limited amount of material extracted, oxygen-containing materials constitute a negligible quantity of the extract when acetonitrile is employed as a solvent. When the appropriate reagents were not suitably soluble in acetonitrile, acetonitrile and toluene were used, with toluene acting as a mutual medium for both the reagent and the microwave receptor. It is permitted to use mixed solvents in microwave reactions as long as one is a microwave receptor and they do not interfere with the reaction pathway or each other.

3.3.2 Investigation into the distribution of microwave radiation in the microwave cavity

The microwave oven in which the testing was carried out was the Sharp Carousel II R-84801. The procedure is as outlined in section 3.2.1. Table 3.04 shows the variation in temperature relative to the beaker's starting position (the position of the beaker before microwave heating was initiated) on the turntable. Distance zero indicates the centre of the turntable, with negative numbers indicating beaker starting positions to left of the centre and positive numbers indicating beaker starting positions to the right of the centre, along the horizontal diameter of the turntable. The diameter of the turntable was 0.36 metres and testing was carried out in triplicate :

Table 3.04

Temperature of water relative to its position on the microwave turntable

Distance from the centre of the turntable (m)	Temperature from 3 consecutive runs °C
+ 0.06	56, 56, 54
+ 0.12	54, 57, 54
+ 0.18	56, 58, 55
0.00	70, 69, 69
- 0.06	54, 57, 56
- 0.12	56, 53, 54
- 0.18	55, 56, 56

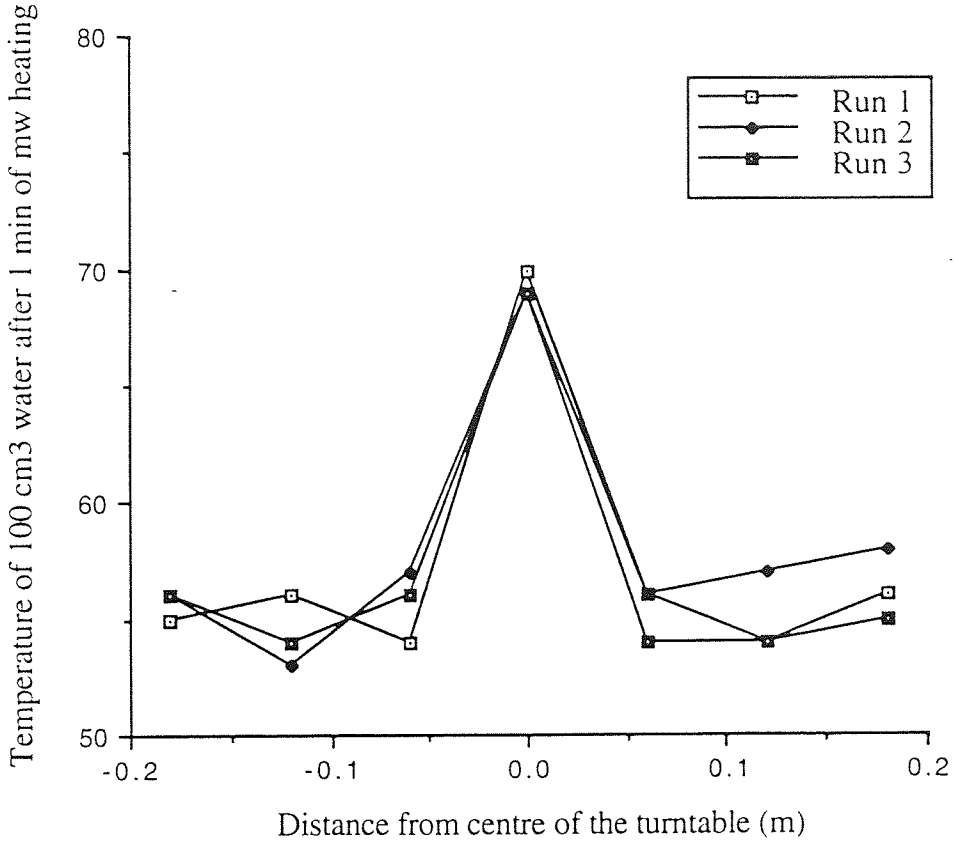

Fig 3.05

Variation in the temperature of 100 cm^3 water relative to its starting position on the microwave turntable

The tests show that there is indeed a variation in microwave flux, which is dependant upon the position of the reaction vessel within the microwave cavity. It is the centre of the microwave cavity which appears to be the position of greatest microwave flux. If the beaker is placed at the centre of the turntable during one run and then at the edge of the turntable on a consecutive run then, assuming the starting conditions are the same, differences in temperature of up to 17°C can result between the two runs. Further testing revealed that if the reaction vessel was placed on a circumference from its position on the diameter and microwave heating initiated, the temperature of the water varied between ± 6°C under the same reaction conditions. These results conclude that it is important to position the reaction vessel in the same position (i.e the centre of the turntable - the position of greatest microwave flux) for each successive experiment to ensure comparability of results. It should also be noted that over a period of time the magnetron tends to degenerate and operate less efficiently - this is especially true for domestic microwave ovens.

3.3.3 Stannylation of model compounds

The FT-IR spectra for the reagents can be found in Appendix II. Data for the model compounds used in these experiments is shown in Table 3.05 :

Two different stannylating reagents were tested.

(a) Tributyltin chloride

Tributyltin chloride (m.wt 325.49) is a colourless corrosive liquid of density 1.20 gcm^{-3}. It has a b.pt of 172 °C and is toxic by inhalation, ingestion and contact.

Initially stannylation of 2,6-dimethylphenol (the least hindered phenolic compound) was attempted via both microwave and reflux methods - the procedures are outlined in sections 2.6.1(a) and 2.6.1(b) respectively. The proposed reaction is the stannylation of the hydroxyl functionality in the model compounds :

$$R\text{-}OH + n\text{-}Bu_3SnCl \rightarrow R\text{-}O\text{-}SnBu_3 + HCl$$

Using the microwave method the reagents were heated for 15, 30, 45 and 60 minutes in separate reactions. Fig 3.06 shows the IR spectra obtained after a reaction time of 15 mins in the microwave oven. There are 2 spectra in the plot - the spectrum at the top is that of the unreacted 2,6-dimethylphenol compound and beneath it is the reaction product. The hydroxyl functionality is still intact in the reaction product, as indicated by the band at 3600 - 3200 cm^{-1}. The product also shows an intense peak at approximately 2950 cm^{-1} which corresponds to C-H stretching of the butyl groups in the reagent and another peak at approximately 600 cm^{-1} corresponding to C-Sn asymmetric stretching. The peak corresponding to O-H stretching is also still visible at approximately 1300 cm^{-1}. Similar spectra were also obtained for the 30, 45 and 60 min reactions (figs 3.07 - 3.08). It is evident from the FT-IR spectra that the microwave-driven stannylation of 2,6-dimethylphenol using the n-tributyltin chloride reagent was unsuccessful.

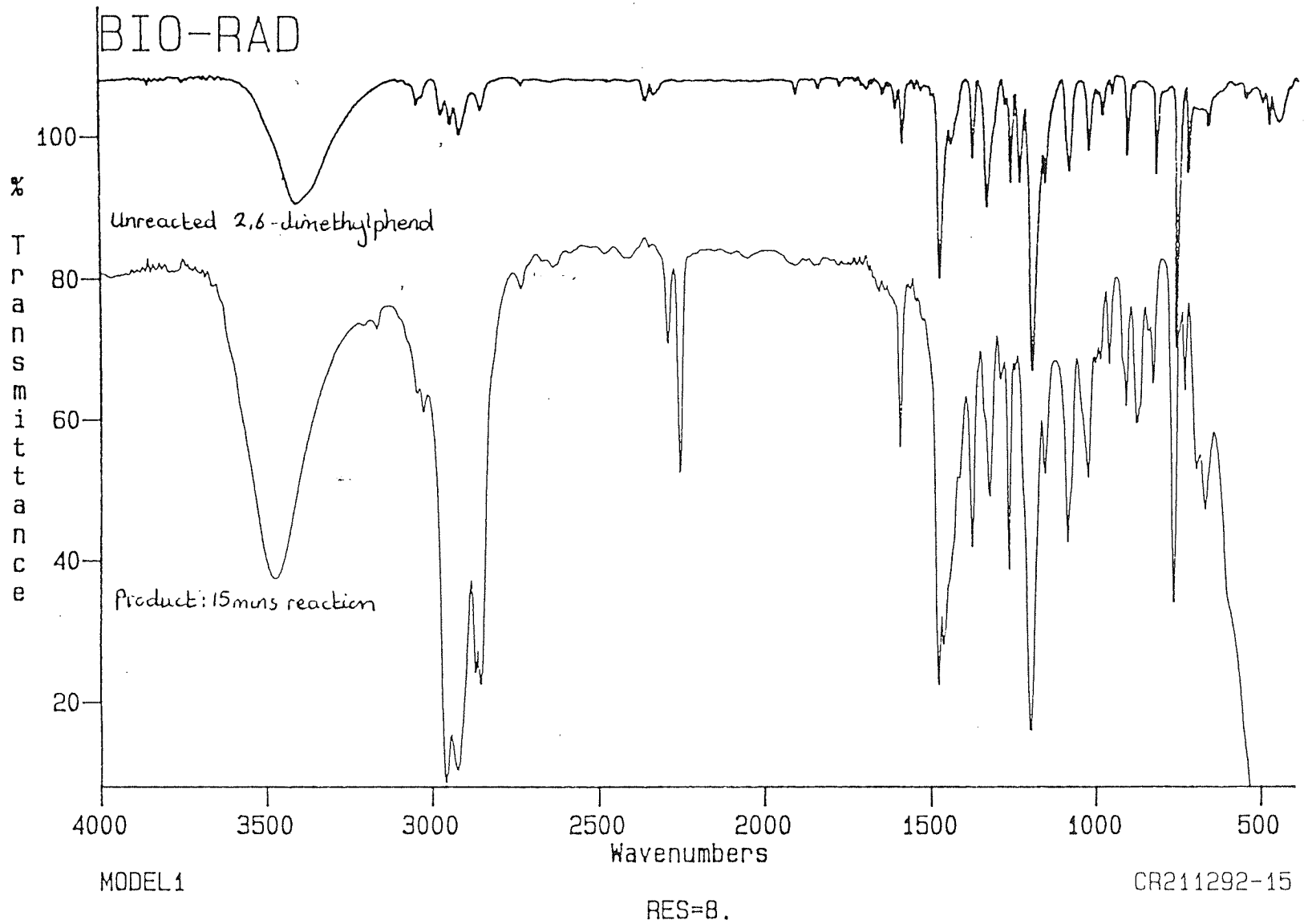

Fig3.06
IR spectra of 2,6-dimethylphenol after 15 mins stannylation with Bu_3SnCl in the mw oven and the unreacted 2,6-dimethylphenol

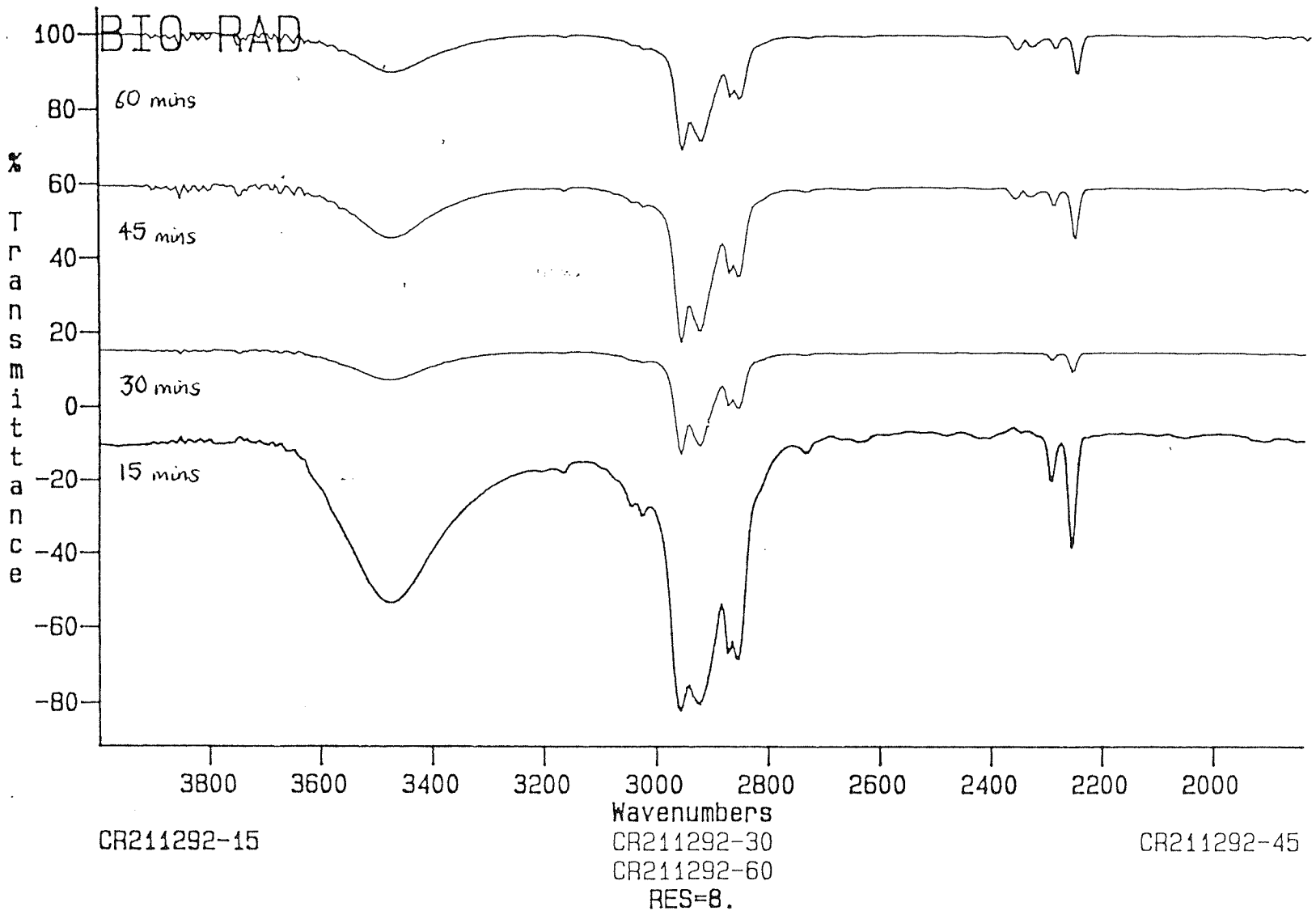

Fig3.07
IR spectra of 2,6-dimethylphenol after 15, 30, 45 and 60 mins stannylation with Bu_3SnCl in the mw oven (4000 - 2000 cm^{-1})

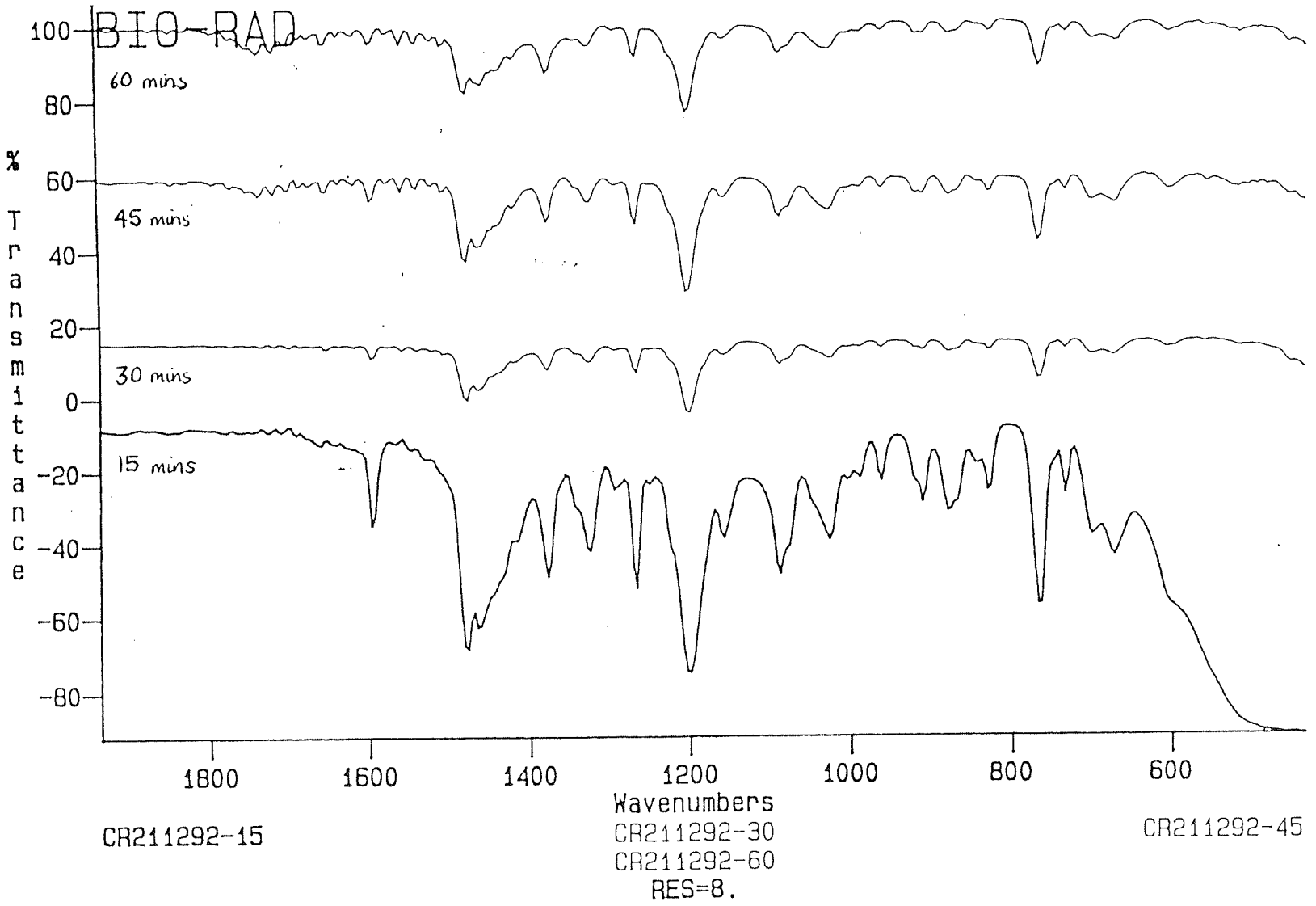

Fig3.08
IR spectra of 2,6-dimethylphenol after 15, 30, 45 and 60 mins stannylation with Bu_3SnCl in the mw oven (2000 - 400 cm^{-1})

Table 3.05 Data for model compounds

Model compund	Formula	Appearance	m.wt	b.pt °C	m.pt °C
2,6-dimethylphenol	$(CH_3)_2C_6H_3OH$	white crystalline solid	122.17	203	46-48
2,6-diisopropylphenol	$[(CH_3)_2CH]_2C_6H_3OH$	light yellow liquid	178.28	256	18
2,6-di-tert-butylphenol	$(C_4H_9)_2C_6H_3OH$	yellow/brown crystalline solid	206.33	253	35-38
2,6-diphenylphenol	$(C_6H_5)_2C_6H_3OH$	white crystalline solid	246.31	___	100-102
2-phenylphenol	$(C_6H_5)C_6H_4OH$	white solid	170.21	282	57-59
2,4,6-tri-tert-butylphenol	$(C_4H_9)_3C_6H_2OH$	brown crumbly solid	262.44	277	129-132

Next reflux of the reagents was carried out for 4 days, but again the FT-IR spectrum (fig 3.09) indicates that stannylation was unsuccessful. Reflux was also attempted using toluene solvent, instead of acetonitrile. Again the reagents were refluxed for 4 days and the toluene was then rotary-evaporated off. A yellow solution was obtained from which, on cooling, white crystals precipitated. These were filtered and analysed by FT-IR. Spectroscopic analysis (fig 3.10) showed that these crystals were unreacted 2,6-dimethylphenol.

The unwillingness of the n-tributyltin chloride reagent to react seems to suggest that this reagent is very sensitive to reaction conditions. The Sn-Cl bond is covalent but polarised and the extent of polarisation can be greatly influenced by the nature of the medium and the other reagents present - both radical and polar reactions have been known to occur. Dissociation is possible as a limiting case :

$$R_3Sn^{\delta+}\text{-}\ Cl^{\delta-} \leftrightarrow R_3Sn^{+} + Cl^{-}$$

The n-tributyltin chloride reagent also reacts with water resulting in rapid and reversible hydrolysis :

$$2Bu_3SnCl + H_2O \leftrightarrow Bu_3SnOSnBu_3 + 2HCl$$

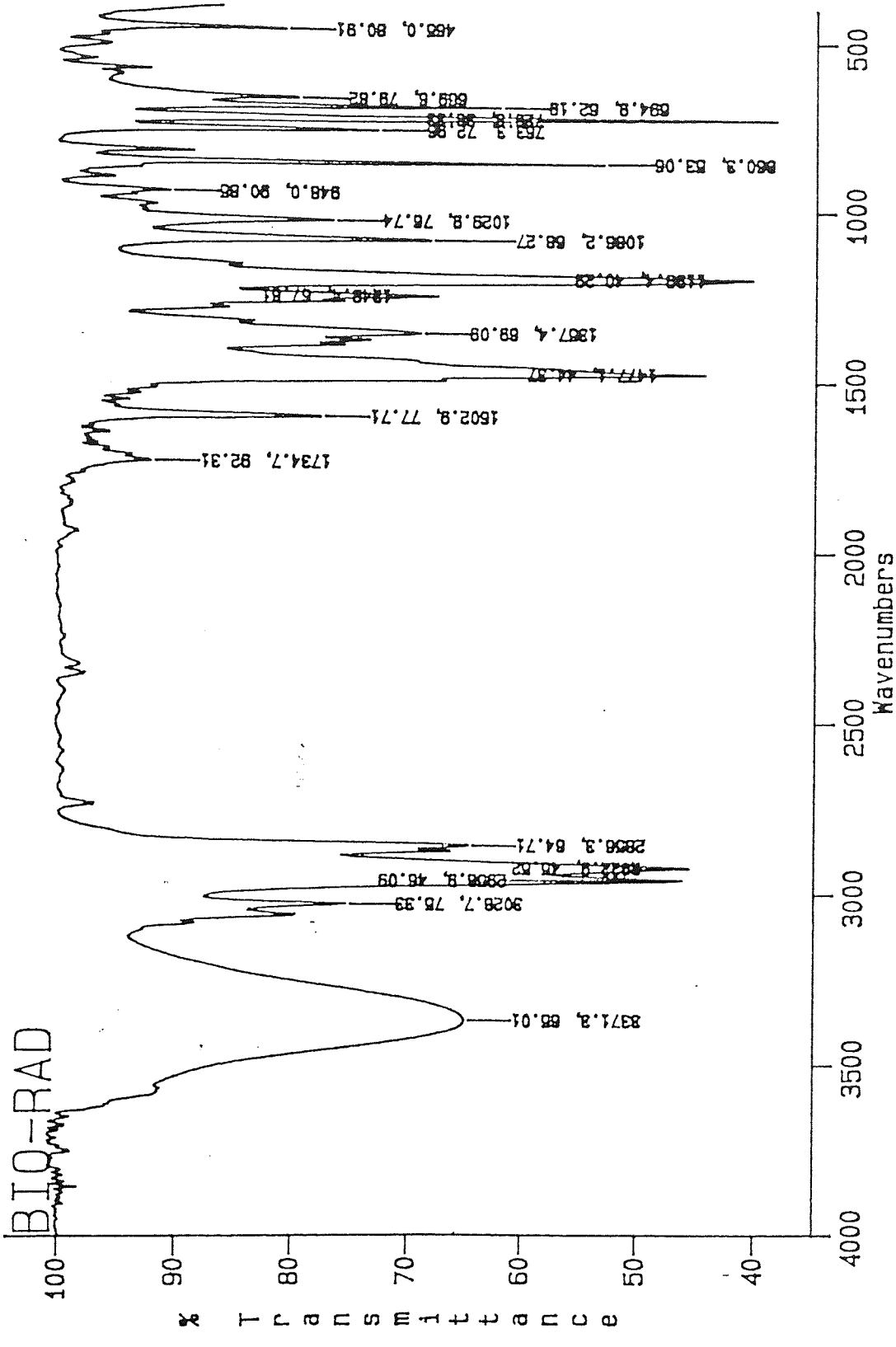

Fig3.09
IR spectrum of 2,6-dimethylphenol after 4 days stannylation via reflux with Bu_3SnCl and acetonitrile

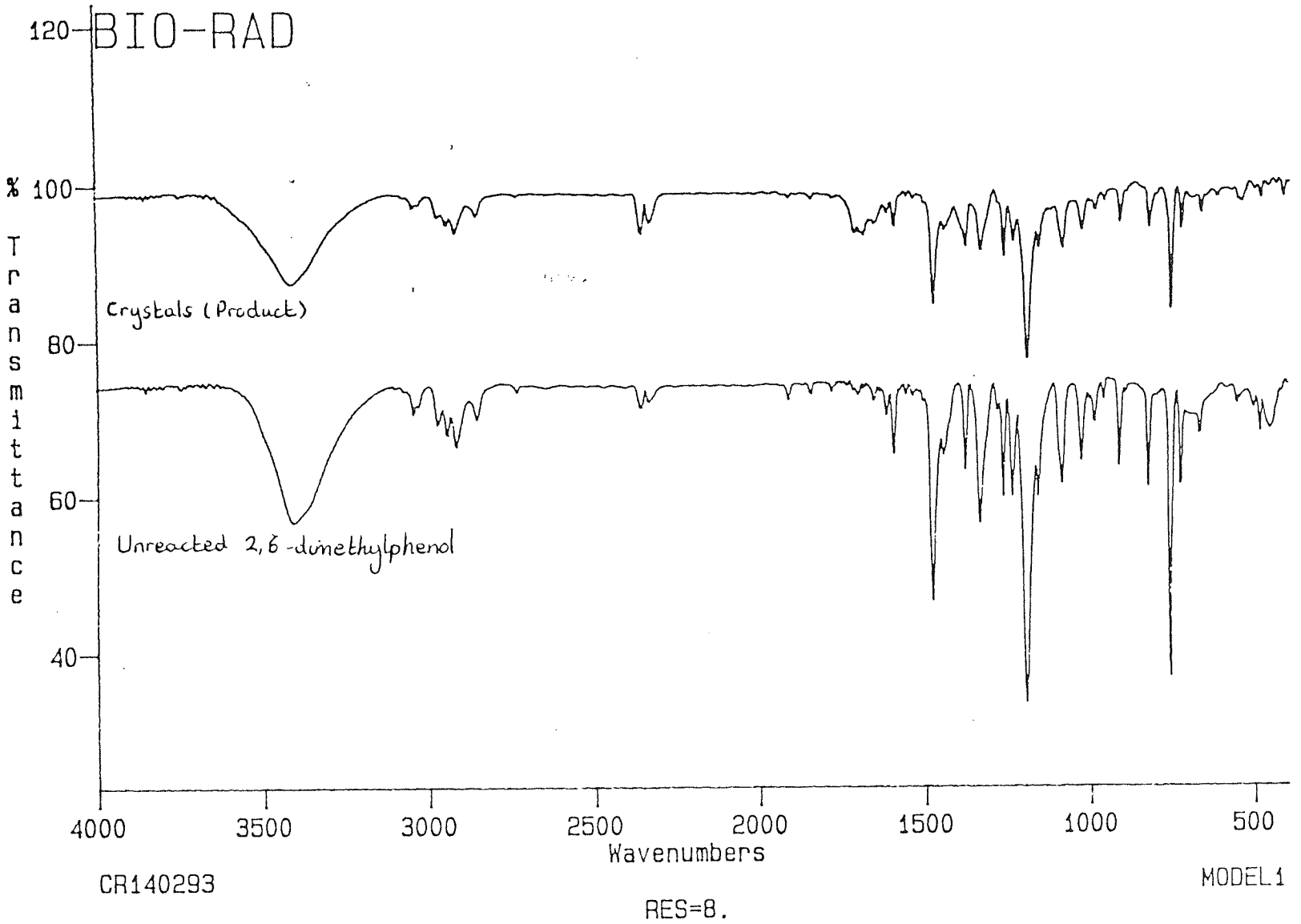

Fig3.10
IR spectra of 2,6-dimethylphenol after 4 days stannylation via reflux with Bu_3SnCl and toluene and unreacted 2,6-dimethylphenol

The product of this reaction is bis-tributyltin oxide (TBTO) - a stannoxane. If this reaction is occurring then *this* product should react with the phenolic compound (see later - section 3.3.4) to give a stannylated product. This, however, is not the case and other reactions must be involved - one such reaction may be a backside attack on the hydroxyl group of the substituted-phenolic compound by the acidic tin to form a trigonal bipyramidal complex. This reaction would effectively 'kill' off the reagent rendering further reaction impossible :

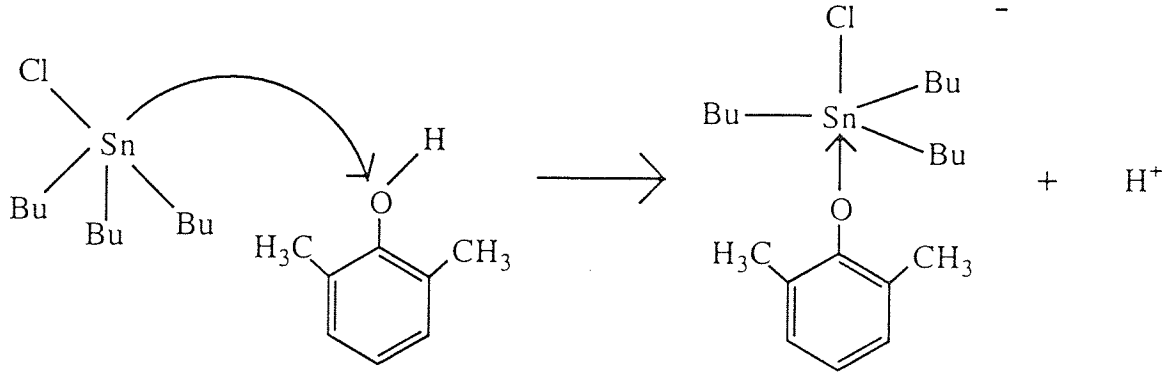

In conclusion n-tributyltin chloride is not an effective stannylating reagent for hydroxyl functionalities due to the fact that side reactions occur preferentially and harsh reaction conditions, such as an inert atmosphere, are required.

(b) Bis-tributyltin oxide (TBTO)

The model compounds were reacted with TBTO using both microwave (section 2.6.2(a)) and reflux (section 2.6.2(b)) techniques.

Initially all the model compounds were reacted by refluxing with TBTO in 20 cm^3 toluene solvent for 2 hours. The products were analysed by FT-IR.

FT-IR data for the stannylation of 2,6-dimethylphenol (fig 3.11) show that derivatisation was successful - this is shown by the disappearance of the -OH bands (O-H stretch at 3600 - 3200 cm^{-1} and O-H bending at 1335 cm^{-1}). The same is also true for the 2,6-diisopropylphenol, 2,6-diphenylphenol and the 2-phenylphenol compounds (figs 3.12 - 3.14). The 2,6-di-tert-butylphenol and 2,4,6-tri-tert-butylphenol compounds showed little inclination to react. The distillate collected in the Dean-Stark trap was analysed by FT-IR and found to be toluene (with small droplets of water at the bottom when stannylation occurred).

It was decided to extend the reflux time and react the 2,6-di-tert-butylphenol compound for 24 hours - but, again no stannylation was observed (fig 3.15). The reaction time was then extended to 3 days, but still no stannylation was observed (fig 3.16). It was decided to try an alternative method of reaction - ultrasound. The reagents (using the 2,6-di-tert-butylphenol compound) were left in a closed glass vessel in an ultrasound bath for 24 hours. The toluene was then distilled off and the product was analysed by FT-IR (fig 3.17). No stannylation was observed.

The next stage involved carrying out the analogous reactions in the microwave oven using acetonitrile solvent instead of toluene - toluene is not a good microwave-receptor solvent.

Stannylation was observed for 2,6-dimethylphenol (fig 3.18), 2,6-diisopropylphenol (fig 3.19), 2-phenylphenol (fig 3.20) and 2,6-diphenylphenol (fig 3.21) after only 1 min of microwave heating. The 2,6-di-tert-butylphenol and 2,4,6-tri-tert-butylphenol showed no inclination to react either after 1 min or 60 mins heating in the microwave oven.

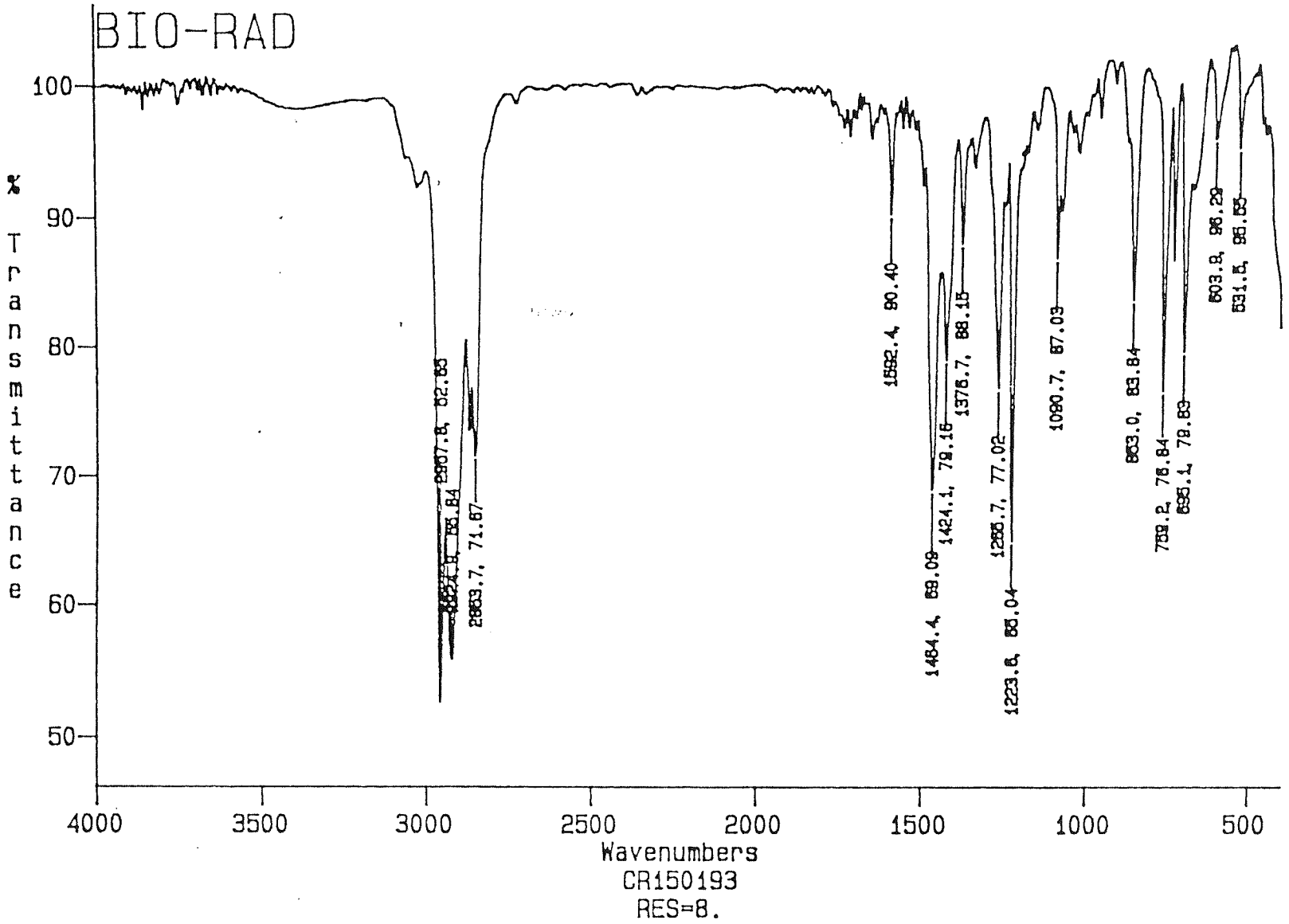

Fig3.11
IR spectrum of 2,6-dimethylphenol after 2 hrs stannylation
via reflux with TBTO and toluene

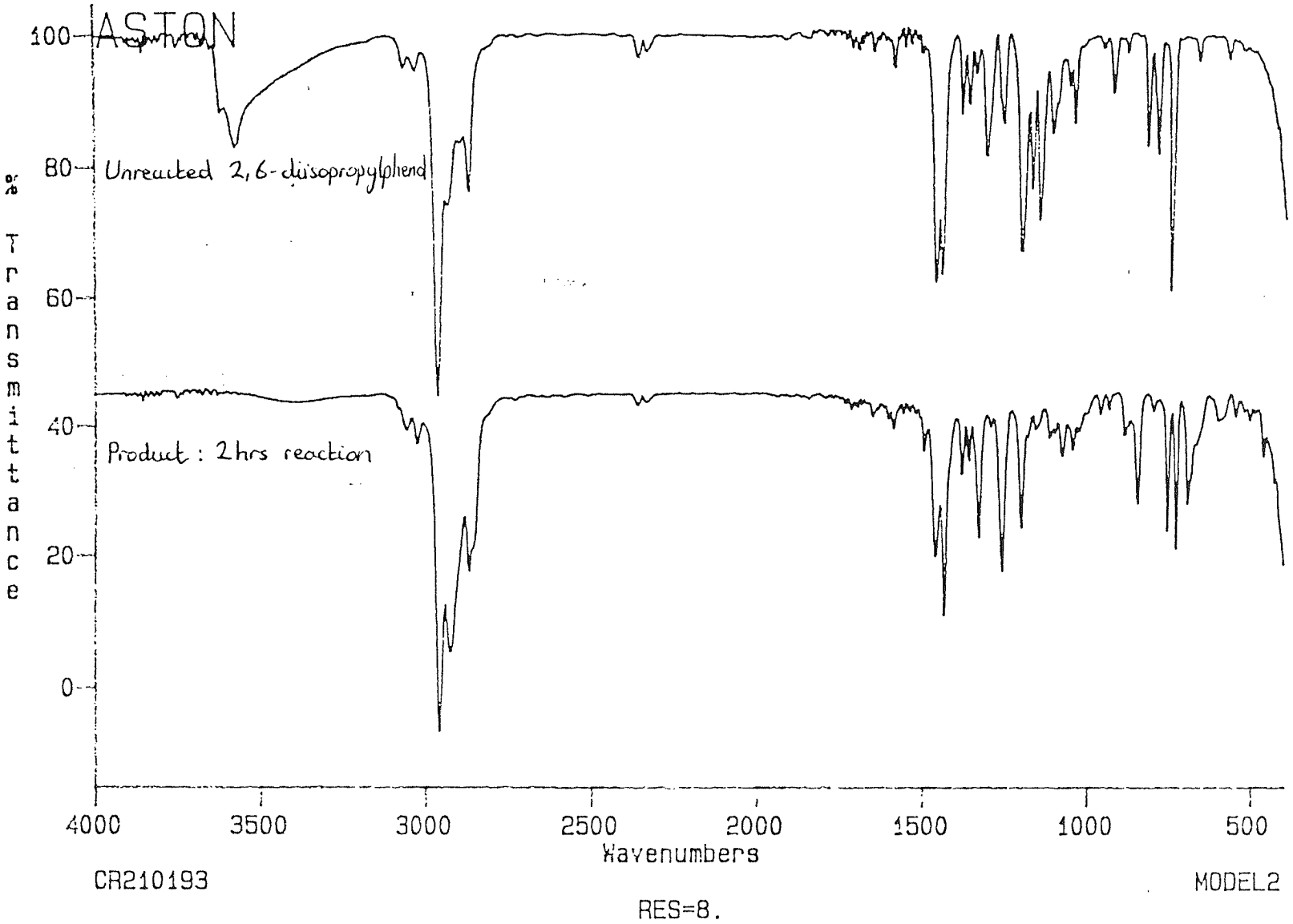

Fig3.12
IR spectra of 2,6-diisopropylphenol after 2 hrs stannylation via reflux with TBTO and toluene and unreacted 2,6-diisopropylphenol

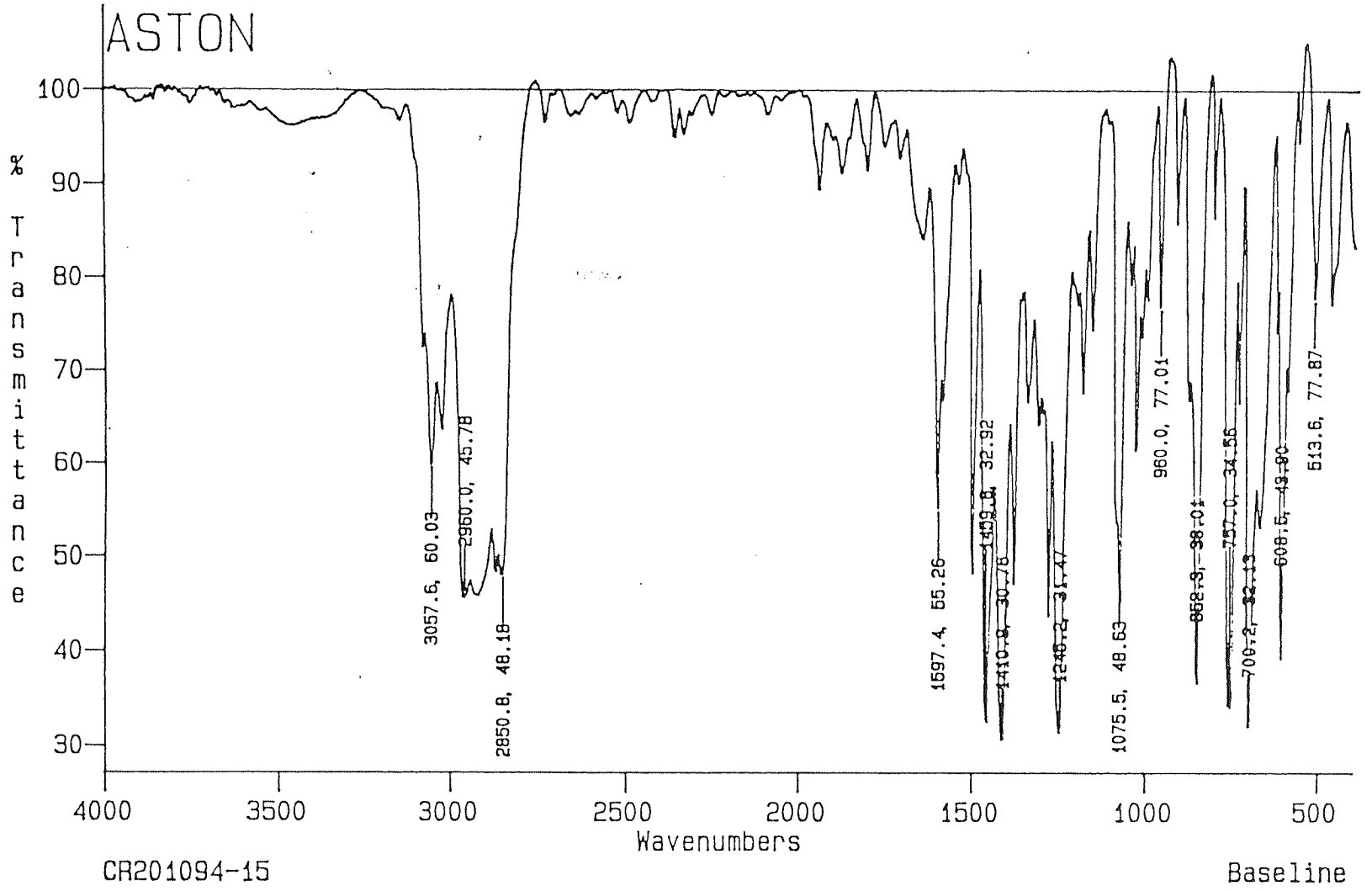

RES=8.

Fig3.13
IR spectrum of 2,6-diphenylphenol after 2 hrs stannylation via reflux with TBTO and toluene

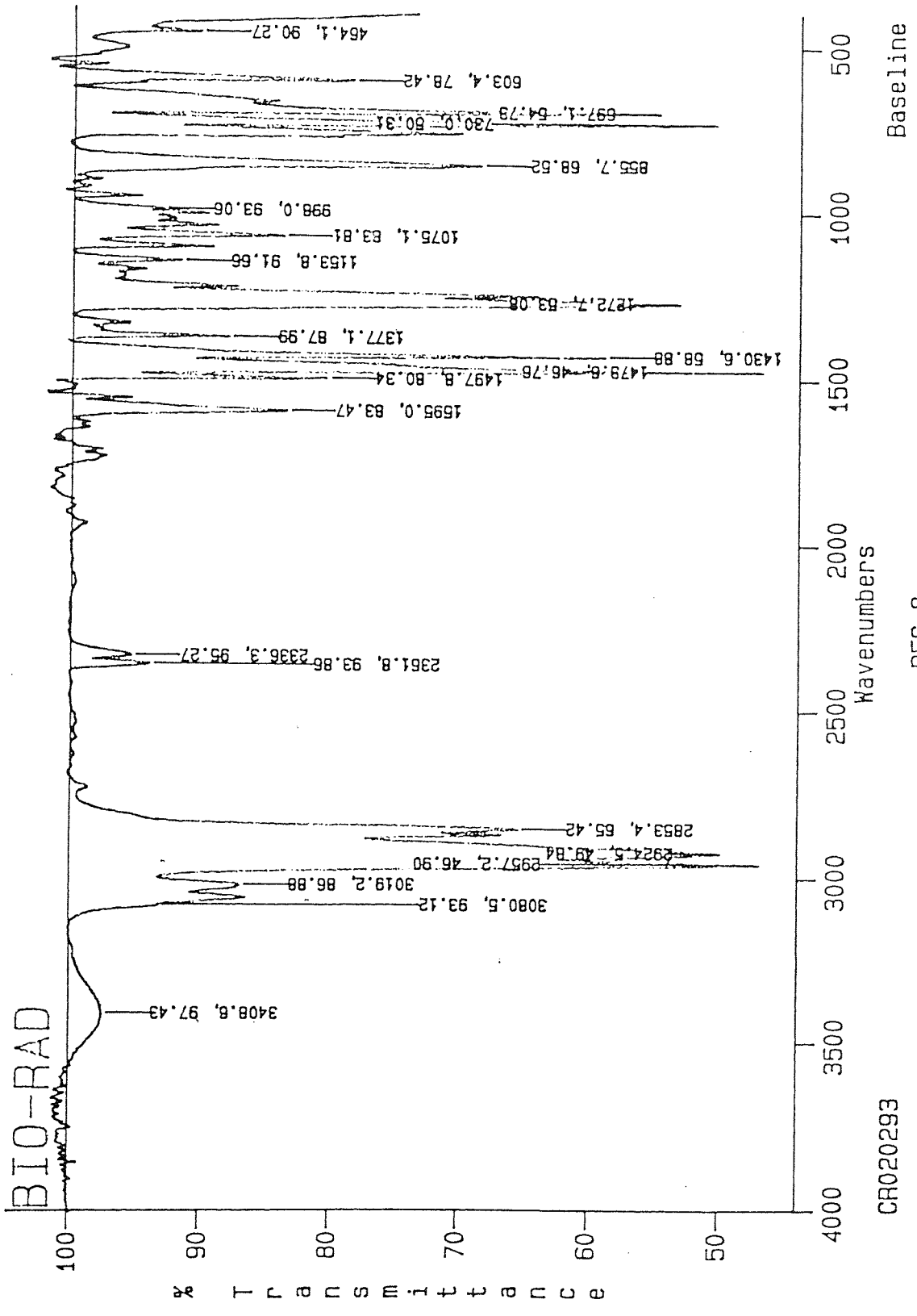

Fig3.14
IR spectrum of 2-phenylphenol after 2 hrs stannylation via reflux with TBTO and toluene

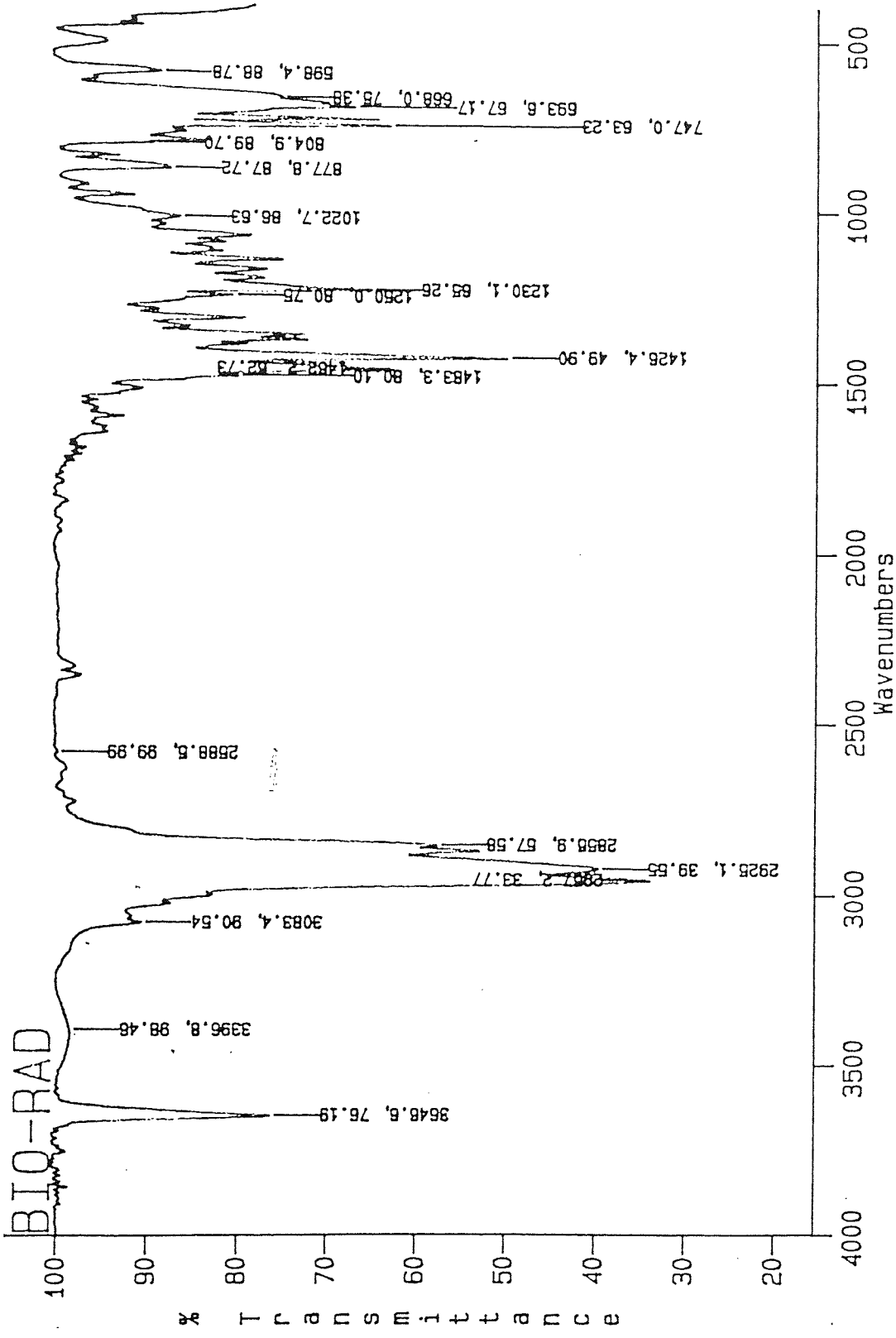

IR spectrum of 2,6-di-tert-butylphenol after 24 hrs stannylation via reflux with TBTO and toluene

Fig3.15

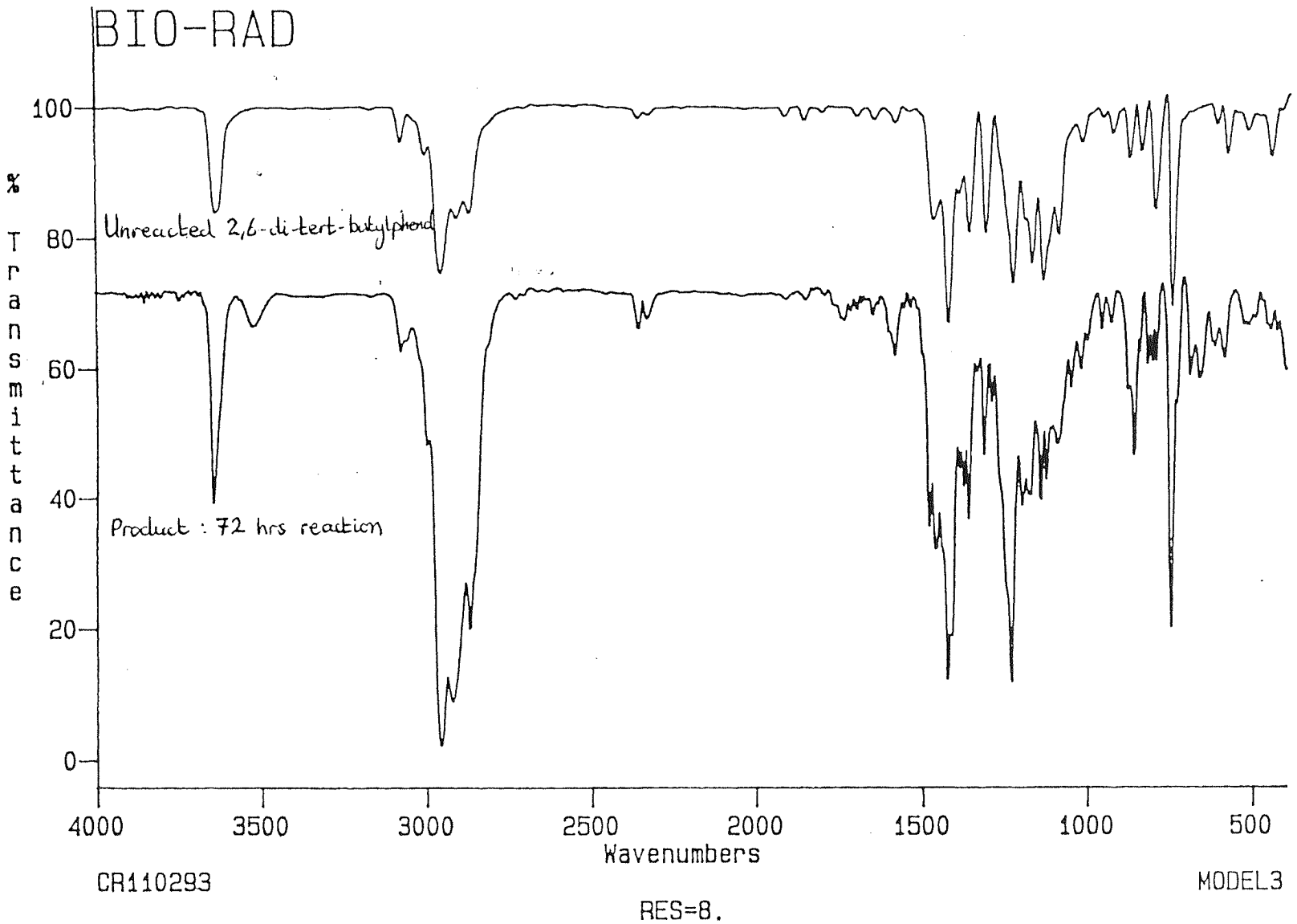

Fig3.16
IR spectra of 2,6-di-tert-butylphenol after 72 hrs stannylation via reflux with TBTO and toluene and unreacted 2,6-di-tert-butylphenol

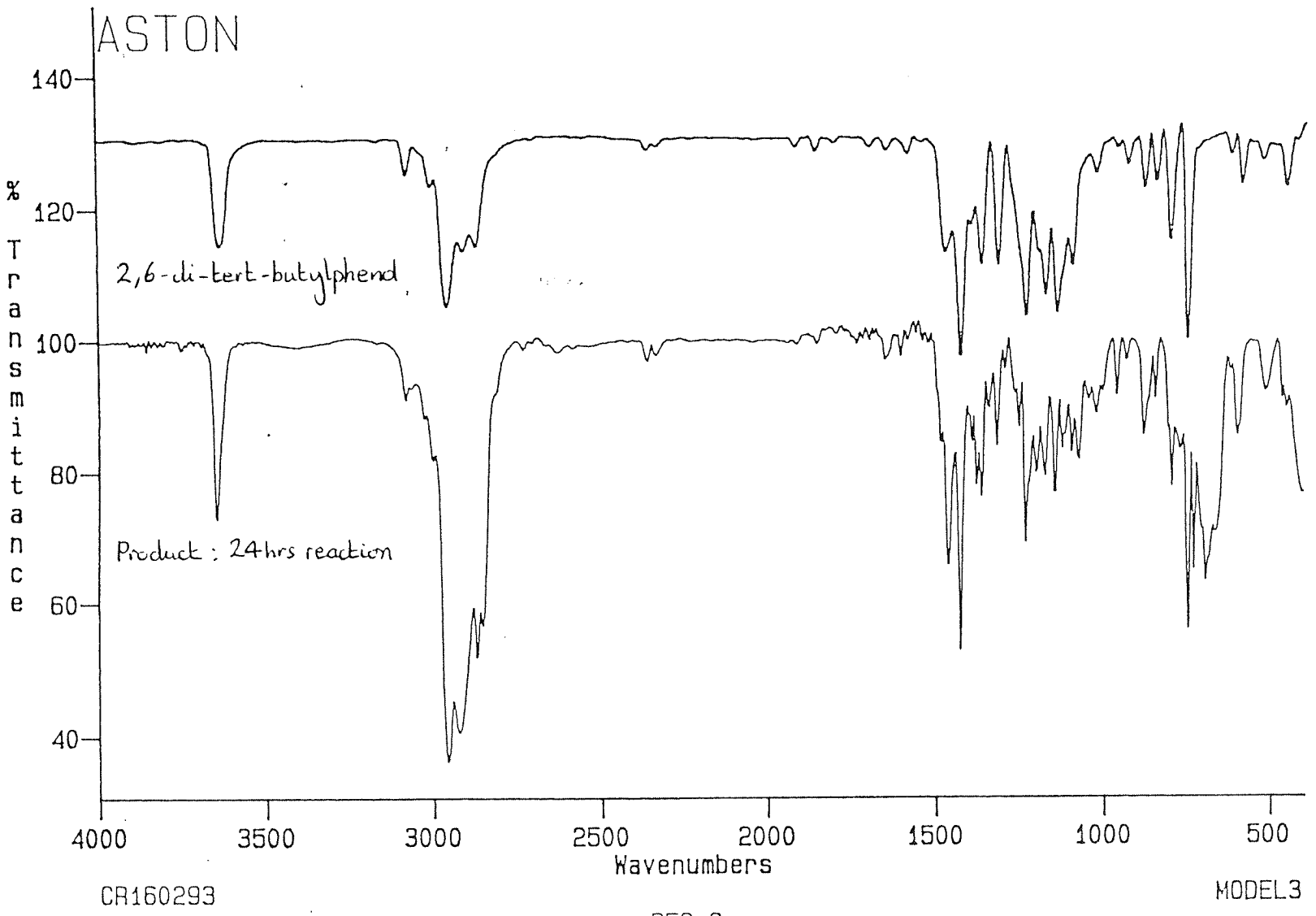

Fig3.17
IR spectra of 2,6-di-tert-butylphenol after 24 hrs stannylation via ultrasound bath using TBTO and toluene and unreacted 2,6-di-tert-butylphenol

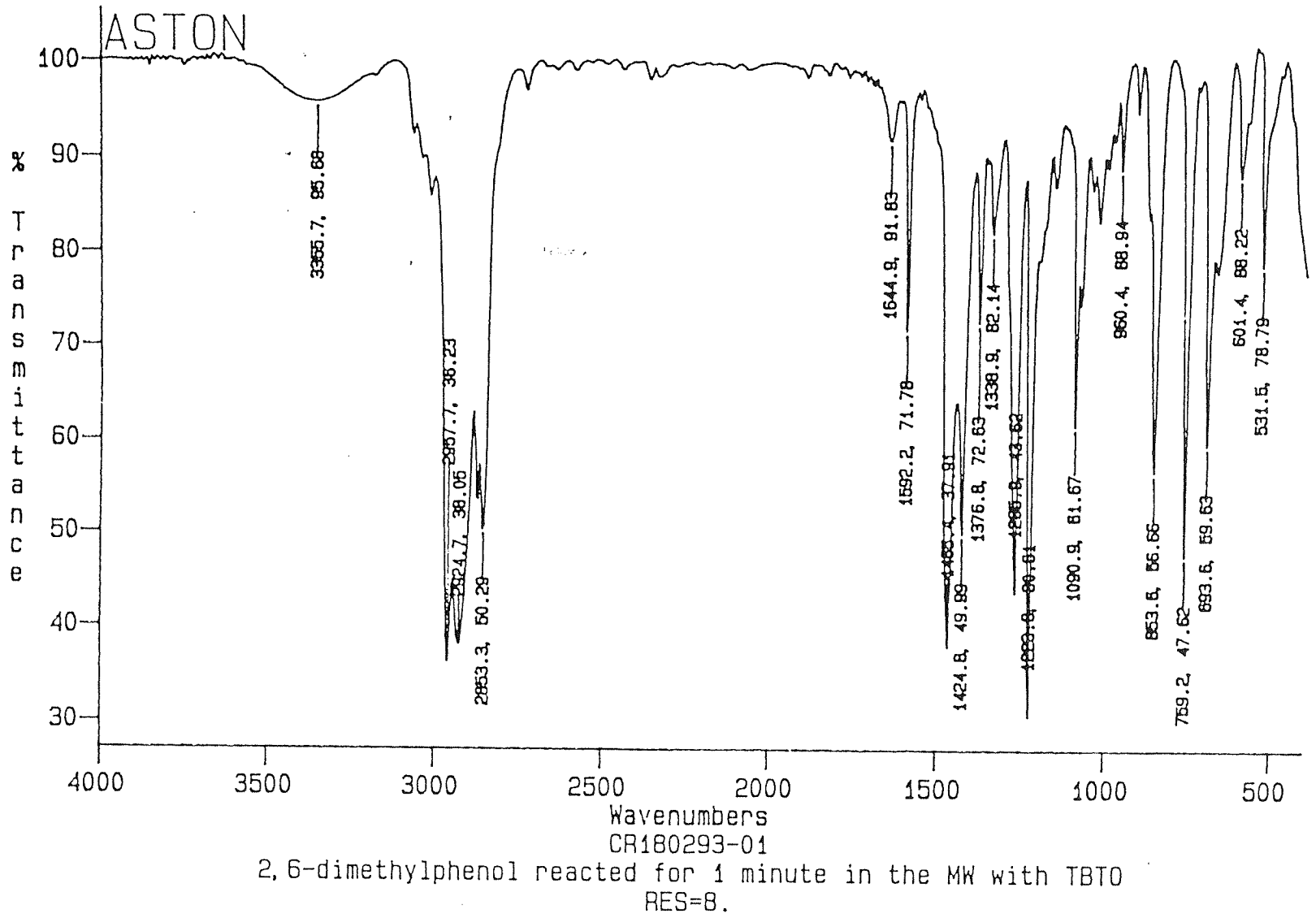

Fig3.18
IR spectrum of the stannylated 2,6-dimethylphenol after 1 min mw heating

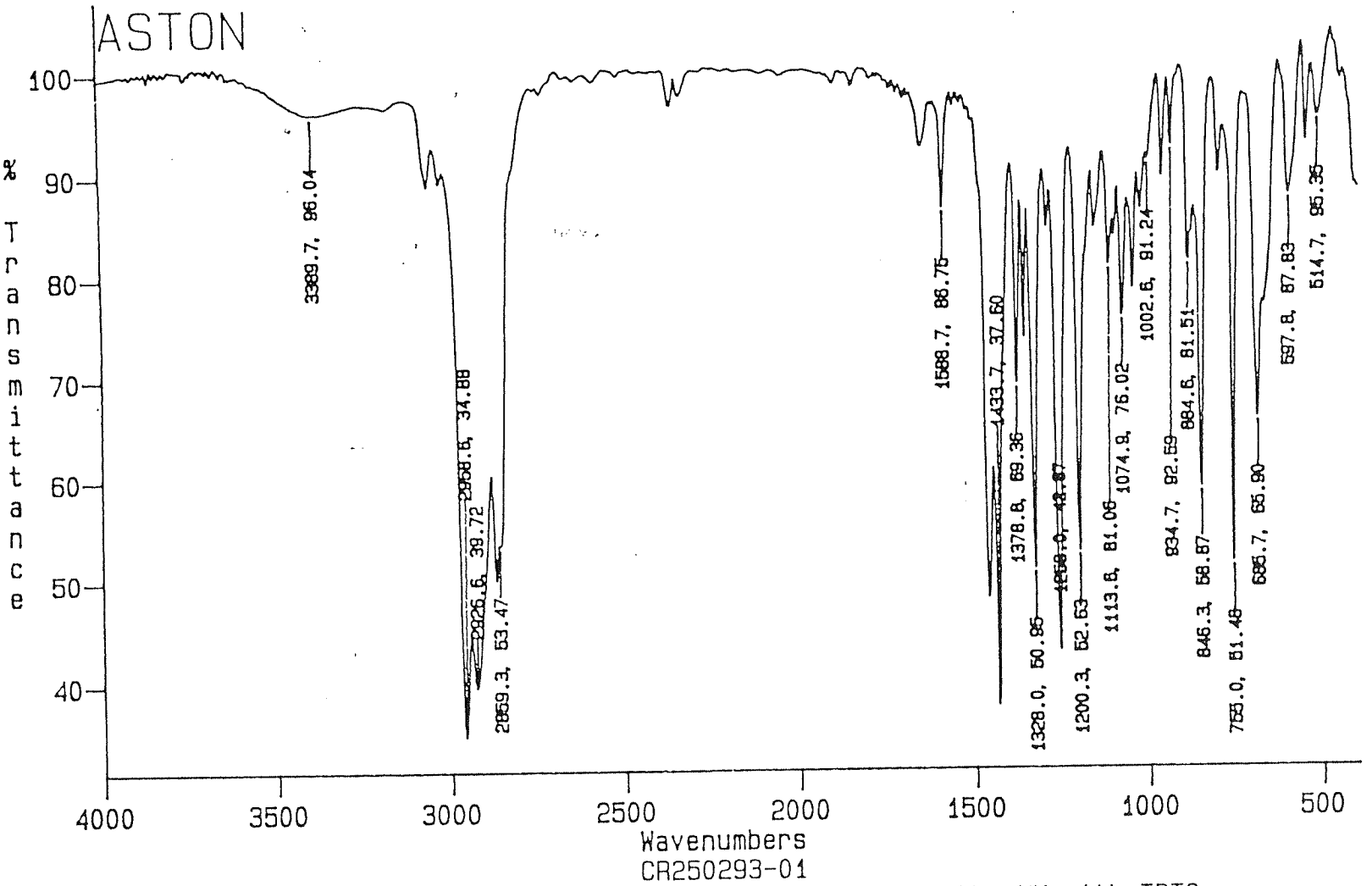

CR250293-01
2, 6-diisopropylphenol reacted for 1 minute in the MW with TBTO
RES=8.

Fig3.19.
IR spectrum of the stannylated 2,6-diisopropylphenol after 1 min mw heating

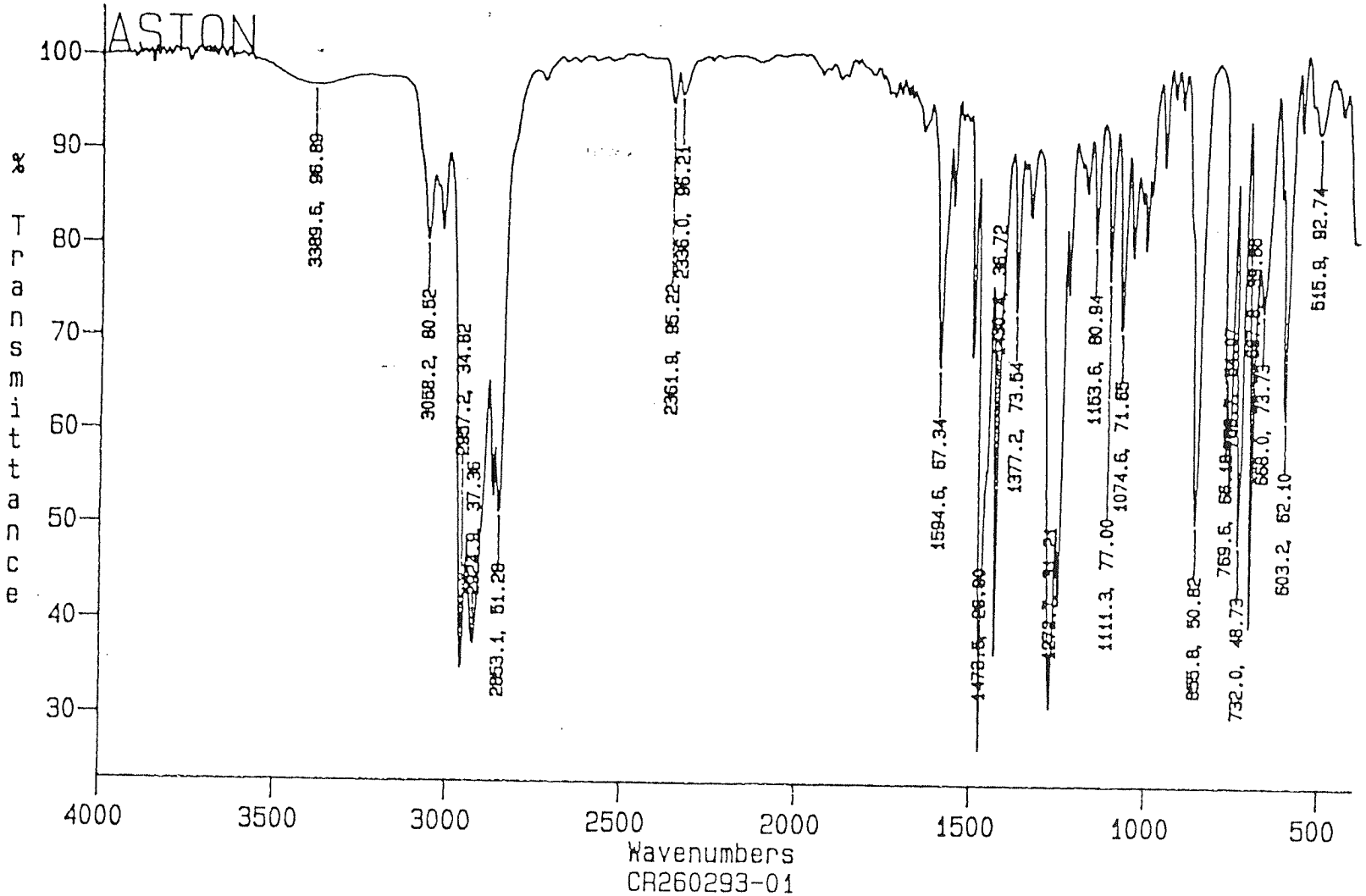

CR260293-01
2-phenylphenol reacted in the MW for 1 minute with TBTO
RES=8.

Fig3.20
IR spectrum of the stannylated 2-phenylphenol after 1 min mw heating

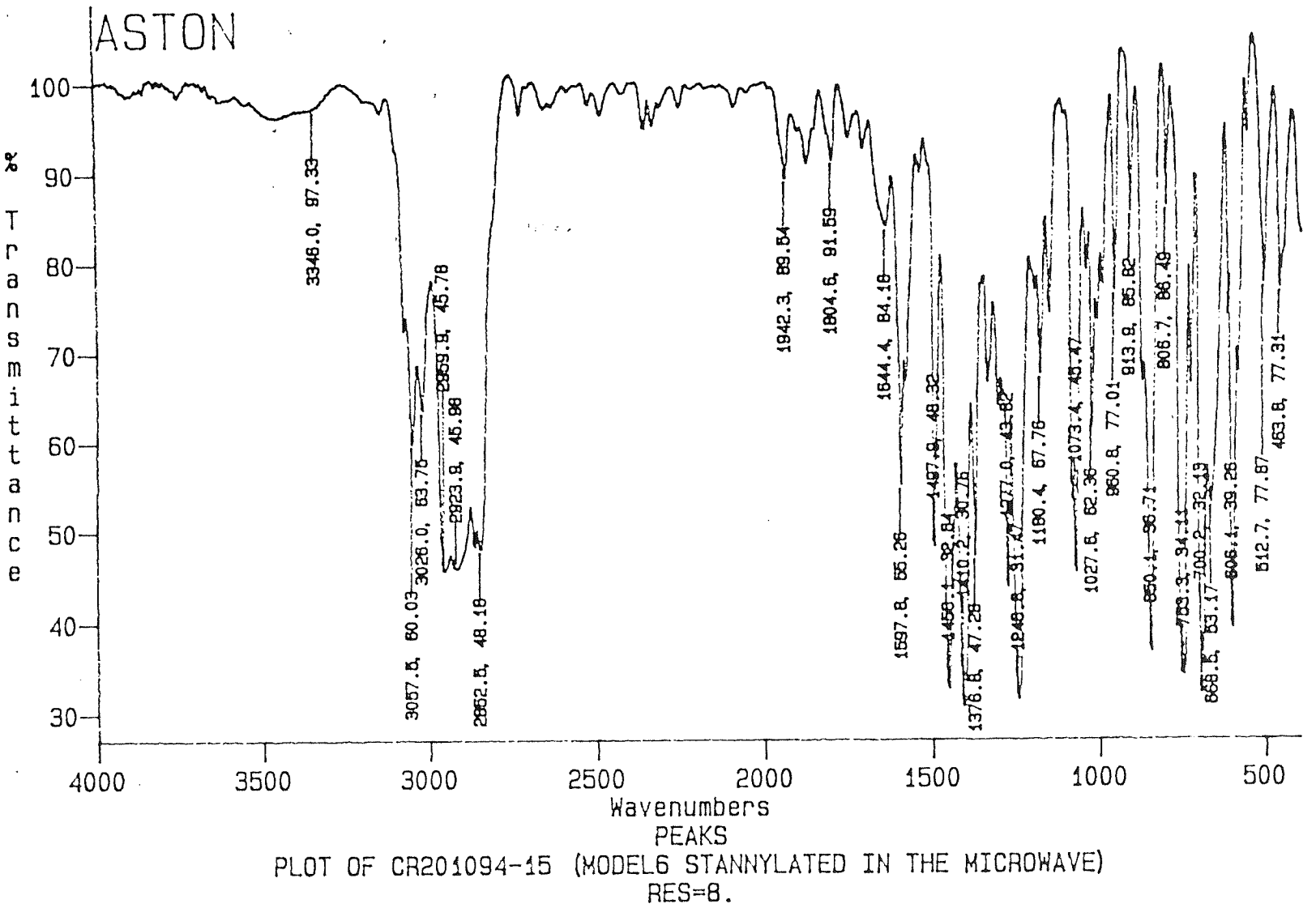

Fig3.21
IR spectrum of the stannylated 2,6-diphenylphenol after 1 min mw heating

Table 3.06 Stannylation of model compounds using reflux methods

Model compound	Reflux time	Evidence of stannylation from FT-IR
2,6-dimethylphenol	2 hrs	yes
2,6-diisopropylphenol	2 hrs	yes
2-phenylphenol	2 hrs	yes
2,6-diphenylphenol	2 hrs	yes
2,4,6-tri-tert-butylphenol	2 hrs	no
2,6-di-tert-butylphenol	2 hrs	no
	24 hrs	no
	72 hrs	no
(ultrasound)	24 hrs	no

Table 3.07

Stannylation of model compounds using microwave methods

Model compound	Microwave heating time (min)	Evidence of stannylation from FT-IR
2,6-dimethylphenol	1.0	yes
2,6-diisopropylphenol	1.0	yes
2-phenylphenol	1.0	yes
2,6-diphenylphenol	1.0	yes
2,4,6-tri-tert-butylphenol	1.0	no
	60.0	no
2,6-di-tert-butylphenol	1.0	no
	60.0	no

The stannylated 2,6-dimethylphenol, 2,6-diisopropylphenol and 2,6-diphenylphenol were analysed by gas chromatography.

(a) 2,6-dimethylphenol

Using the reflux method 3 major peaks were observed on the GC plot. The first of these is at RT (residence time in minutes) 0.751 - a blank gas chromatograph experiment using just the model compound dissolved in toluene showed that this peak is due to the toluene solvent. The other 2 peaks are in close proximity at RT 3.303 and 3.517 (fig 3.22). It is highly probable that the product has a slightly higher boiling-point than the unreacted phenol due to the bonding of a high m.wt entity - the tributyltin derivative. Consequently we would expect the peak at RT 3.517 to be our product. This indicates a conversion of [(50.02341 / 75.81604) 100%] ≈ 66% for the 2,6-dimethylphenol compound. The other minor peaks in the GC plot are probably due to impurities in the TBTO, such as tributyltin hydroxide. The microwave method showed a 100% conversion with the product peak at RT 3.873 (fig 3.23).

(b) 2,6-diisopropylphenol

For the reflux method the main product appears at RT 4.105 indicating 100% conversion. The solvent peak is at RT 0.785 and the other minor peaks are due to impurities in the 2,6-diisopropylphenol compound (fig 3.24). With the microwave method the product is at RT 4.567 and the acetonitrile peak is at RT 0.633. In this instance there is again 100% conversion (fig 3.25).

(c) 2,6-diphenylphenol

Using the reflux method GC analysis reveals only 2 peaks - the first of these is a combination of ether (used to clean the syringe before extraction and injection of the sample in the gas chromatograph) and toluene (the reflux solvent). The second peak is the product. GC analysis indicates 100% conversion after 2 hrs reflux (fig 3.26). The microwave method reveals 2 major peaks. The first of these is the acetonitrile solvent peak and the other major peak (third peak on GC plot) is the product. Again the GC plot indicates 100% conversion (fig 3.27). The small peak at RT 1.467 is probably due to impurities in the TBTO.

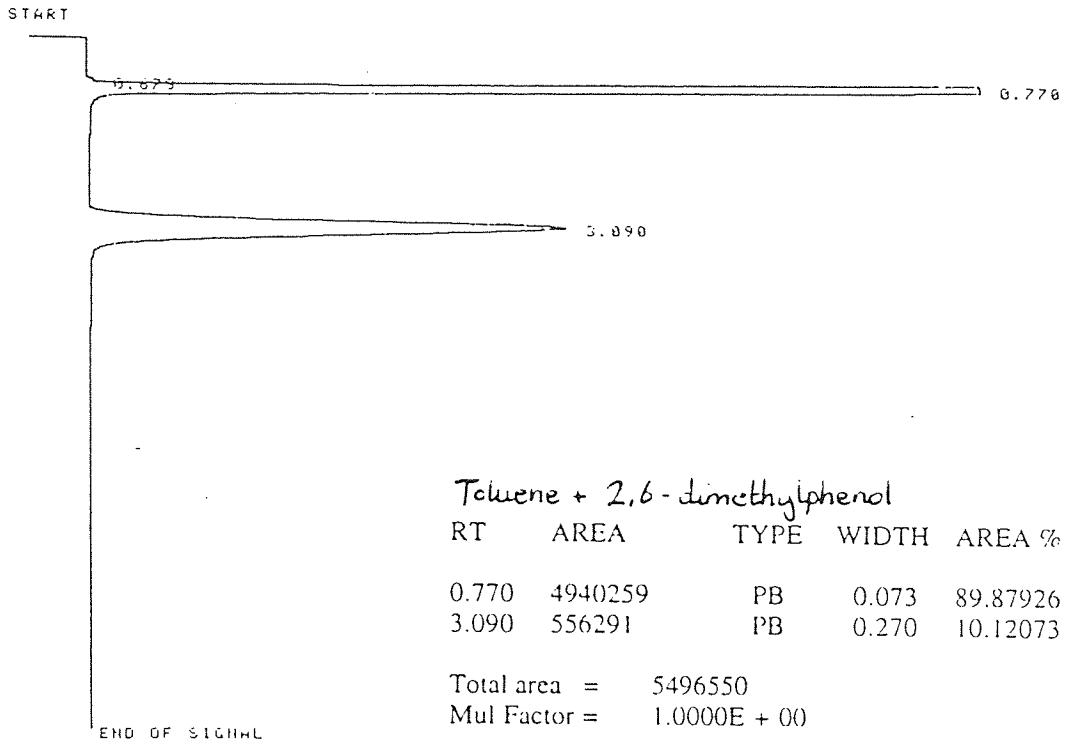

Toluene + 2,6-dimethylphenol

RT	AREA	TYPE	WIDTH	AREA %
0.770	4940259	PB	0.073	89.87926
3.090	556291	PB	0.270	10.12073

Total area = 5496550
Mul Factor = 1.0000E + 00

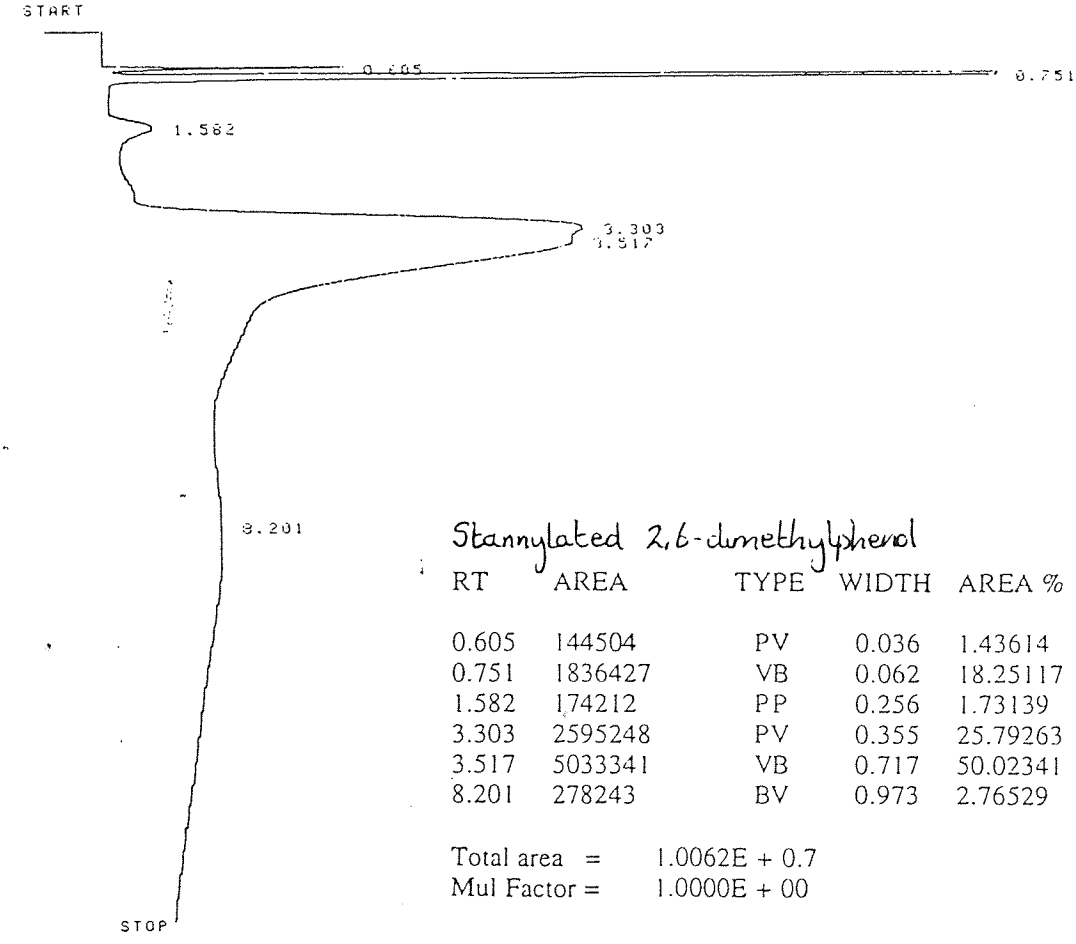

Stannylated 2,6-dimethylphenol

RT	AREA	TYPE	WIDTH	AREA %
0.605	144504	PV	0.036	1.43614
0.751	1836427	VB	0.062	18.25117
1.582	174212	PP	0.256	1.73139
3.303	2595248	PV	0.355	25.79263
3.517	5033341	VB	0.717	50.02341
8.201	278243	BV	0.973	2.76529

Total area = 1.0062E + 0.7
Mul Factor = 1.0000E + 00

Fig3.22
GC plot of the stannylated 2,6-dimethylphenol compound (reflux method)

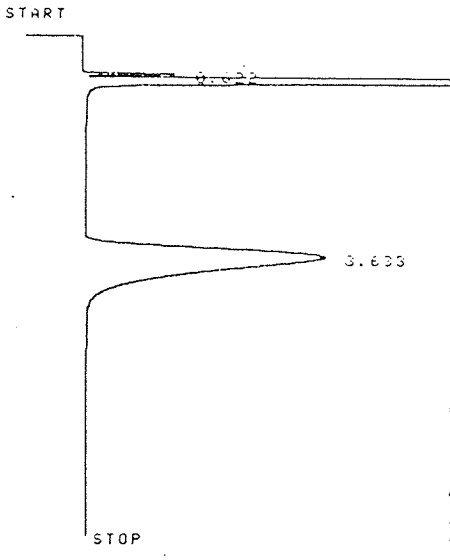

Acetonitrile + 2,6-dimethylphenol

RT	AREA	TYPE	WIDTH	AREA %
0.622	102657	PV	0.033	1.57925
0.705	2768789	VB	0.079	42.59446
3.633	3628902	PB	0.442	55.82629

Total area = 6500346
Mul Factor = 1.0000E + 00

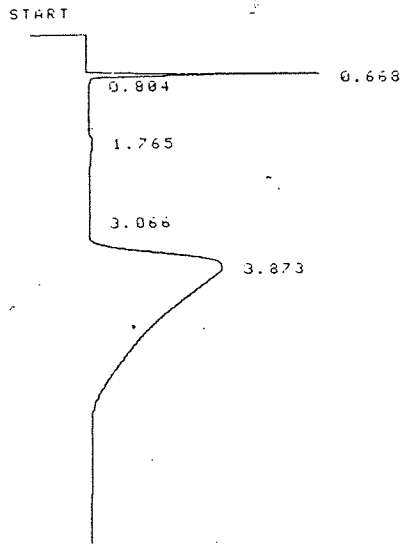

Stannylated 2,6-dimethylphenol

RT	AREA	TYPE	WIDTH	AREA %
0.668	325257	PV	0.041	3.53628
0.804	8149	VB	0.093	0.08860
1.765	70444	VV	0.336	0.76589
3.066	38891	VV	0.478	0.42283
3.873	8754973	VB	5.232	95.18642

Total area = 9.1977E + 0.6
Mul Factor = 1.0000E + 00

Fig3.23
GC plot of the stannylated 2,6-dimethylphenol compound (microwave method)

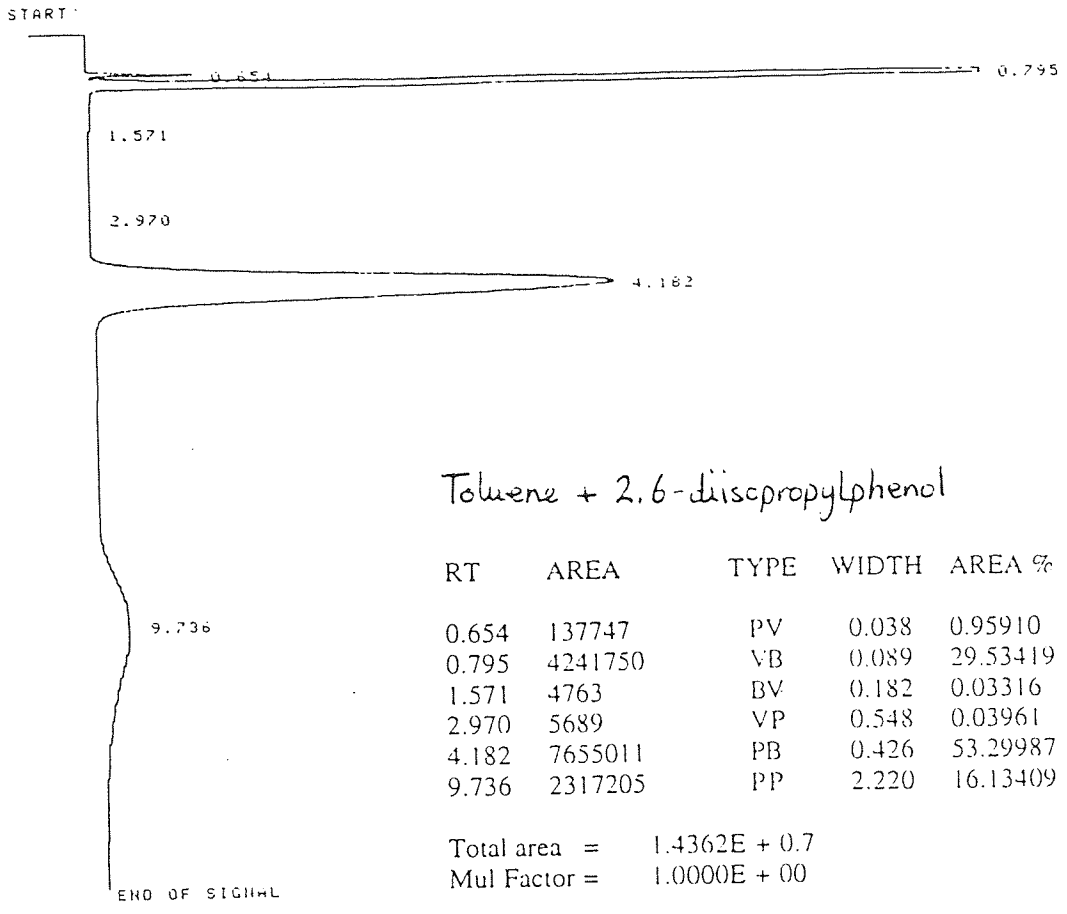

Toluene + 2,6-diisopropylphenol

RT	AREA	TYPE	WIDTH	AREA %
0.654	137747	PV	0.038	0.95910
0.795	4241750	VB	0.089	29.53419
1.571	4763	BV	0.182	0.03316
2.970	5689	VP	0.548	0.03961
4.182	7655011	PB	0.426	53.29987
9.736	2317205	PP	2.220	16.13409

Total area = 1.4362E + 0.7
Mul Factor = 1.0000E + 00

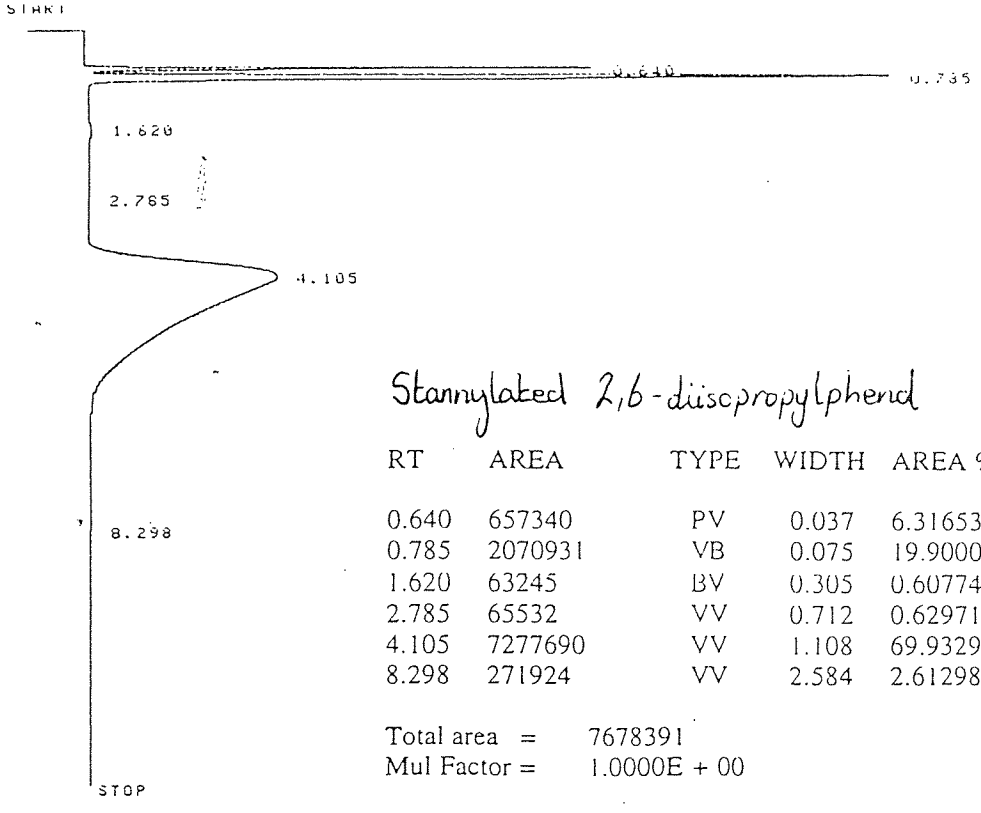

Stannylated 2,6-diisopropylphenol

RT	AREA	TYPE	WIDTH	AREA %
0.640	657340	PV	0.037	6.31653
0.785	2070931	VB	0.075	19.90006
1.620	63245	BV	0.305	0.60774
2.785	65532	VV	0.712	0.62971
4.105	7277690	VV	1.108	69.93299
8.298	271924	VV	2.584	2.61298

Total area = 7678391
Mul Factor = 1.0000E + 00

Fig3.24
GC plot of the stannylated 2,6-diisopropylphenol compound (reflux method)

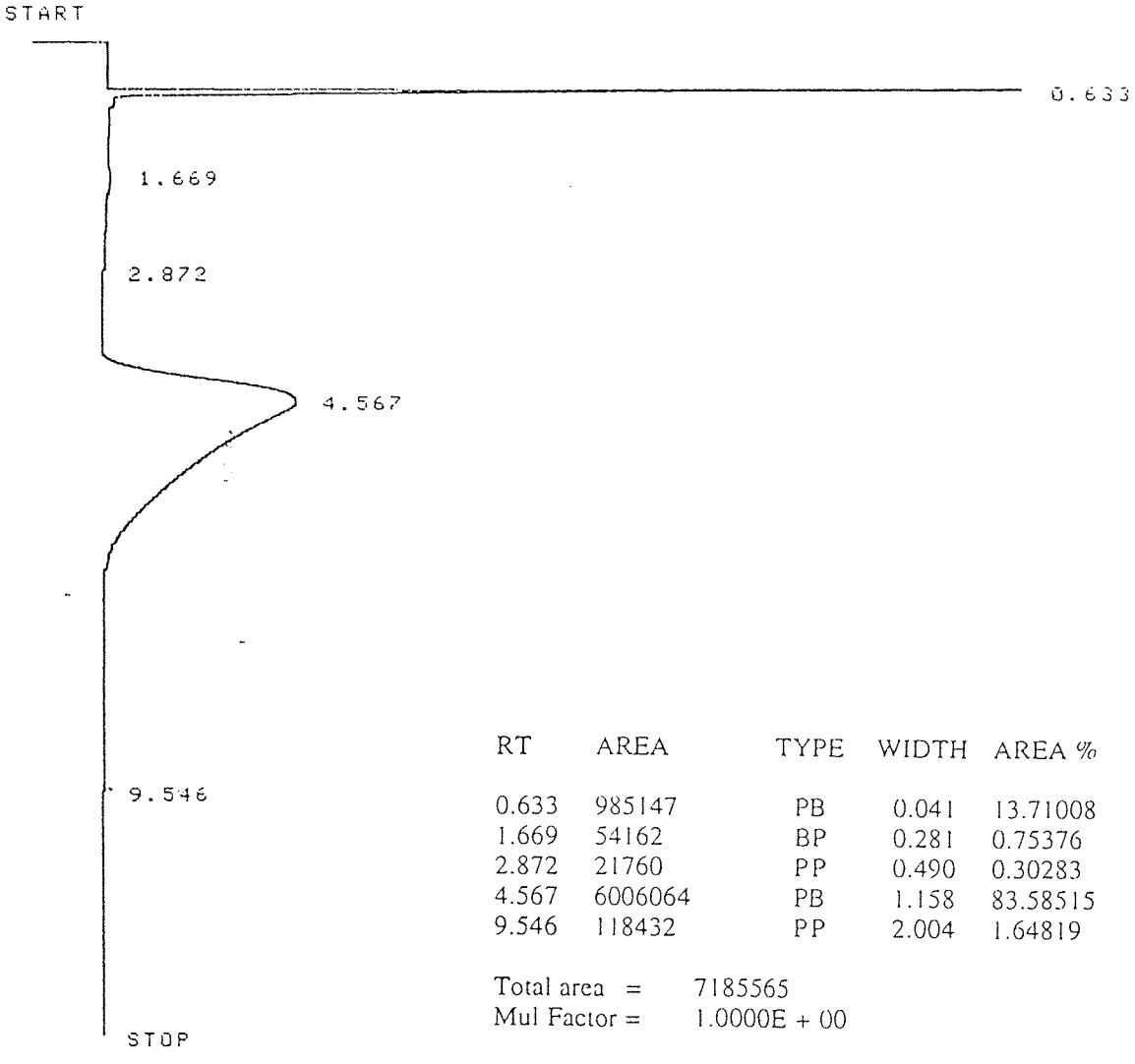

RT	AREA	TYPE	WIDTH	AREA %
0.633	985147	PB	0.041	13.71008
1.669	54162	BP	0.281	0.75376
2.872	21760	PP	0.490	0.30283
4.567	6006064	PB	1.158	83.58515
9.546	118432	PP	2.004	1.64819

Total area = 7185565
Mul Factor = 1.0000E + 00

Fig3.25
GC plot of the stannylated 2,6-diisopropylphenol compound (microwave method)

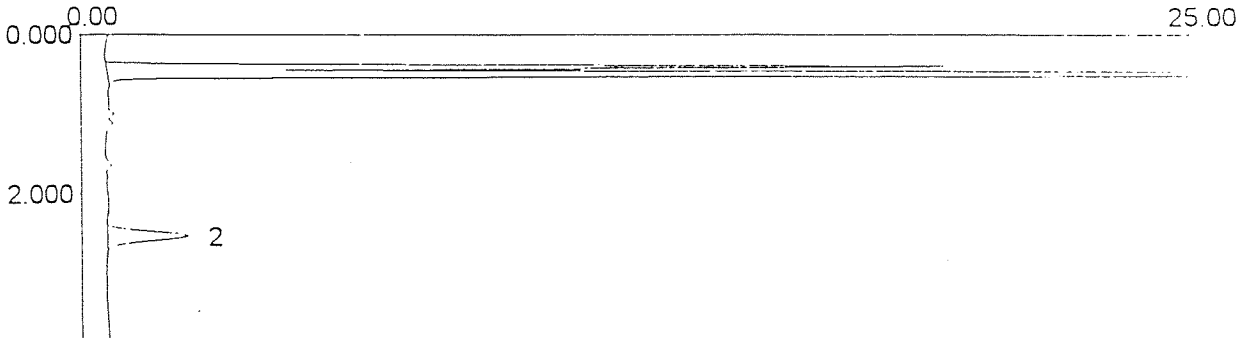

Stannylated 2,6-diphenylphenol

RT	AREA	TYPE	WIDTH	AREA %
0.500	286.706	BB	0.619	95.062
2.533	14.892	BT	0.596	4.938

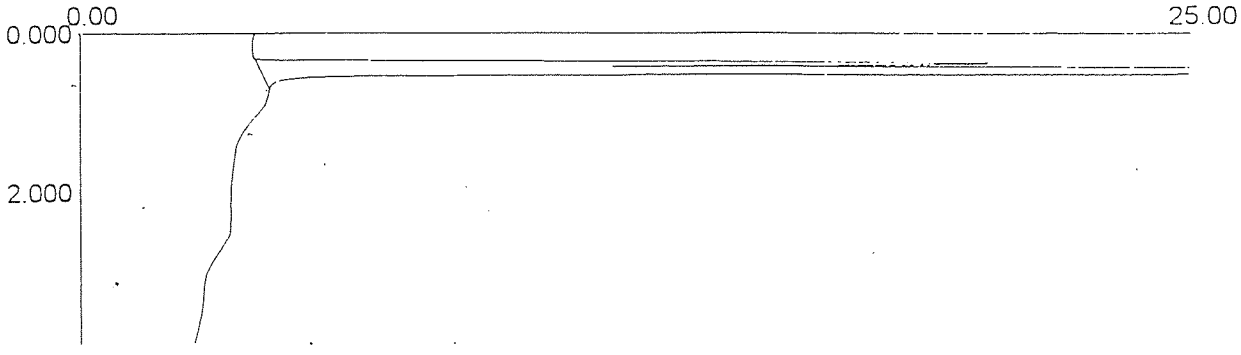

Toluene

RT	AREA	TYPE	WIDTH	AREA %
0.483	455.952	BB	4.140	100.000

Fig3.26
GC plot of the stannylated 2,6-diphenylphenol compound
(reflux method)

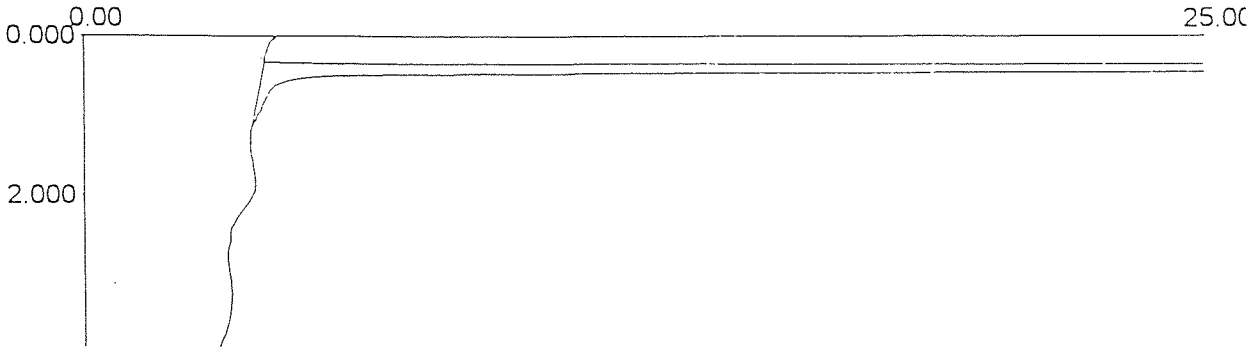

Acetonitrile

RT	AREA	TYPE	WIDTH	AREA %
0.417	446.455	BT	3.983	100.000

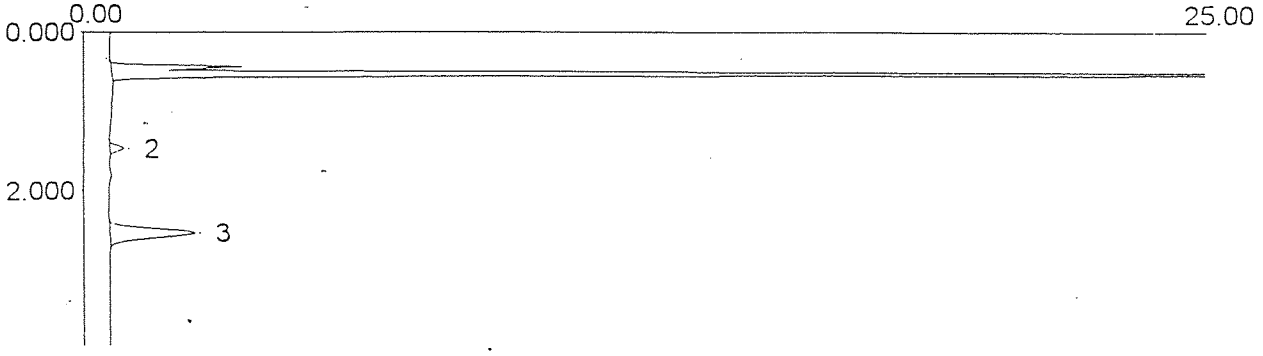

Stannylated 2,6-diphenylphenol

RT	AREA	TYPE	WIDTH	AREA %
0.533	108.146	BB	0.634	86.634
1.467	1.576	BB	0.593	1.263
2.533	15.108	BB	0.587	12.103

Fig3.27
GC plot of the stannylated 2,6-diphenylphenol compound
(microwave method)

Table 3.08 GC analyses of stannylated model compounds

Stannylated compound	Main peaks (residence time RT)	Assignments	% Conversion
2,6-dimethylphenol			
reflux method	0.751	toluene	66
	3.303	unreacted model cmpd*	
	3.517	stannylated model cmpd	
microwave method	0.668	acetonitrile	100
	3.873	stannylated model cmpd	
2,6-diisopropylphenol			
reflux method	0.785	toluene	100
	4.105	stannylated model cmpd	
microwave method	0.633	acetonitrile	100
	4.567	stannylated model cmpd	
2,6-diphenylphenol			
reflux method	0.500	toluene	100
	2.533	stannylated model cmpd	
microwave method	0.533	acetonitrile	100
	2.533	stannylated model cmpd	

*cmpd=compound

The GC data corroborates the FT-IR spectra for the stannylated model compounds and shows that in all cases, with the exception of the reflux method using the 2,6-dimethylphenol compound, all the model compound was converted to the stannylated derivative. In the case of 2,6-dimethylphenol, the microwave method shows a distinct advantage over classical reflux methods in its ability to drive reactions quickly and efficiently to completion. This is one of the major advantages of using microwave methodology.

The stannylated samples were also analysed by nmr spectroscopy. Two isotopes - ^{117}Sn and ^{119}Sn - were investigated in order to determine which would give a clearer nmr spectrum. The standard used was tetramethyltin. The TBTO reagent gave a signal at approximately 93 ppm, with the ^{119}Sn isotope producing a better signal (figs 3.28 - 3.29). The stannylated 2,6-dimethylphenol (reflux method) gave a clear signal at approximately 116 ppm - again a better resolution was obtained using the ^{119}Sn isotope (figs 3.30 - 3.31). The microwave method for the 2,6-dimethylphenol compound yielded a single sharp ^{119}Sn peak at approximately 115 ppm (fig 3.32). The stannylated 2,6-diisopropylphenol compound gave peaks at approximately 113 ppm (reflux method) and 112 ppm (microwave method) - fig 3.33 and fig 3.34 respectively. The stannylated 2,6-diphenylphenol produced a very well-defined peak at approximately 127 ppm for both the reflux and the microwave methods (figs 3.35 and 3.36 respectively) and the stannylated 2-phenylphenol produced signals at approximately 121 ppm (reflux method - figs 3.37 - 3.38) and 120 ppm (microwave method - fig 3.39). It appears that for a given amount of instrument time the signal / noise ratio is superior for the ^{119}Sn nucleus compared to the ^{117}Sn nucleus.

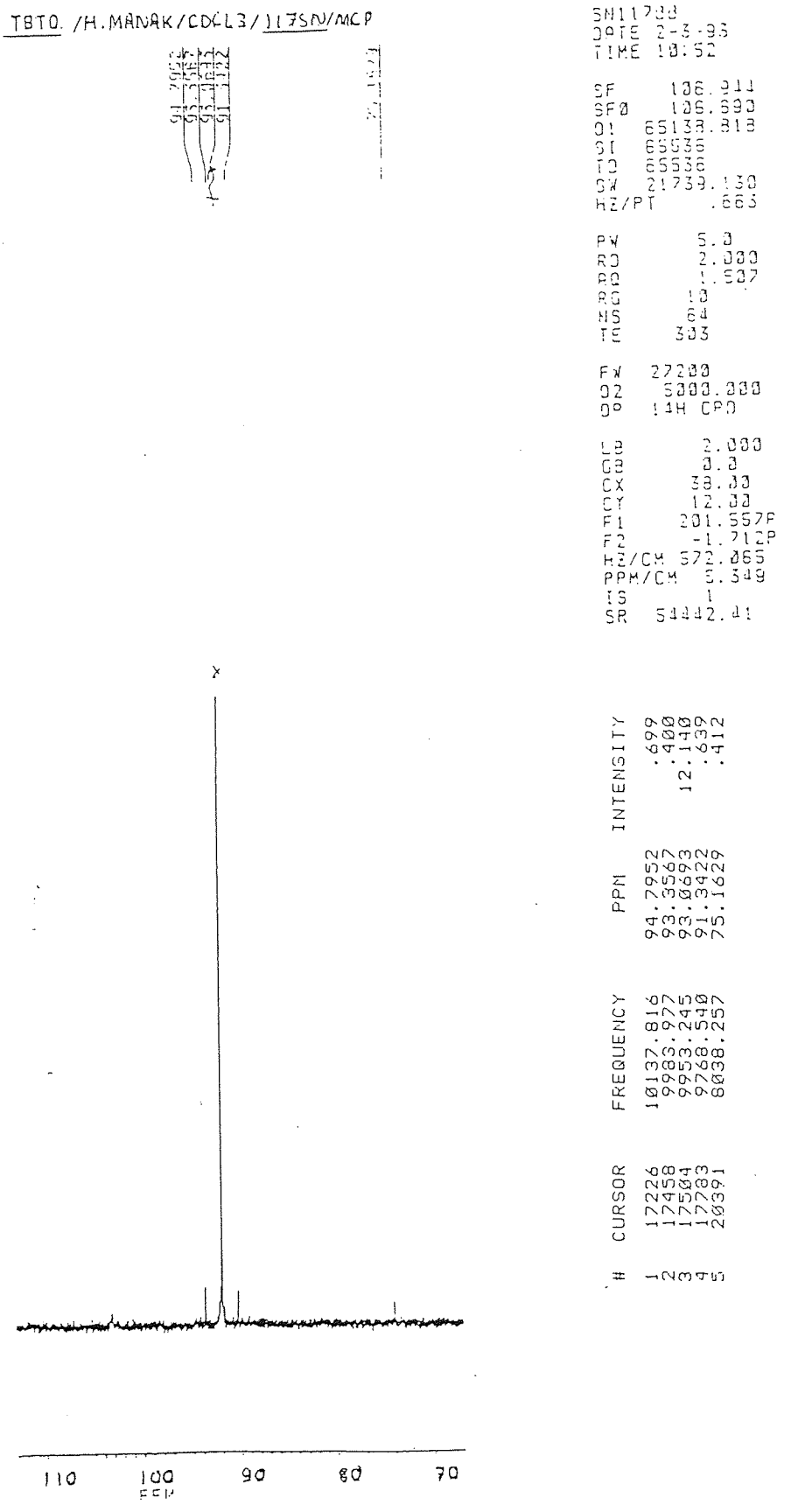

#	CURSOR	FREQUENCY	PPM	INTENSITY
1	17226	10137.816	94.7952	.699
2	17458	9983.977	93.3567	.400
3	17504	9953.245	93.0693	12.140
4	17783	9768.540	91.3422	.639
5	20391	8038.257	75.1629	.412

Fig3.28
^{117}Sn nmr of TBTO

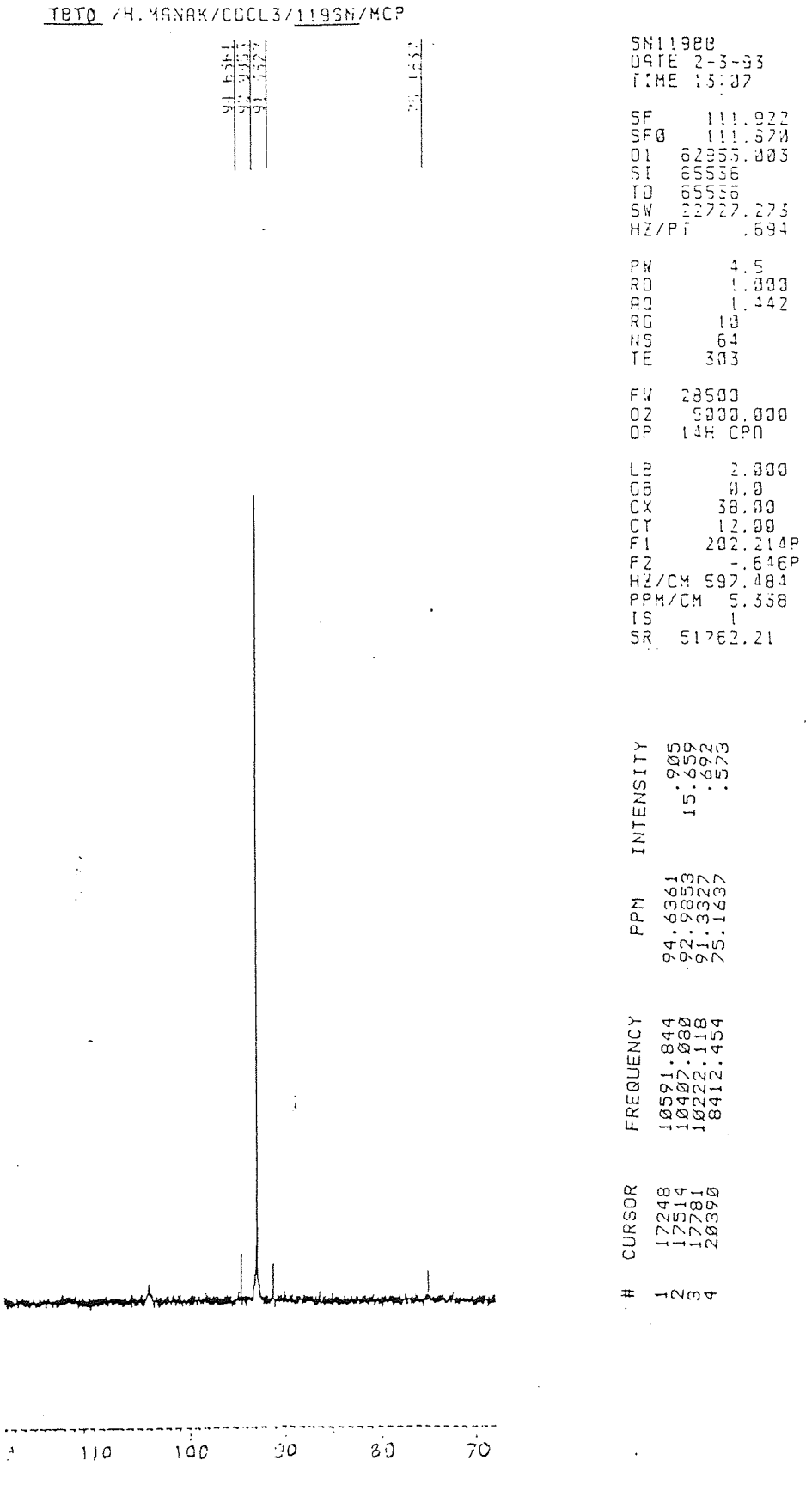

Fig3.29
^{119}Sn nmr of TBTO

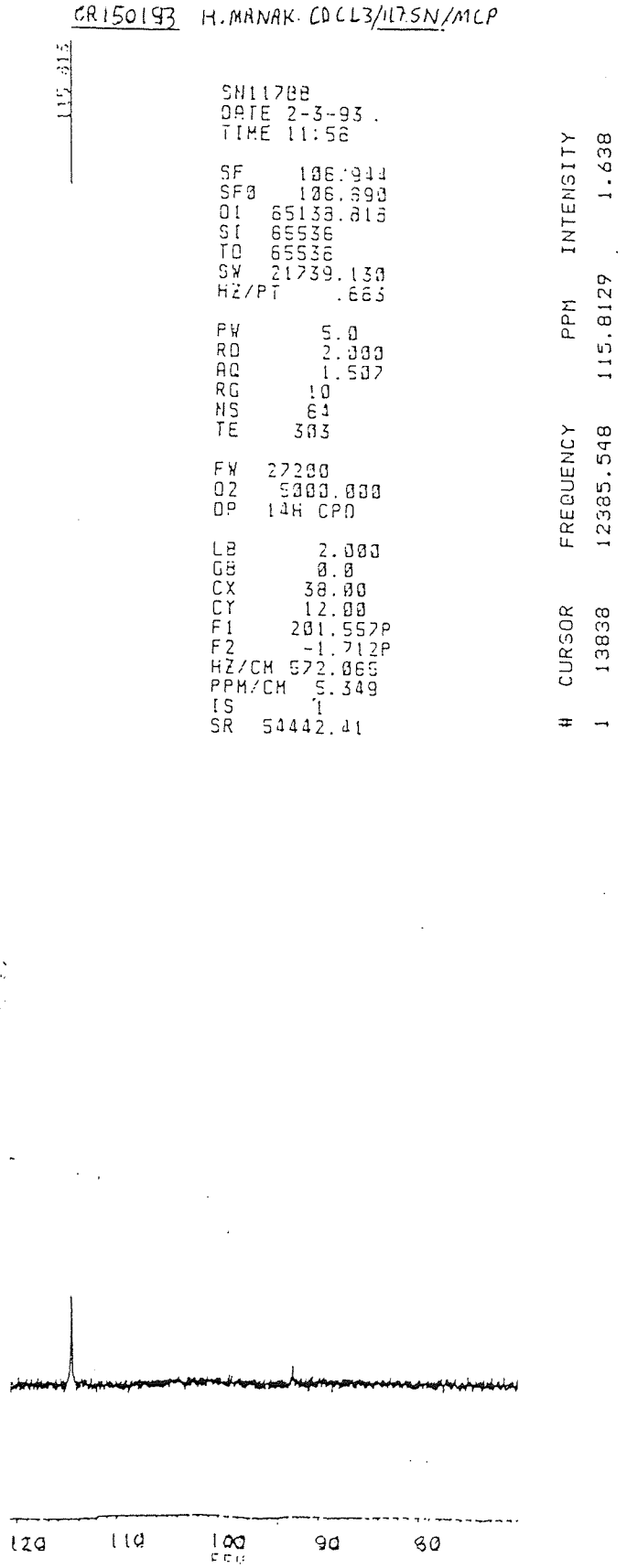

Fig3.30
^{117}Sn nmr of the stannylated 2,6-dimethylphenol compound (reflux method)

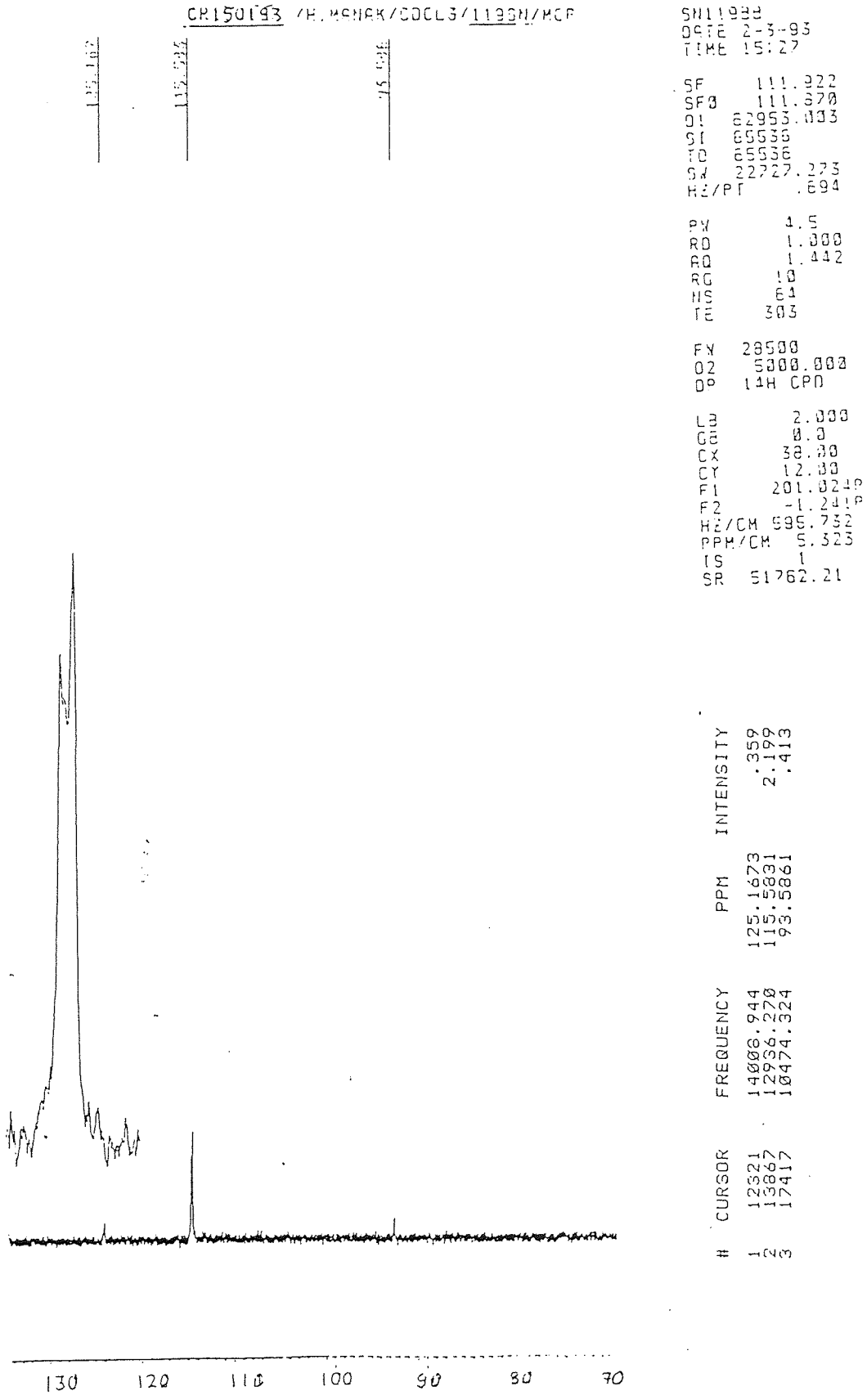

Fig3.31
^{119}Sn nmr of the stannylated 2,6-dimethylphenol compound (reflux method)

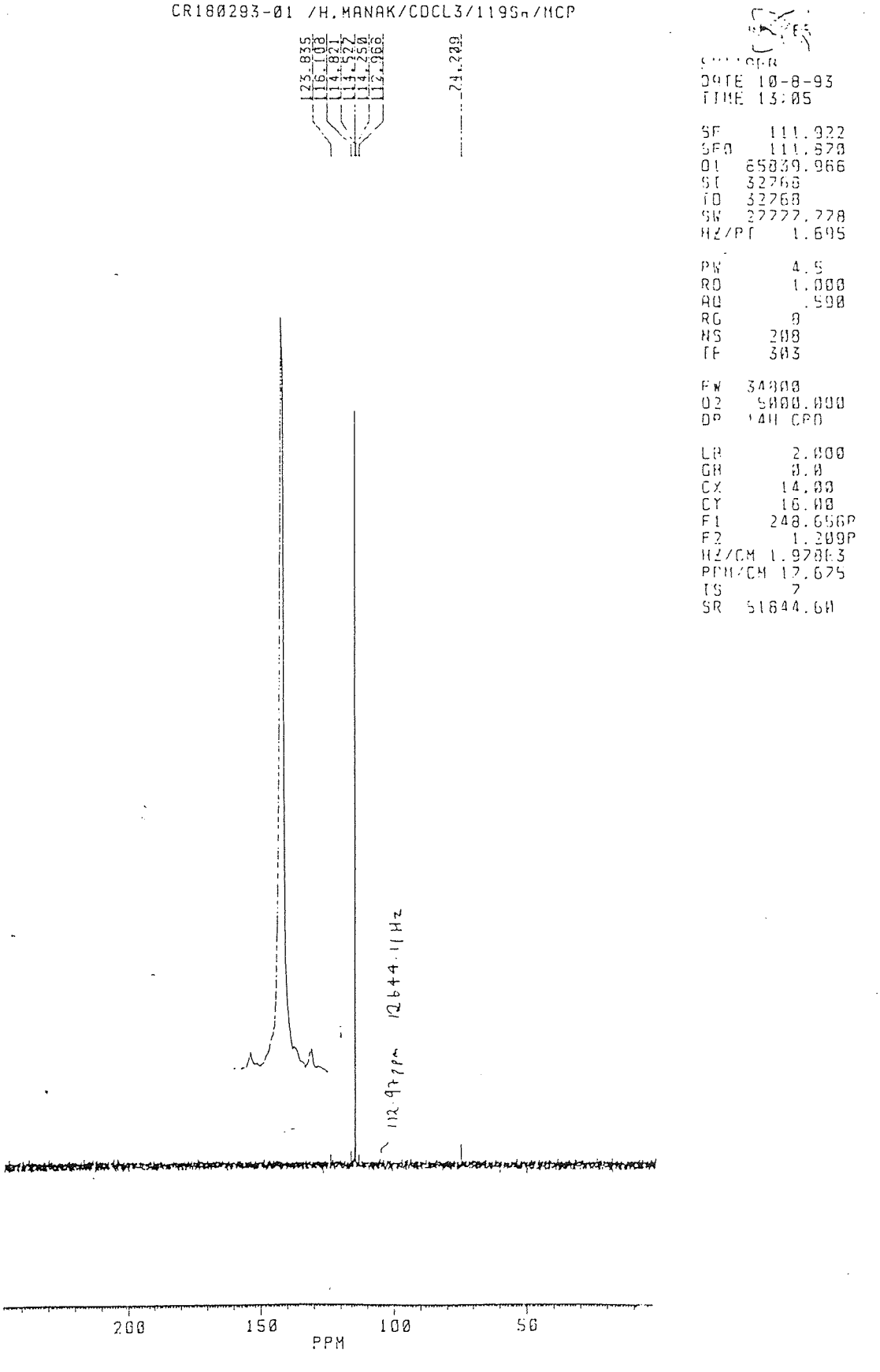

Fig3.32
^{119}Sn nmr of the stannylated 2,6-dimethylphenol compound (microwave method)

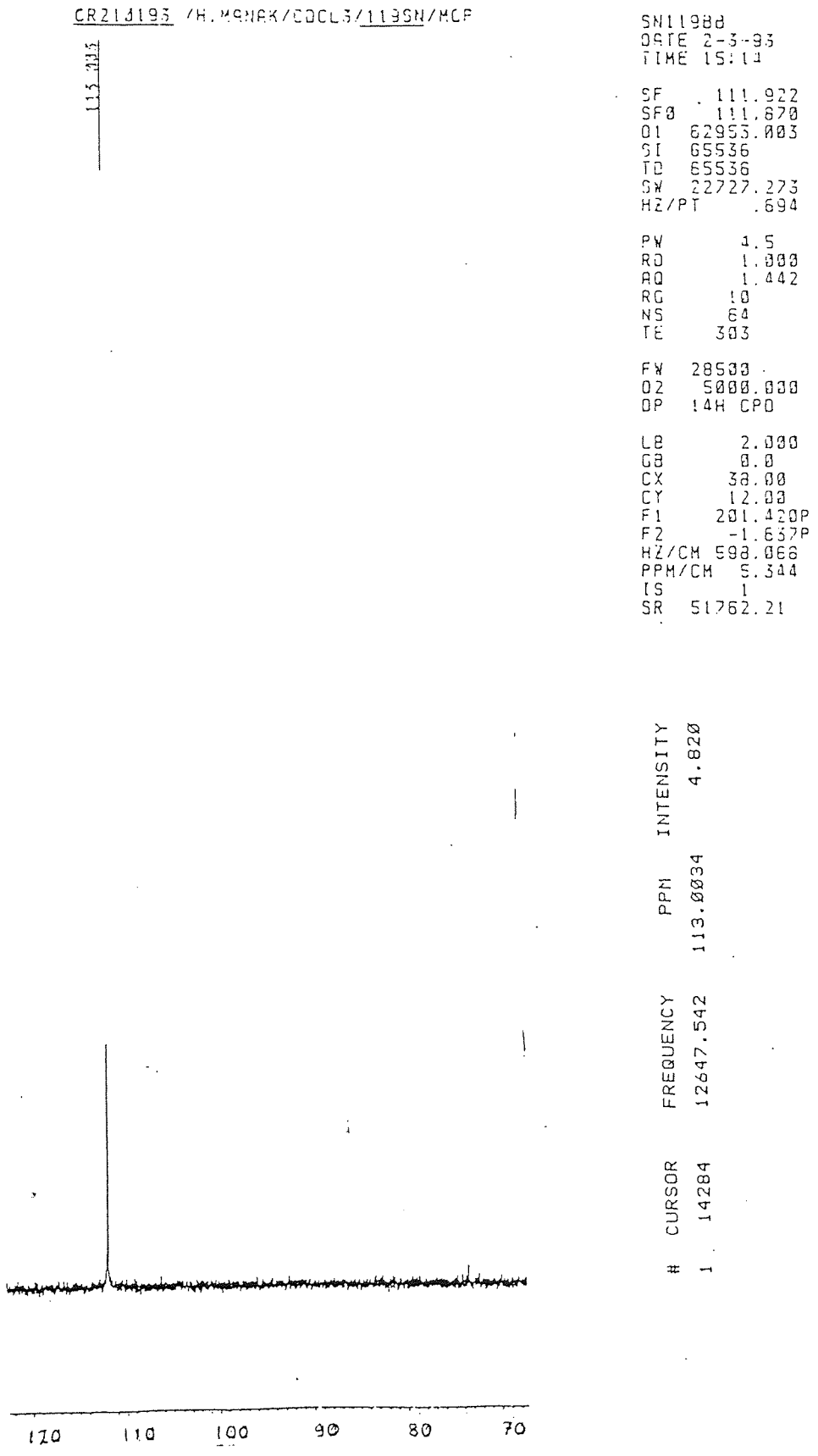

Fig3.33
^{119}Sn nmr of the stannylated 2,6-diisopropylphenol compound (reflux method)

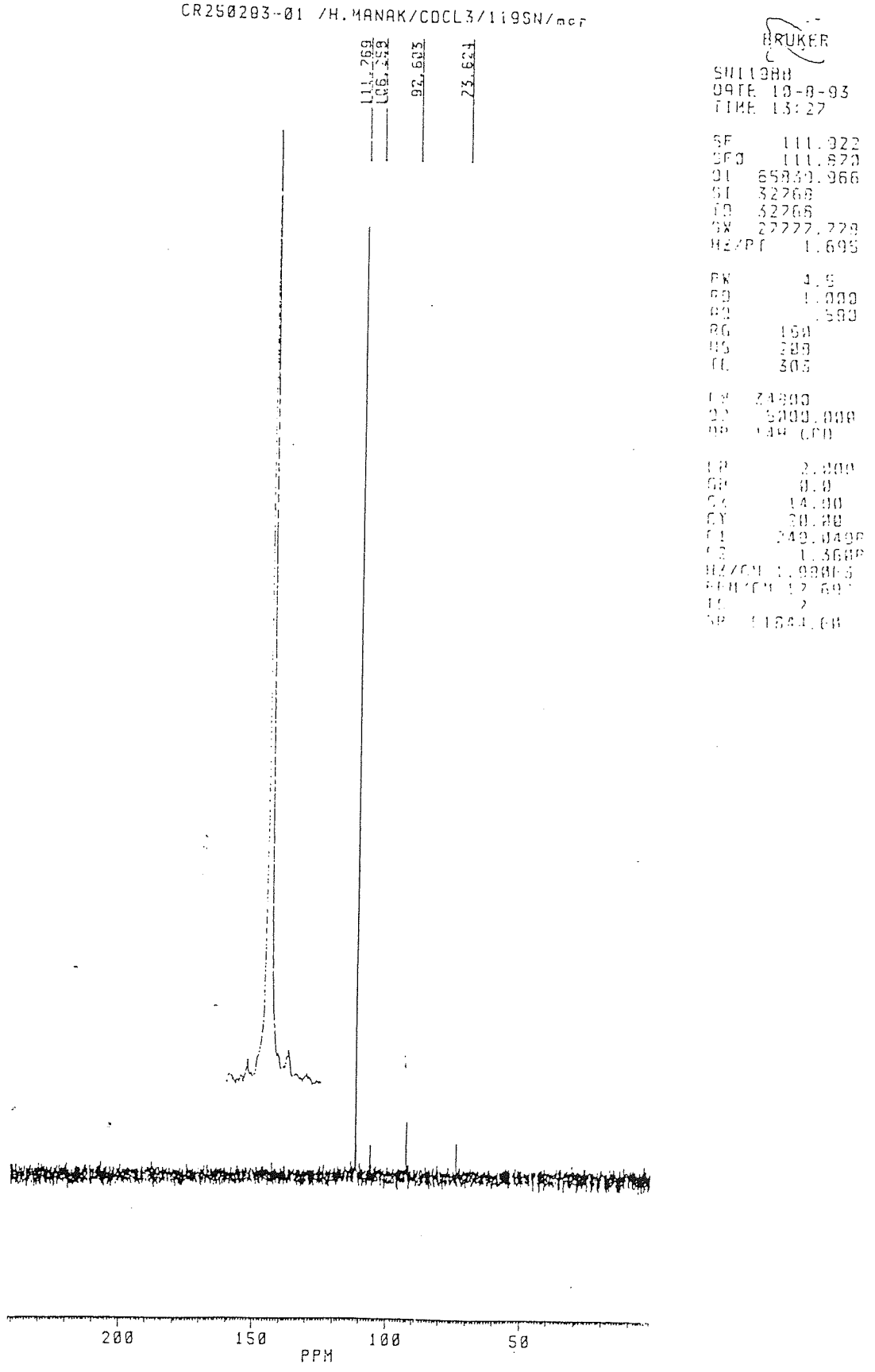

Fig3.34
^{119}Sn nmr of the stannylated 2,6-diisopropylphenol compound (microwave method)

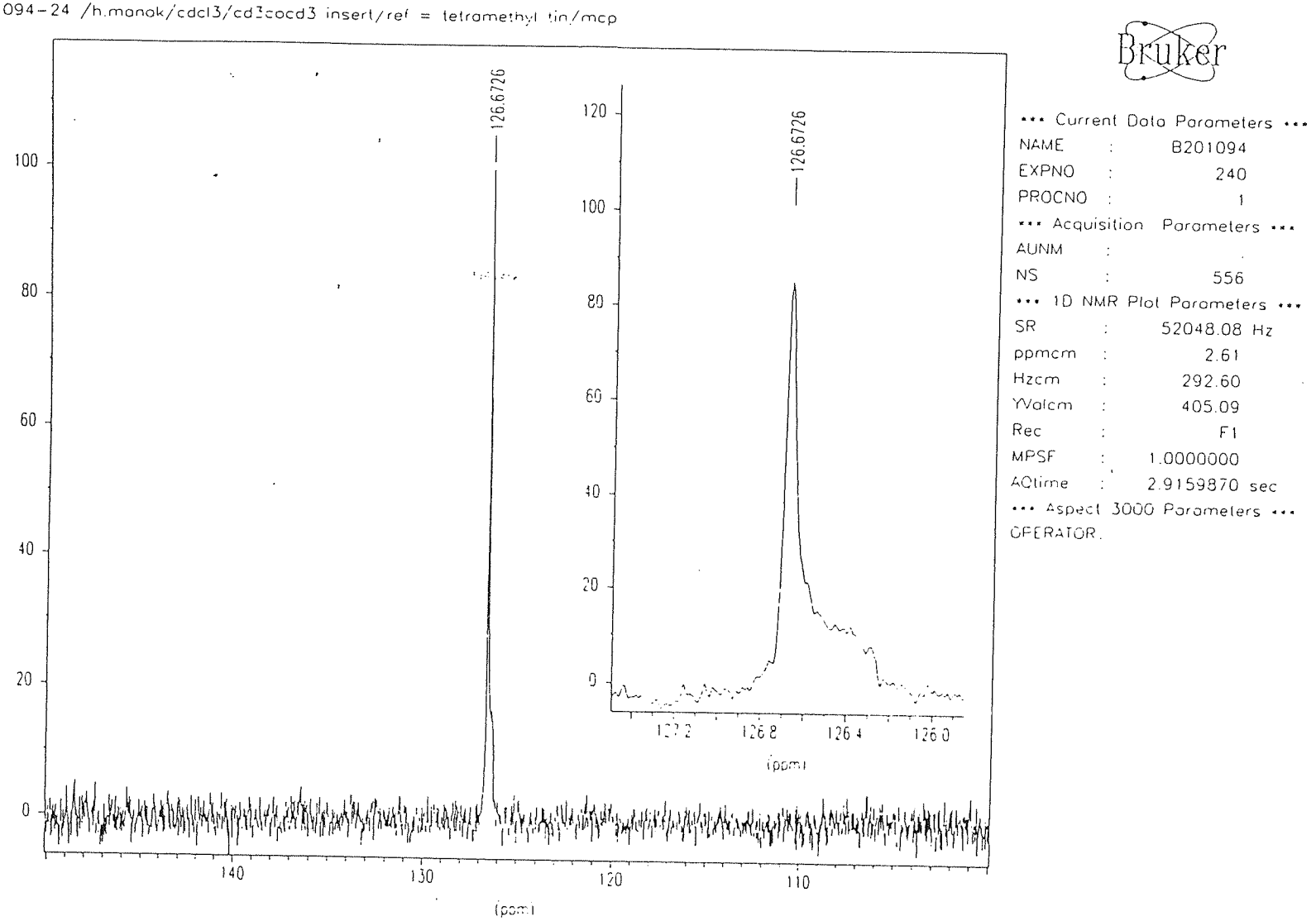

Fig3.35
^{119}Sn nmr of the stannylated 2,6-diphenylphenol compound
(reflux method)

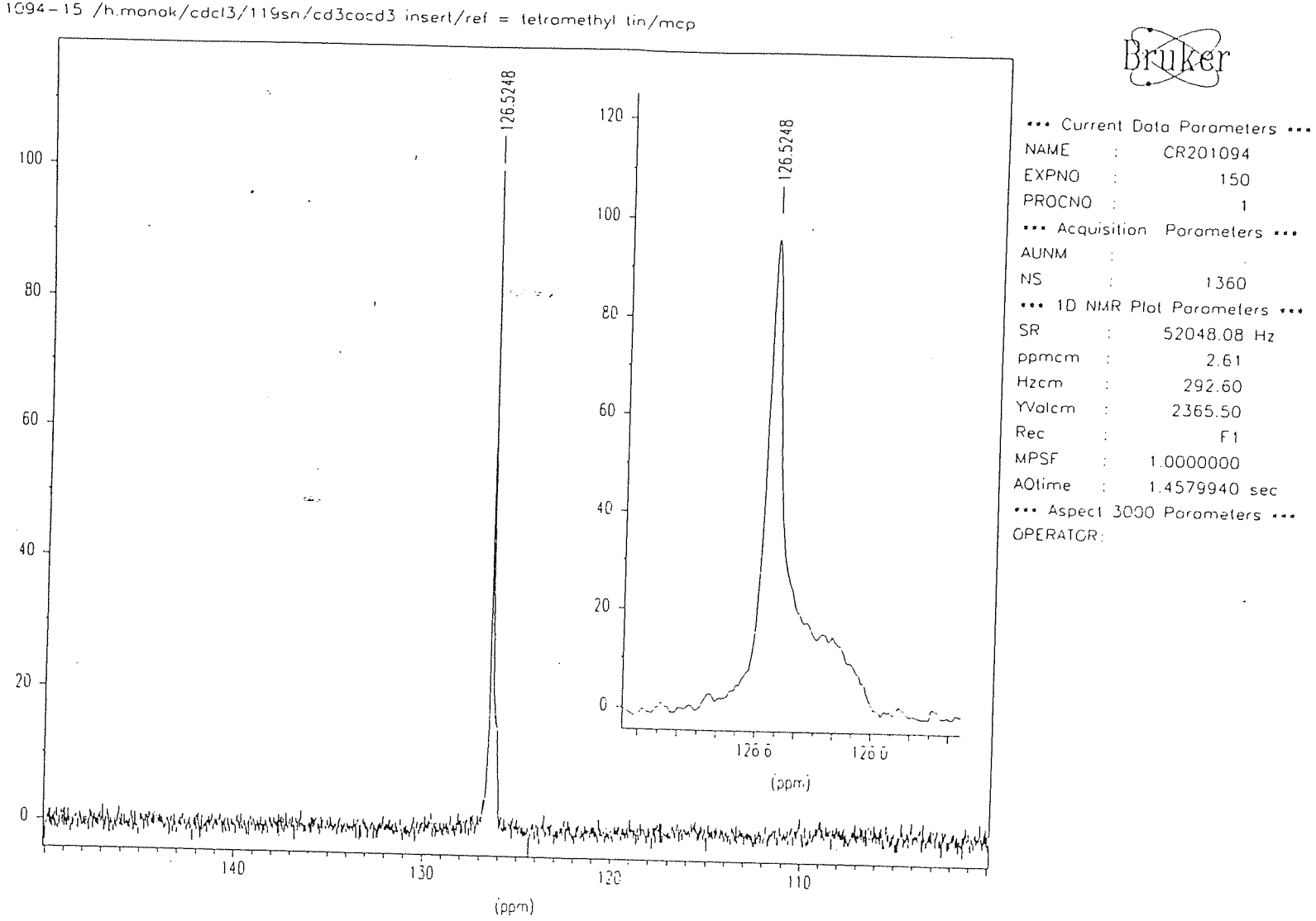

Fig3.36
^{119}Sn nmr of the stannylated 2,6-diphenylphenol compound
(microwave method)

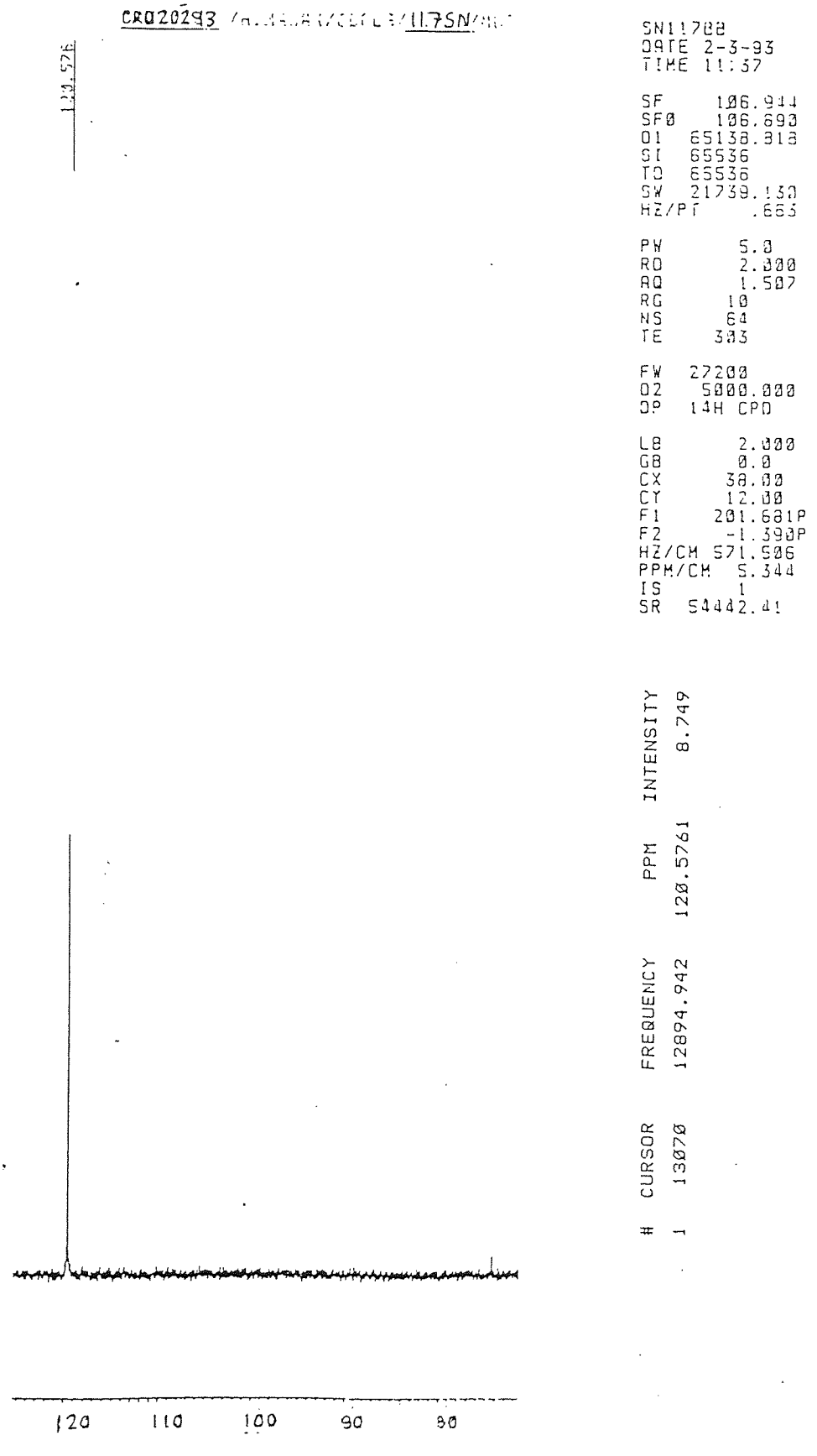

Fig3.37
^{117}Sn nmr of the stannylated 2-phenylphenol compound (reflux method)

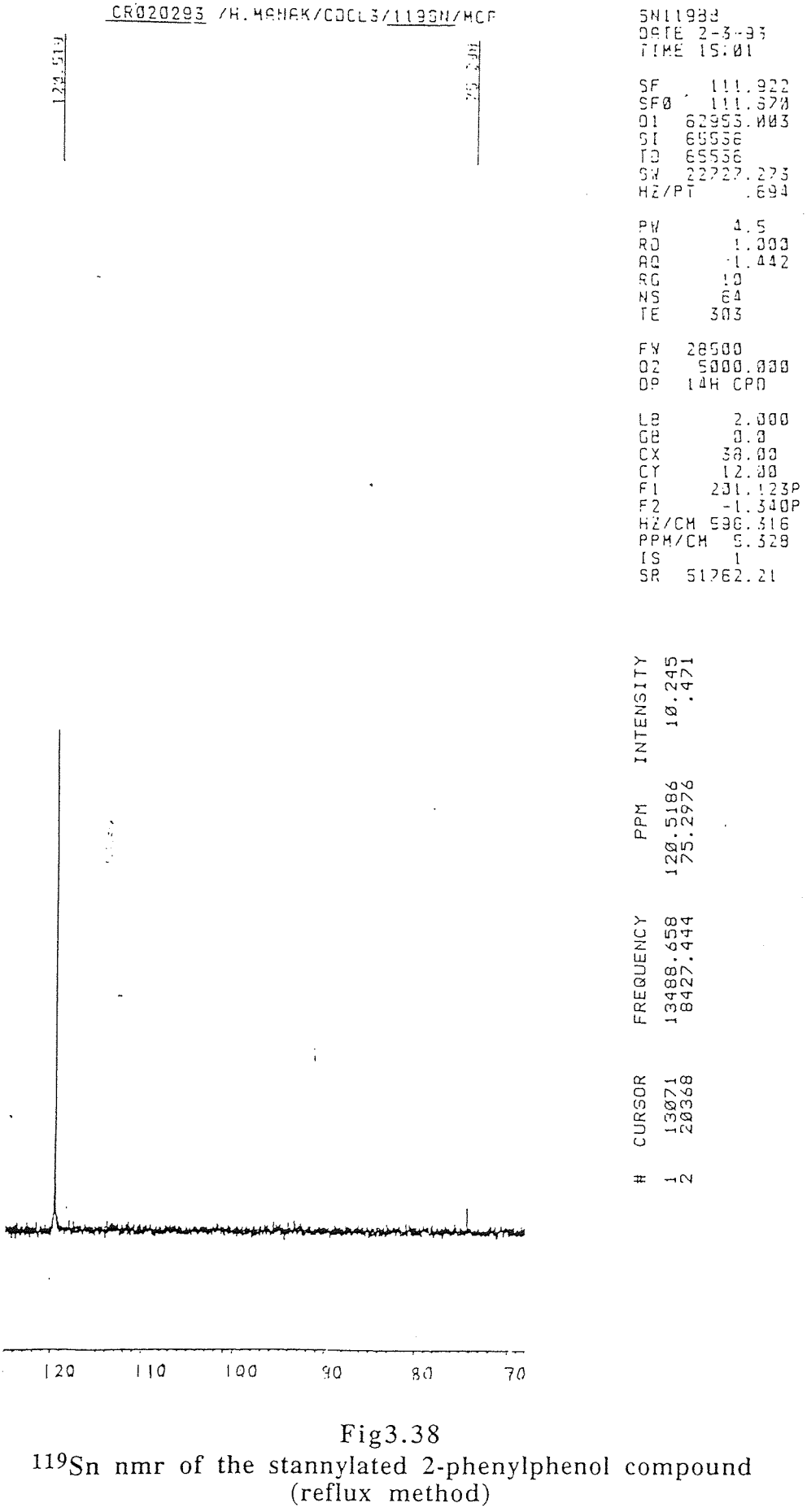

Fig3.38
^{119}Sn nmr of the stannylated 2-phenylphenol compound
(reflux method)

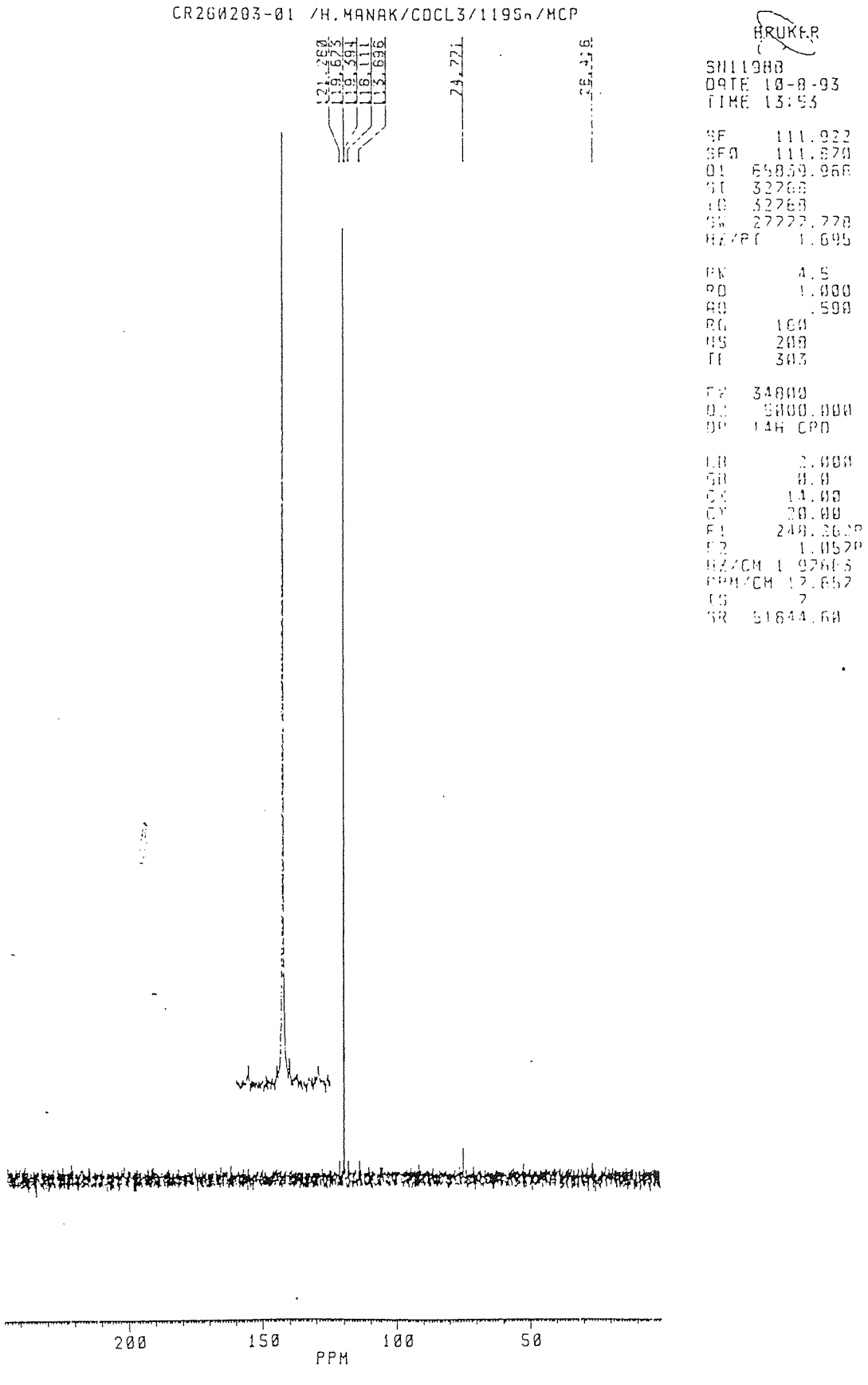

Fig3.39
^{119}Sn nmr of the stannylated 2-phenylphenol compound (microwave method)

Table 3.09 Chemical shifts for stannylated model compounds

Stannylated compound	δ (ppm) (reflux method)	δ (ppm) (microwave method)	Comments
2,6-dimethylphenol	115.8 (^{117}Sn) 115.6 (^{119}Sn)	114.5 (^{119}Sn)	^{119}Sn gave a better signal than ^{117}Sn
2,6-diisopropylphenol	113.0 (^{119}Sn)	111.8 (^{119}Sn)	
2,6-diphenylphenol	126.7 (^{119}Sn)	126.5 (^{119}Sn)	
2-phenylphenol	120.6 (^{117}Sn) 120.5 (^{119}Sn)	119.7 (^{119}Sn)	^{119}Sn gave a better signal than ^{117}Sn

TBTO produced chemical shifts at 93.1 ppm (^{117}Sn) and 93.0 ppm (^{119}Sn)

^{119}Sn was shown to be more sensitive than ^{117}Sn (both have a spin 1/2). The reason for this is because of the slightly greater abundance of ^{119}Sn (8.58%) compared to ^{117}Sn (7.61%) and the greater receptivity (on a scale where the receptivity of ^{13}C is taken as 1.0) of ^{119}Sn (25.2) compared to ^{117}Sn (19.54). Both ^{119}Sn and ^{117}Sn have similar gyromagnetic ratios and typical values of T_1 are between 2.0 - 0.02 seconds (which is rapid for a spin 1 / 2 nucleus).

As can be seen from Table 3.09 there are slight changes in chemical shift (±1.2 ppm) for the same reaction. These chemical shift changes can be attributed to various factors including solvent effects, magnetic fluctuations and temperature variations when the sample was analysed.

The model compound work has shown that TBTO is a more suitable reagent for our purposes than Tributyltin chloride, which preferentially undergoes side-reactions. This points to an important conclusion concerning the methodology - microwave heating will not necessarily accelerate only a reaction of particular analytical interest, but the rates of side reactions may also be accelerated. Consequently it is desirable to select reagents with no or minimum side reactions, such as TBTO. Another drawback of utilising the triorganotin chloride reagent in the microwave oven is that there is a loss of reagent due to volatility, as well as accelerated loss of reagent due to side reactions.

Because the Sn nucleus (atomic radius 1.40 Å) is larger than the Si nucleus (atomic radius 1.17 Å) we would expect an order of accessibility with the more sterically demanding substituted-phenols finding it more difficult to react with the stannylating reagent - the TBTO. The work in this chapter has shown this to be true. The more hindered phenols such as 2,6-di-tert-butylphenol, are less likely to react because the steric demand of the ortho-substituents is too great. The 2,6-dimethylphenol, 2,6-diisopropylphenol, 2,6-diphenylphenol and 2-phenylphenol compounds all reacted after only 1 minute in the microwave oven (the mono- and di-substituted phenylphenols reacted well because, although their substituents are fairly bulky, they lie in a planar plane and are able to 'skewer' away from the hydroxyl functional group allowing the reagent room to attack), whereas 2,6-di-tert-butylphenol and 2,4,6-tri-tert-butylphenol showed no inclination to react at all.

The results also show the ability of microwave radiation to drive reactions to equilibrium much more rapidly and efficiently than conventional (reflux) methods. Rate acceleration up to 120 times faster was achieved for the stannylation of the model compounds when using microwave methodology.

The ^{119}Sn nmr data for the stannylated model compounds shows that distinct peaks are obtained for different substituted-phenolic compounds. This could afford valuable data on the nature of phenolic groups in coals - stannylation of the phenolic group could introduce a magnetic label into the coal, which could be analysed by ^{119}Sn MASNMR to ascertain which hydroxyl groupings are present. However, due to steric differences, not all the phenolic groups will be stannylated - this would allow us to map out the extent of the more hindered phenolic groups in coal i.e the more sterically demanding n-Bu_3Sn- derivative will show a lower apparent -OH content for a given coal than that determined by using, say Me_3Si- derivatives, thus enabling the proportion of more hindered -OH groups to be established. Subsequently it would be possible to map out the density of -OH sites of differing degrees of steric hindrance by treatment of the same coal with a range of reagents of differing steric demand.

3.3.4 Stannylation of coals

The coals used in the stannylation experiments were Creswell, Cortonwood (Silkstone), Gedling and Ollerton. Three particle sizes were investigated for Creswell coal. These were <500>212 μm, <212>90 μm and ≤90 μm. All other coals were of particle size ≤212 μm. Table 3.10 shows the analytical data for the coals. The attempted reaction may be summarised as :

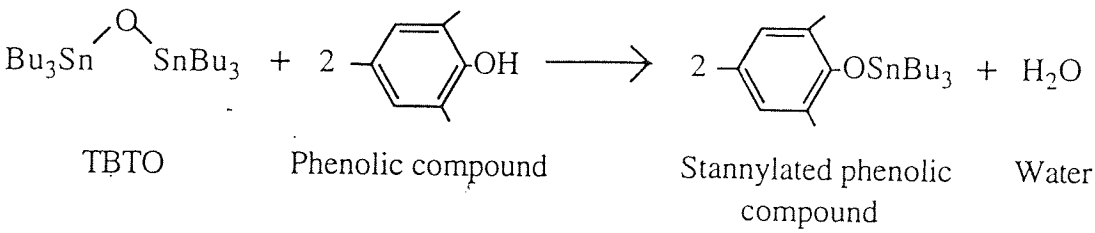

The TBTO reagent also reacts with thiol, carboxylic acid and aliphatic hydroxyl groups - if present in the coal. The coals used in this study do not contain appreciable amounts of carboxylic acid groupings and the total S content is only about 1.0% ; thus the main reaction occurring will be that of the TBTO with hydroxyl, and in particular phenolic functional groups.

Table 3.10 Analytical data for coals

Analysis	Component	Basis	Creswell (% w/w)	Cortonwood (% w/w)	Gedling (% w/w)	Ollerton (% w/w)
Proximate	Moisture	ad[a]	2.5	1.0	10.0	6.1
	Ash	ad	2.6	2.2	2.0	3.4
	Fixed C	ad	60.2	62.1	53.5	55.7
	Volatile matter	dmmf[b]	36.8	34.7	34.5	38.7
	Mineral matter	db[c]	3.39	2.73	2.76	4.45
Ultimate	Carbon	dmmf	86.2	87.2	81.6	83.5
	Hydrogen	dmmf	5.2	5.6	5.2	5.0
	Oxygen	dmmf	5.6	4.8	10.3	8.3
	Nitrogen	dmmf	1.91	1.70	1.70	1.85
	Chlorine	db	0.21	0.09	0.46	0.57
Forms of Sulfur	S (total)	db	1.40	0.98	0.98	1.6
	S (organic)	db	0.95	0.60	0.89	1.10
	S (pyritic)	db	0.40	0.36	0.07	0.40
	S (sulfate)	db	< 0.05	0.02	0.02	< 0.1
Calorific value	KJ / Kg	daf[d]	35380	36200	33580	34280
Maceral Analysis (% vol)	Exinite	mmf[e]	07	09	15	10
	Vitrinite	mmf	81	82	65	74
	Inertinite	mmf	12	09	20	16

[a]ad = as analysed (air dry) basis. [b]dmmf = dry, mineral matter free basis. [c]db = dry basis. [d]daf = dry, ash-free basis. [e]mmf = mineral matter free

The reaction is essentially a condensation reaction and occurs fairly rapidly and exothermically. A polar mechanism appears to be operating whereby the lone pair of electrons on the oxygen of the organotin reagent acts as a nucleophile towards the phenolic hydrogen, which is rendered positive and detached as a proton. The electrophilic tin centre then attacks the electron-rich phenolic oxygen to give the stannylated product and water as a by-product. The reactions were carried out as outlined in sections 2.6.2(a) and 2.6.2(d). With the microwave experiments acetonitrile was used as the solvent. It is possible to characterise the products by ^{119}Sn MASNMR because the ^{119}Sn chemical shift depends upon the nature of the substituted-phenol compound which is being stannylated - as shown by the model compound work.

The first coal to be stannylated was Creswell, which is a middle rank coal (86.2% C, 5.6% O). Three different particle sizes were tested (<500>212 μm, <212>90 μm and ≤90 μm). The <500>212 μm size coal was reacted with TBTO, using acetonitrile solvent, in the microwave oven for 5, 10 and 30 mins in separate reactions. An analogous bench top reaction was also carried out using TBTO and toluene solvent - the reagents were refluxed for 24 hrs. The <212>90 μm particle size coal was also reacted for 5, 10 and 30 mins in the microwave oven and for 24 hours on the bench top (refluxing in toluene). The ≤90 μm particle size coal was subjected to 5, 45, 75 and 120 mins of microwave heating in separate reactions and reacted for 24 hrs on the bench top refluxing in toluene.

Fig 3.40 shows the FT-IR spectrum of the Creswell coal. The -OH band is clearly visible at 3410 cm^{-1}. Other absorption bands commonly found in the IR spectra of coals are shown in Table 3.11 :

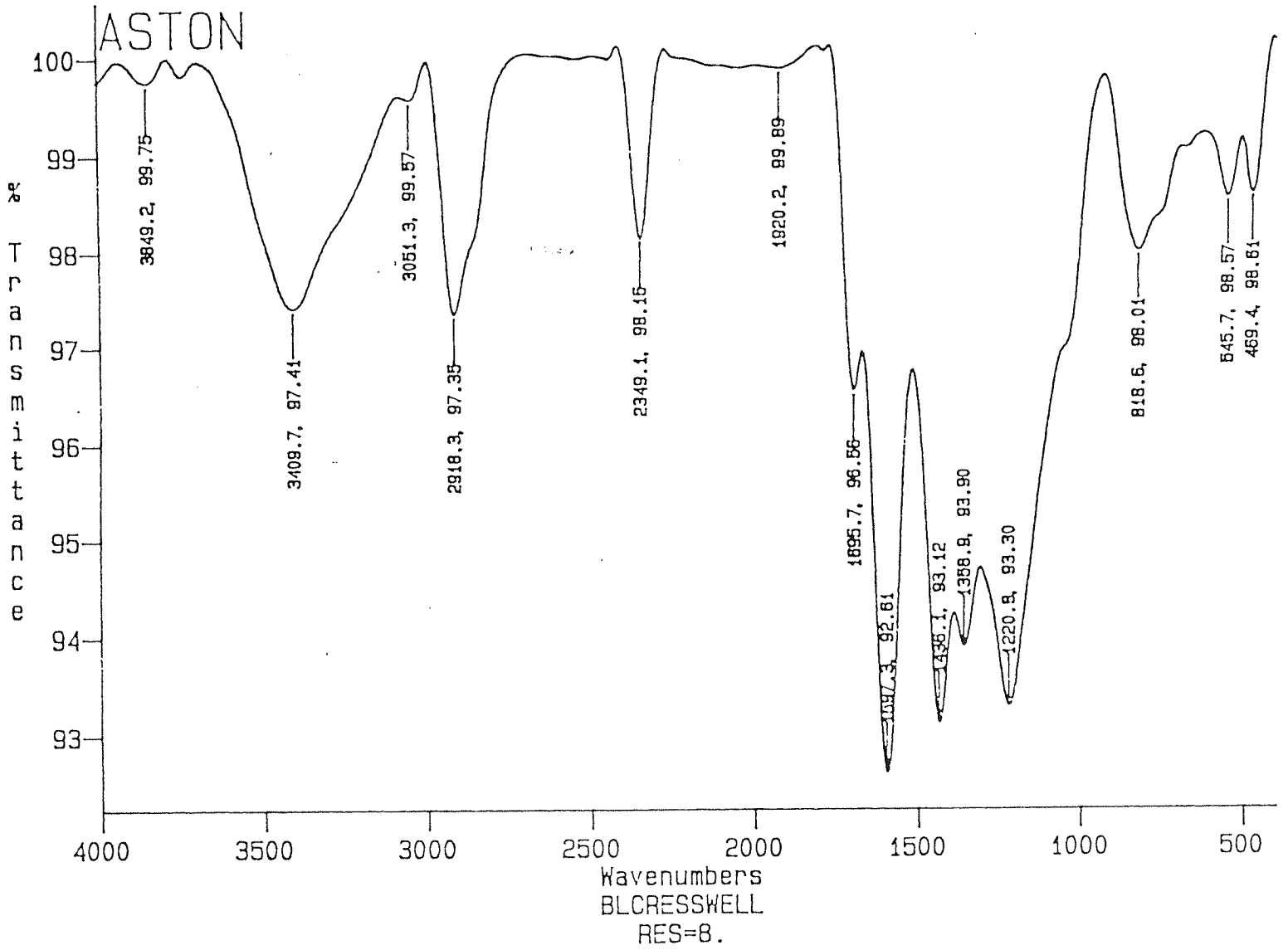

Fig3.40 .
IR spectrum of the raw Creswell coal <500>212 μm

Table 3.11 Absorption bands in the IR spectra of coal

Band position cm^{-1}	Assignment
3300	-OH (stretching), -NH (stretching)
3030	Aromatic C-H (stretching)
2940	Aliphatic C-H (stretching)
2925	$-CH_3$ (stretching), $-CH_2$ (stretching)
2860	Aliphatic C-H (stretching)
1700	C=O (stretching)
1600	Aromatic C=C (stretching), C=O, -OH
1500	Aromatic C=C (stretching)
1450	Aromatic C=C (stretching), $-CH_3$ (asymmetric deformation) $-CH_2$ (scissor deformation)
1380	$-CH_3$ (symmetric deformation), cyclic $-CH_2$
1300-1000	Phenolic and alcoholic C-H (stretching) C_{ar}-O-C_{ar} (stretching), C_{al}-O-C_{al} (stretching) C_{ar}-O-C_{al} (stretching)
900-700	"Aromatic" bands

The prominent band which occurs at about 1600 cm^{-1} in the IR spectra of coals has been variously assigned to :

(a) Polynuclear aromatic structures connected by predominantly aliphatic - CH_2 -
(b) Hydrogen-bonded or -OH chelated carbonyl groups
(c) Electron-transfer between aromatic carbon sheets
(d) Non-crystalline pseudographitic, but not necessarily aromatic, C-C configurations

Other important IR spectral bands are given in Table 3.12 :

Table 3.12 IR absorptions of organotin compounds

Bond	IR bands (cm^{-1})	Assignments
Sn-C (in Sn-Bu)	585-605	asymmetric stretch
	500-515	symmetric stretch
Sn-O (in $(R_3Sn)_2O$)	737-790vs	asymmetric stretch
	395-415m	symmetric stretch
Sn-O (in Sn-O-C)	960-1100	stretch
Sn-OH	885-910s	deformation

vs = very strong m = medium s = strong

Fig 3.41 shows the IR spectrum of the product from the microwave reaction of the <500>212 μm particle size Creswell coal after 5, 10 and 30 mins in the microwave oven. The IR spectrum shows that there is a definite reduction of the -OH band at about 3400 cm^{-1} indicating stannylation has taken place. There is also a small band at approximately 1100 cm^{-1} indicative of Sn-O-C bond formation. As the microwave heating time increases there is only a very slight reduction in the intensity of the -OH stretching band - indicating that the majority of the reaction has already taken place after only 5 mins heating in the microwave oven. The results from the 24 hrs reflux experiment for the <500>212 μm size coal (fig 3.42) also indicate that some stannylation has taken place, but in this case the degree of stannylation appears to be less than that obtained after 5 mins in the microwave oven.

The stannylation of the <212>90 μm particle size Creswell coal was also shown to occur after only 5 mins in the microwave oven (fig 3.43). There was no significant improvement in stannylation for this particle size after 10 mins or 30 mins further heating in the microwave oven. Again, the reflux method showed that reaction had occurred after 24 hrs (fig 3.44), but not to the same extent as after 5 mins microwave heating.

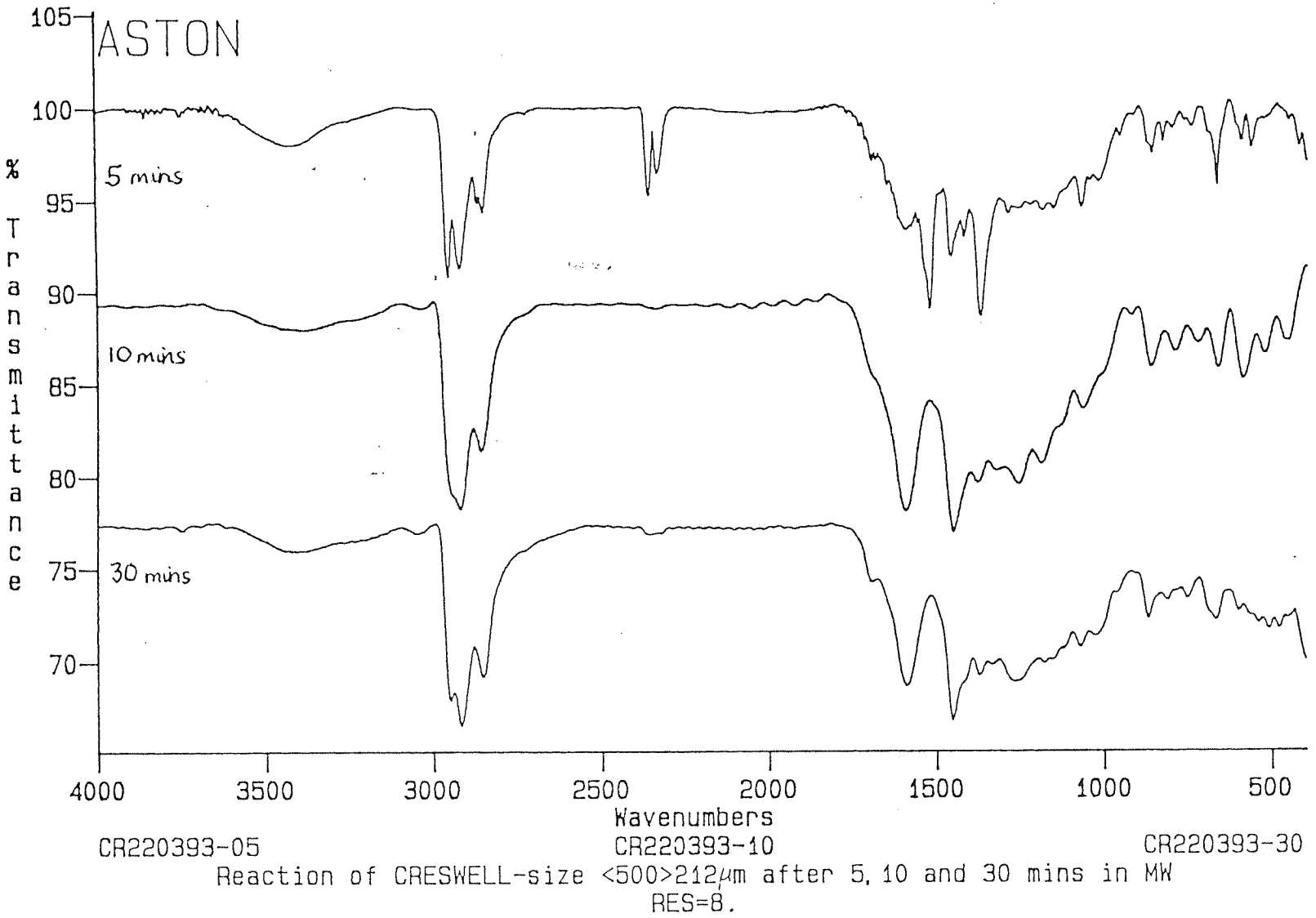

Fig3.41
IR spectra of the stannylated Creswell coal <500>212 μm
after 5, 10 and 30 mins of mw heating

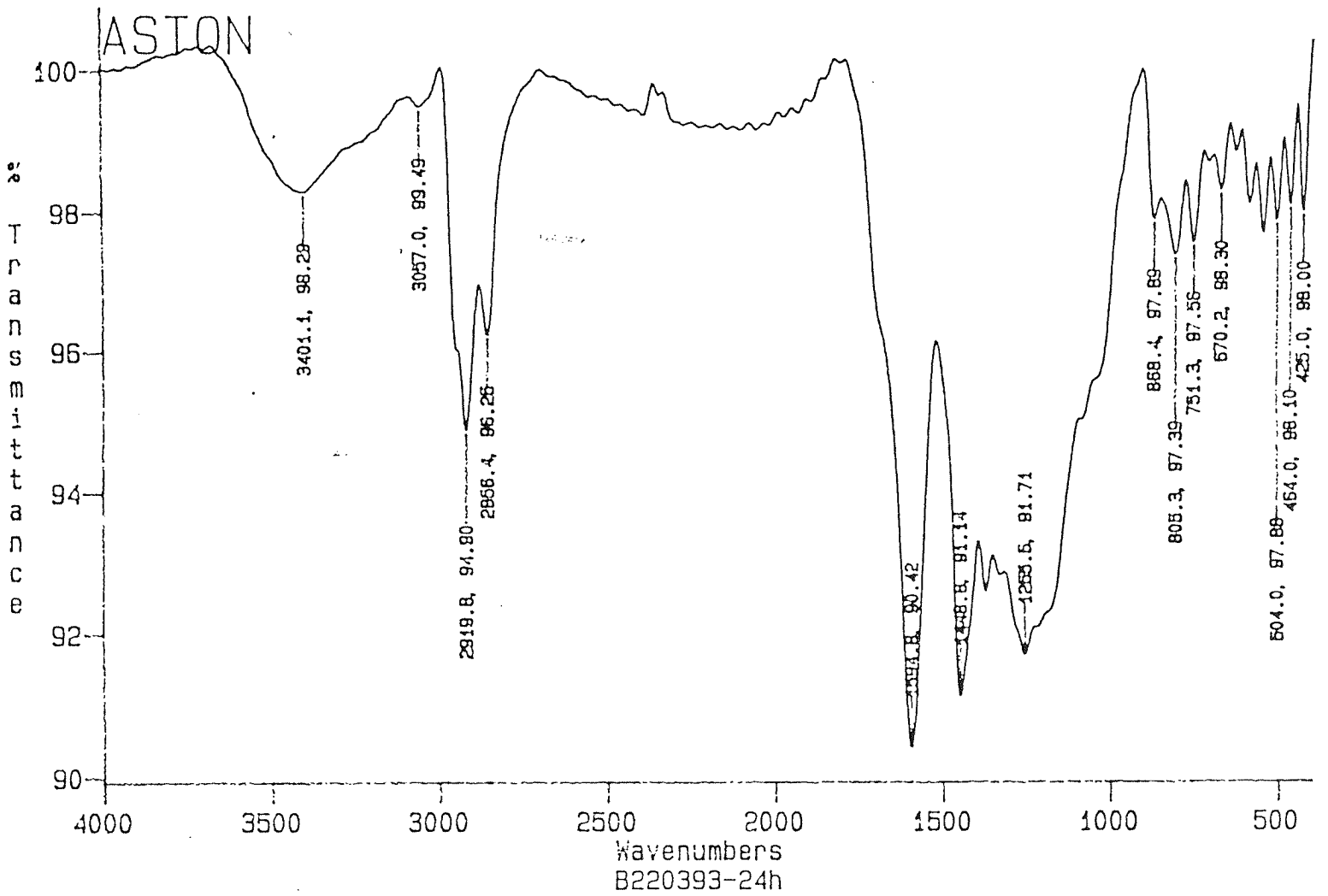

Fig3.42
IR spectra of the stannylated Creswell coal <500>212 μm after 24 hrs reflux

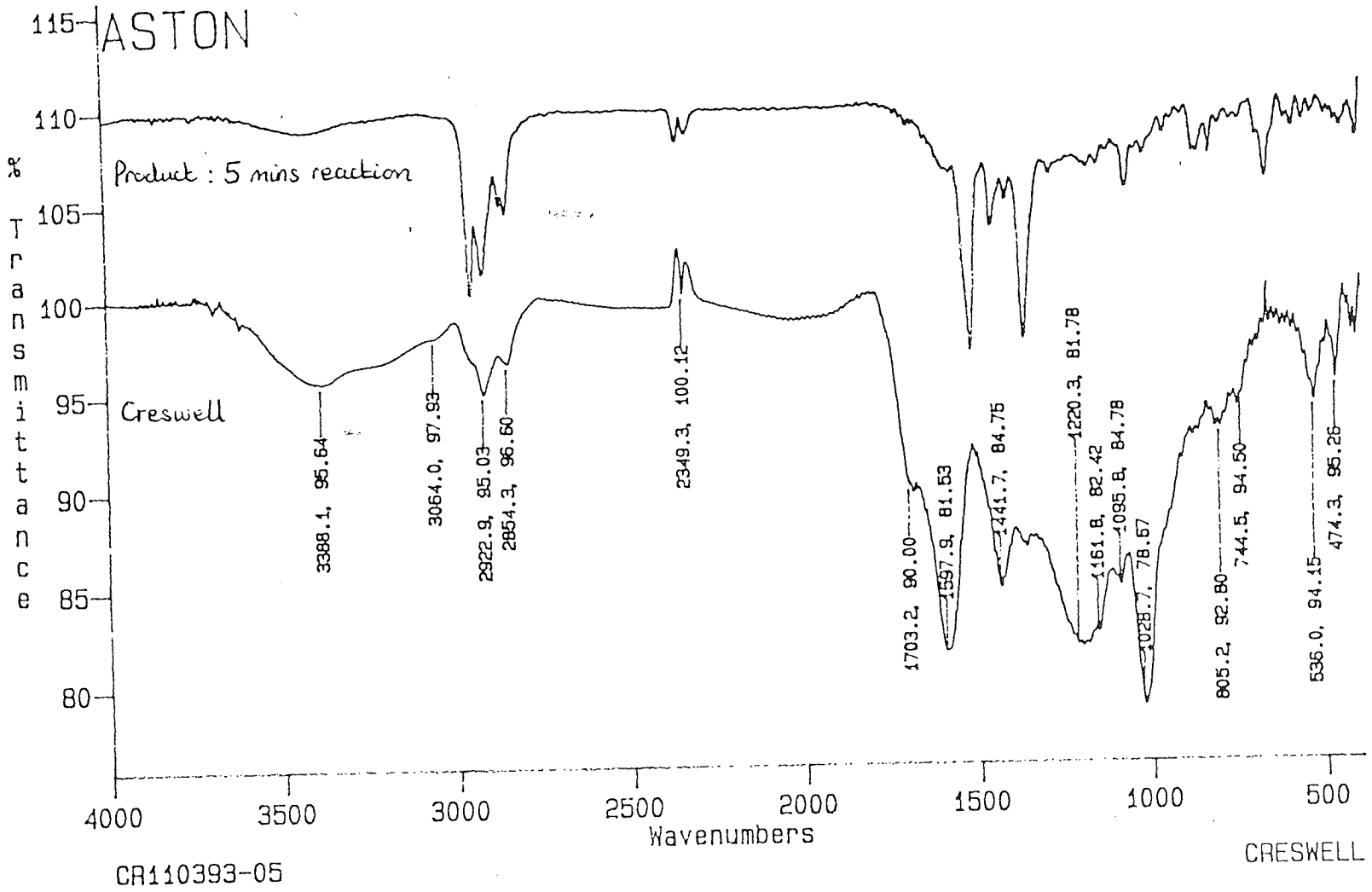

Fig3.43
IR of the stannylated Creswell coal <212>90 μm after 5 mins mw heating

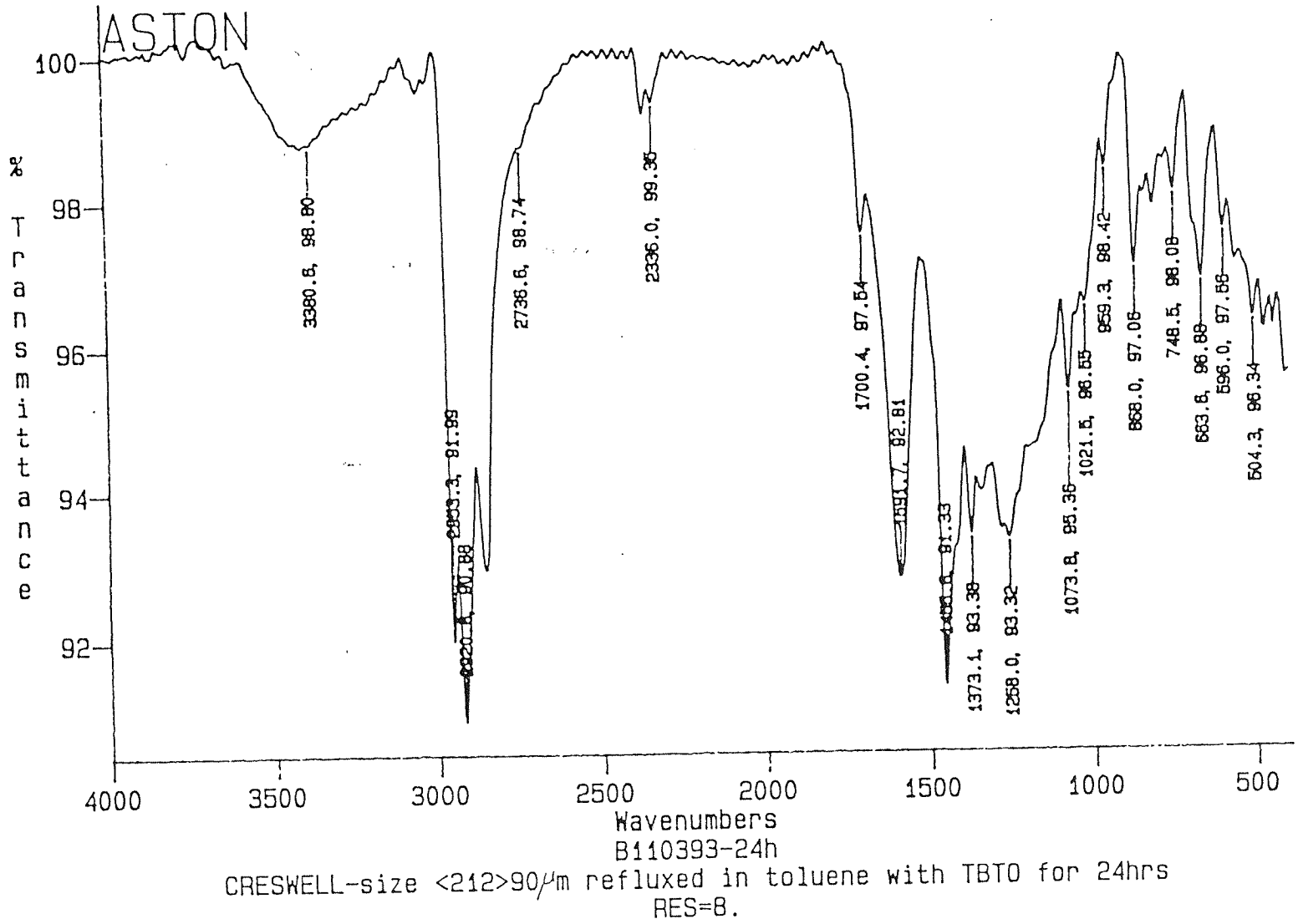

Fig3.44
IR of the stannylated Creswell coal <212>90 μm after 24 hrs reflux in toluene

The final particle size (≤90 μm) showed hardly any reaction after 5 mins in the microwave oven (fig 3.45), and only a slight reaction after 45, 75 and 120 mins of microwave heating (fig 3.46). The extent of reaction after 24 hrs refluxing in toluene was similar to that obtained after only 5 mins reaction time in the microwave oven (fig 3.47) for the ≤90 μm particle size.

Table 3.13 Stannylation of the different particle sizes of Creswell coal

Creswell particle size (μm)	Evidence of stannylation from FT-IR
<500>212	Microwave method : The reaction works after 5 mins and there is a slightly improved reaction after 10 mins, whereafter the reaction does not significantly improve with successive time increments. Reflux method : Some stannylation has taken place after 24 hrs, but there appears to be less stannylation compared to the microwave method.
<212>90	Microwave method : The reaction works after 5 mins. No significant improvement in reaction after a further 10 mins or 30 mins microwave heating. Reflux method : Some stannylation after 24 hrs, but not as much as after 5 mins in the microwave oven.
≤ 90	Microwave method : Hardly any reaction after 5 mins, but there was a limited reaction after 45, 75 and 120 mins. This reaction was not as complete as the <500>212 μm and <212>90 μm particle size reactions. Reflux method : Hardly any reaction after 24 hrs reflux.

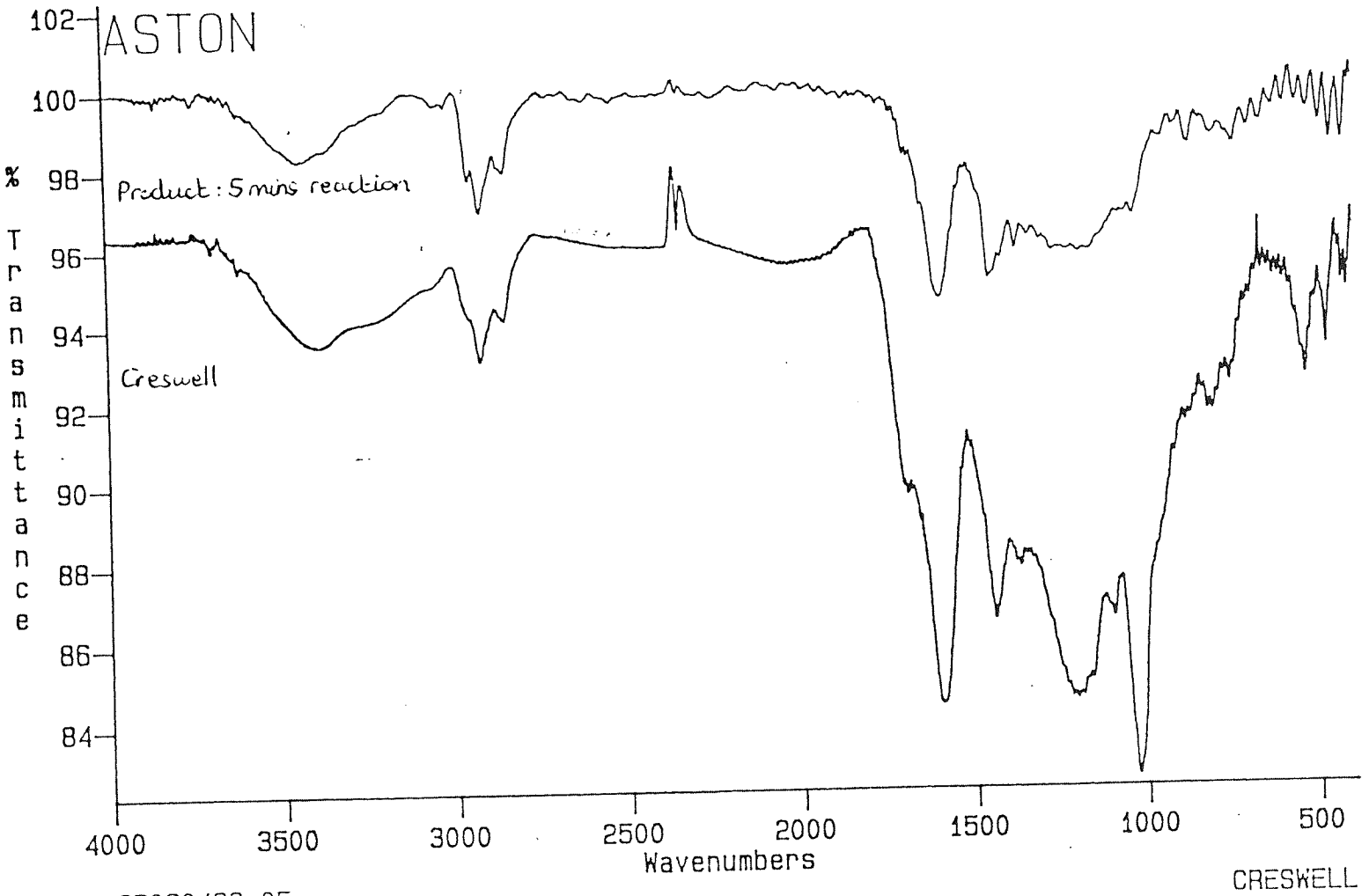

Fig3.45
IR of the stannylated Creswell coal ≤90 μm after 5 mins mw heating

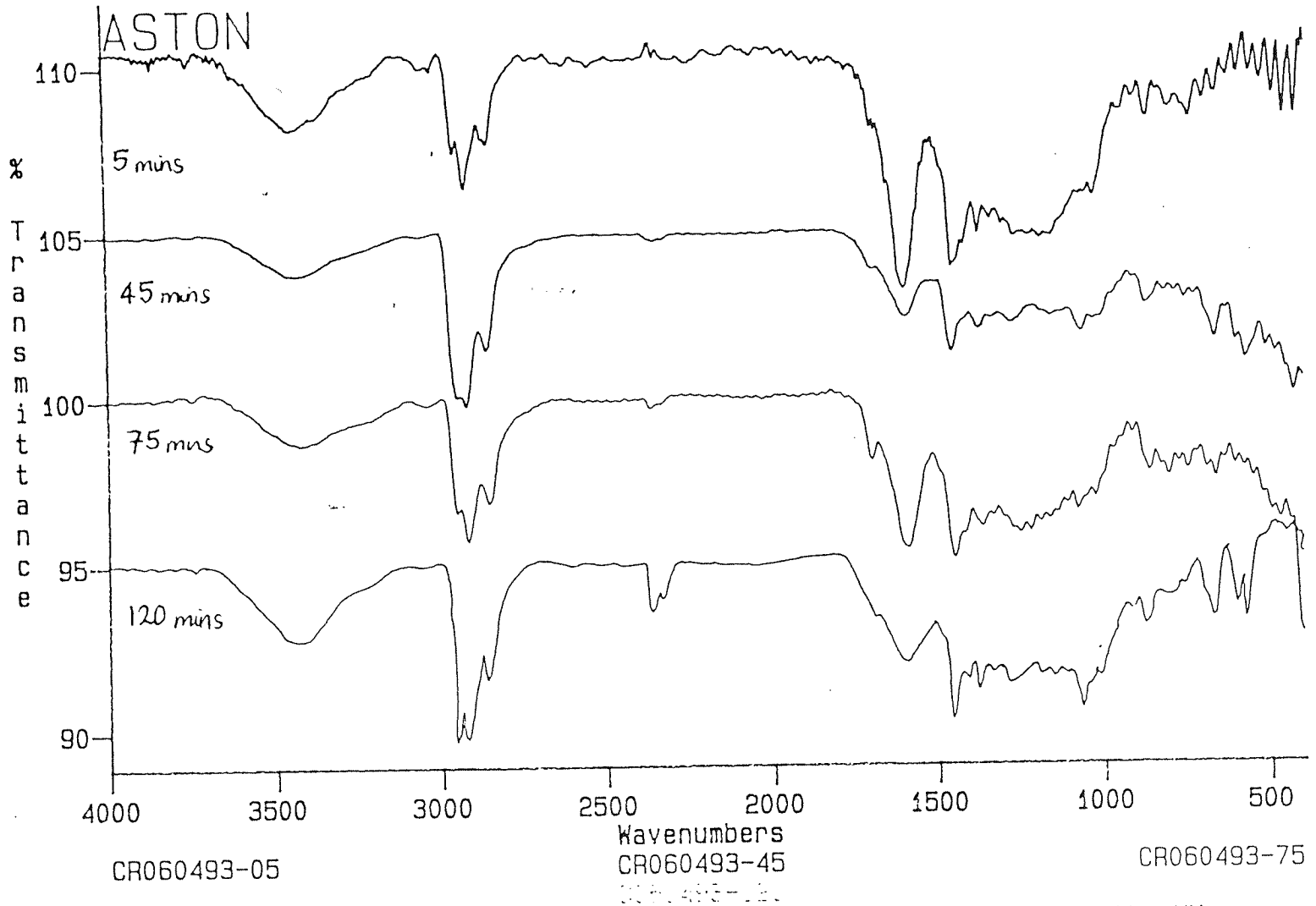

Reaction of CRESWELL-size 90μm after 5, 45, 75 and 120mins in the MW RES=8.

Fig3.46
IR of the stannylated Creswell coal ≤90 μm after
5, 45 and 75 and 120 mins mw heating

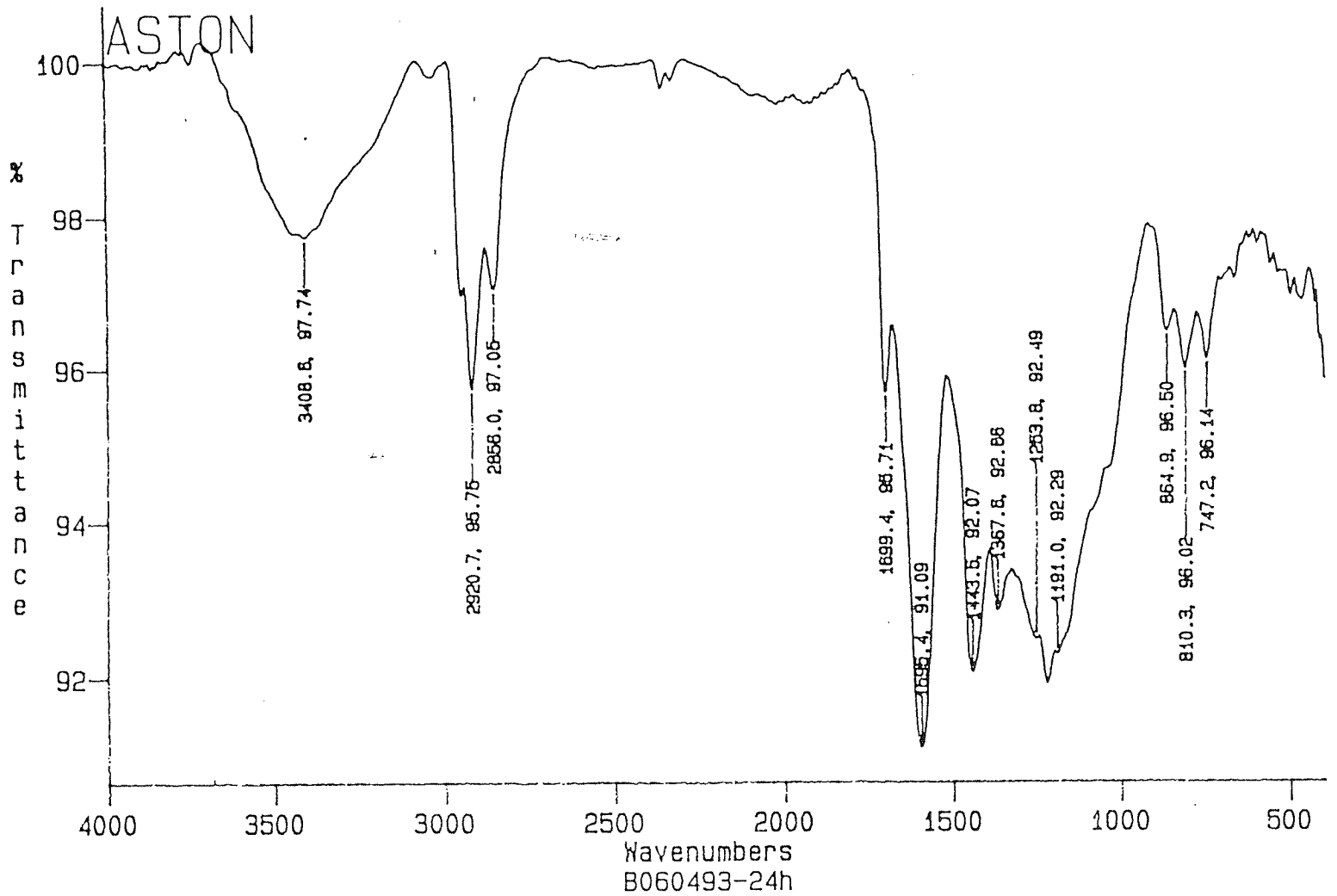

Fig3.47
IR of the stannylated Creswell coal ≤90 μm after 24 hrs reflux in toluene

^{119}Sn MASNMR shows that the stannylated <500>212 μm Creswell coal (reacted for 30 mins in the microwave oven) gives a fairly broad signal with a major peak at 110 ppm (fig 3.48) - this corresponds to the stannylation of 2,6-dimethylphenol-type structures (see section 3.3.3). The stannylated <212>90 μm particle size (reacted for 5 mins in the microwave oven) shows a much clearer resonance (fig 3.49) peak at 106 ppm. According to data collected by E.Raffi et al[61], this signal corresponds to the stannylation of phenolic compounds such as 2,3-dimethylphenol, 2,4,6-trimethylphenol, 3-methylphenol, 2,5-dimethylphenol and mono-substituted 2-, 3- and 4-ethylphenol i.e phenolic compounds with small steric demand - this correlates well with the work done on model compounds in section 3.3.3. A similar ^{119}Sn MASNMR spectrum is obtained for the <212>90 μm particle size stannylated Creswell coal using the reflux method (fig 3.50). The ≤90 μm particle size Creswell (reacted for 120 mins in the microwave oven) produced no signal in the ^{119}Sn range (fig 3.51), but this is not too surprising considering the reaction, as indicated by FT-IR, did not appear to proceed very far.

From the results it appears that the <212>90 μm particle size reacted best, very closely followed by the <500>212 μm particle size and finally the ≤90 μm particle size. It is not fully understood why the ≤90 μm particle size shows such little inclination to react, but one explanation may be that because of the larger surface area of the ≤90 μm particle size coal, it undergoes greater atmospheric oxidation - this results in a large increase in ether linkages in the coal, which could effectively trap the large stannylating reagent and hinder its progress in trying to reach the hydroxyl functionalities. Also, because the different particle sizes of the coal are from the same 'cut' of one Creswell sample (the same sample of Creswell coal has been passed successively through 500 μm, 212 μm and 90 μm wire-mesh sieves), it is possible that particles such as bi- and trimacerites (containing groups such as phenolic functional groups) could be 'lost' during earlier separations, thereby leaving the smaller particle size with an overall deficiency in functionality. Another factor to consider is that when grinding to very low particle sizes, more mineral matter (such as pyrite) and ash-forming particles (such as clay and sand) may be released into the ground coal. These entities may have a 'damping' effect on the reaction - the presence of a greater proportion of mineral matter results in less coal being available for reaction.

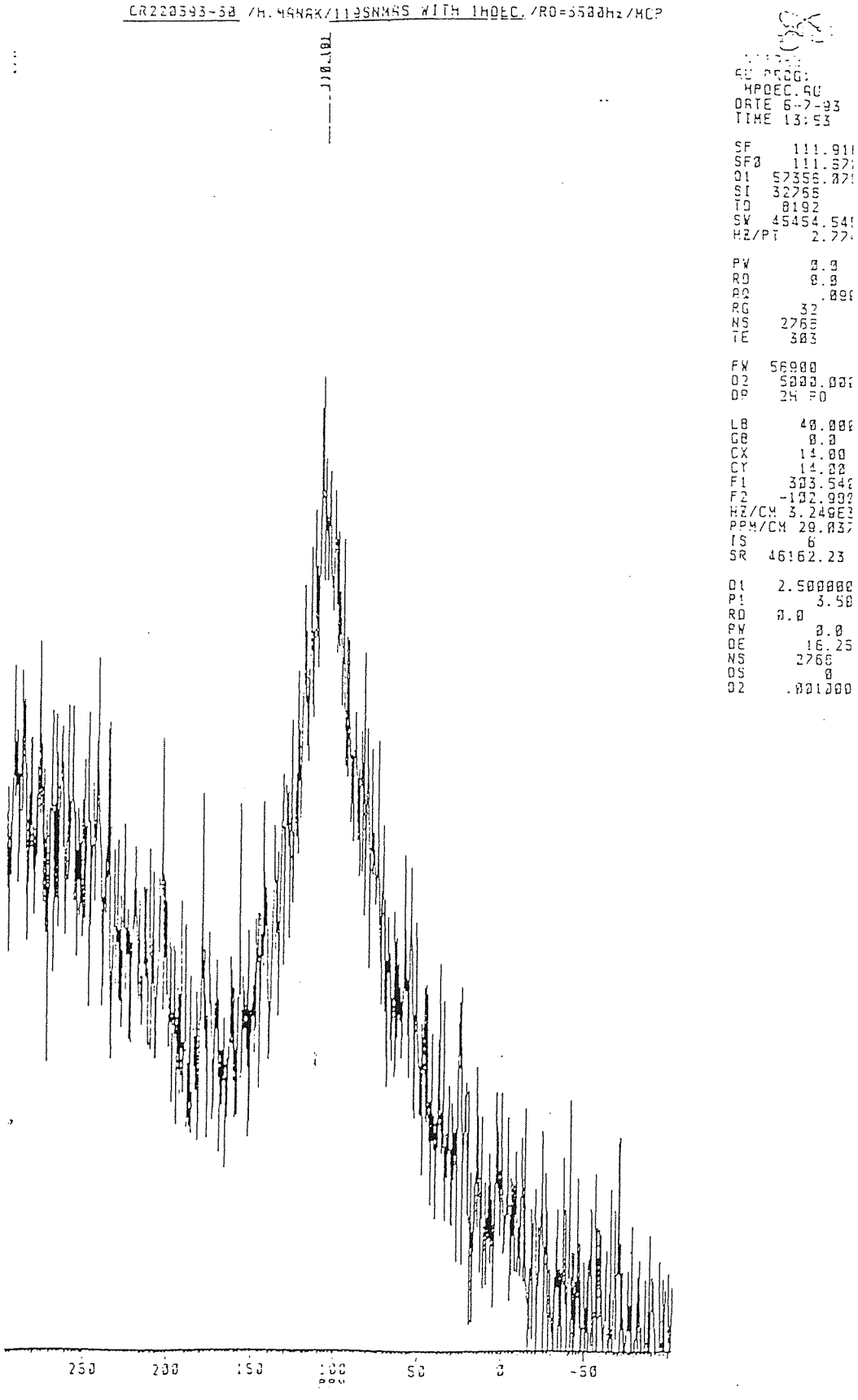

Fig3.48
^{119}Sn MASNMR of the stannylated Creswell coal <500>212 μm after 30 mins mw heating

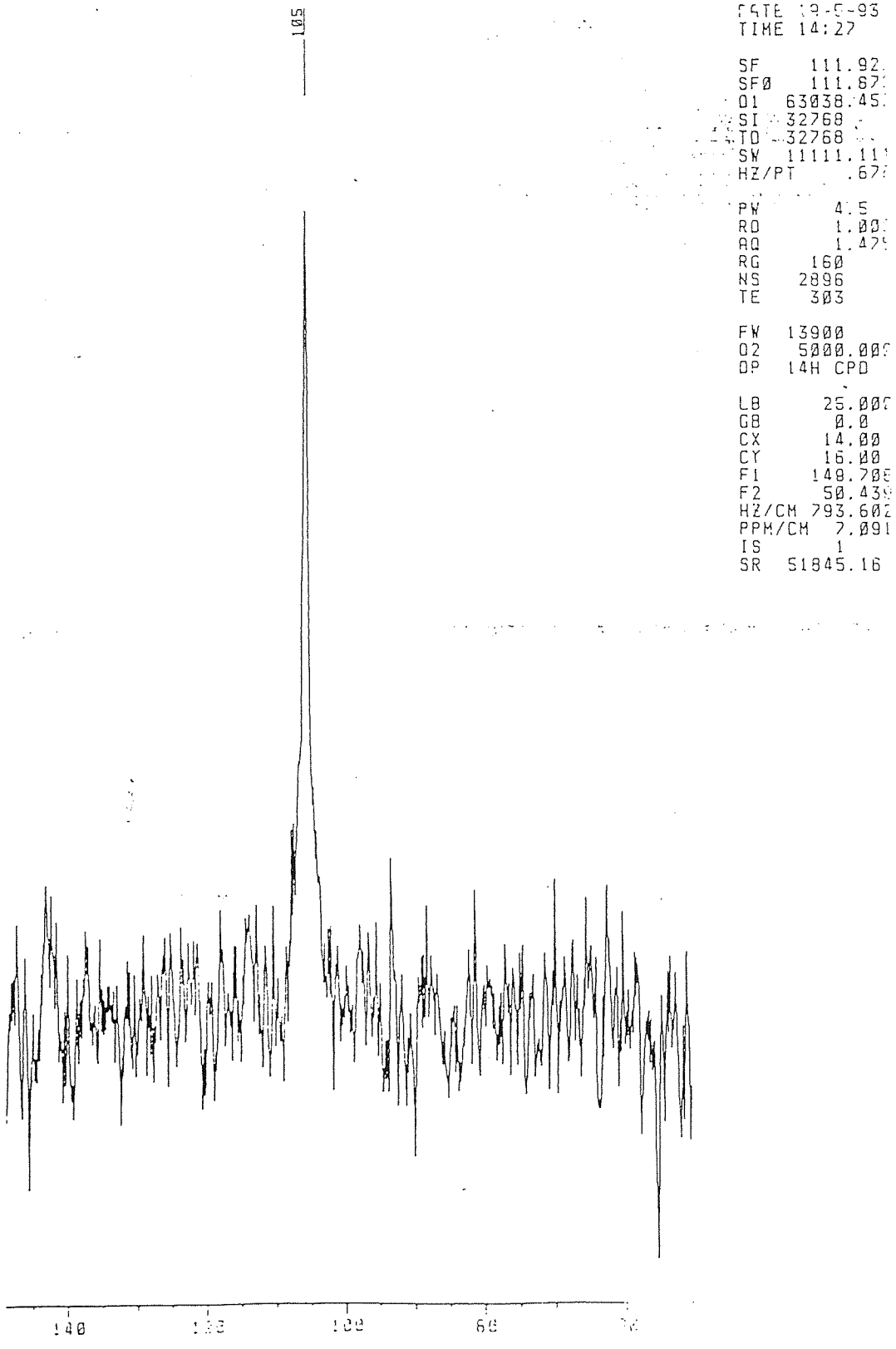

Fig3.49
^{119}Sn MASNMR of the stannylated Creswell coal <212>90 μm after 5 mins mw heating

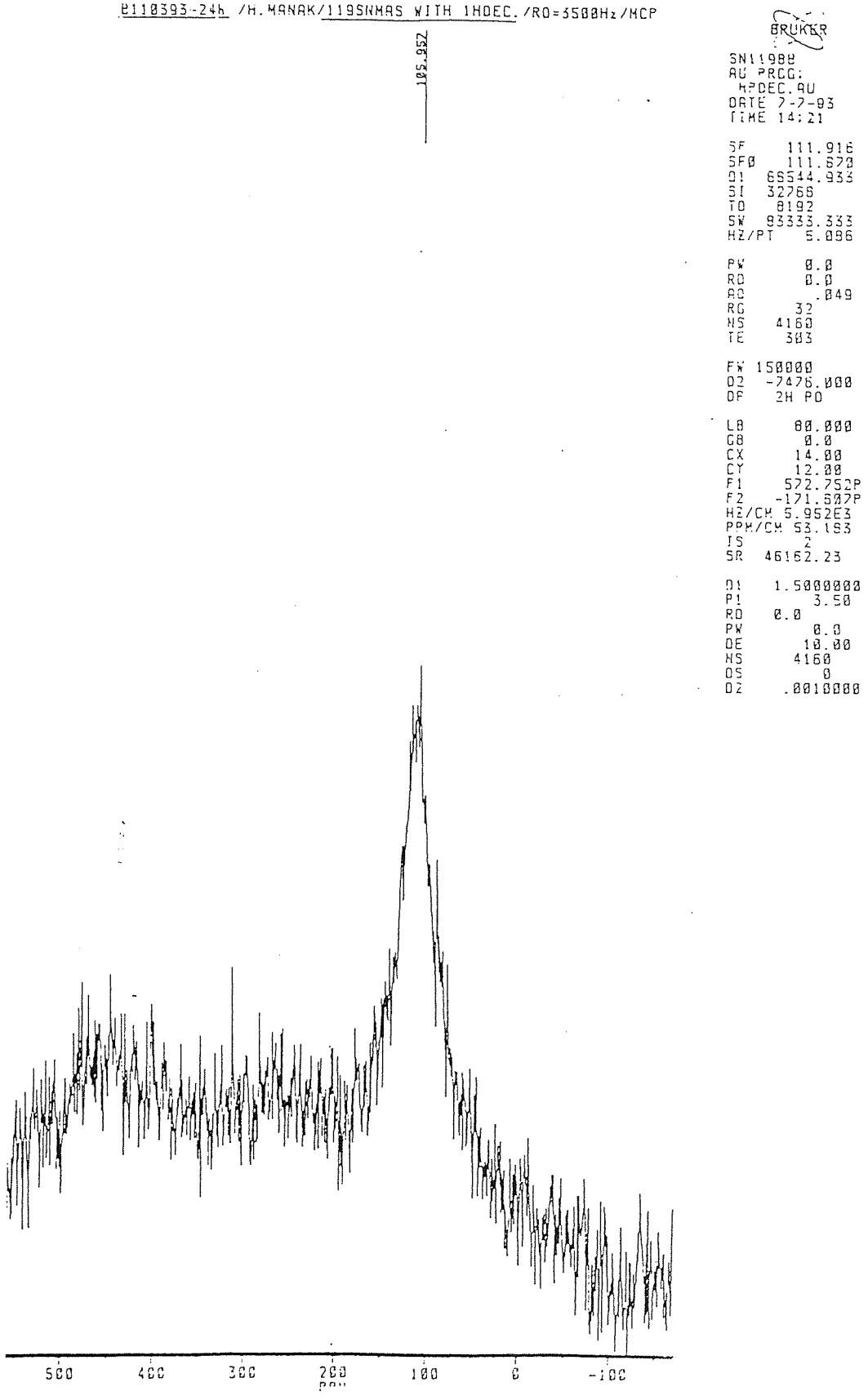

Fig3.50

^{119}Sn MASNMR of the stannylated Creswell coal <212>90 μm after 24 hrs reflux in toluene

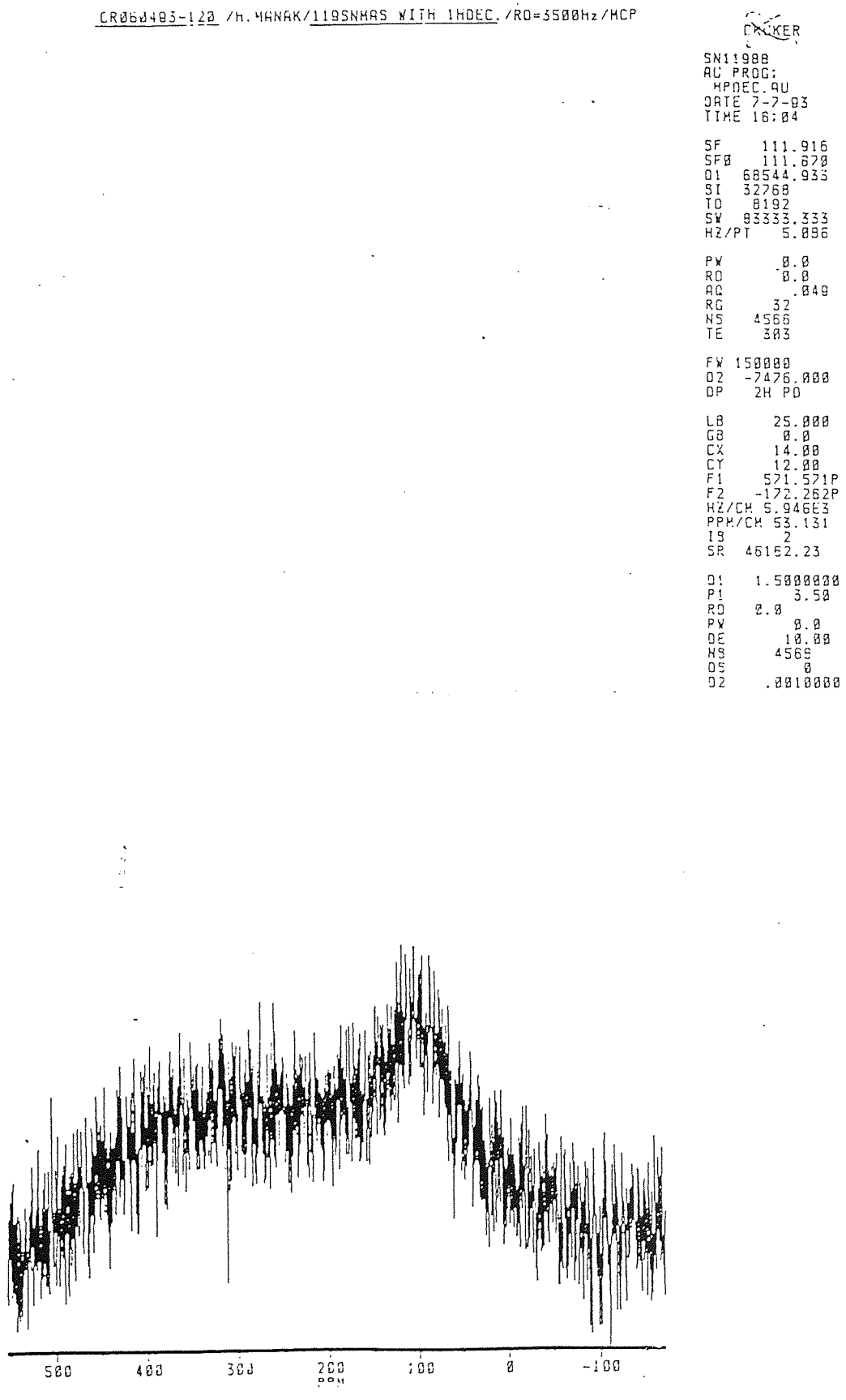

Fig3.51
^{119}Sn MASNMR of the stannylated Creswell coal ≤90 μm after 120 mins mw heating

The Cortonwood coal (≤212 μm) was reacted for 5 mins and 60 mins with TBTO and acetonitrile solvent in the microwave oven. Fig 3.52 shows the FT-IR spectra of the Cortonwood coal - the -OH stretching band at 3400 cm^{-1} is very prominent. Fig 3.53 shows the Cortonwood coal after 5 mins and 60 mins reaction in the microwave oven. The spectra shows that there is very little reaction after 5 mins, but there is a noticeable reduction in the -OH band intensity after 60 mins indicating some reaction has taken place.

The Gedling coal (≤212 μm) was reacted for 5, 30 and 60 mins in the microwave oven using TBTO and acetonitrile solvent. Fig 3.54 shows the FT-IR of the Gedling coal - again the -OH stretching absorptions are very noticeable. Fig 3.55 shows the IR spectra of the coal after 5, 30 and 60 mins reaction in the microwave oven. The spectra shows that there is hardly any reaction after 5 mins or 30 mins, but a significant reaction after 60 mins (similar to the Cortonwood coal). Fig 3.56 shows the comparison between the raw Cortonwood coal and the reacted (60 mins in microwave oven) Cortonwood coal.

The Ollerton coal was reacted for 5, 60 and 120 mins in the microwave oven using TBTO and acetonitrile solvent. There was no change after 5 mins, but some reaction after 60 mins which did not improve significantly even after 120 mins of microwave heating (figs 3.57 - 3.58).

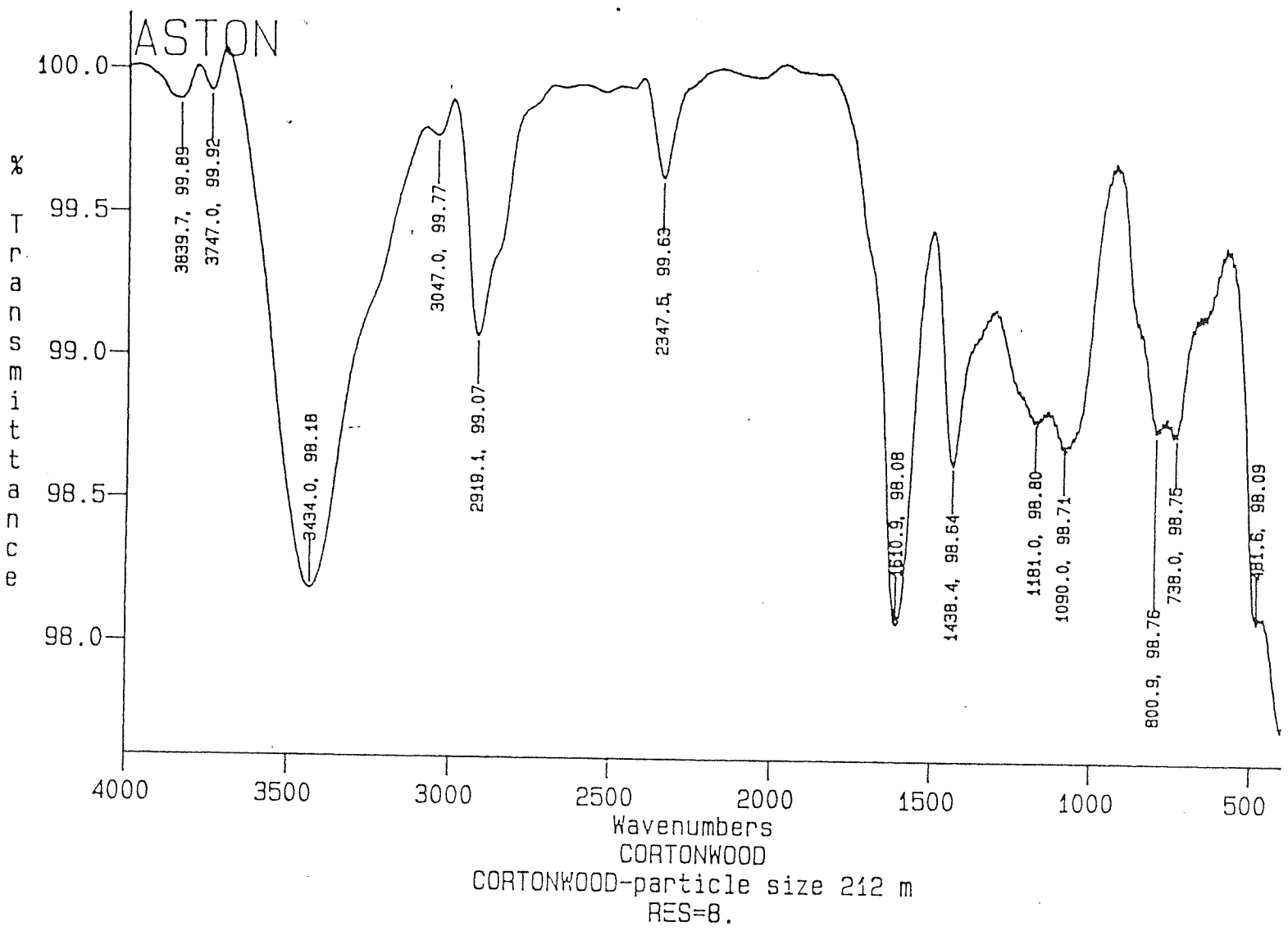

Fig3.52
IR of the raw Cortonwood coal ≤212 μm

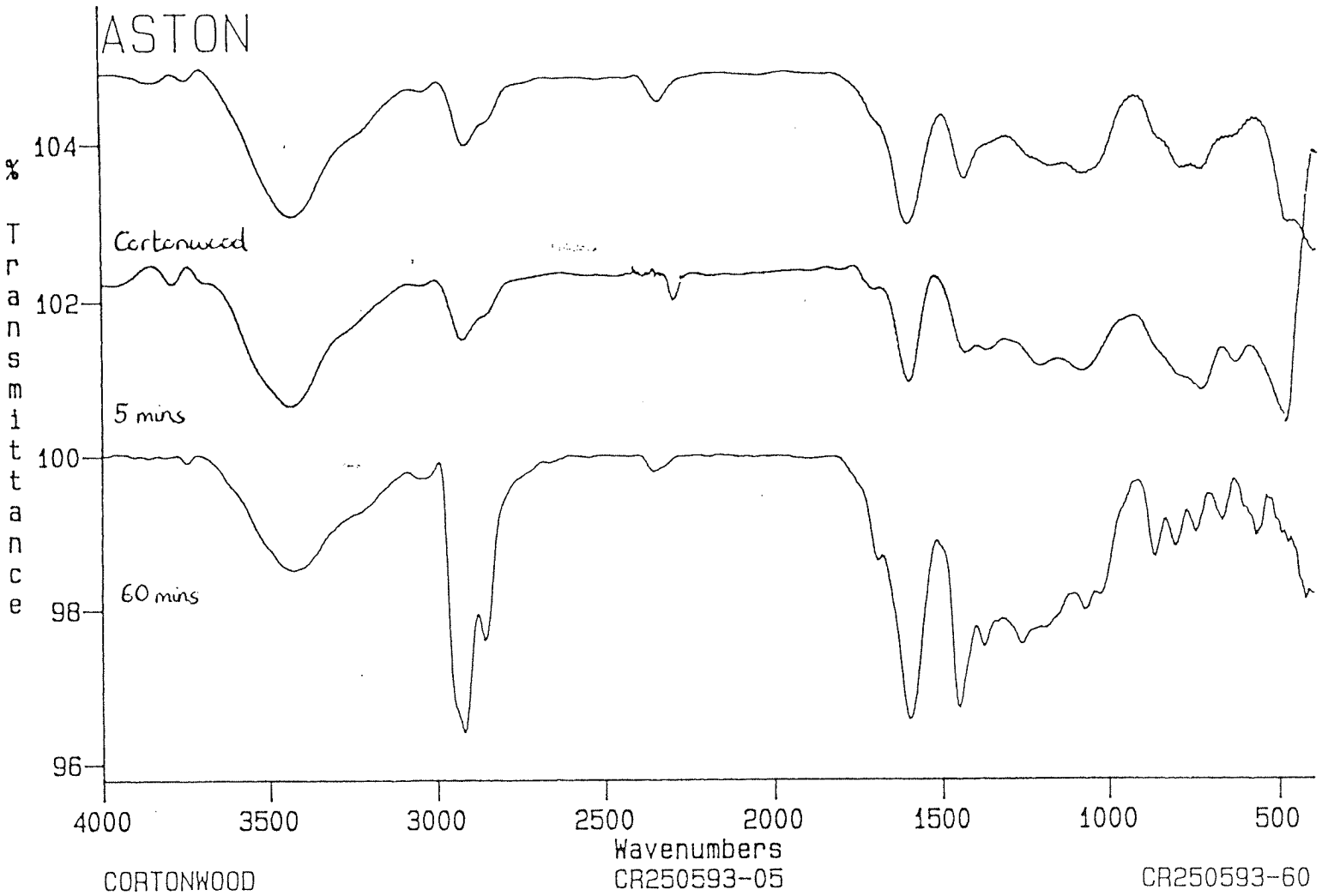

Fig3.53
IR of the stannylated Cortonwood coal ≤212 μm after
5 mins and 60 mins mw heating

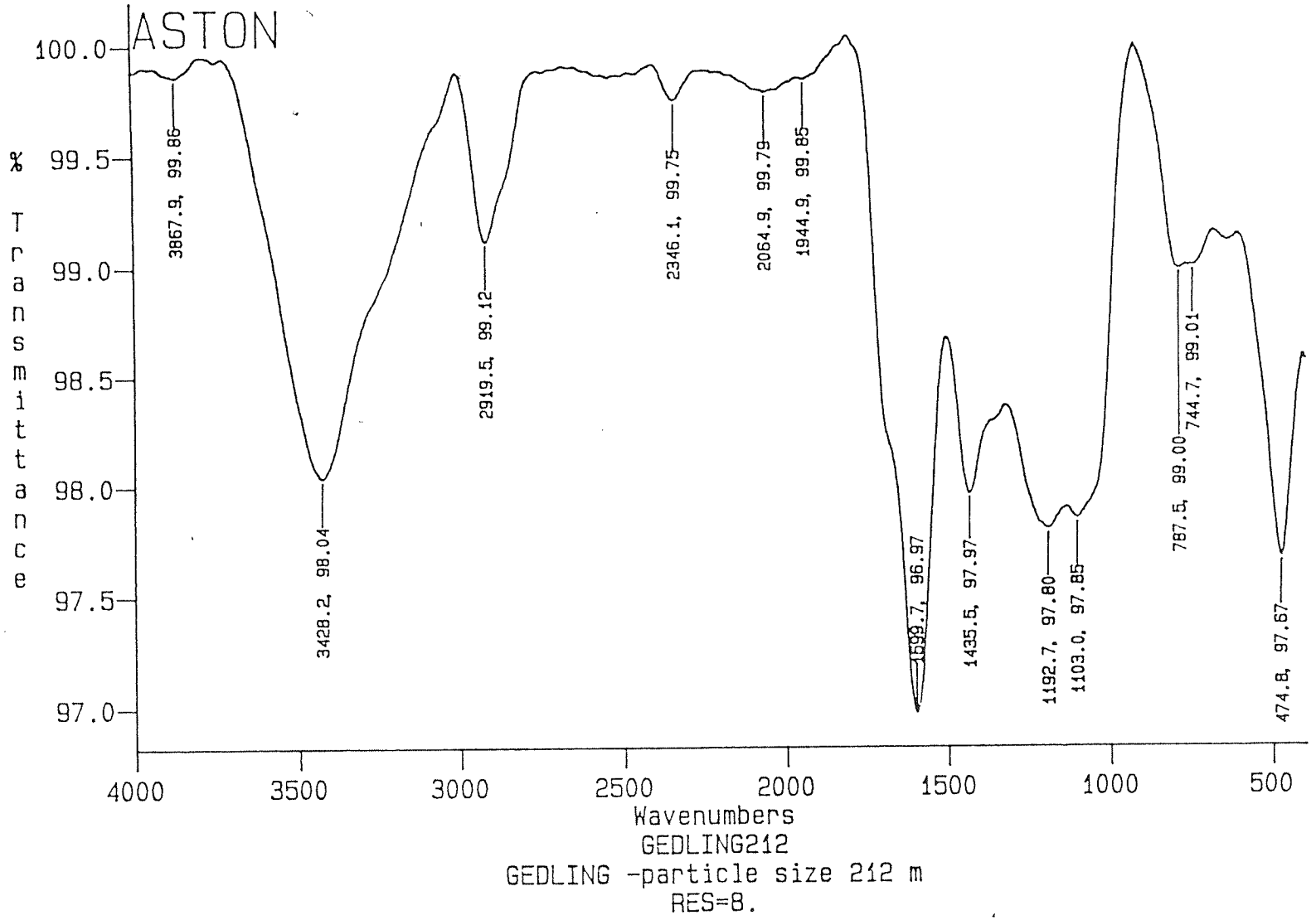

Fig3.54
IR of the raw Gedling coal ≤212 μm

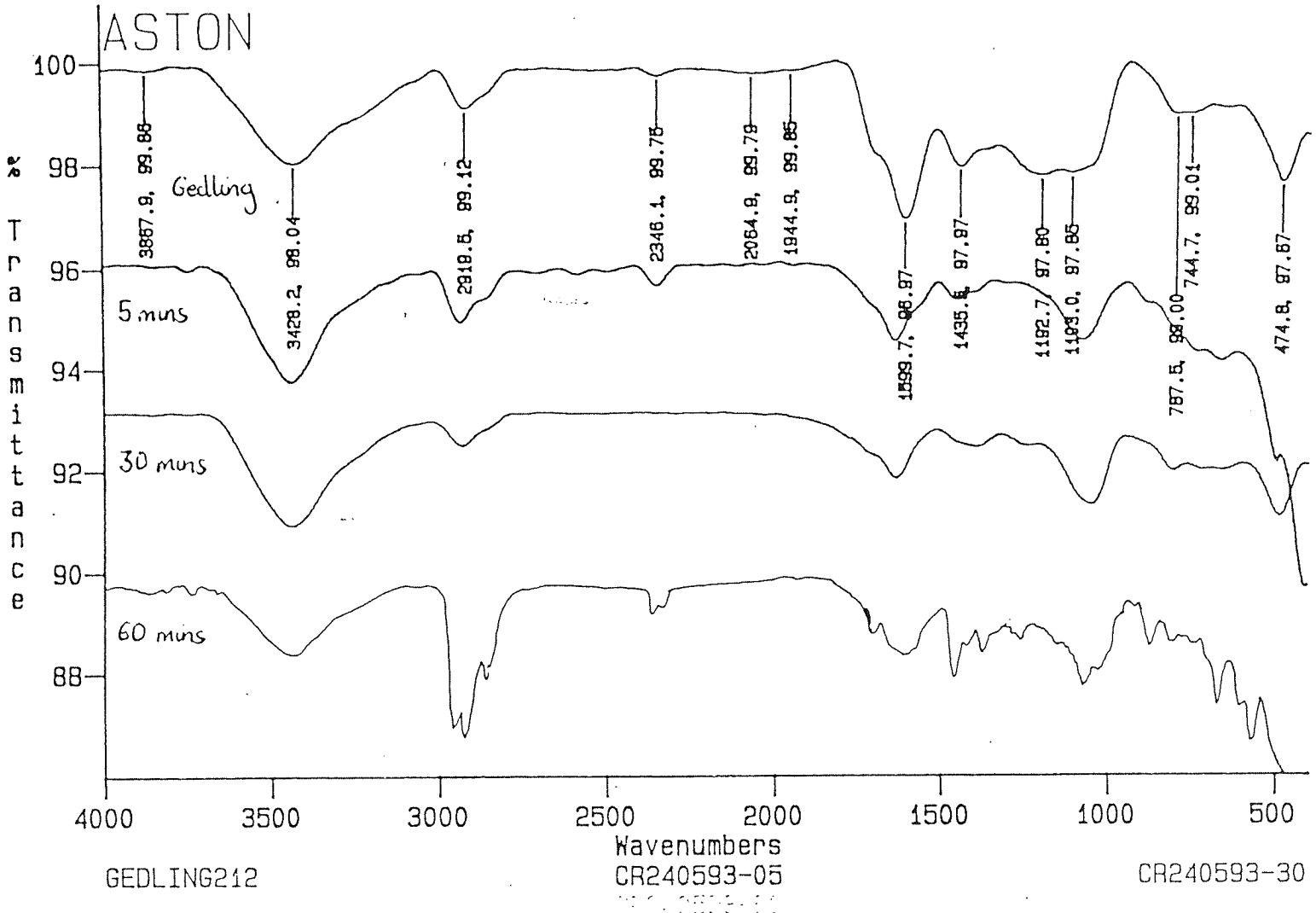

Reaction of GEDLING-size 212μm in MW after 5, 30 and 60 mins
RES=8.

Fig3.55
IR of the stannylated Gedling coal ≤212 μm after
5, 30 and 60 mins of mw heating

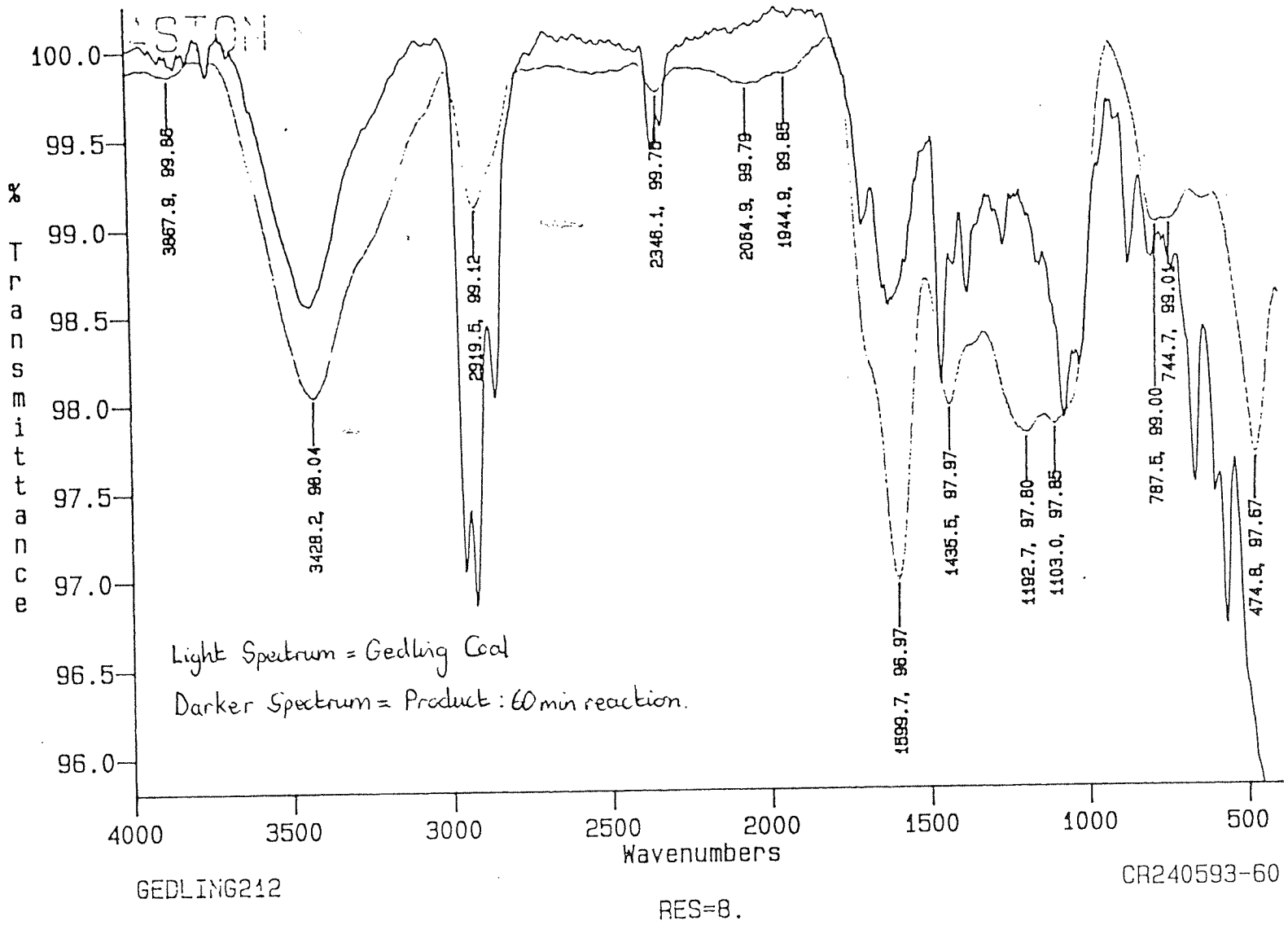

Fig3.56
IR of the stannylated Gedling coal ≤212 μm after 60 mins mw heating

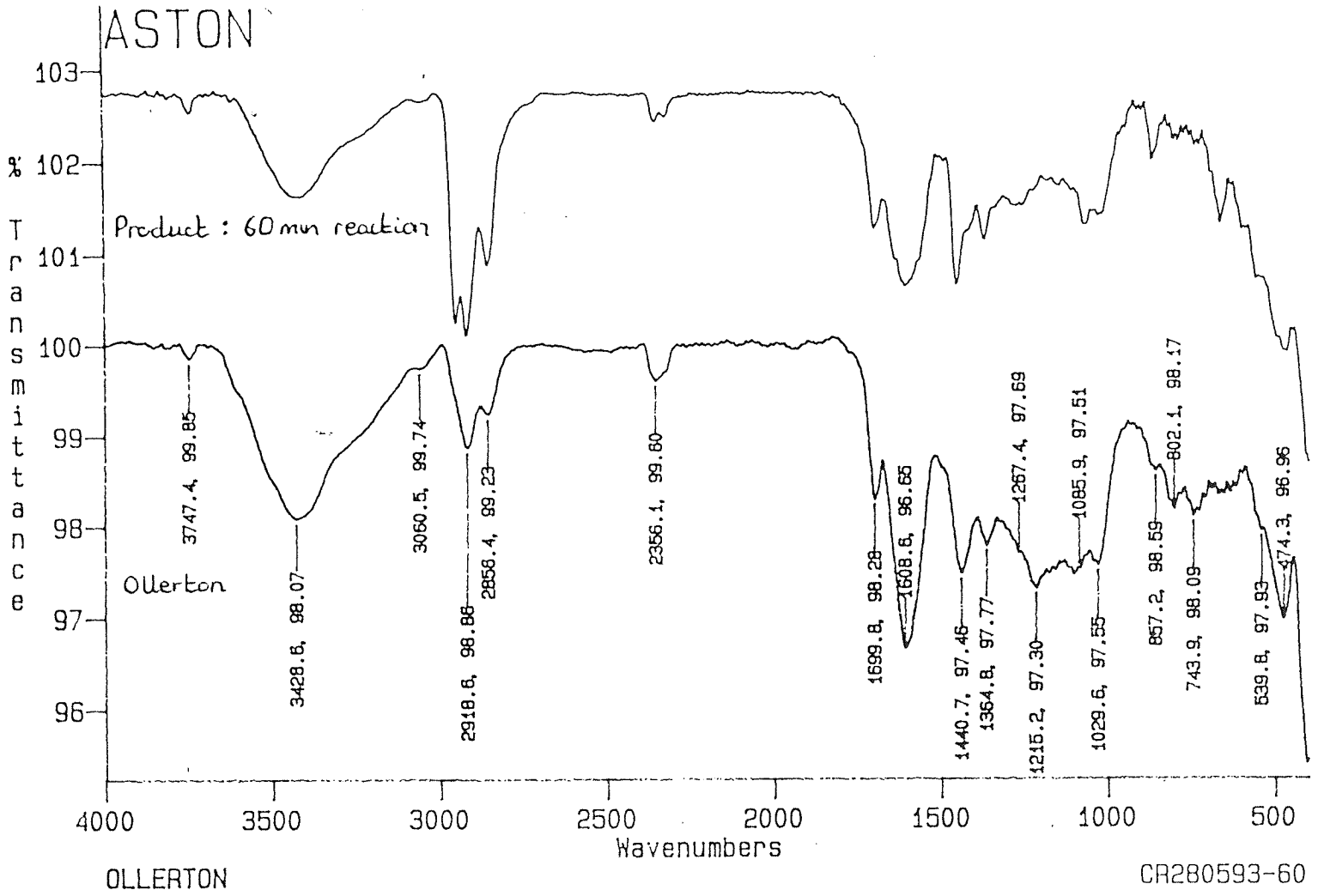

RES=8.

Fig3.57
IR of the stannylated Ollerton coal ≤212 μm after 60 mins mw heating

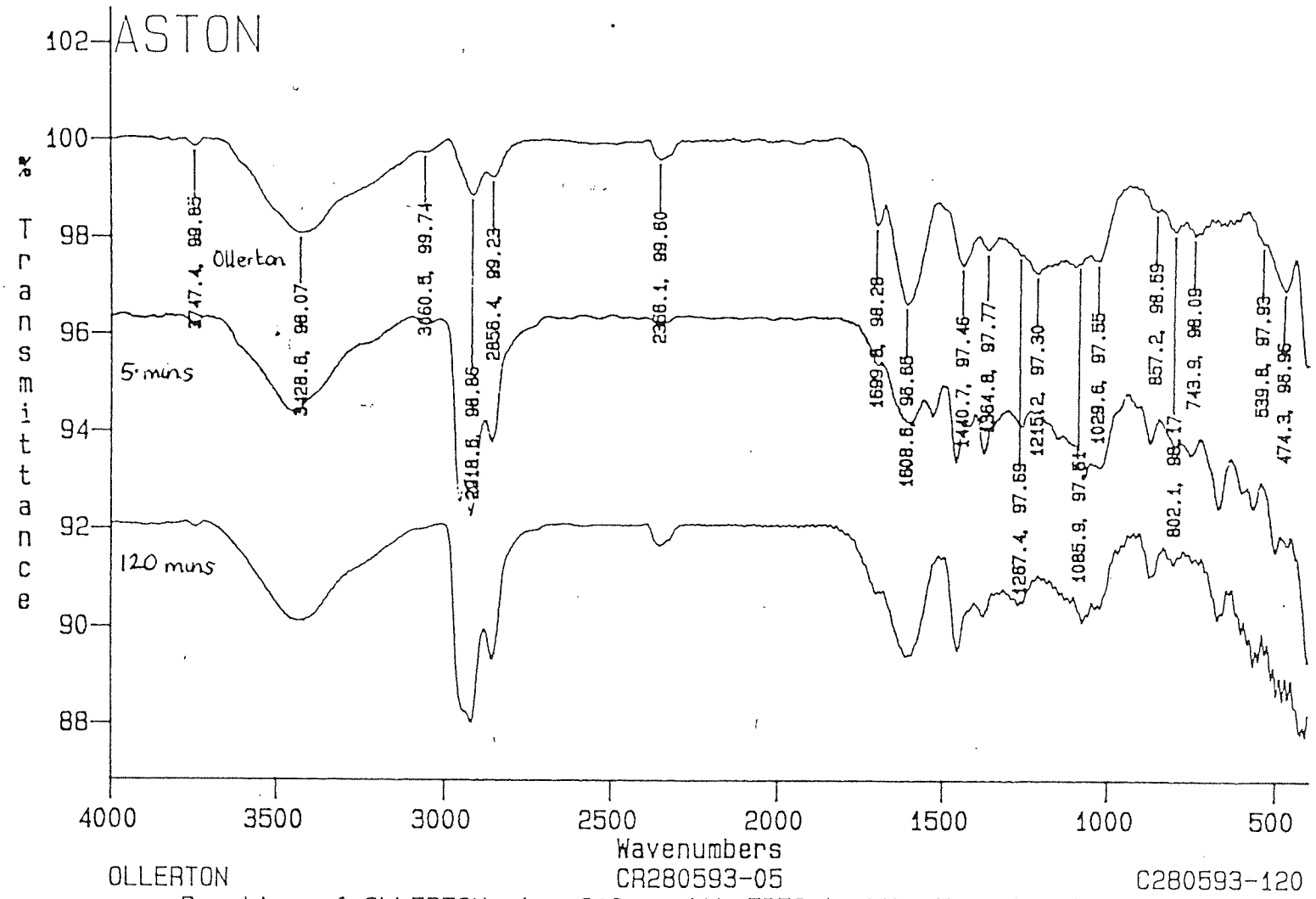

Fig3.58
IR of the stannylated Ollerton coal ≤212 μm after 5 mins and 120 mins mw heating

Table 3.14 Stannylation of Cortonwood, Gedling and Ollerton coals in the microwave oven

Coal - particle size ≤ 212 μm	Evidence of stannylation from FT-IR
CORTONWOOD	Hardly any reaction after 5 mins. Some reaction after 60 mins.
GEDLING	Hardly any reaction after 5 mins / 30 mins. Some reaction after 60 mins.
OLLERTON	Hardly any reaction after 5 mins. Some reaction after 60 mins. No further reaction after 120 mins.

Of the four coals tested, Creswell appears to be the most reactive. In comparison to Creswell, Cortonwood (which is of a similar rank) showed little reactivity for the same particle size. One explanation for this unreactivity could be that Cortonwood contains slightly less oxygen than Creswell (5.6% w/w O for Creswell compared to 4.8% w/w O for Cortonwood). Because both coals are of a similar rank we would expect more hydroxyl functional groups to be present in the Creswell coal and hence a more rapid reaction, because the reagent only needs to diffuse short distances before reaction occurs resulting in a greater reduction in the -OH band in the IR spectra with respect to reaction time. But if this statement were true we would expect to find rapid reactions occurring with the Gedling and Ollerton coals (10.3% w/w O and 8.3% w/w O respectively), which we do not! One reason for the inactivity of the Gedling and Ollerton coals may be due to the fact that they contain relatively large amounts of inertinite (20% vol and 16% vol respectively) in their maceral make-up. Inertinite, as the name suggests, is a fairly unreactive material and could hinder the reaction pathway between the TBTO reagent and the hydroxyl functionalities. If this is the case then a more in-depth analysis of the macerals which constitute the coal is required - see section 3.3.5 and chapter 4.

Another more probable explanation is that the unreactive coals contain a higher degree of more hindered phenolic groups and the large TBTO reagent finds it difficult to attack the hydroxyl functionality, because of the large steric demand. A significant amount of the oxygen present in the unreactive coals may also exist in functionality other than the hydroxyl group - this aspect is investigated in chapter 4.

3.3.5 Stannylation of Creswell macerals

Attempts were made to stannylate the Creswell and Cortonwood macerals, as only these coals had produced satisfactory maceral separations (see section 4.3.1). All three of the Creswell macerals were stannylated for 60 mins in the Sharp Carousel II microwave oven. Figs 3.59a - 3.59c show the FT-IR spectra of the unreacted Creswell exinite, vitrinite and inertinite macerals respectively. The exinite maceral group shows appreciable -OH content (as shown by the peak centred at 3334 cm^{-1}) and a greater degree of aliphatic character (aliphatic C-H stretching at 2919 cm^{-1}) than the vitrinite and inertinite macerals. The Creswell vitrinite maceral again shows appreciable -OH content (-OH stretching peak centred at 3333 cm^{-1}) and significant aliphatic character (aliphatic C-H stretching at 2917 cm^{-1}). The Creswell inertinite maceral, however, appears to have relatively less -OH and less aliphatic character compared to the other two maceral groups. There are also three peaks at 753 cm^{-1}, 812 cm^{-1} and 865 cm^{-1}, which are more discernible in the Creswell inertinite IR plot - these are due to substituted benzene groups and indicate a greater aromatic character. Fig 3.60 shows a multispectral IR display showing all three Creswell macerals on the same plot for comparison.

Fig 3.61 shows the IR spectrum for the stannylated Creswell exinite maceral. Although peaks due to stannylation are evident at 586 cm^{-1} (asymmetric Sn-C stretching), 1376 cm^{-1} (symmetric -CH_3 deformations) and 1460 cm^{-1} (C-H deformations), there is still a significant peak due to -OH stretching centred at 3430 cm^{-1}. There is also a peak at 1074 cm^{-1} which is probably due to Sn-O-C asymmetric stretching. Fig 3.62 shows the IR spectrum for the stannylated Creswell vitrinite maceral group. Again, peaks due to stannylation can be observed at 1075 cm^{-1} (Sn-O-C), 586 cm^{-1} (Sn-C), 1377 cm^{-1} (-CH_3 deformations) and 1462 cm^{-1} (C-H), but the -OH stretching vibration at 3415 cm^{-1} is still a dominant peak on the plot. Fig 3.63 shows the FT-IR plot for the stannylated Creswell inertinite maceral. In this instance, the peaks due to stannylation are much weaker compared to the other two stannylated macerals, which appears to suggest an inferior reaction. Fig 3.64 shows an IR comparison of the three stannylated Creswell macerals.

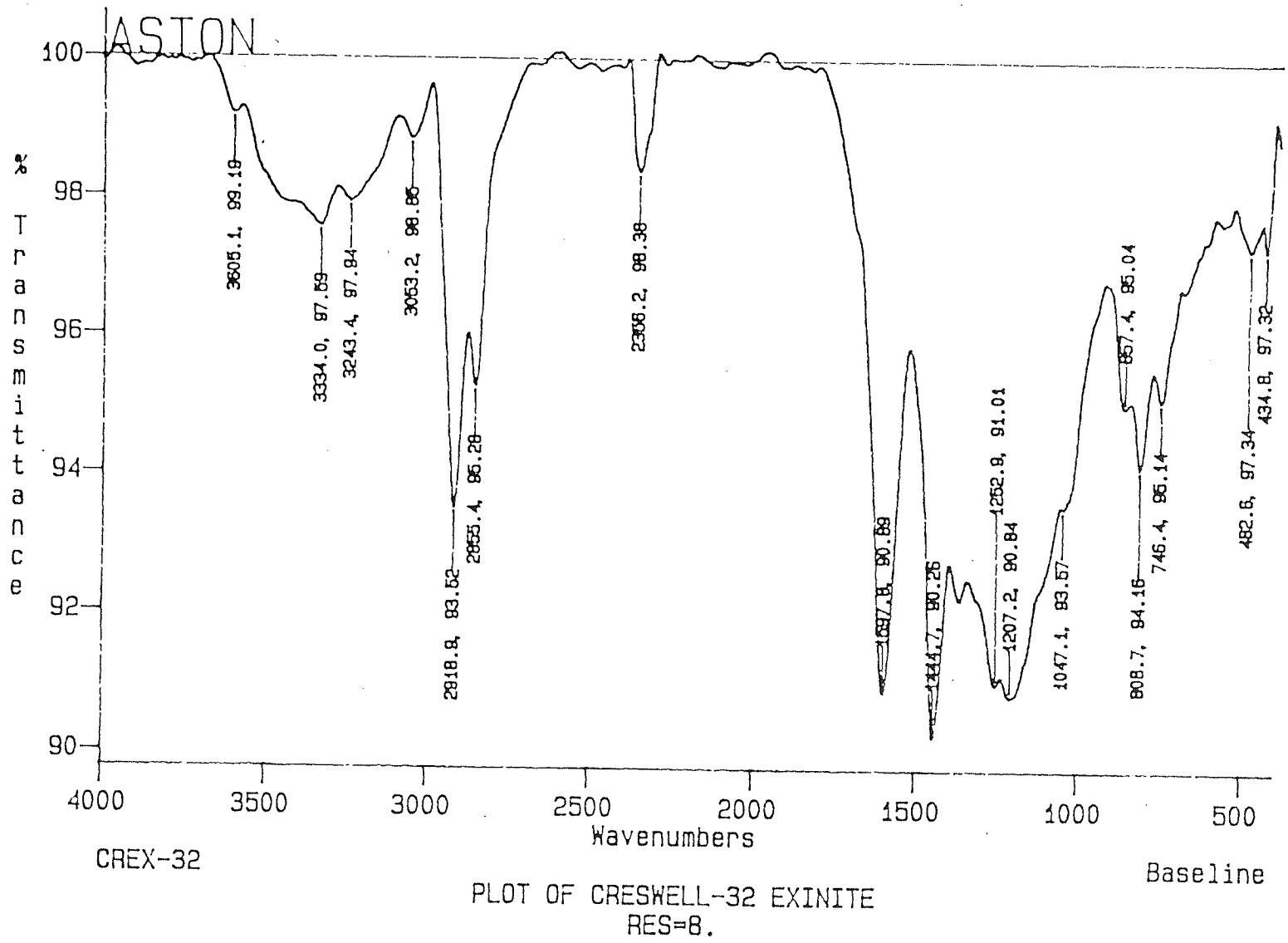

Fig3.59a
IR of the Creswell ≤32 μm exinite maceral

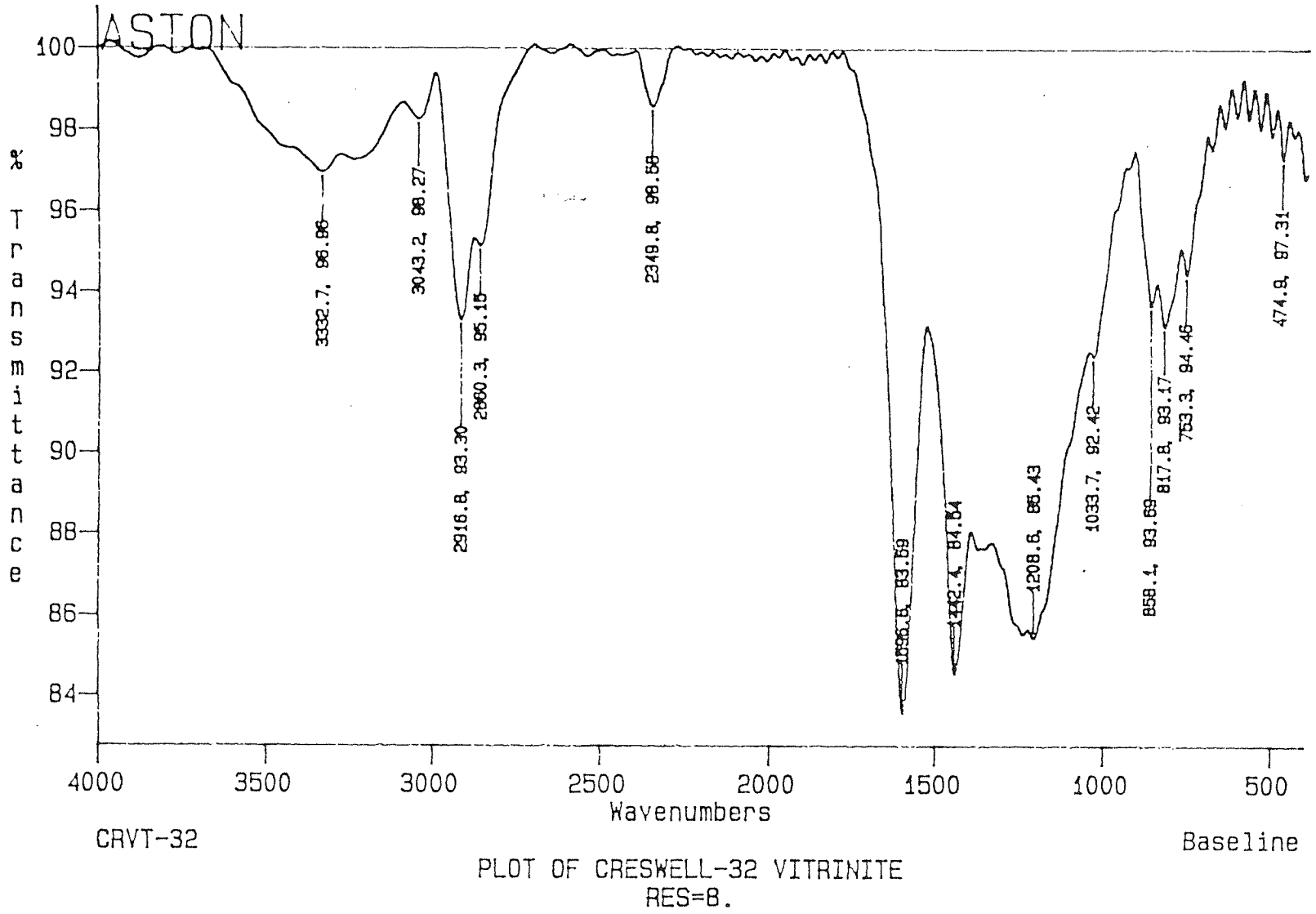

Fig3.59b
IR of the Creswell ≤32 μm vitrinite maceral

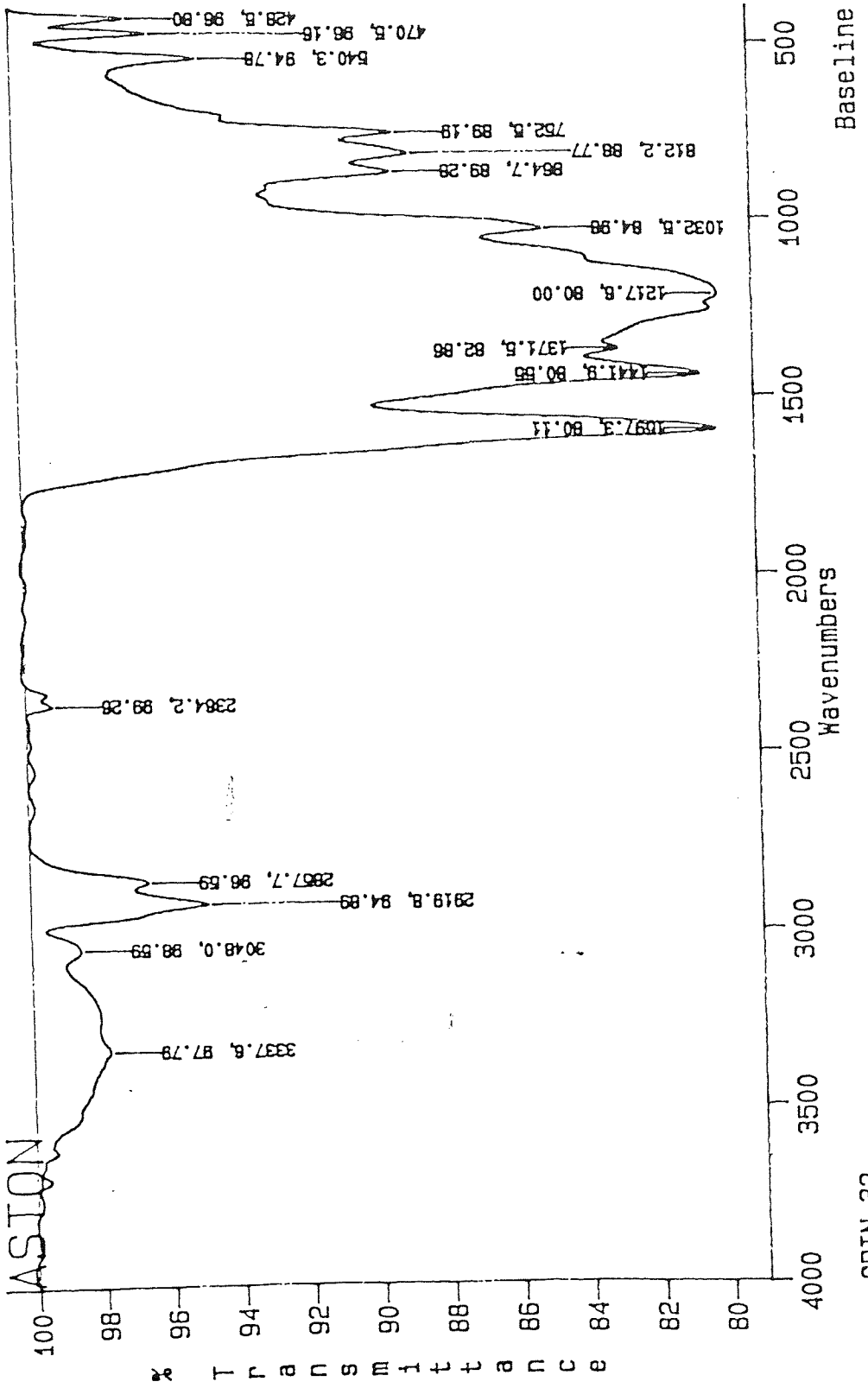

Fig3.59c
IR of the Creswell ≤32 μm inertinite maceral

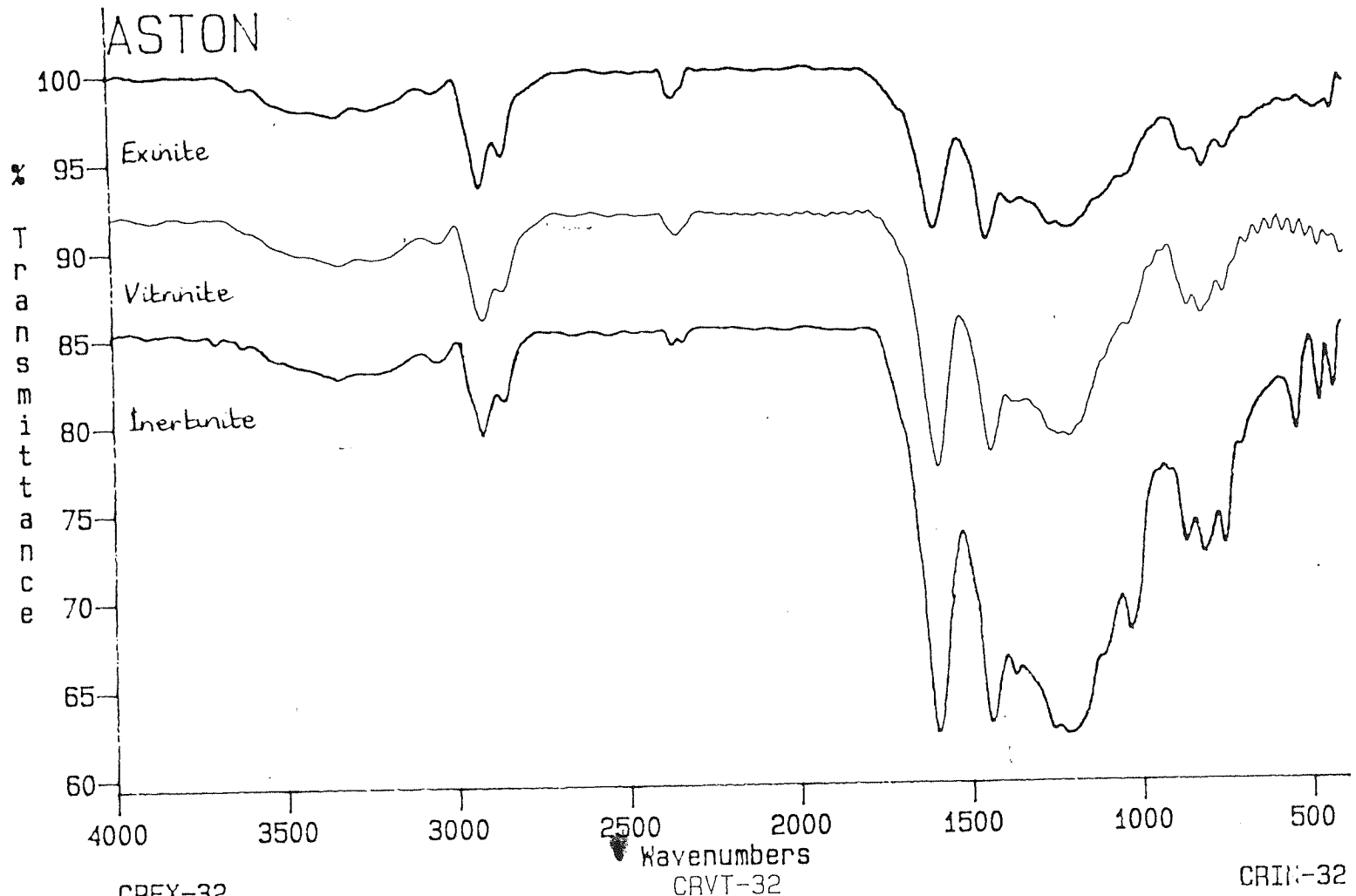

Fig3.60
IR comparison of the Creswell ≤32 μm macerals

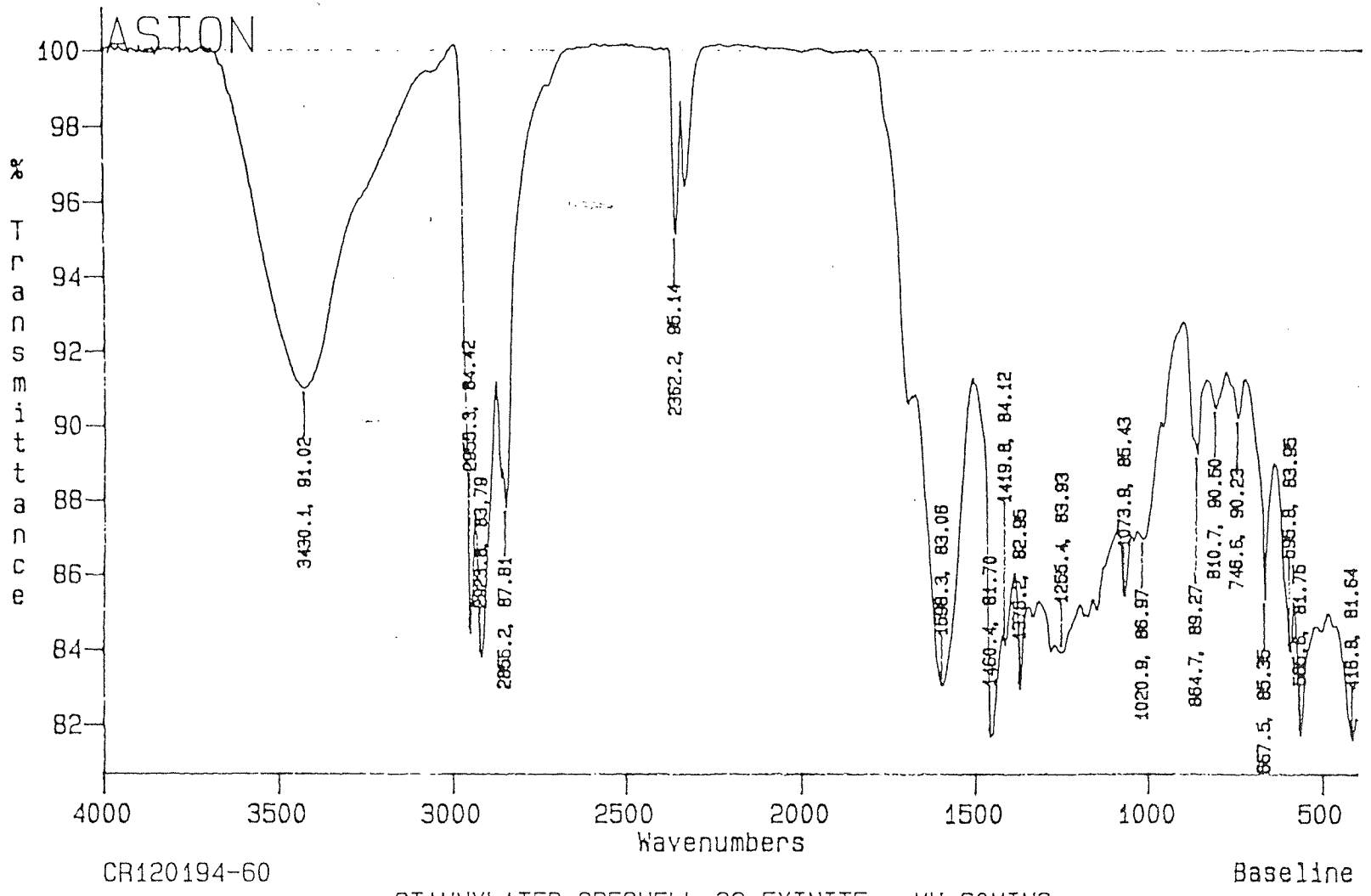

Fig3.61
IR of the stannylated Creswell ≤32 μm exinite after 60 mins mw heating

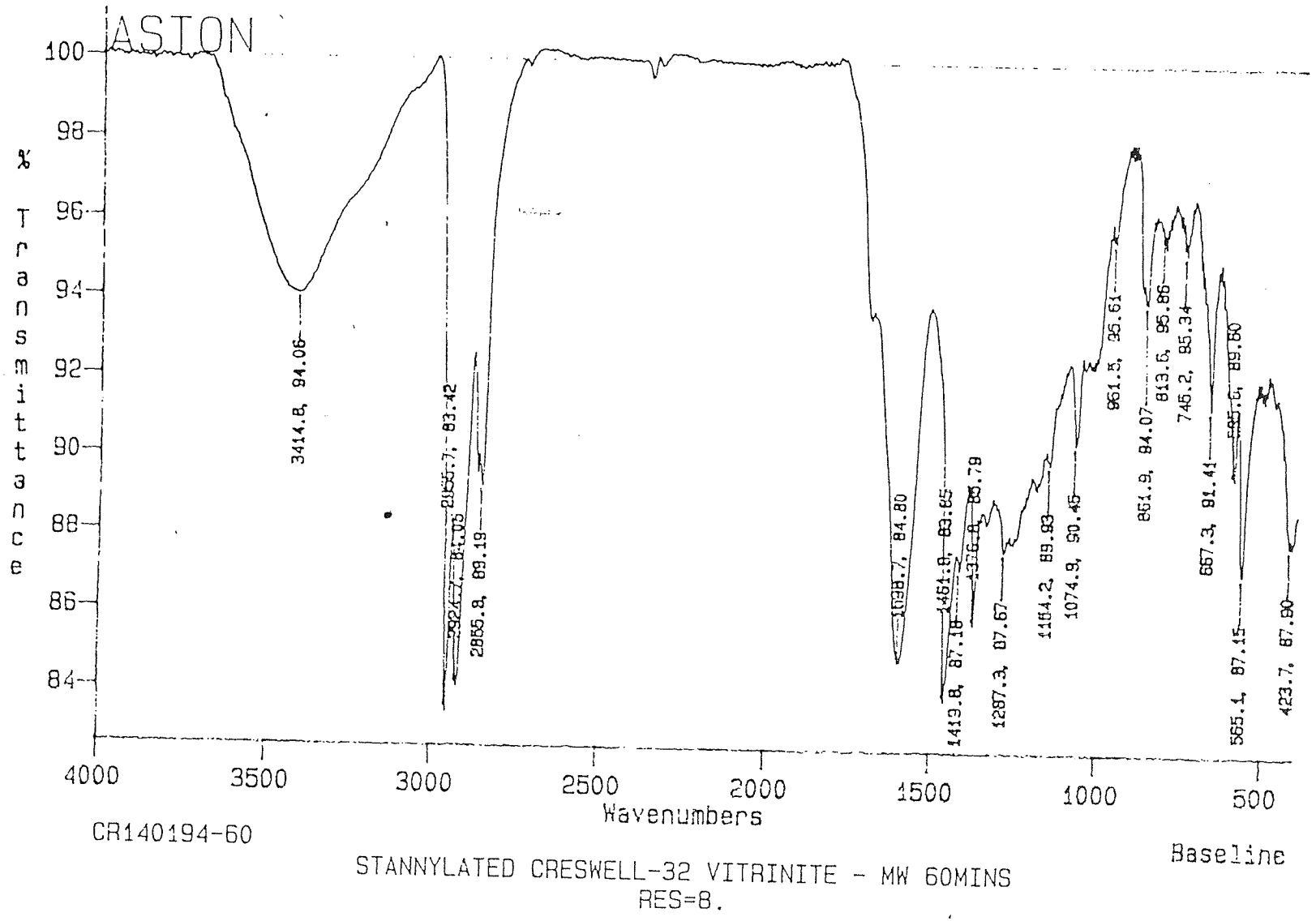

Fig3.62
IR of the stannylated Creswell ≤32 μm vitrinite after 60 mins mw heating

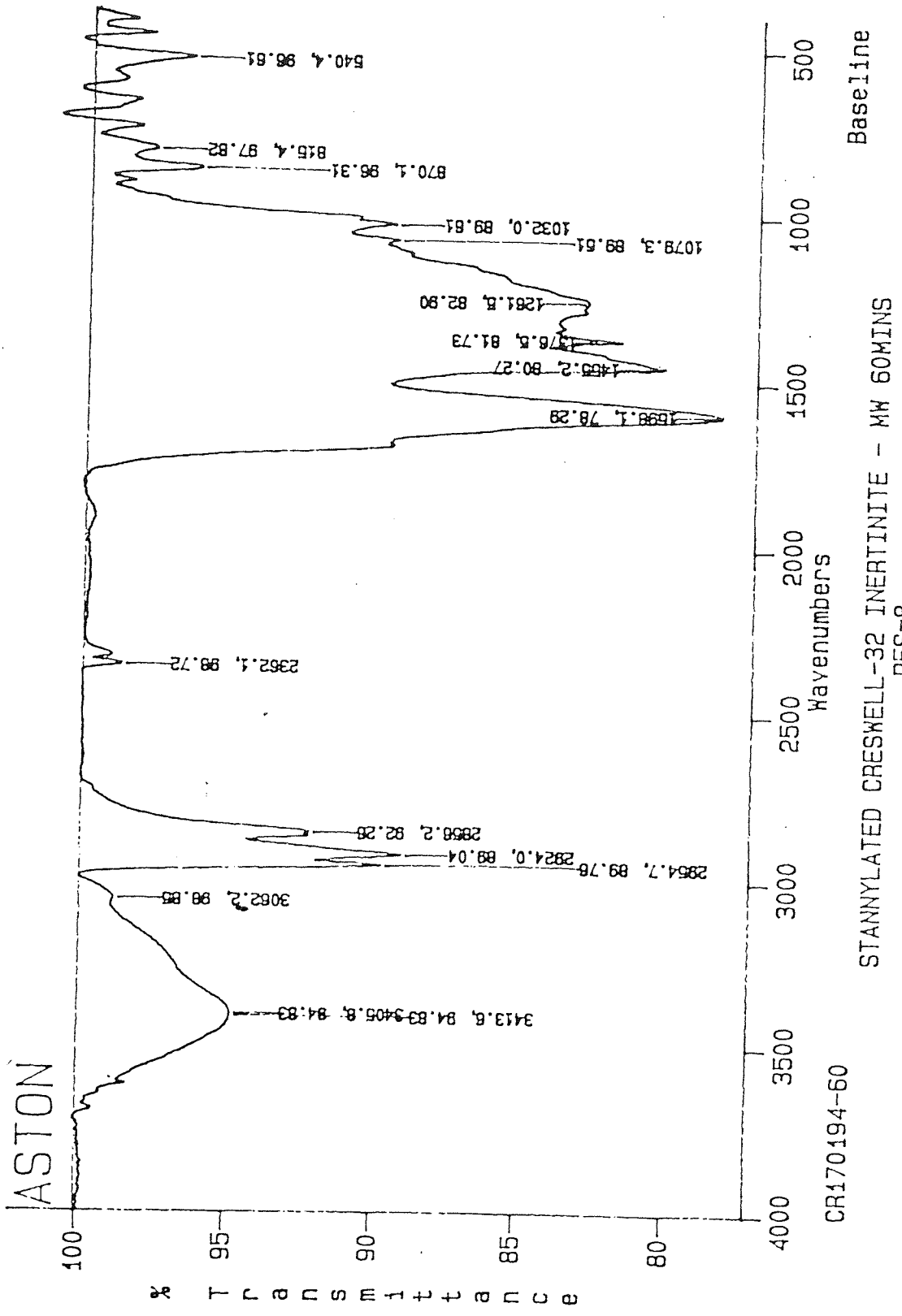

Fig3.63
IR of the stannylated Creswell ≤32 μm inertinite after 60 mins mw heating

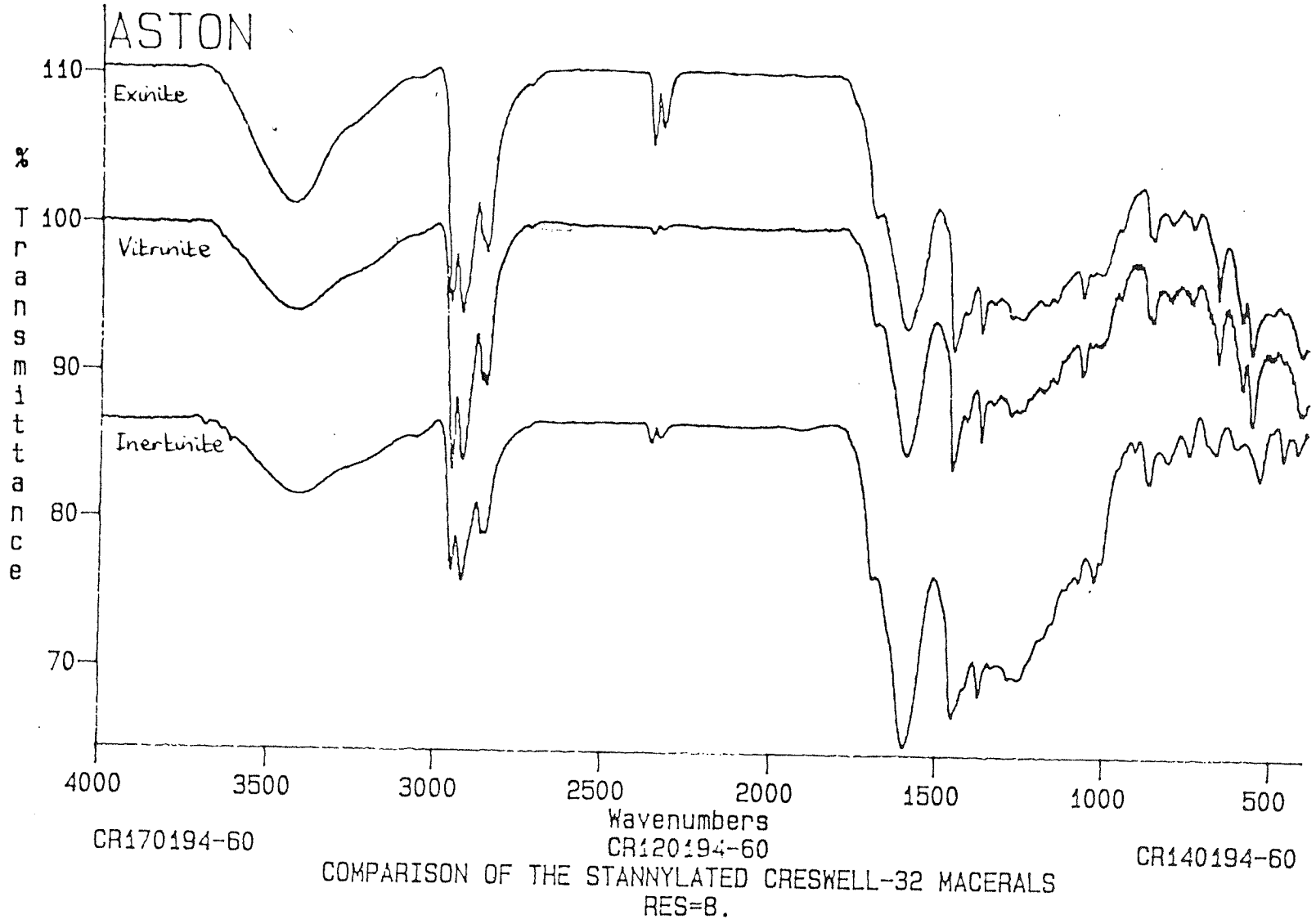

Fig3.64
IR comparison of the stannylated Creswell ≤32 μm macerals

In order to confirm that none of the absorptions, obtained during IR analysis of the stannylated coal macerals, were due to the TBTO reagent adsorbed onto the coal, a test experiment was carried out. This involved soxhlet-extraction of the stannylated Creswell vitrinite with toluene for 24 hrs. Because TBTO is very soluble in toluene, we would expect all the adsorbed TBTO, if present, to be removed by dissolution over this time period, thereby ensuring complete removal of any excess TBTO reagent. The soxhlet-extracted stannylated Creswell vitrinite and the solution obtained after extraction were then analysed by FT-IR to determine whether any extraction had taken place. Fig 3.65 shows IR spectra displaying the stannylated Creswell vitrinite both before and after soxhlet-extraction with toluene. The two spectra are effectively the same with no significant differences between them. Fig 3.66 shows the IR spectra of toluene and the solution obtained after 24 hrs soxhlet-extraction. The plot shows that no TBTO reagent, or any other chemicals, have been extracted. This demonstrates that the peaks due to stannylation, obtained during IR analysis of the stannylated coal macerals, are not due to excess TBTO reagent adsorbed onto the coal macerals during reaction.

Table 3.15 IR analysis of the stannylated Creswell macerals

Stannylated Creswell Maceral	Sn-O-C (cm^{-1})	Sn-C (cm^{-1})	$-CH_3$ (cm^{-1})	C-H (cm^{-1})
Exinite	1074	586	1376	1460
Vitrinite	1075	586	1377	1462
Inertinite	1079	—	1377	1455

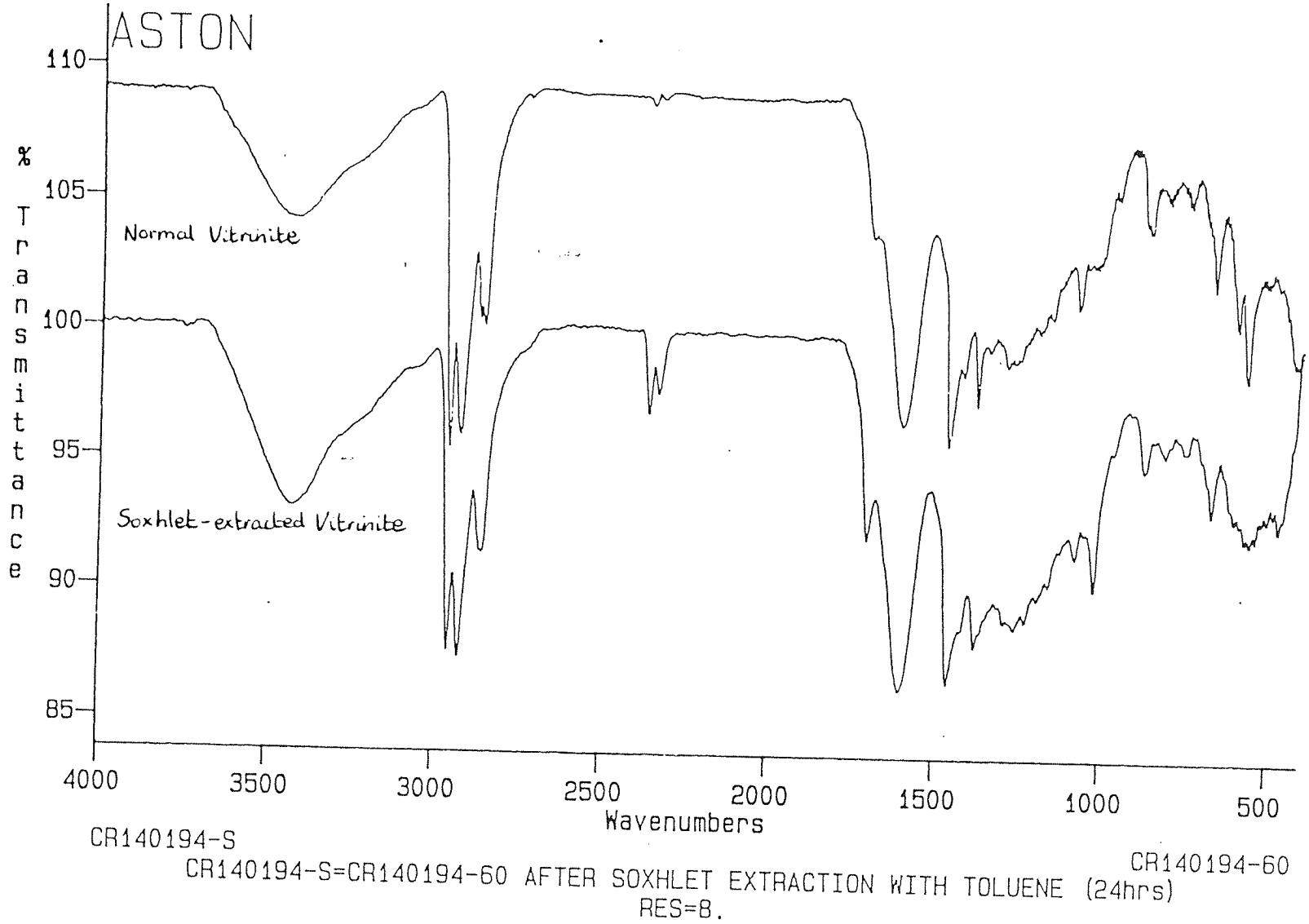

Fig3.65
IR comparison of 24 hr soxhlet-extracted stannylated Creswell ≤32 μm vitrinite and the normal stannylated Creswell ≤32 μm vitrinite maceral

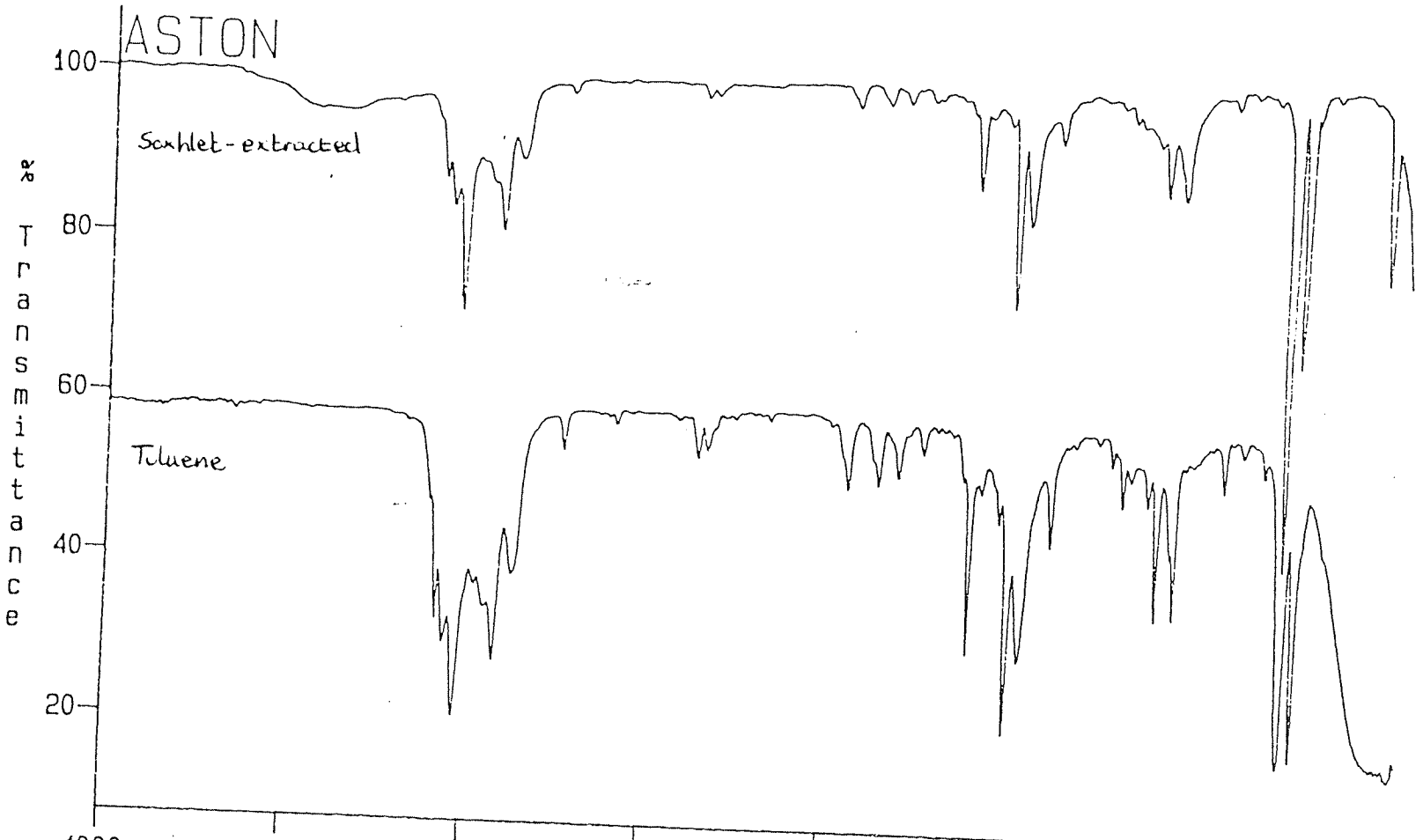

Fig3.66
IR comparison of solution obtained from stannylated Creswell ≤32 μm soxhlet-extraction and toluene

The Creswell macerals and stannylated Creswell macerals were also analysed by solid-state CP MASNMR. Figs 3.67a - 3.67c show the ^{13}C CP MASNMR spectra of the unreacted Creswell exinite, vitrinite and inertinite respectively. Each spectrum has two main broad peaks - the broad peak between 0 - 60 ppm denotes mainly aliphatic carbon, whilst the broad peak between 100 - 160 ppm is predominantly due to aromatic carbon moieties. The ^{13}C CP MASNMR spectrum for the Creswell exinite maceral shows that a significant proportion of the structure consists of aliphatic moieties compared to the other two maceral groups. The Creswell vitrinite maceral also shows significant aliphatic structure, though this is not as extensive as the exinite maceral, and the Creswell inertinite maceral shows relatively little aliphatic character - its structure is dominated mainly by aromatic carbon moieties. The stannylated Creswell coal macerals were analysed by solid-state ^{119}Sn CP MASNMR. The nmr spectra are reported relative to a tetraphenyltin solid standard - the tetraphenyltin signal appears at 120.42 ppm downfield from tetramethyltin. It was decided to use tetraphenyltin as the standard, because tetramethyltin was considered too toxic and volatile for practical use. The chemical shifts obtained, however, may be reported relative to tetramethyltin by subtracting 120.42 ppm from the resonance chemical shift value reported relative to tetraphenyltin. Fig 3.68 shows the ^{119}Sn CP MASNMR spectrum of the TBTO reagent. The resonance appears at 203.2 ppm relative to the tetraphenyltin standard (82.8 ppm relative to tetramethyltin - the value reported in the literature[61] is 83.0 ppm). Fig 3.69a shows the ^{119}Sn CP MASNMR spectrum of the stannylated Creswell exinite maceral. The spectrum shows prominent peaks at 230.4 ppm and 269.9 ppm (110.0 ppm and 149.5 ppm relative to tetramethyltin). The peak at 230.4 ppm denotes stannylation of less sterically-hindered phenols, such as 2,6-dimethylphenol and 2,6-diisopropylphenol, whilst the peak at 269.9 ppm is probably due to stannylation of groups such as substituted naphthol groups. There is also a prominent resonance at -19.3 ppm (-139.7 ppm relative to tetramethyltin) - this resonance could be due to a Bu_3SnOH type structure. Fig 3.69b shows the ^{119}Sn CP MASNMR spectrum of the stannylated Creswell vitrinite maceral - even after an overnight run on the nmr spectrometer and 6320 scans, only one resonance is discernible at -19.4 ppm (postulated to be due to Bu_3SnOH formation). Fig 3.69c shows the ^{119}Sn CP MASNMR spectrum of the stannylated Creswell inertinite maceral. The main product peaks appears at 222.0 ppm and 226.9 ppm (101.6 ppm and 106.48 ppm respectively relative to tetramethyltin) indicating stannylation of mono-, di- and tri-substituted methylphenols, mono- and di-substituted isopropylphenols and mono-substituted butylphenols. Again, there is a prominent peak at approximately -19.0 ppm.

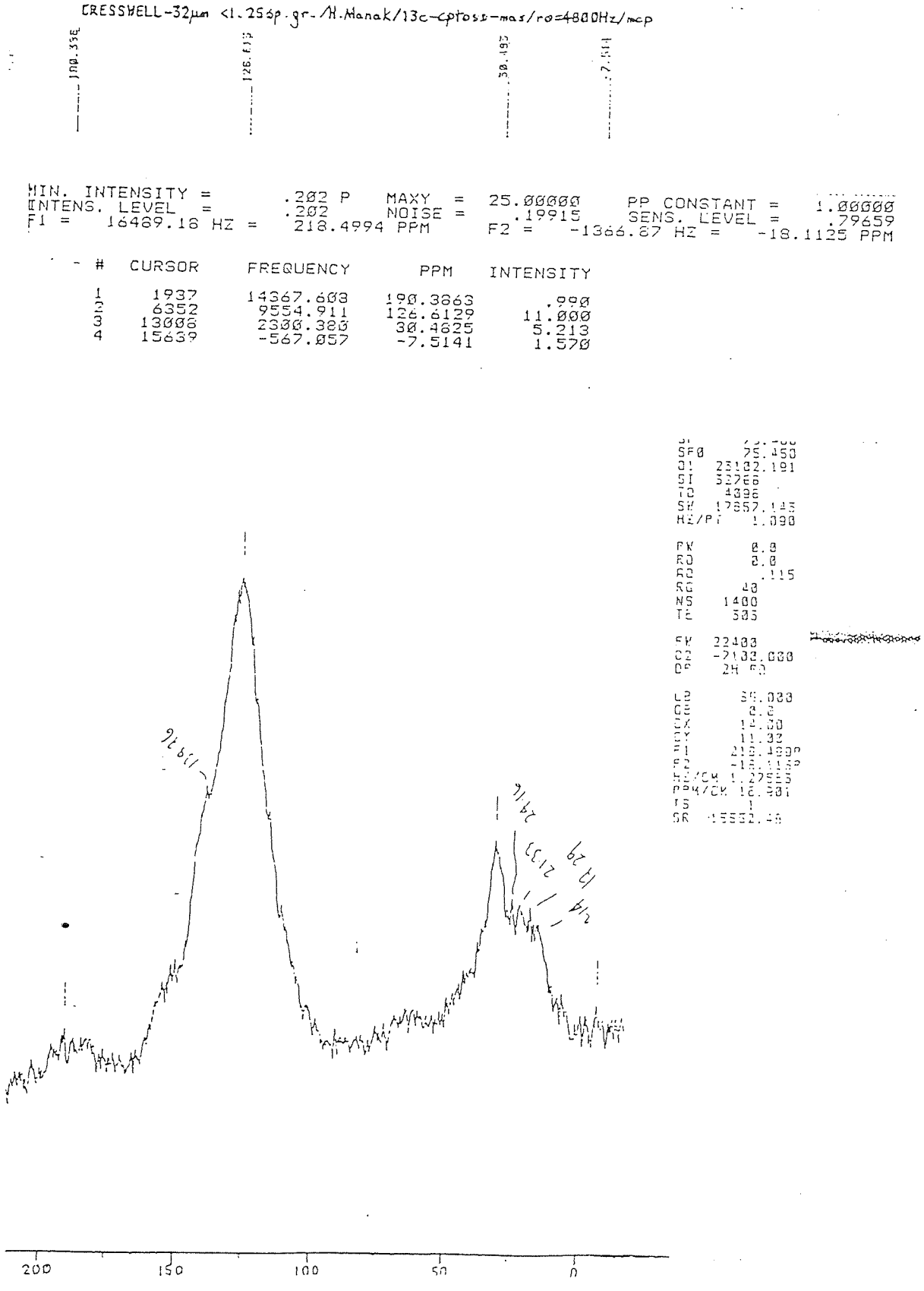

Fig3.67a
^{13}C CP MASNMR of the Creswell ≤32 µm exinite maceral

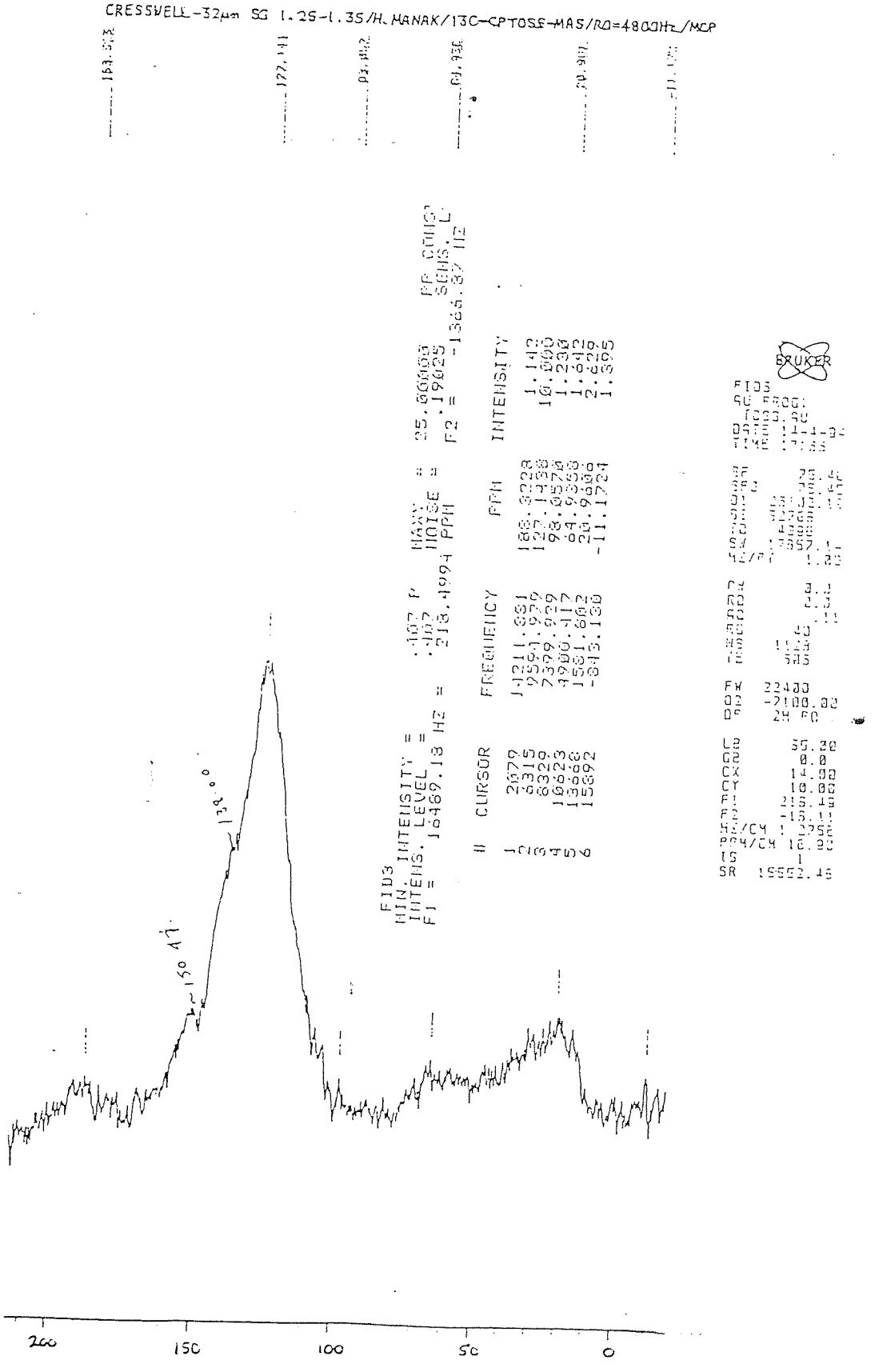

Fig3.67b

^{13}C CP MASNMR of the Creswell ≤32 µm vitrinite maceral

CRESSWELL-32μm-SG1.35-1.45/H.MANAK/13C-CPTOSS-HAS/RO=4800Hz/HCP

MIN. INTENSITY = .217 F MAXY = 25.00000 PP
INTENS. LEVEL = .217 NOISE = .12486 SE
F1 = 16489.16 HZ = 218.4994 PPM F2 = -1366.8

#	CURSOR	FREQUENCY	PPM	INTENSITY
1	278	16175.538	214.3433	.690
2	1934	14370.511	190.4248	.695
3	2046	14248.602	188.8093	1.018
4	2298	13973.134	185.1591	.737
5	2510	13742.398	182.1016	.945
6	2766	13463.930	178.4116	.824
7	3149	13046.448	172.8795	.558
8	3513	12649.813	167.6237	.347
9	3804	12332.447	163.4182	.657
10	4333	11755.654	155.7751	1.450
11	4661	11375.951	150.7436	1.923
12	6419	9481.926	125.6457	10.000
13	8129	7617.966	100.9463	.650
14	8298	7434.364	98.5133	.815
15	8434	7285.630	96.5425	.675
16	8832	6852.034	90.7968	.721
17	9044	6620.614	87.7303	.716
18	9467	6137.752	81.3316	.952
19	9989	5591.444	74.0927	1.036
20	10467	5135.162	68.0464	1.444
21	10656	4946.267	65.5686	1.690
22	11274	4190.546	55.5293	1.388
23	11864	3547.318	47.0058	1.169
24	12166	3218.793	42.6525	1.128
25	12823	2502.241	33.1574	1.799
26	13314	1966.943	26.0641	1.522
27	13710	1535.412	20.3459	1.423
28	13992	1228.467	16.2785	1.365
29	14275	-170.330	-2.2571	.512
30	15883	-832.641	-11.0334	.576

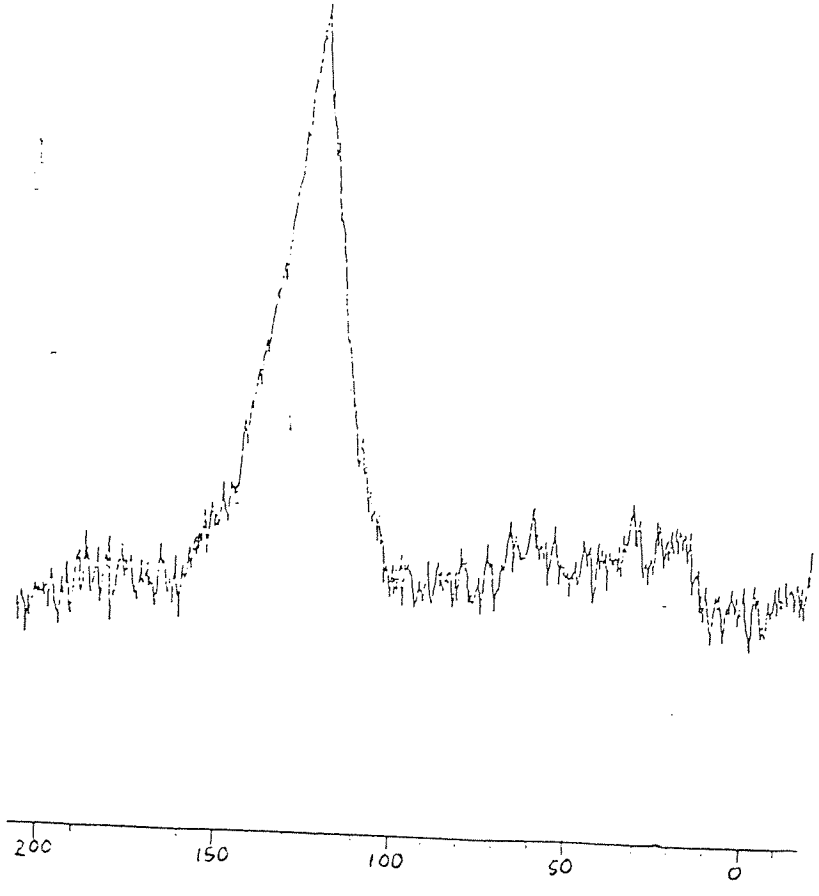

Fig3.67c
^{13}C CP MASNMR of the Creswell ≤32 μm inertinite maceral

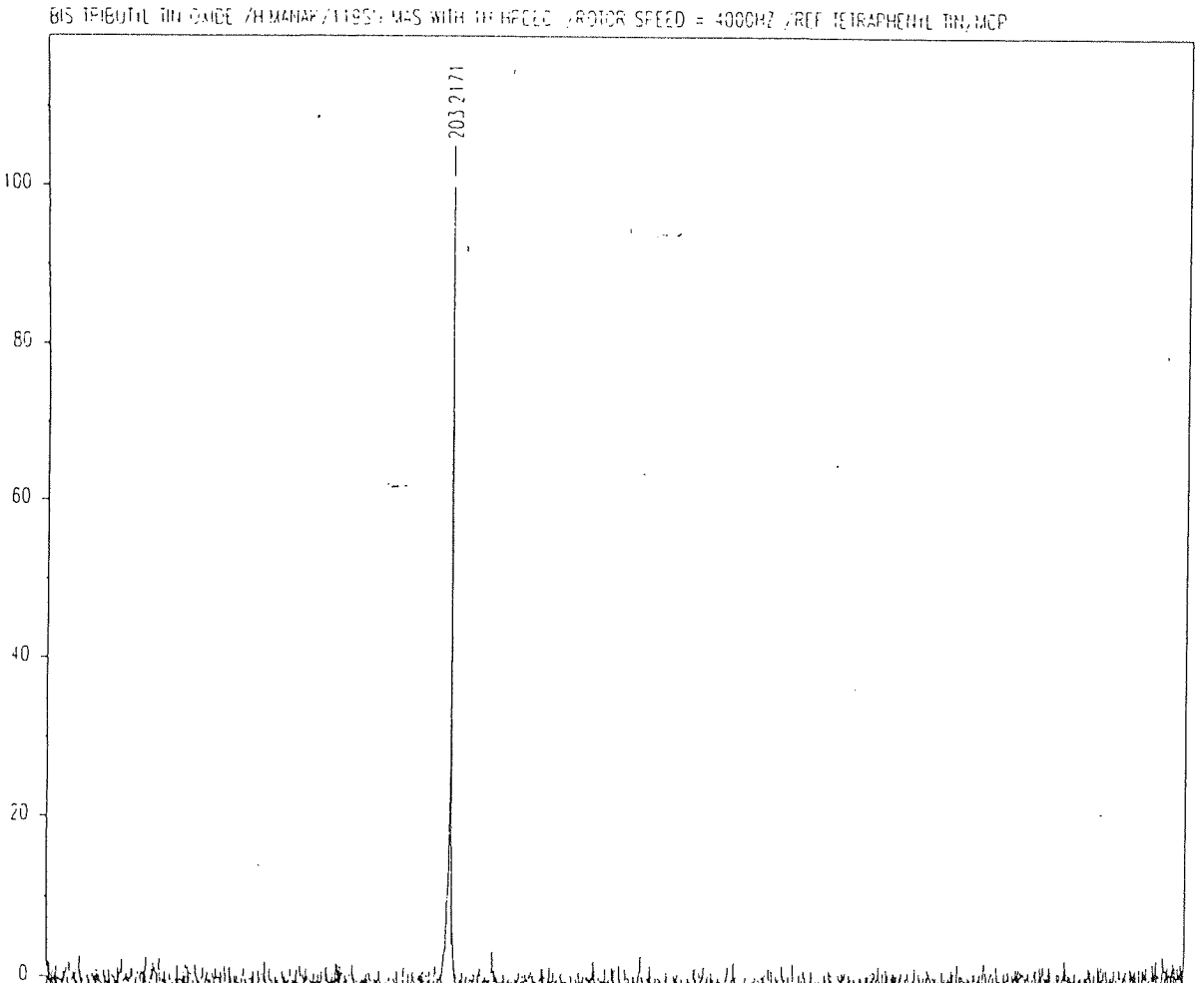

··· Current Data Parameters ···

NAME	:	BTBOSN
EXPNO	:	1
PROCNO	:	1

··· Acquisition Parameters ···

AUNM	:	HPDEC.AU
NS	:	8

··· 1D NMR Plot Parameters ···

SR	:	-16591.53 Hz
ppmcm	:	38.78
Hzcm	:	4340.28
%Volcm	:	1601.71
Rec	:	F1
MPSF	:	1.0000000
AQtime	:	0.0122870 sec

··· Aspect 3000 Parameters ···

OPERATOR :

203·22
120·42
$Ph_1 J_{Sn} = 0.$

82·80 doublets from Tetramethyltin

Fig3.68
^{119}Sn MASNMR of the TBTO reagent

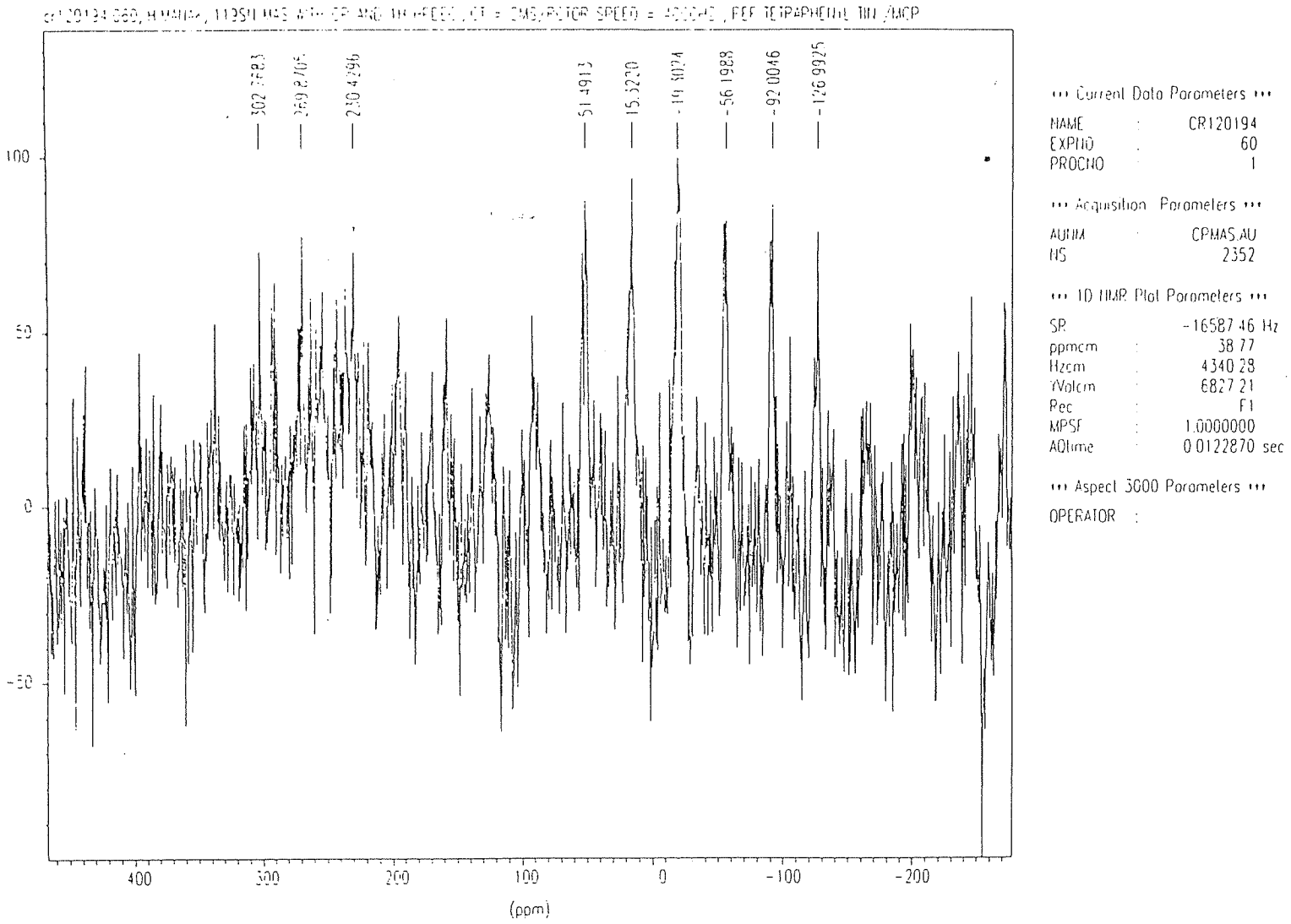

Fig3.69a

^{119}Sn CP MASNMR of the stannylated Creswell ≤32 μm exinite maceral

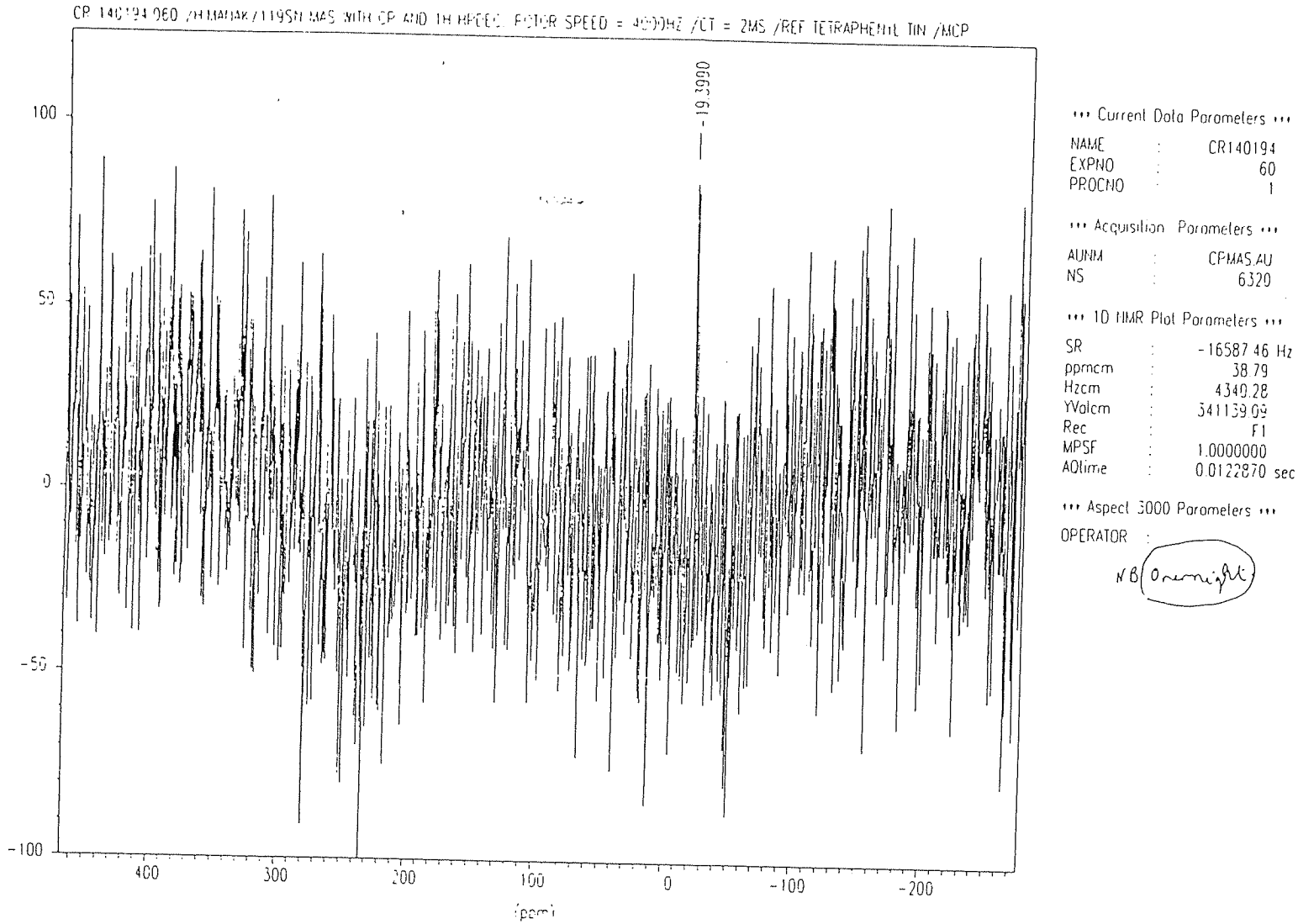

Fig3.69b

^{119}Sn CP MASNMR of the stannylated Creswell ≤32 μm vitrinite maceral

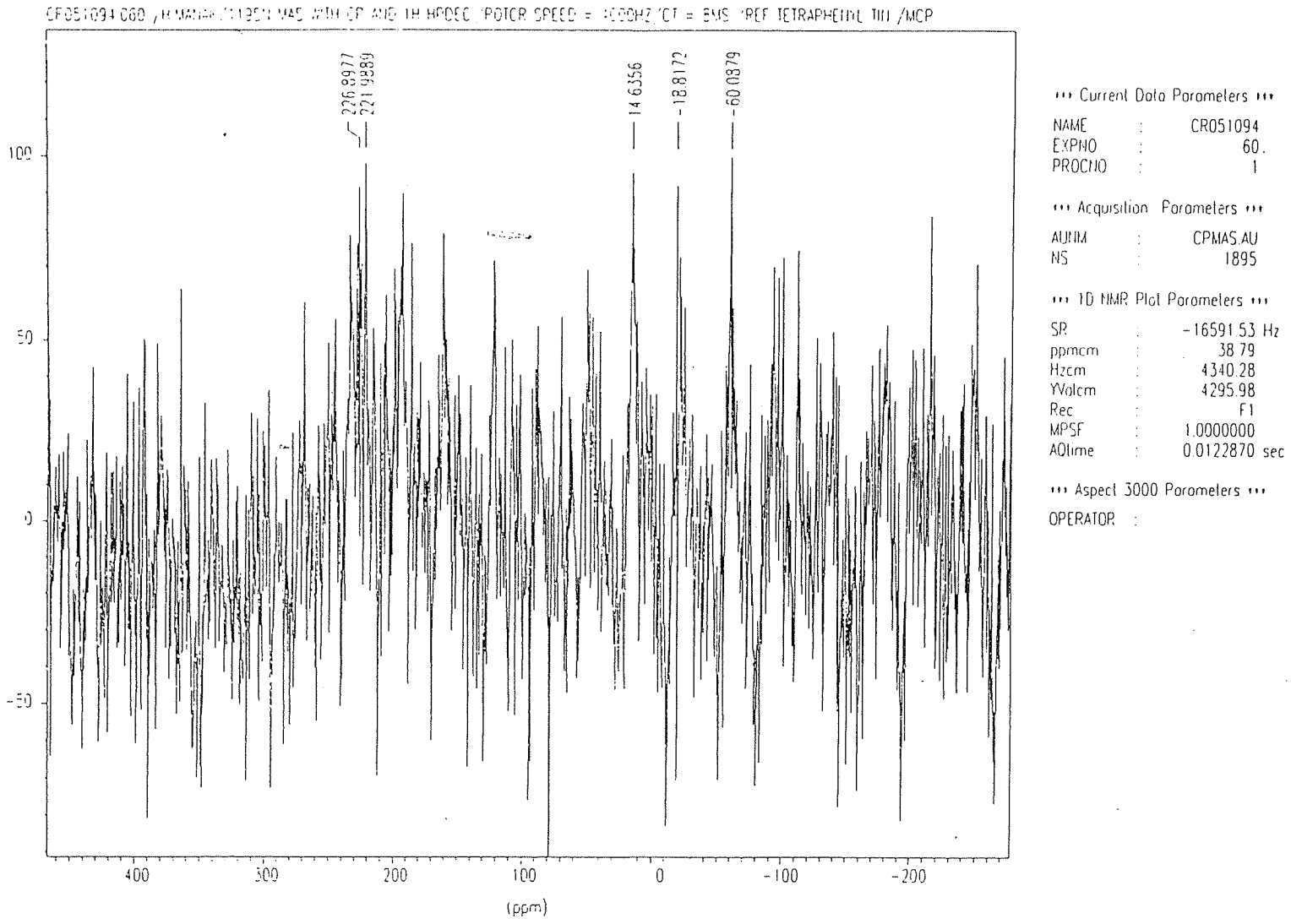

Fig3.69c

^{119}Sn CP MASNMR of the stannylated Creswell ≤32 μm inertinite maceral

The stannylated Creswell macerals were also analysed by X-ray photoelectron spectroscopy (XPS). The extra-nuclear electrons of atoms and molecules exist in orbitals of well-defined energies. Electron spectroscopy enables the different binding energies, or ionisation potentials (IPs), of electrons in different orbitals to be measured. Because these orbital IPs are characteristic features of the parent atom or molecule, electron spectroscopy affords a possible means of compound identification. Essentially, the energy spectrum of the electrons ejected from a sample under bombardment with monoenergetic X-rays is measured. The energies of the ejected electrons differ according to their orbitals of origin and may be cross-referenced to a data base in order to identify the elements present and / or provide information about the structure of the sample. Fig 3.70a and 3.70b show the XPS spectra for the stannylated Creswell exinite maceral. Spin-orbit coupling of states produced two bands with binding energies of approximately 495eV and 486 eV - these values correspond to Sn in an Sn-O environment. The approximate ratio of C : O : Sn recorded is 3.7 : 0.8 : 1.0. If we assume that the Sn and O present interact on a 1 : 1 mole ratio, then it appears that the bulk of the oxygen has been stannylated. This, however, is not the case, as XPS is a surface technique (detecting down to approximately 50 Å) and does not take into account the bulk structure of the sample. It may well be true that nearly all the oxygen near the surface has been stannylated, but this does not imply that the reagent has successfully diffused through the structure to react with the rest of the oxygen in the bulk of the sample. Fig 3.71 shows the XPS spectrum for the stannylated Creswell vitrinite maceral. Again, a binding energy of approximately 486 eV is detected indicating a Sn-O structure. The approximate C : O : Sn ratio is 5.2 : 0.8 : 1.0. The ratio of Sn : O is the same as in the stannylated Creswell exinite maceral, but in this case there appears to be a greater carbon content indicating, assuming that there is only a small contribution from the butyl groups of the TBTO reagent, a greater degree of aromaticity for the Creswell vitrinite. Fig 3.72 shows the XPS spectrum of the stannylated Creswell inertinite maceral group. An electron binding energy of approximately 486 eV is detected denoting a Sn-O structure. The C : O : Sn ratio is 14.1 : 2.1 : 1.0. The higher carbon content seems to indicate a greater degree of aromaticity in the Creswell inertinite compared to the other two maceral groups and the low ratio of Sn : O denotes that not much, in fact less than half, of the oxygen near the surface of the sample has been derivatised. Table 3.16 summarises the XPS results.

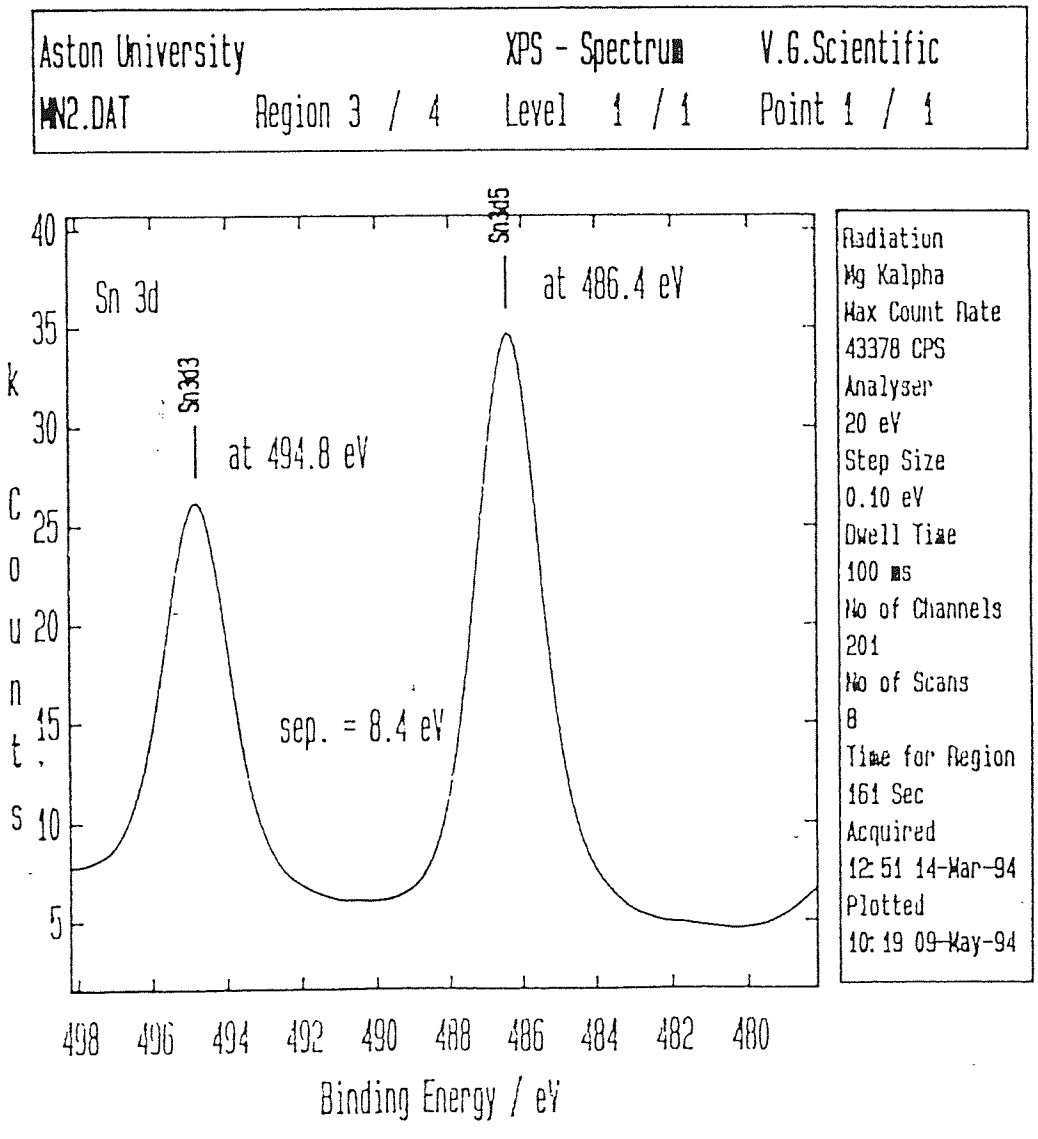

Fig3.70a
XPS of the stannylated Creswell ≤32 μm exinite maceral

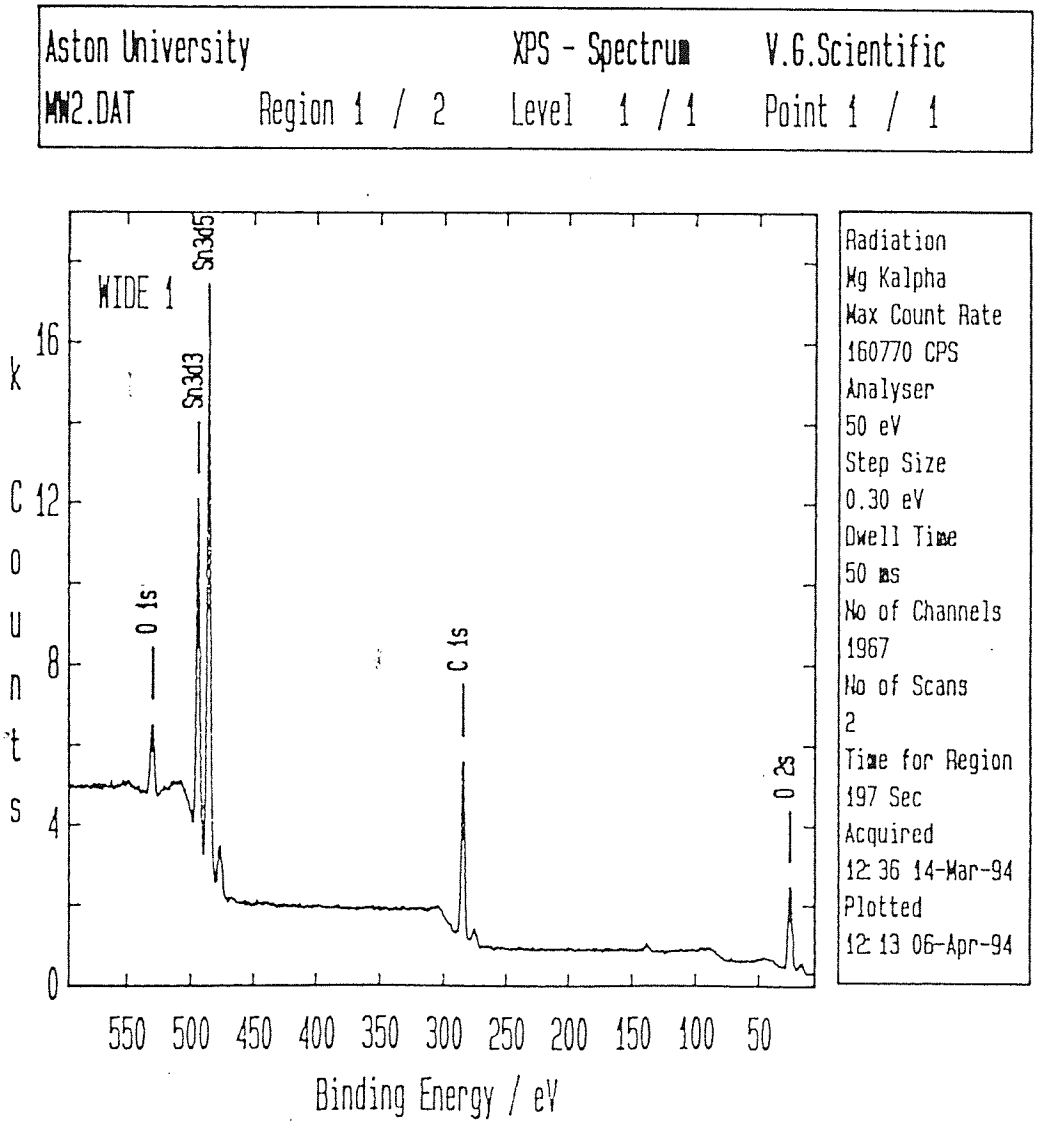

Fig3.70b
XPS of the stannylated Creswell ≤32 μm exinite maceral II

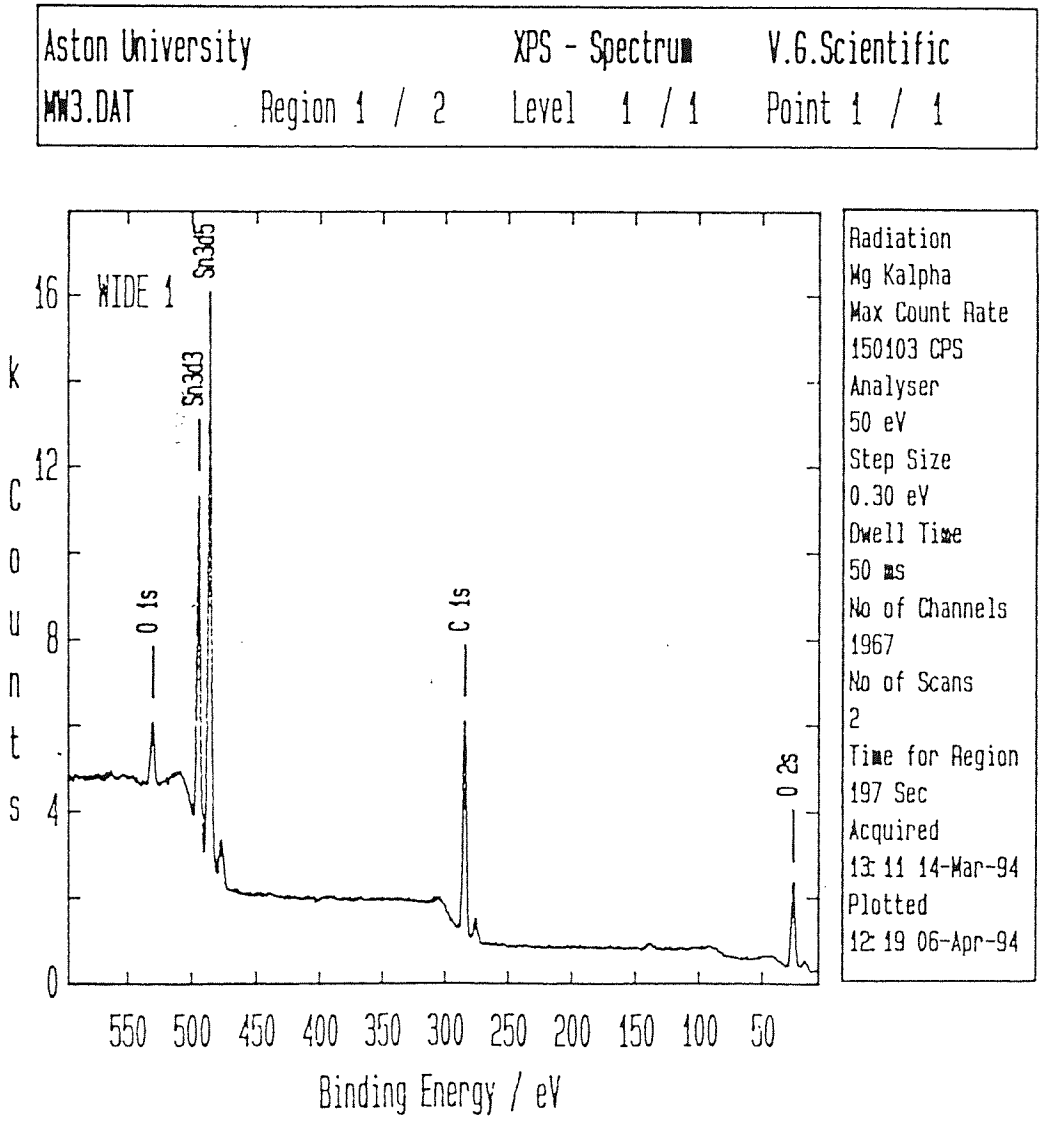

Fig3.71
XPS of the stannylated Creswell ≤32 μm vitrinite maceral

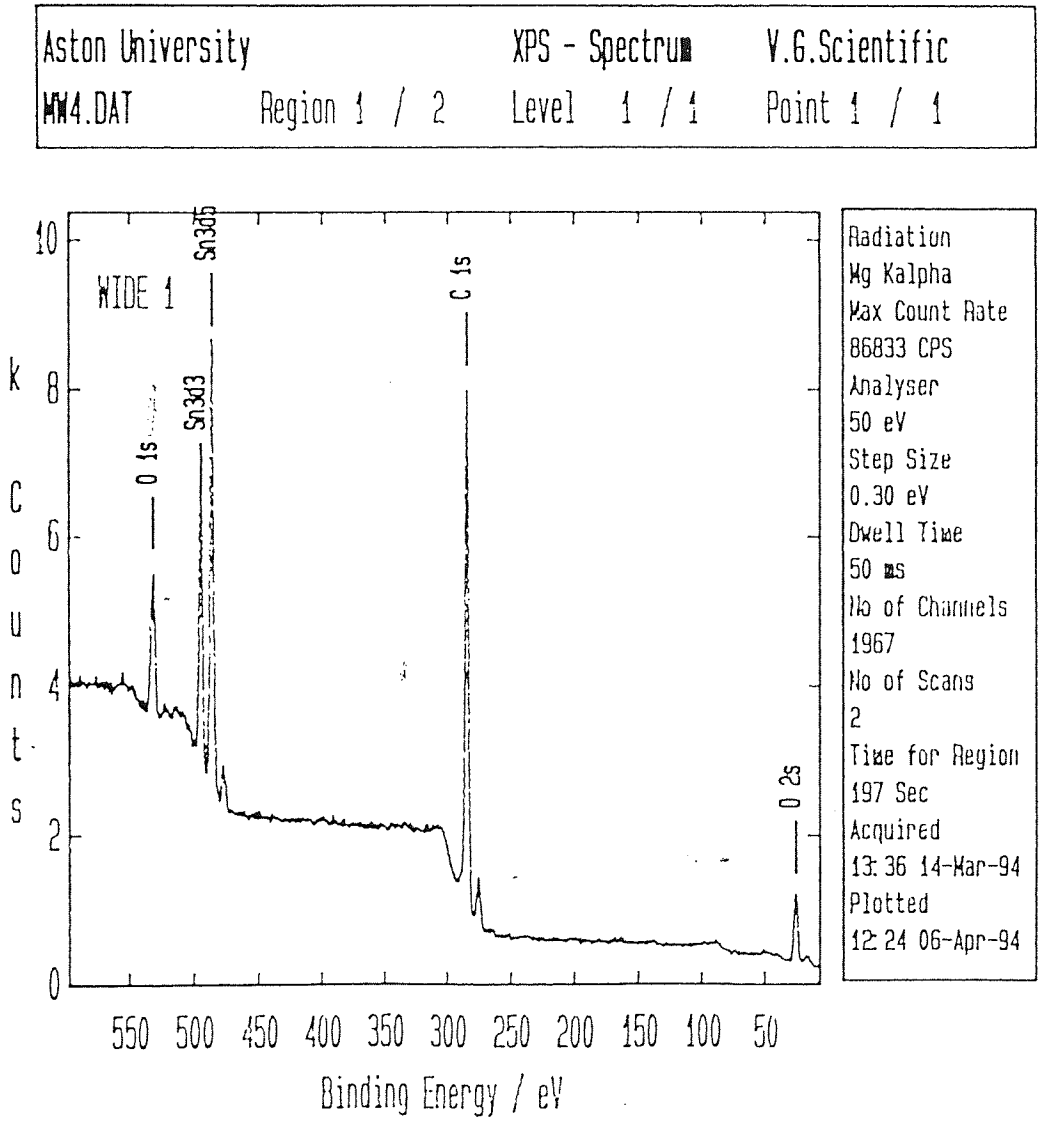

Fig3.72
XPS of the stannylated Creswell ≤32 μm inertinite maceral

Table 3.16 XPS Results for the stannylated Creswell macerals

Stannylated Creswell Maceral	Element Identification	Atomic [%]	Atomic Ratio	Peak Intensity kCeV / S	Binding energy eV
Exinite	C 1s	67.53	3.7	21.58	284.60
	O 1s	14.42	0.8	13.14	530.40
	Sn $3d^5$	18.05	1.0	84.38	486.40
Vitrinite	C 1s	74.64	5.2	25.49	284.60
	O 1s	11.08	0.8	10.78	530.30
	Sn $3d^5$	14.29	1.0	71.37	486.40
Inertinite	C 1s	82.06	14.1	30.94	284.60
	O 1s	12.11	2.1	13.01	531.80
	Sn $3d^5$	05.83	1.0	32.15	486.70

In summary, IR analysis of the unreacted Creswell macerals shows that the exinite and vitrinite macerals both have an appreciable -OH content with the exinite maceral group showing a greater aliphatic character. The Creswell inertinite maceral group, however, shows a lower relative concentration of -OH, less aliphatic character and a greater degree of aromaticity. There is some ambiguity, however, as to how much of this -OH is actually due to the phenolic groups present in the macerals and how much is due to tenaciously held moisture (which reacts to form Bu_3SnOH with the stannylating reagent). The IR analysis of the stannylated Creswell macerals shows that significant stannylation has occurred with the exinite and vitrinite maceral groups, even though the -OH peak is still evident on the IR plots, and that relatively less stannylation has occurred with the Creswell inertinite maceral group. Solid-state ^{13}C CP MASNMR analysis of the unreacted Creswell macerals shows a similar trend to that observed with the IR results i.e the aromatic character appears to increase in going from exinite to vitrinite to inertinite. The ^{119}Sn CP MASNMR results are somewhat ambiguous. Low intensity resonance peaks were observed for the stannylated exinite and inertinite maceral groups, but no product resonance peak was observed for the stannylated vitrinite maceral. A resonance at approximately -19 ppm was observed on all three nmr spectra. This peak is postulated to be due to Bu_3SnOH, which is formed by the reaction of the stannylating reagent with inherent moisture present in the macerals. The presence of this resonance may imply that the major reaction occurring in the macerals, is that of TBTO with moisture, as opposed to TBTO with phenolic functional groups. The XPS results show that some stannylation appears to have taken place. The Sn : O ratio suggests that a similar degree of stannylation has taken place with the exinite and vitrinite maceral groups, with relatively less stannylation occurring with the Creswell inertinite maceral - these results are consolidated by the IR analyses. The XPS results also show that there appears to be an increase in aromaticity in going from exinite to vitrinite to inertinite - a trend also seen with the ^{13}C CP MASNMR analyses.

3.3.6 Stannylation of the Cortonwood macerals

As with the Creswell macerals, the Cortonwood macerals were each reacted for 60 mins in the Sharp Carousel II microwave oven. Figs 3.73a -3.73c show the FT-IR spectra of the unreacted Cortonwood exinite, vitrinite and inertinite macerals respectively. Subjectively, the exinite and vitrinite macerals appear to show similar -OH contents and a similar degree of aliphatic character, whereas the Cortonwood inertinite shows markedly less -OH content and less aliphatic character compared to the other two maceral groups. Fig 3.74 shows a multispectral IR display showing all three Cortonwood macerals on the same plot for comparison.

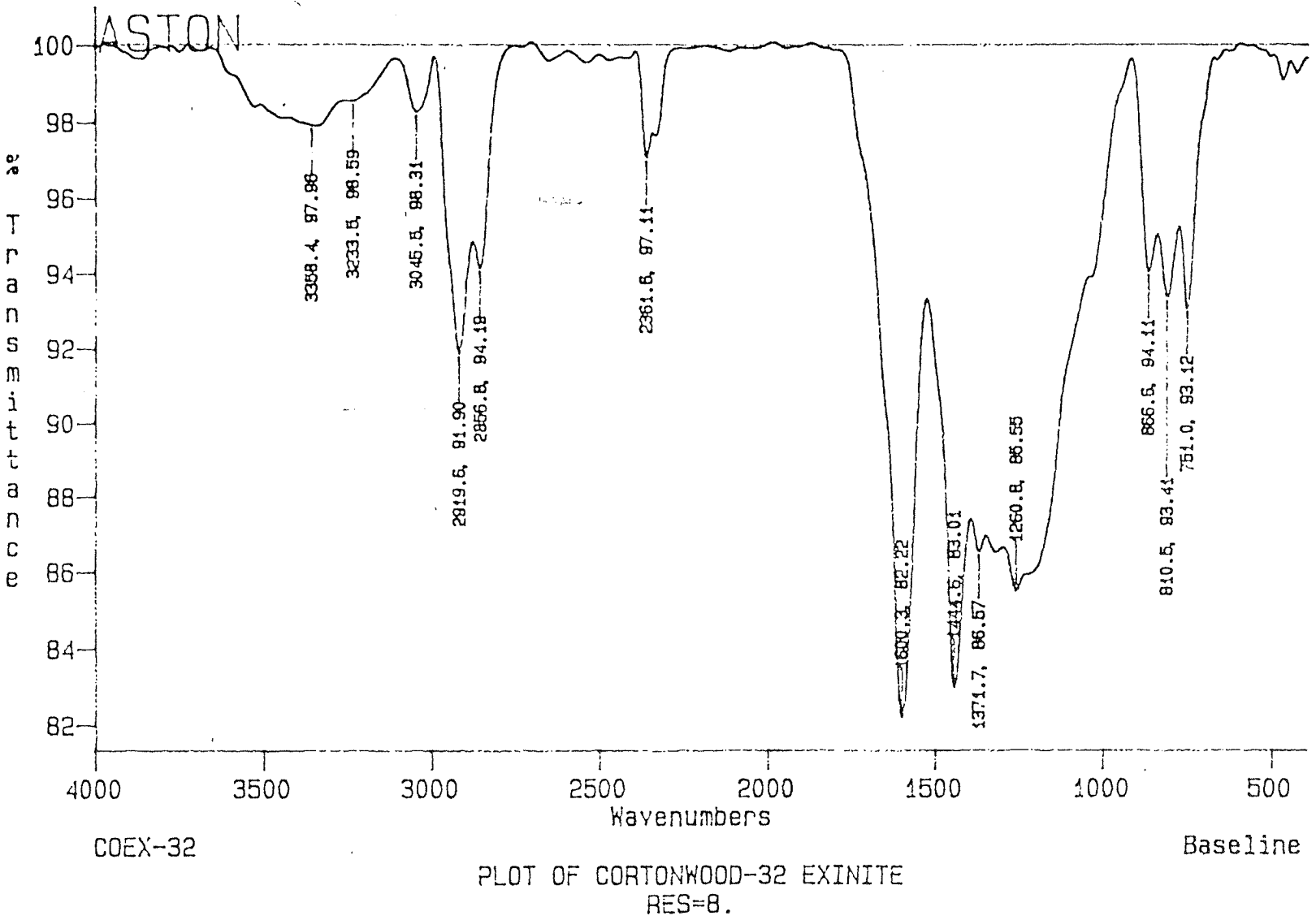

Fig3.73a
IR of the Cortonwood ≤32 μm exinite maceral

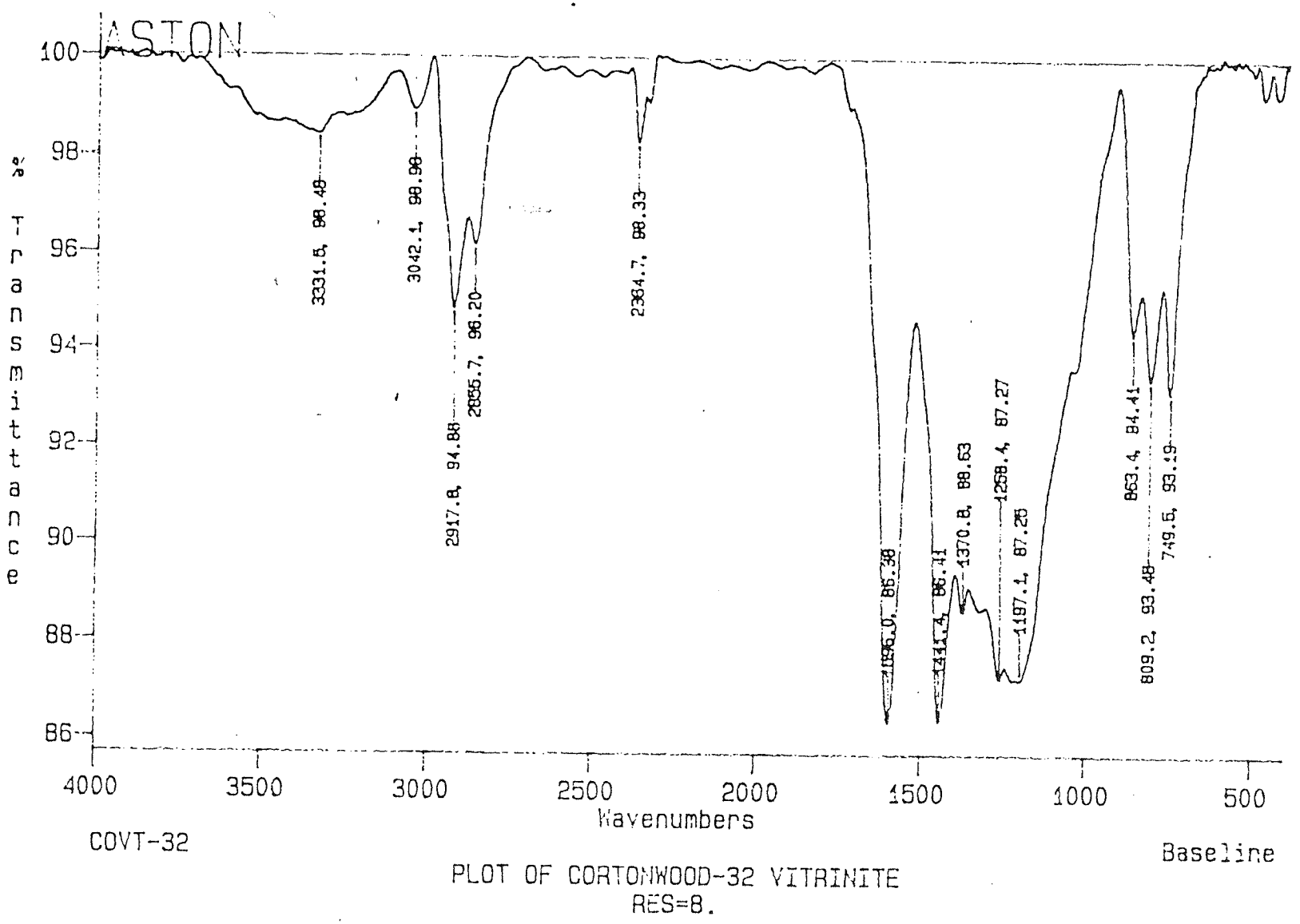

Fig3.73b
IR of the Cortonwood ≤32 μm vitrinite maceral

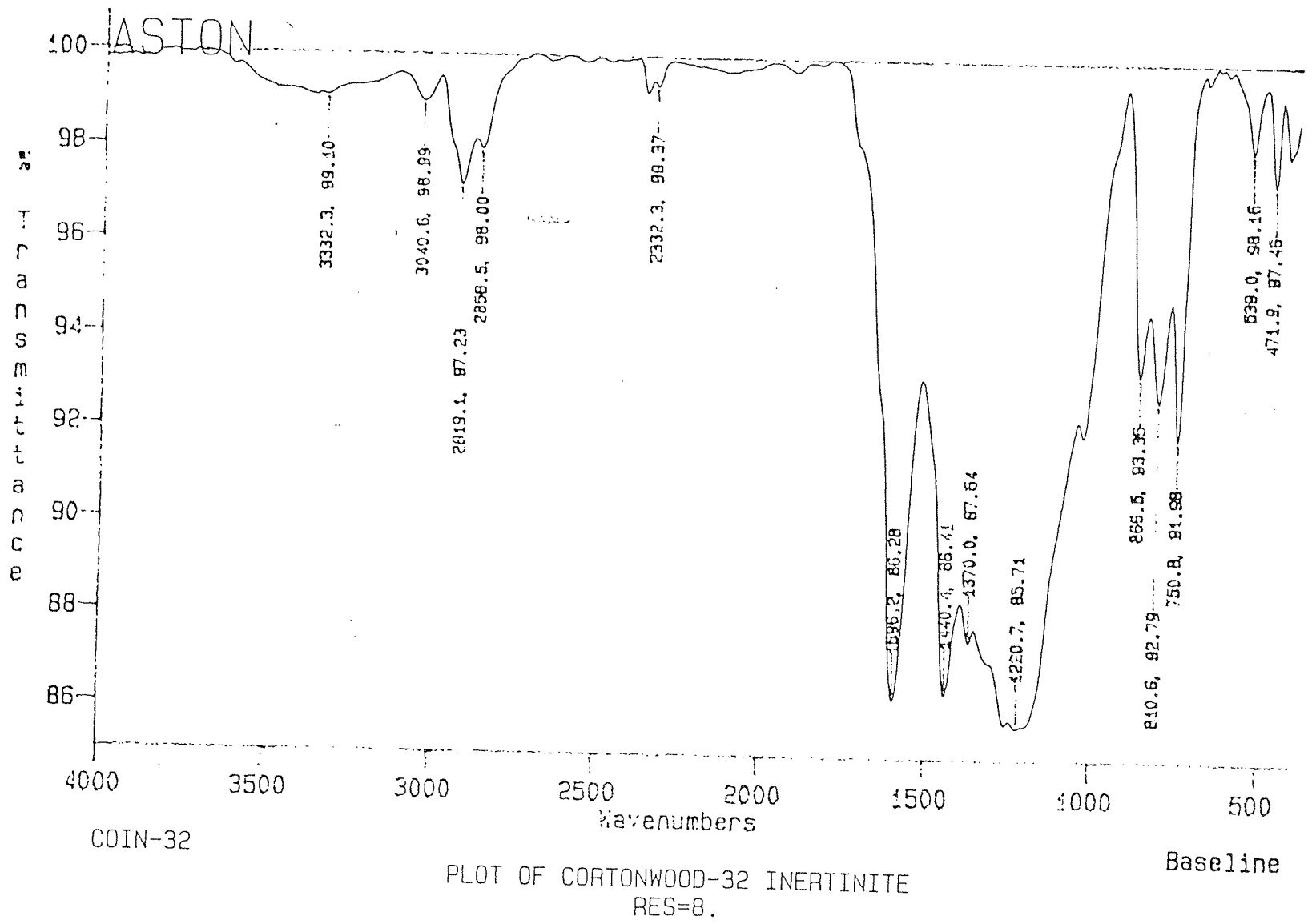

Fig3.73c
IR of the Cortonwood ≤32 μm inertinite maceral

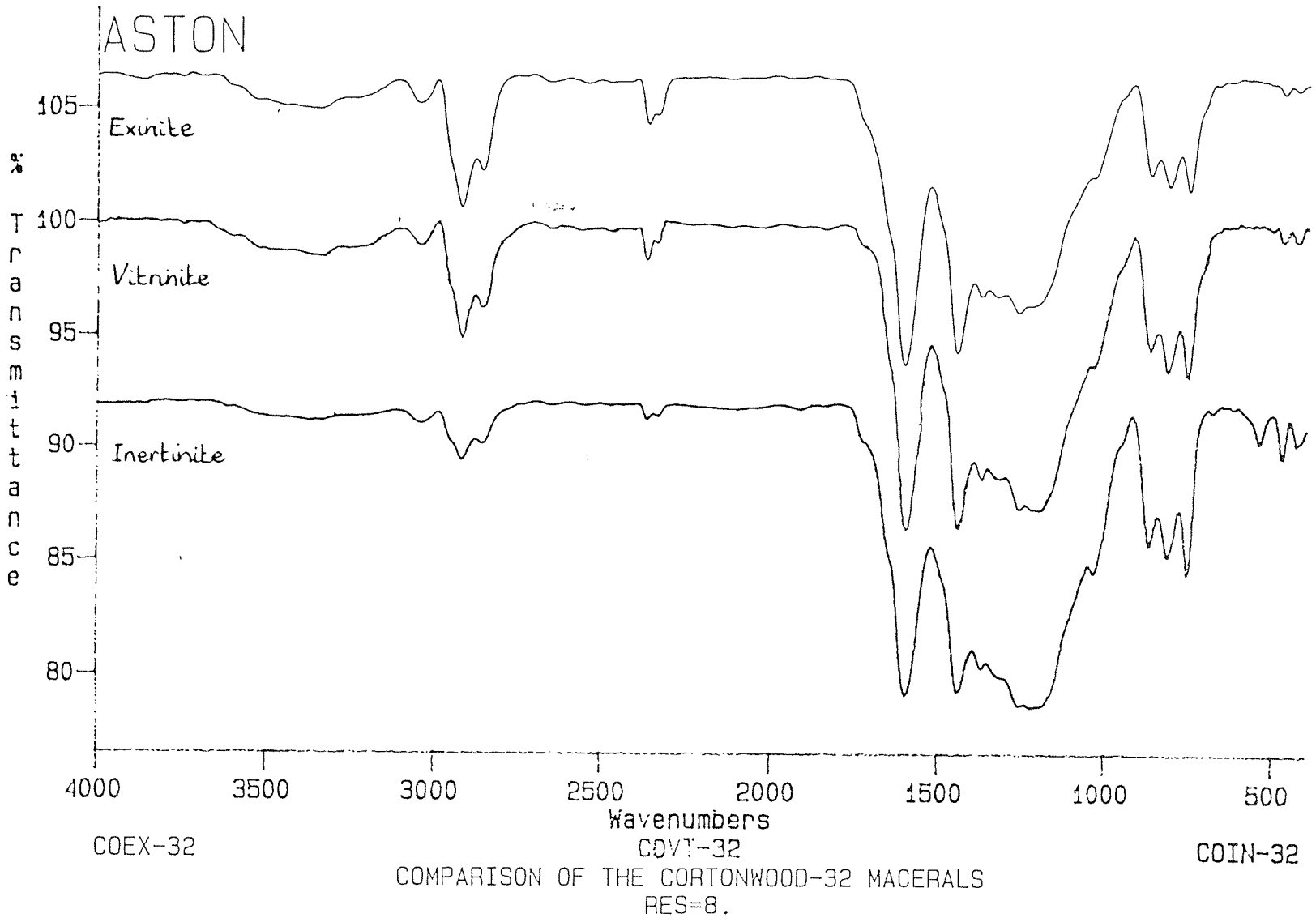

Fig3.74
IR comparison of the Cortonwood ≤32 μm macerals

Fig 3.75 shows the IR spectrum for the stannylated Cortonwood exinite. Peaks indicating that some stannylation has occurred can be observed at 1069 cm^{-1} (Sn-O-C stretching), 585 cm^{-1} (Sn-C asymmetric stretching), 1376 cm^{-1} (symmetric $-CH_3$ deformations) and 1456 cm^{-1} (C-H deformations). A significant peak due to -OH stretching does, however, still exist centred at 3430 cm^{-1}. Fig 3.76 shows the IR spectrum of the stannylated Cortonwood vitrinite maceral. Again, peaks denoting that some stannylation has taken place can be seen at 1072 cm^{-1} (Sn-O-C), 598 cm^{-1} and 507 cm^{-1} (asymmetric and symmetric Sn-C respectively), 1377 cm^{-1} ($-CH_3$ deformations) and 1457 cm^{-1} (C-H), but the -OH stretching absorption centred at 3427 cm^{-1} is still a dominant peak on the plot. Fig 3.77 shows the IR spectrum for the stannylated Cortonwood inertinite maceral. As with the other two maceral groups, peaks pertaining to stannylation may be observed at 1070 cm^{-1} (Sn-O-C stretching), 584 cm^{-1} and 596 cm^{-1} (asymmetric and symmetric Sn-C stretching respectively), 1368 cm^{-1} (symmetric $-CH_3$ deformations) and 1461 cm^{-1} (C-H deformations), but the -OH peak centred at 3444 cm^{-1} still persists.

Table 3.17 IR analysis of the stannylated Cortonwood macerals

Stannylated Cortonwood Maceral	Sn-O-C (cm^{-1})	Sn-C (cm^{-1})	$-CH_3$ (cm^{-1})	C-H (cm^{-1})
Exinite	1069	585	1376	1456
Vitrinite	1072	598	1377	1457
Inertinite	1070	584	1368	1461

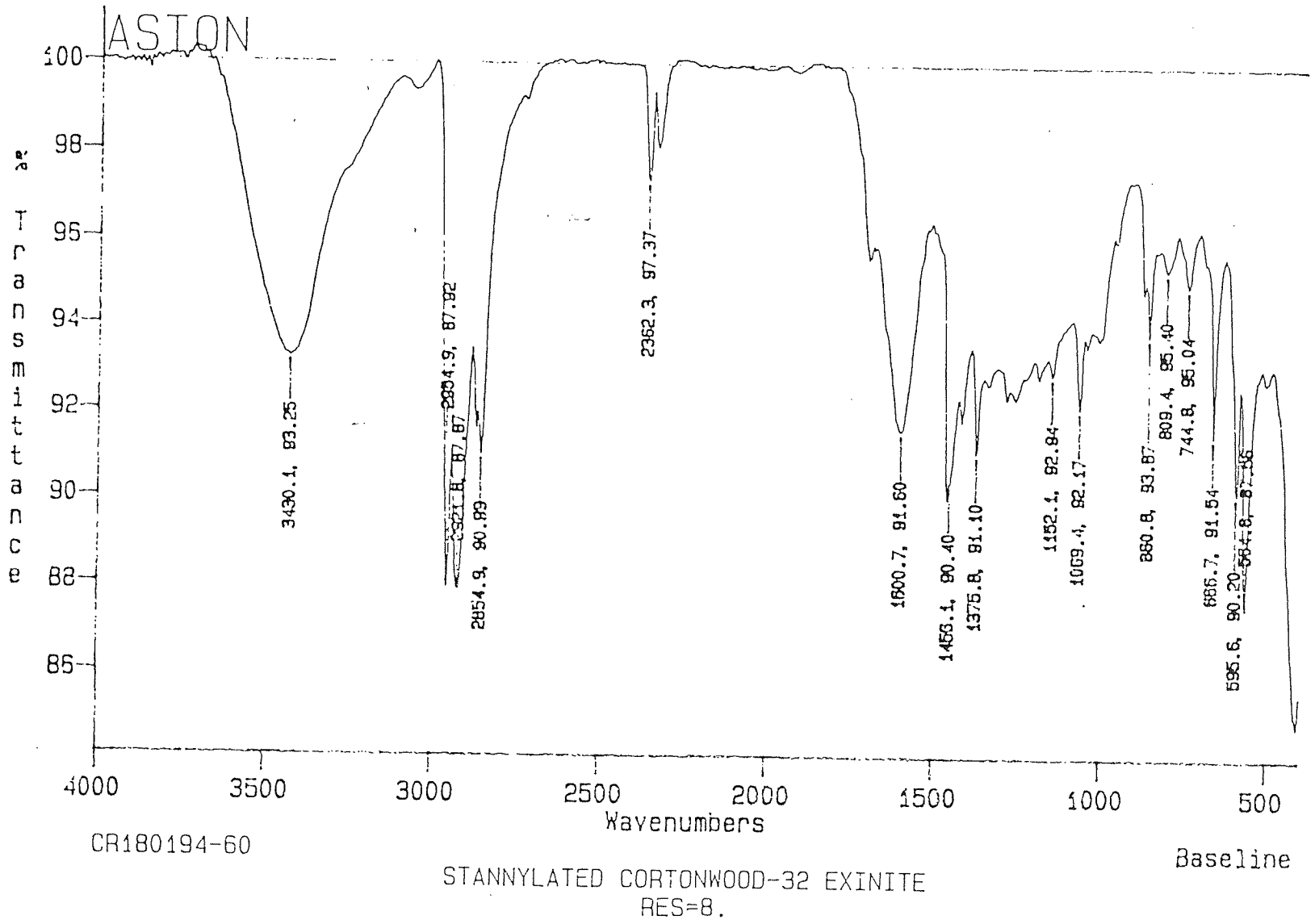

Fig3.75
IR of the stannylated Cortonwood ≤32 μm exinite after 60 mins mw heating

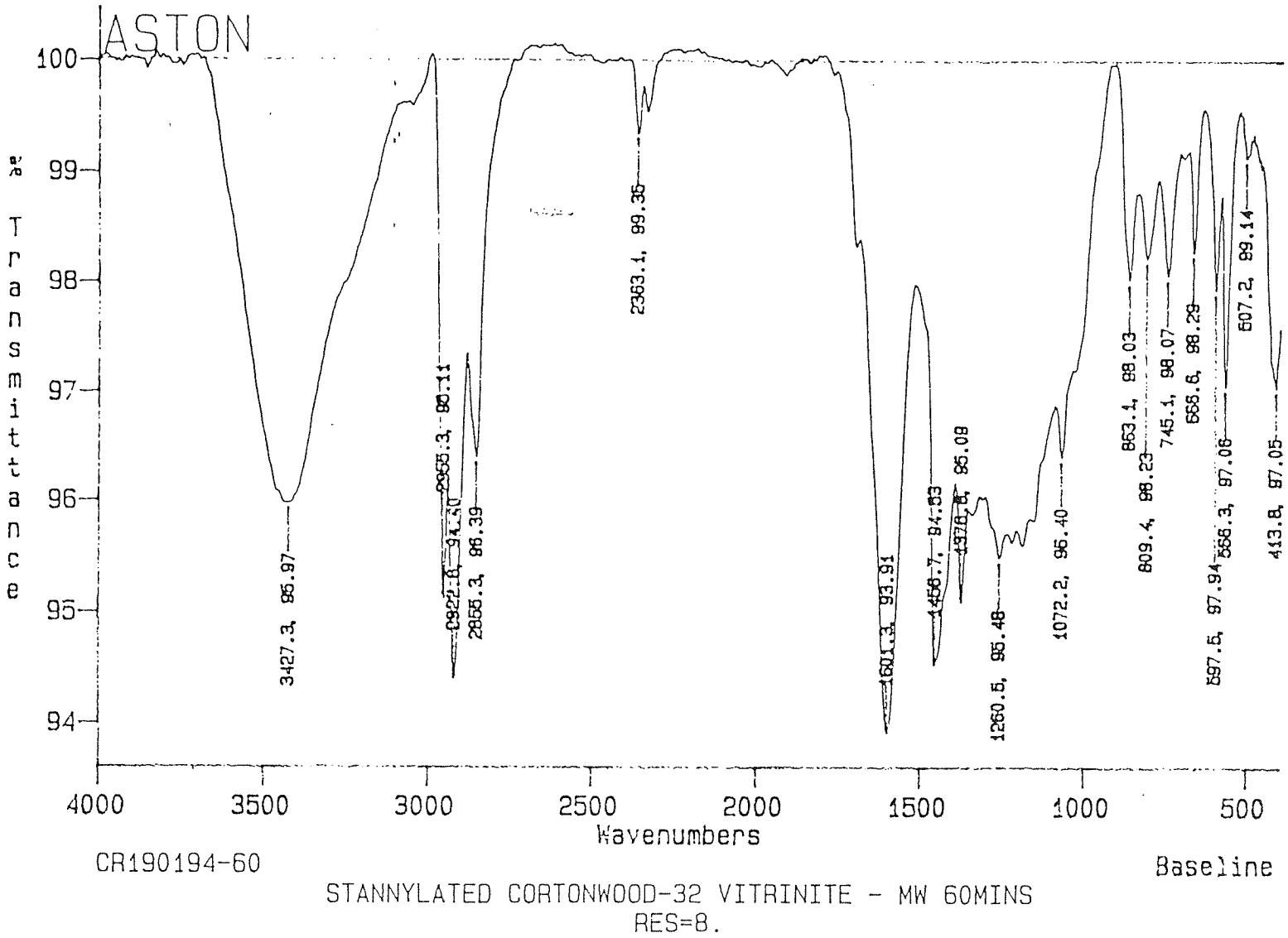

Fig3.76
IR of the stannylated Cortonwood ≤32 μm vitrinite after 60 mins mw heating

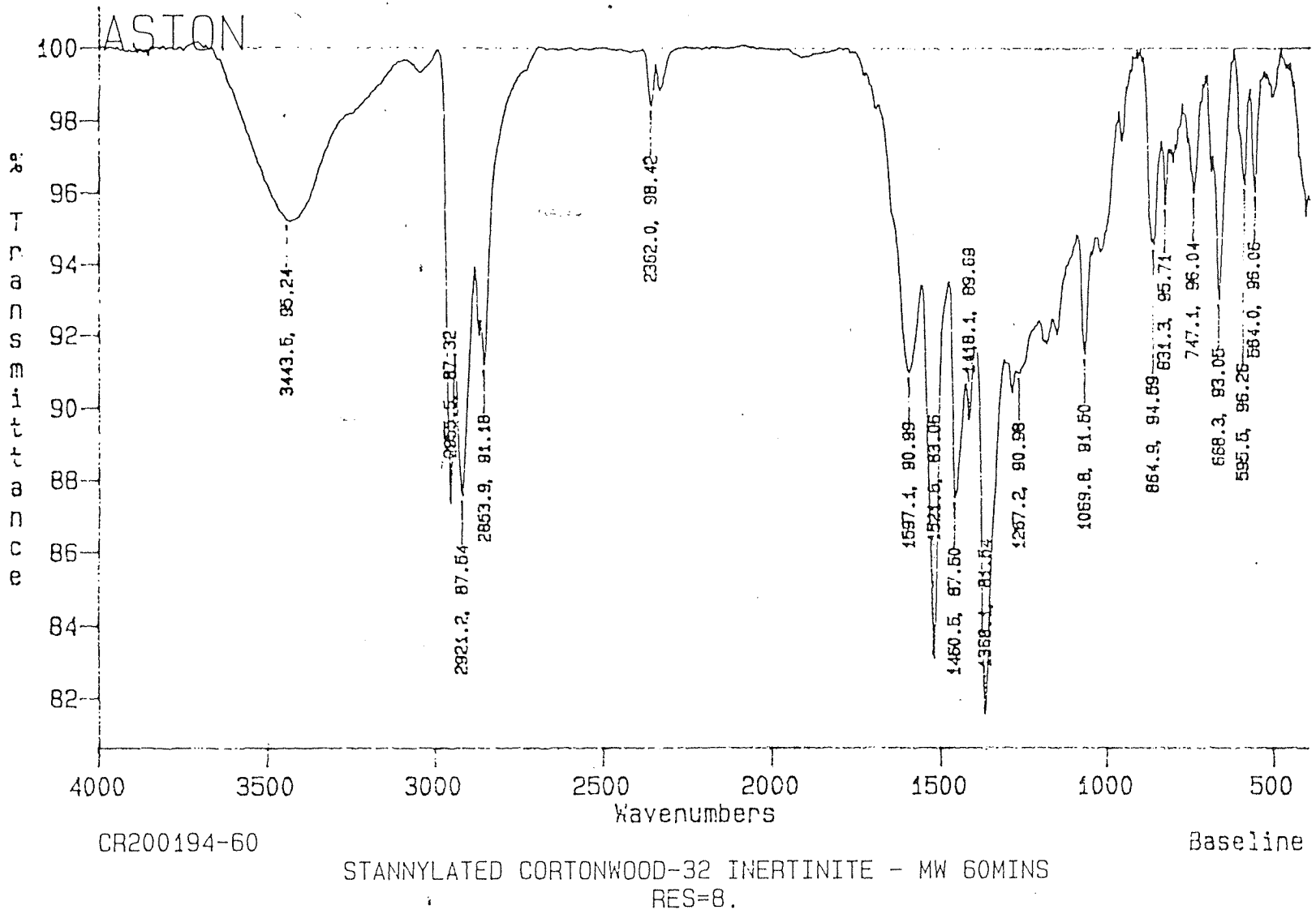

Fig3.77
IR of the stannylated Cortonwood ≤32 μm inertinite after 60 mins mw heating

The coal macerals were also analysed by solid-state ^{13}C CP MASNMR. Figs 3.78a - 3.78c show the ^{13}C CP MASNMR spectra of the unreacted Cortonwood exinite, vitrinite and inertinite macerals respectively. Each spectrum exhibits two main peaks - the broad peak between 0 - 70 ppm denotes mainly aliphatic carbon, whilst the broad peak between 100 - 160 ppm is due mainly to aromatic carbon moieties. The ^{13}C CP MASNMR spectrum for the Cortonwood exinite maceral shows that a significant proportion of the structure consists of aliphatic carbon moieties compared to the other two maceral groups. The Cortonwood vitrinite maceral also shows significant aliphatic carbon structure, though not as extensive as the exinite maceral. By contrast, the Cortonwood inertinite maceral shows much less aliphatic character and its structure is dominated mainly by aromatic carbon moieties. The stannylated Cortonwood macerals were analysed by ^{119}Sn CP MASNMR. All chemical shifts are reported relative to a tetraphenyltin standard. Fig 3.79a shows the ^{119}Sn CP MASNMR spectrum of the stannylated Cortonwood exinite maceral. Only one main resonance is evident at -19.4 ppm (-139.8 ppm relative to tetramethyltin). This peak also appears on each of the stannylated Creswell maceral ^{119}Sn CP MASNMR spectra. The folded spinning sidebands indicate that the chemical shift anisotropy is very large. Fig 3.79b shows the ^{119}Sn CP MASNMR spectrum for the stannylated Cortonwood vitrinite maceral. Again, there is only one major absorption at -20.6 ppm (-141.1 ppm relative to tetramethyltin). The spinning sidebands are again very much in evidence. Fig 3.79c shows the ^{119}Sn CP MASNMR spectrum for the stannylated Cortonwood inertinite maceral. In this case there is a main resonance at 226.0 ppm (105.6 ppm relative to tetramethyltin) and the peak which appears at approximately -19 ppm in all the other stannylated maceral's ^{119}Sn CP MASNMR spectra is noticeable by its absence. The peak at 226 ppm appears to denote stannylation of less sterically-hindered mono-, di- and tri-substituted methylphenols and mono-substituted ethylphenols.

In summary, IR analysis of the unreacted Cortonwood macerals showed a similar trend to that observed with the Creswell macerals i.e the exinite and vitrinite macerals both show appreciable -OH content with the exinite maceral showing more aliphatic character, whereas the Cortonwood inertinite maceral shows a lower relative concentration of -OH, less aliphatic character and a greater degree of aromaticity. The IR analyses of the stannylated Cortonwood macerals appear to show that stannylation has occurred in all cases. An interesting difference emerges here between the Creswell and Cortonwood inertinite macerals.

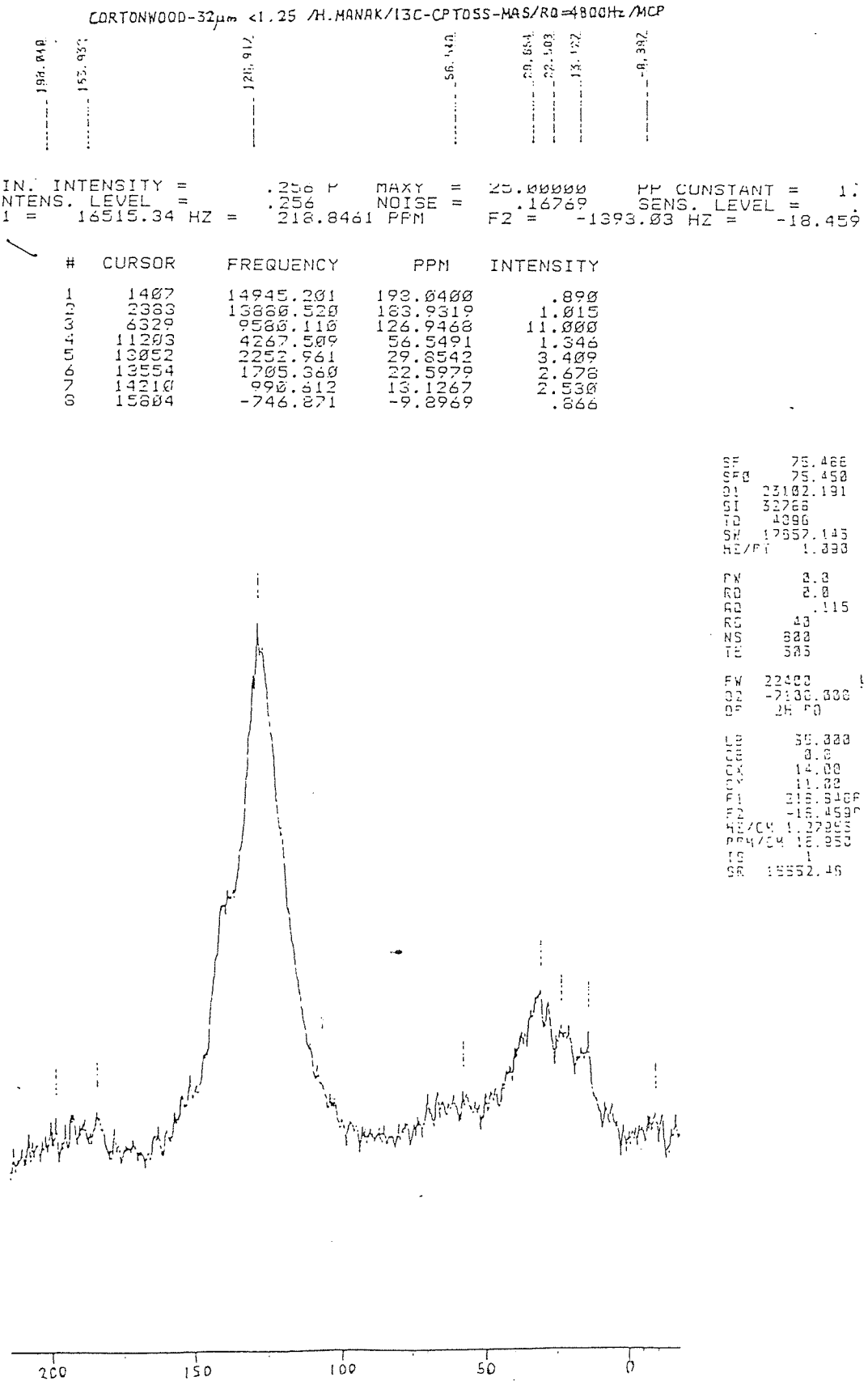

Fig3.78a

^{13}C CP MASNMR of the Cortonwood ≤32 µm exinite maceral

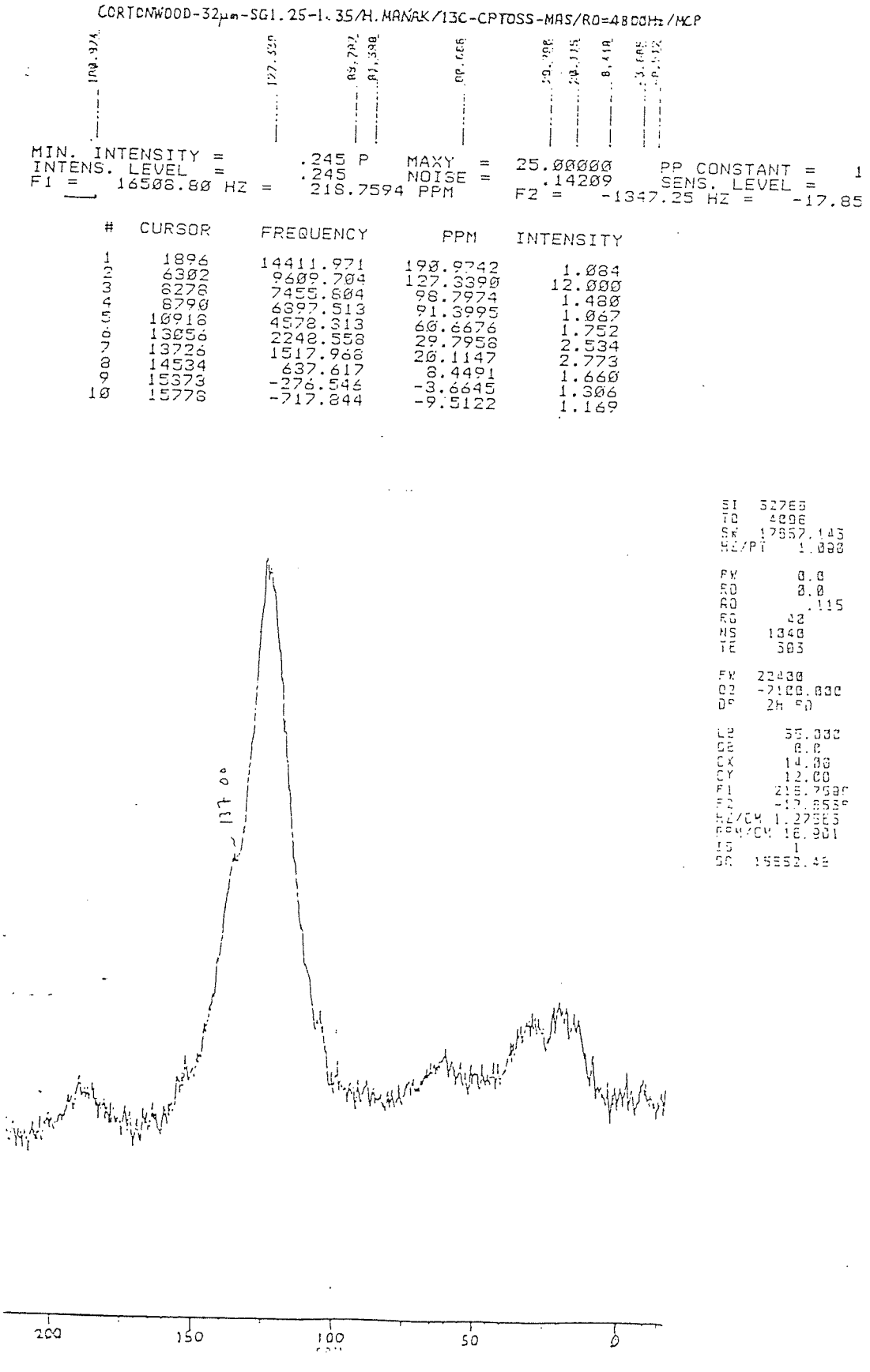

Fig3.78b

^{13}C CP MASNMR of the Cortonwood ≤32 µm vitrinite maceral

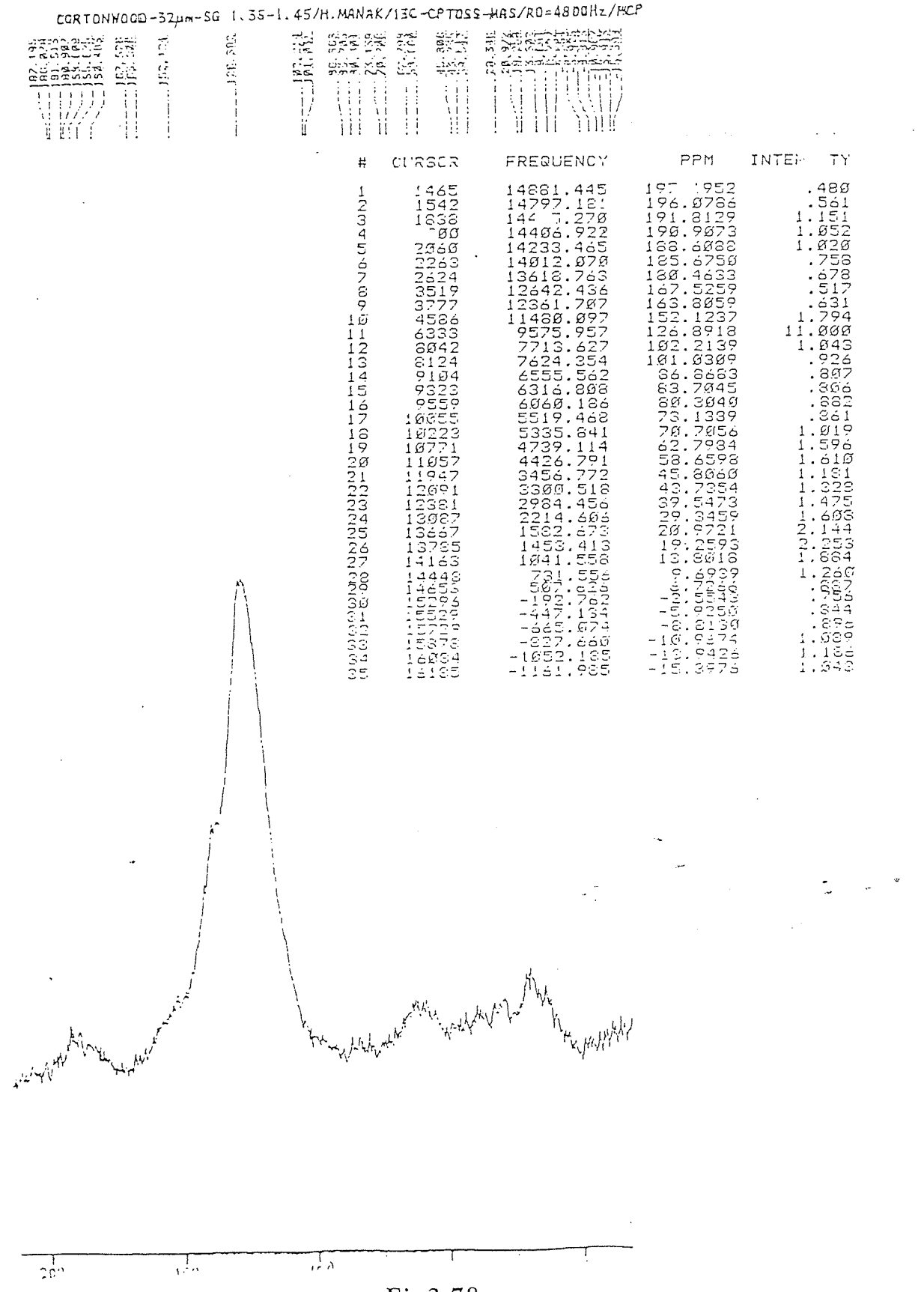

Fig3.78c

^{13}C CP MASNMR of the Cortonwood ≤32 μm inertinite maceral

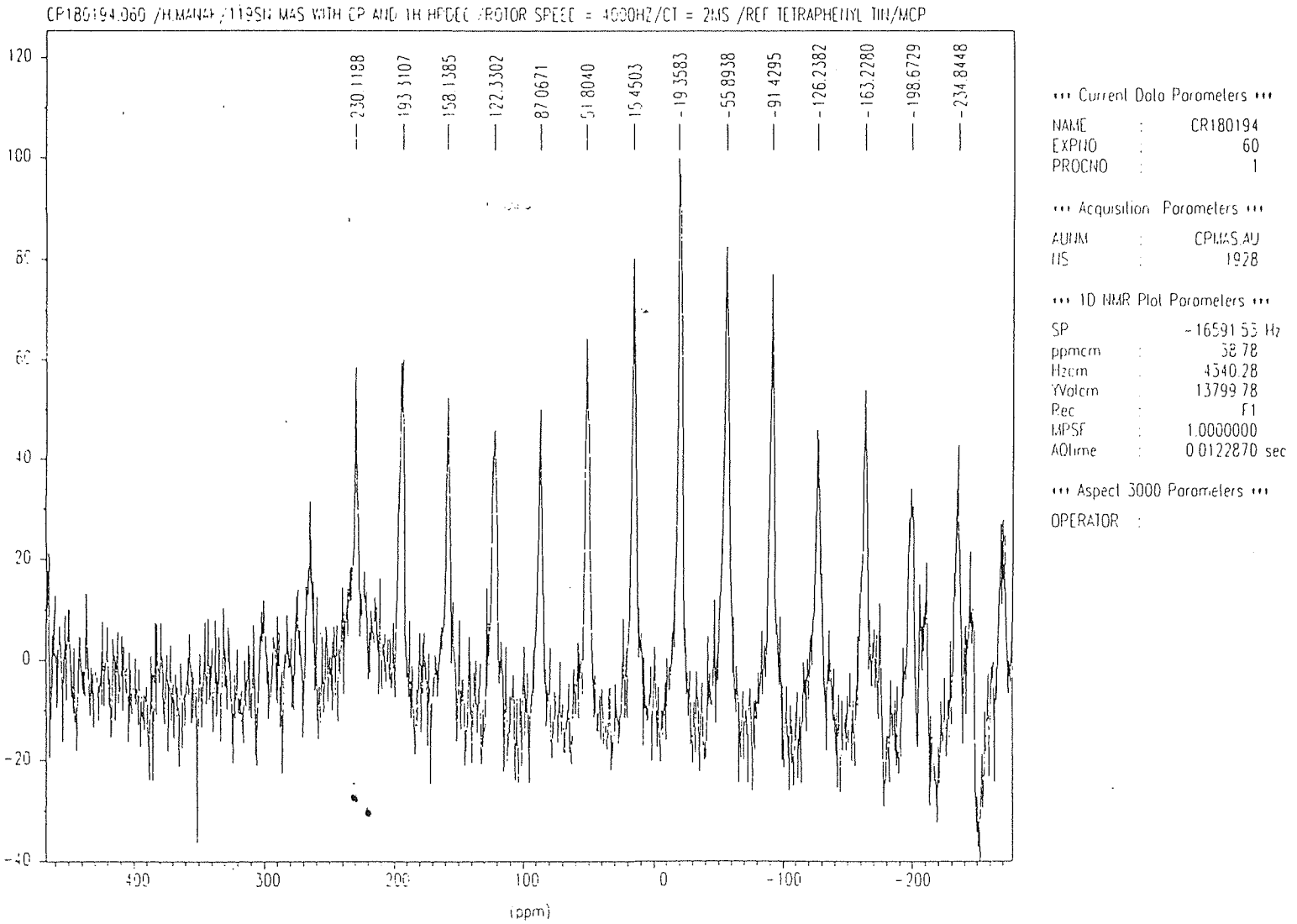

Fig3.79a

^{119}Sn CP MASNMR of the stannylated Cortonwood ≤32 μm exinite

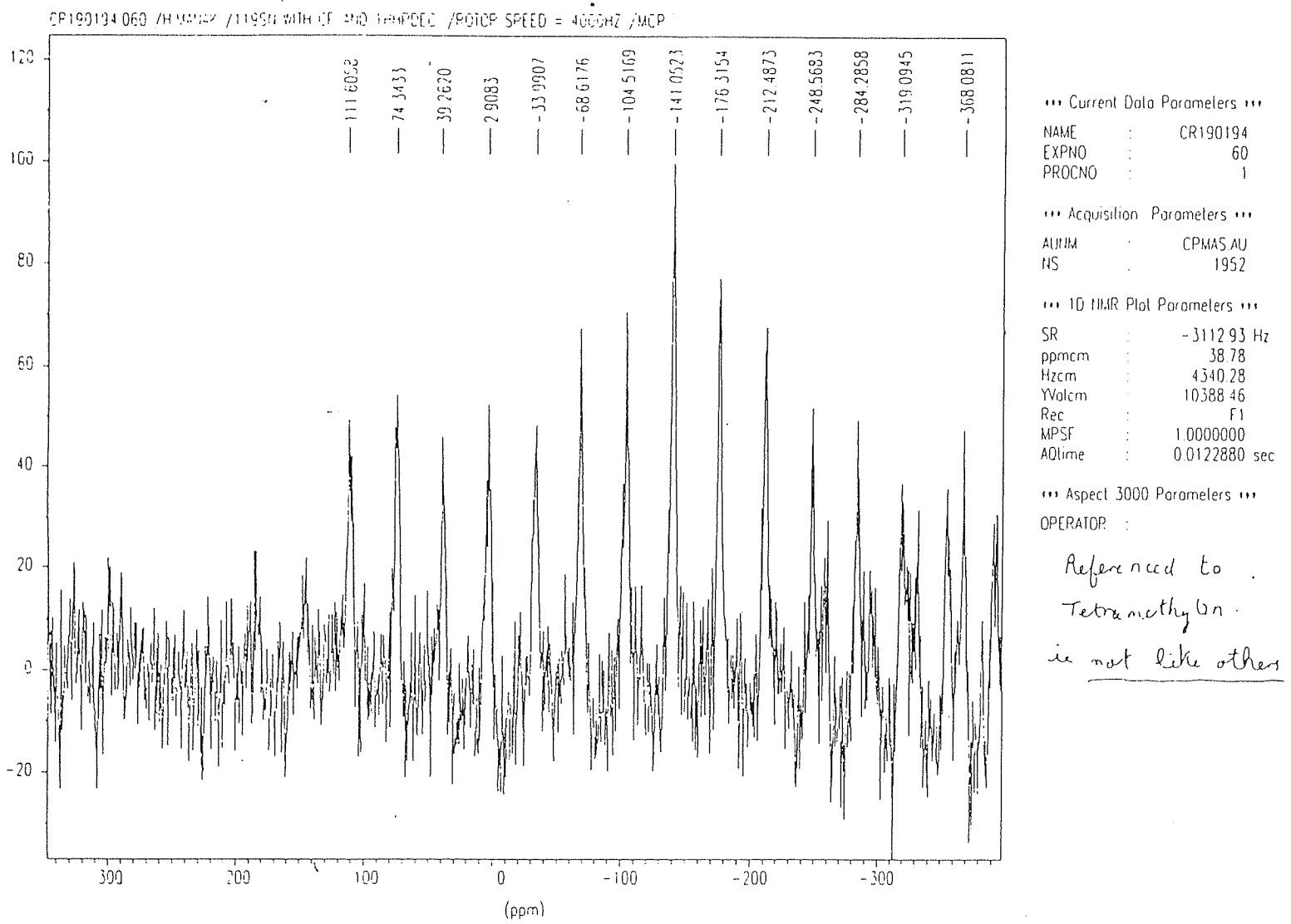

Fig3.79b

^{119}Sn CP MASNMR of the stannylated Cortonwood ≤32 μm vitrinite

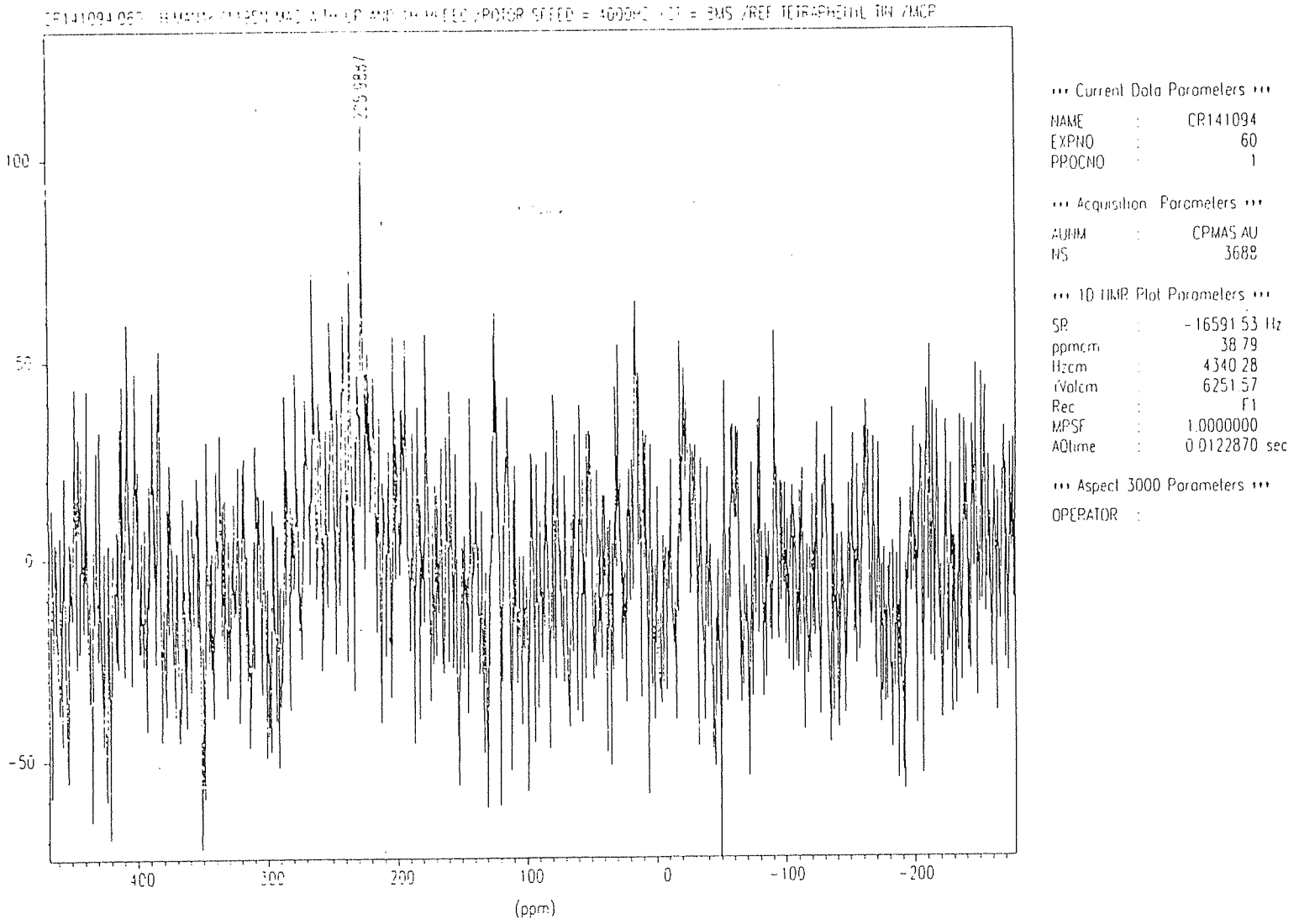

Fig3.79c

^{119}Sn CP MASNMR of the stannylated Cortonwood ≤32 μm inertinite

The stannylated Creswell inertinite's IR spectrum produced stannylation peaks with a lower intensity compared to those obtained for the stannylated Cortonwood inertinite maceral - this suggests a greater degree of stannylation in the Cortonwood inertinite, which would seem to imply that the hydroxyl functionality in the Cortonwood inertinite is less sterically-hindered compared to the Creswell inertinite maceral. The ^{119}Sn CP MASNMR spectra of the stannylated Cortonwood macerals produced some surprising results. The Cortonwood exinite and vitrinite do not appear to have reacted very well at all. They both produced a ^{119}Sn resonance at approximately -19 ppm. It has been postulated that this peak is due to the formation of Bu_3SnOH - a decomposition product of the TBTO reagent. This would also explain the apparent increase in the -OH band of the IR spectra of the stannylated Cortonwood exinite and vitrinite macerals. The stannylated Cortonwood inertinite, however, produced a very good ^{119}Sn spectrum with a single main resonance appearing in a region where we would expect the Sn to be in a less sterically-crowded environment. Consequently, it appears that the Cortonwood exinite and vitrinite macerals contain more sterically-hindered hydroxyl functional groups, which are difficult to derivatise with the TBTO stannylating reagent being employed, whereas the Cortonwood inertinite maceral appears to contain much more accessible hydroxyl functional groups and less inherent moisture compared to the other two macerals. By contrast, ^{119}Sn CP MASNMR analysis of the stannylated Creswell macerals showed that stannylation had occurred for the Creswell exinite and inertinite maceral groups, but no stannylation was observed for the Creswell vitrinite maceral. This suggests that the more sterically-hindered hydroxyl functional groups in Creswell coal exist mainly in the Creswell vitrinite maceral. This work has highlighted the fact that there is tenaciously held moisture associated with all coals and coal macerals and care must be taken when analysing the -OH region of the IR spectrum (3600 - 3200 cm^{-1}) - there will always be a band due to the moisture present. Consequently, it is more prudent to look at the derivatisation absorption bands in order to determine whether a reaction has actually occurred. Also, because this inherent moisture contains -OH groups, which we are attempting to derivatise, we must expect some reaction between the derivatising reagent and the moisture in the coal / coal maceral. In conclusion, the TBTO reagent does indeed appear to effect stannylation of the coals and coal macerals, but due to its large size, it is a very sterically-demanding reagent and only the more accessible -OH groups in the coal / coal maceral are derivatised.

Addendum

Whilst in the process of writing up this thesis, two new stannylating reagents have come to light in the literature. These have been used by Ye and Verkade[88] to successfully stannylate a set of 29 phenols, thiophenols, carboxylic acids and alcohols. The two reagents are N-trimethylstannylaniline $Me_3SnNHPh$ and N,N-bis(tri-n-butylstannyl)aniline $(n\text{-}Bu_3Sn)_2NPh$, with the latter appearing to be the more effective of the two. The ^{119}Sn nmr of the stannylated model compounds have been measured in pyridine solution at 240K and chemical shifts precise to $\pm$ 0.1 ppm have been obtained after only a 20 min acquisition time and 200 scans. Ye and Verkade have also managed to derivatise a pyridine extract from a sample of Illinois No.6 coal with $(n\text{-}Bu_3Sn)_2NPh$ and tentatively identify four of the phenol groups observed.